

THESIS
N 4445f
1997
c. 2

$^{40}\text{Ar}/^{39}\text{Ar}$ GEOCHRONOLOGY OF
THE MIocene SILICIC LAVAS
OF THE SOCORRO-MAGDALENA AREA,
NEW MEXICO, U.S.A.

by
Hal H. Newell

Submitted in Partial Fulfillment of the
Requirements of the Degree of
Masters of Science in Geochemistry
August 1997

NMIMT
Library
SOCORRO, NM

Department of Earth and Environmental Science
New Mexico Institute of Mining and Technology
Socorro, New Mexico, USA

MAR 03 1998
38538629

ABSTRACT

$^{40}\text{Ar}/^{39}\text{Ar}$ dating of mineral separates provides a precise chronology for the Miocene silicic volcanism in the Socorro-Magdalena area contemporaneous with the evolution of the central Rio Grande rift. The volcanism is apparently associated with the formation of the Socorro accommodation zone. This study increases the resolution and accuracy of the ages of silicic lavas erupted from the area.

$^{40}\text{Ar}/^{39}\text{Ar}$ dates on mineral separates were obtained by single-crystal laser fusion, laser step-heating, and incremental furnace heating procedures. The most precise ages (typically ± 0.5 to 1%) were produced from sanidine mineral analyses. Ages on additional minerals pairs of plagioclase, biotite, or hornblende from individual rock samples allowed comparisons between the various mineral ages. The apparent ages of all biotite separates are older than the more accurate age results from sanidine from corresponding samples. No definitive explanation for the older apparent ages of the biotites was discovered. All methods of analysis for the biotite data yielded older ages, including isochron analysis which should exclude the influence of homogeneously distributed excess ^{40}Ar . Plagioclase and hornblende results were the least precise and did not produce reliable ages.

Silicic lavas were erupted in the Socorro-Magdalena area from 18.5 until 7.0 Ma, within four geographically defined centers of volcanism. The Squaw Peak centers were active from 18.5 to 11.5 Ma, the Magdalena Peak centers were active from 13.8 to 13.0 Ma, the Pound Ranch centers were active approximately 12 to 11.3 Ma, and the Socorro Peak centers were active from 11.6 to 7.0 Ma. Chronological trends apparent with the new $^{40}\text{Ar}/^{39}\text{Ar}$ ages include a pulse of volcanism between 14.5 and 11.3 Ma, when all four volcanic centers were active. The apparent eruption ages also record older volcanism in the western part of the field and the youngest eruption ages in the eastern regions.

ACKNOWLEDGMENTS

I would like to thank all of the people who have given me their time and expertise to help produce this thesis. My committee of Philip Kyle, Bill McIntosh, and Richard Chamberlin has given time, guidance, and support, ranging from the field, to the lab, and on the computer.

Additional field assistance was provided by my good friends at Tech and elsewhere. They are listed by percent abundance in the field and their current residence: Dave Ennis, of Las Cruces; Hannah Rye, of Salt Lake City; Pat Mattie, of Las Vegas; Brad Yonaka, of The Jungle, Venezuela; Scott Howe, of Cameroon, West Africa; Mom, of Lewisville; and Thom's Volcanology class.

Key assistance in the mineral separate lab and with the mass spectrometer was given by Rich Esser, Lisa Peters, and Matt Heizler.

General guidance was supplied by Bob Osburn, Robert Appelt, Joe Stroud, and all of the other unnamed co-conspirators at Tech. I relied heavily on Danny Bobrow's masters thesis (1984) to initially define the field area and the units.

Access to land was graciously granted by: Dennis Hunter of EMRTC, Smokey Pound, Buddy Tiegner, and Thomas Pressgrove of Muleshoe Ranch and the movie crew.

The New Mexico Geochronological Research Lab supplied all the technical and equipment needs of this research, thanks again to Bill and Matt for their enthusiastic support of this and other student research. Philip Kyle provided financial support of a RA while at Tech, partial support of field vehicles came from the NM Bureau of Mines, and the Tech Graduate Office provided a graduate student research grant.

I would like to thank Tara, my wife, for all of her encouragement, patience, and support during my time in Socorro. Finally, I would like to dedicate this thesis to my grandparents, Grandma C. and the late Bill Carson, who first introduced me to New Mexico and rocks.

TABLE OF CONTENTS

TITLE PAGE	i
ABSTRACT	
ACKNOWLEDGMENTS	ii
TABLE OF CONTENTS	iv
INTRODUCTION	1
GEOLOGIC SETTING	3
PREVIOUS WORK	
Squaw Peak centers	8
Magdalena Peak centers	9
Pound Ranch centers	11
Socorro Peak centers	12
	14
ANALYTICAL METHODS	
Methods of Evaluation	15
Mineral Ages	19
	24
⁴⁰ Ar/ ³⁹ Ar RESULTS	
Analytical Errors	27
Mineral to Mineral Comparisions	29
Unit Ages	30
	35
DISCUSSION OF MINERAL AGES	
Sanidine Ages	40
Biotite Age Interpretations	40
Plagioclase and Hornblende Age Analyses	43
	50
GEOCHRONOLOGY OF MIOCENE SILICIC VOLCANISM	
Squaw Peak centers	51
Magdalena Peak centers	52
Pound Ranch centers	53
Socorro Peak centers	54
Geochemical Modeling and Timing of the SAZ	55
Other Rio Grande rift Related Rhyolitic Volcanism	56
	58

CONCLUSIONS	60
REFERENCES	62

APPENDICES

Appendix 1	Sample Locations
Appendix 2	Sample Map
Appendix 3	Irradiation Information
Appendix 4	Age Summary for all $^{40}\text{Ar}/^{39}\text{Ar}$ Analyses
Appendix 5.a.	Laser Fusion Numeric Data
Appendix 5.b.	Funace Step-Heating Numeric Data
Appendix 5.c.	Two-Step Laser Fusion Numeric Data
Appendix 6.a.	Laser Fusion Graphical Analysis
Appendix 6.b.	Furnace Step-Heating Graphical Analysis
Appendix 6.c.	Two-Step Laser Fusion Graphical Analysis

LIST OF TABLES

Table 1.	Mineral ages	25
Table 2.	Apparent eruption ages	28

LIST OF FIGURES

Figure 1.a.	Rio Grande rift and accomodation zones	2
Figure 1.b.	Aerial extent of Miocene centers	2
Figure 2.	Magdalena and Squaw Peak centers	10
Figure 3.	Socorro Peak and Pound Ranch centers	13
Figure 4.a.	Furnace step-heating, age spectra plot of biotite sample HN-58	20
Figure 4.b.	Furnace step-heating, ideogram plot of biotite sample HN-58	20
Figure 5.	Ideogram of single crystal laser fusion of sanidine sample HN-55	22
Figure 6.a.	Ideogram of single crystal laser fusion of sanidine sample HN-58	23
Figure 6.b.	Ideogram of single crystal laser fusion of sanidine sample HN-17	23

Figure 7.	Furnace step-heating, age spectra plot of hornblende sample HN-6	31
Figure 8.	Comparision of biotite furnace and laser analyses	33
Figure 9.	Comparision of sanidine and biotite analyses	34
Figure 10.	Ideogram of apparent eruption ages	38
Figure 11.	Age versus distance from rift axis	39
Figure 12.a.	Ideogram of single crystal laser fusion of sanidine sample HN-39	42
Figure 12.b.	Isochron of single crystal laser fusion of sanidine sample HN-39	42
Figure 13.a.	Furnace step-heating, age spectra plot of biotite sample HN-2	48
Figure 13.b.	Laser two-step heating, ideogram plot of biotite sample HN-2	48

INTRODUCTION

The Rio Grande rift consists of a series of north-trending, asymmetrical fault-block basins. The half-grabens are bound by northeast-trending accommodation zones (Fig. 1.a), which have developed along preexisting structural lineaments, and allow the basins to alternate in tilt directions from east to west (Chapin and Cather, 1994). Accommodation zones are common features of extensional rifts worldwide (Gibbs, 1984; Bosworth, 1985; Keller, 1991). Bosworth (1986) envisioned that accommodation zones are formed when the lateral propagation of a single detachment system stalls due to fault boundaries migrating inward and forming a "neck" in the rift. At or beyond the neck, the fault system continues and a new sub-basin is formed. In the Rio Grande rift, the best exposed accommodation zone is located in the Socorro-Magdalena area where west-tilted blocks to the north are separated from east-tilted blocks to the south; this rift feature is termed the Socorro accommodation zone (Fig. 1.b)(Chapin, 1989).

Previous investigators of the area of the Socorro accommodation zone have studied the tectonic history (Chamberlin, 1983; Chapin and Cather, 1994) and the volcanic record (Bobrow et al., 1983; Chapin, 1989). However, models for the timing and formation of the

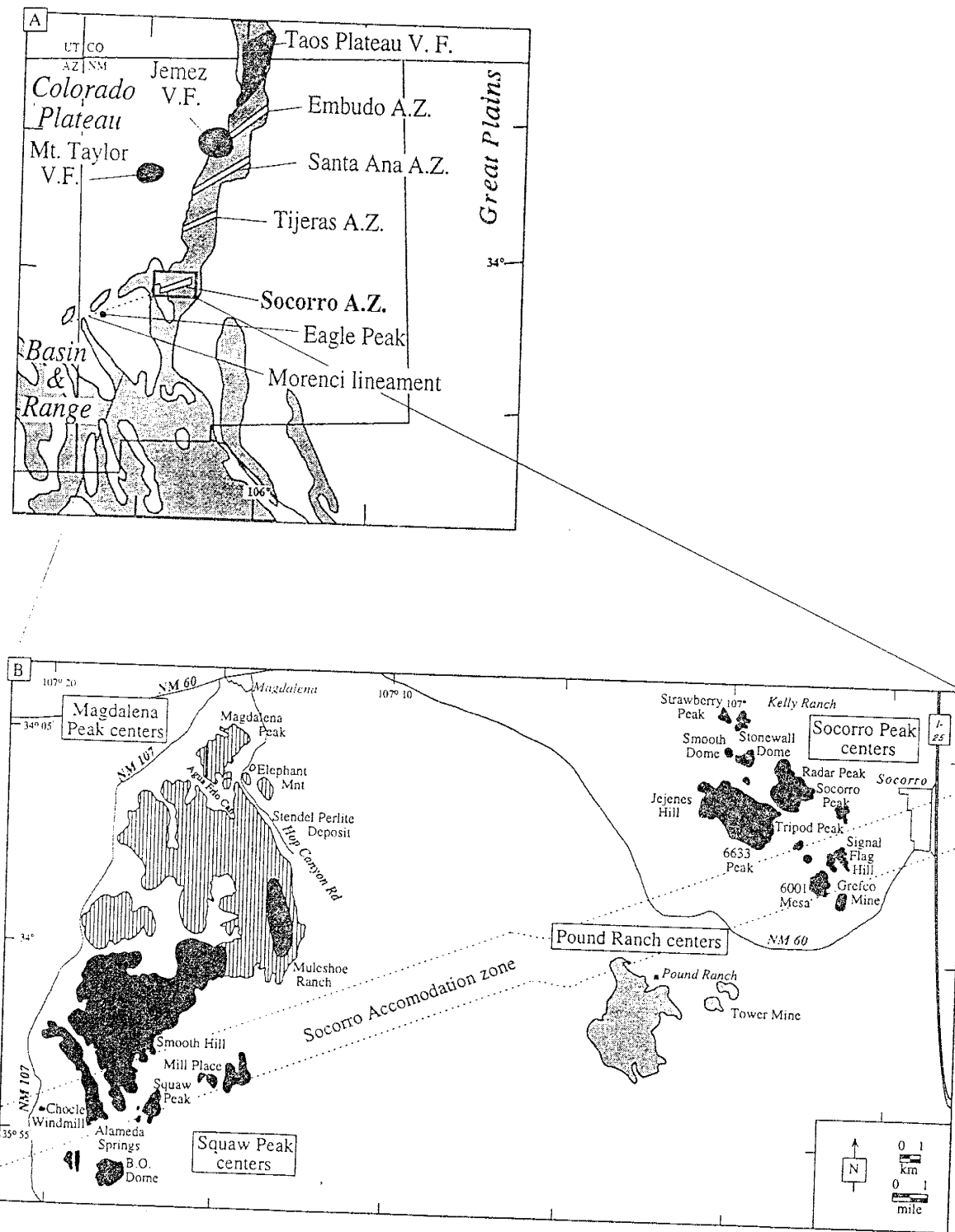


Figure 1.a. Regional map depicting the approximate basin of the Rio Grande rift, the four rift accommodation zones (A.Z.) of New Mexico (After Chapin and Cather, 1994), and some associated volcanic fields (V.F.).

Figure 1.b. The approximate aerial extent of the Miocene silicic centers of the Socorro-Magdalena area (After Bobrow et al., 1983)

Socorro accommodation zone were limited by imprecise K-Ar whole rock and mineral dates (Osburn and Chapin, 1983; Bobrow, 1983).

The main objective of this study was to determine a precise geochronologic framework for the Miocene silicic volcanism in the Socorro-Magdalena area using the $^{40}\text{Ar}/^{39}\text{Ar}$ dating method. An accurate geochronological time frame of the volcanic rocks in the area will aid in the understanding of the extensional kinematics and formation of accommodation zones along the Rio Grande rift and aid in development of geochemical models for rhyolitic volcanism in the area.

An additional goal of this study was to compare apparent ages of coexisting potassium-bearing minerals within a rock sample. Both sanidine and biotite mineral separates produced analytically precise $^{40}\text{Ar}/^{39}\text{Ar}$ ages. However, significant age discordance within mineral and rock samples revealed the need for additional investigation into the accuracy of the biotite, plagioclase, and hornblende mineral ages.

GEOLOGIC SETTING

The Rio Grande rift system extends over 1000 km from central Colorado through to Chihuahua, Mexico and Presidio, Texas (Olsen et al., 1987). In the northern section, the Colorado Plateau bounds the rift to the west, and in the south, the western margin of the rift is transitional into the

Basin and Range province (Fig. 1.a). The Great Plains region bounds the eastern margin of the rift

Tectonic and stratigraphic development of the Rio Grande rift spanned three phases (Baldridge et al., 1991). From the late Oligocene to the early Miocene, the first period resulted from the ductile extension and upwelling of the lithosphere, and produced widespread moderate- to low-angle normal faulting (Olsen, 1987). The onset of rifting was contemporaneous with a period of intense pyroclastic volcanism both within and outside of the rift (Chapin and Cather, 1994). Immediately west of the rift, the Mogollon-Datil volcanic field erupted large volumes of silicic ignimbrites and basaltic andesites between 28.8 and 27.4 Ma (McIntosh et al., 1992), and perhaps signaled the inception of regional extension. Within the rift, broad basins with high relief formed and limited sedimentation began (Chapin and Cather, 1994). Chamberlin's (1983) study of rifting just to the north of Socorro determined that extensional faulting commenced between eruption of the Vicks Peak Tuff and the Lemitar Tuff, most recently dated 28.6 Ma and 28.0 Ma respectively (McIntosh et al., 1992). The rift volcanic rocks of this phase were primarily basaltic andesites, and related calc-alkaline intermediate to silicic rocks (Baldridge et al., 1991).

Following a lull in extension during the early to middle Miocene, the extensional strain rate increased within the Rio Grande rift during the second period of development. Moderate- to high-angle normal faulting resulted in rapid subsidence and sedimentation within the half-grabens of the rift and continued into the late Miocene (Olsen et al, 1987; Chapin and Cather, 1994). Immediately north of the Socorro area, Cather et al. (1994) compared stratal tilt versus age and found the rate of tilting greatly increased between approximately 17 and 10 Ma. This phase of rift development also resulted in widespread magmatism, including basaltic flows and localized intermediate to silicic volcanic eruptions. Geochemical modeling of basalts, in the areas of the highest extension, suggests subcrustal lithospheric thinning (Baldridge et al., 1991).

During Pliocene to recent times, the rate of extension in the rift slowed considerably from former high levels (Chapin and Cather, 1994). Reduced sedimentation rates easily outpaced the minor subsidence of the rift basins and basaltic flows were widespread in the transition zone of the Colorado Plateau and in the central rift (Baldridge et al., 1991).

Four major basins have been identified in the northern to central region of the rift, the San Luis Basin, the Espanola Basin, and the Upper and Lower Albuquerque Basins (Fig. 1.a; Chapin and Cather, 1994). The basins form a chain of asymmetrical half grabens alternating from east-

tilted to west-tilted, reversing across northeast-trending accommodation zones. Studies of these transverse structures found no evidence of significant strike-slip displacement (Chapin, 1989; Faulds et al., 1990). Instead, the Rio Grande rift accommodation zones seem to trace lines of preexisting structural weakness that were activated by rapid extension in the late Oligocene. How these zones "accommodate" up to 70° of tilting in opposite directions is poorly understood (Chapin and Cather, 1994).

The Socorro accommodation zone (SAZ) is a 50 km long by 2 km wide boundary subtly expressed on geologic maps, dividing a domain of west-tilted blocks to the north from east-tilted blocks to the south (Fig. 1.b; Chapin and Cather, 1994). Chapin (1989) proposed that the location of the SAZ was determined by the Morenci lineament, a major northeast-trending crustal flaw perhaps dating back to the Precambrian. The location of the Morenci lineament is indicated by a line of volcanic centers which continues to the southwest from the SAZ. Also prior to existence of the SAZ, three large Oligocene calderas were active in the Socorro-Magdalena area from 32 to 27.4 Ma (Chapin, 1989; McIntosh et al., 1992). The SAZ formed during the period of rapid Oligocene and later Miocene extension of the Rio Grande rift system. Silicic volcanism resumed in the Magdalena area around 18 Ma and continued between 12 and 7 Ma in the Socorro area (Bobrow et al., 1983).

Other studies have identified geochemical alteration and seismic events in the Socorro-Magdalena area which are presumably related to the rift and the SAZ. Dunbar et al. (1996) investigated the scattered outcrops of potassium metasomatism which date to between 15 and 7 Ma. The geochemical alteration was attributed to circulating alkaline-saline brines within a closed-basin playa system (Dunbar et al., 1996). The outcrops of potassium metasomatism are concentrated along the SAZ (Chapin, 1989).

Sanford et al. (1996) proposed that a major crustal flaw, termed the Socorro Fracture Zone (SFZ), crossed the Socorro-Magdalena area. The zone is based upon the concentration of current high seismicity (Sanford et al., 1995) and the trace of a major topographic lineation oriented approximately N70E from the Arizona-New Mexico border to the Texas-Oklahoma border (Thelin and Pike, 1991). The SFZ coincides with the southern border of the SAZ, but the Morenci lineament is located to the southwest of the Socorro fracture zone area (Sanford et al., 1995). Also within the seismically active zone, the Socorro midcrustal magma body is located 19 km below Socorro and spans approximately 4000 km² (Sanford et al., 1977).

PREVIOUS WORK

Previous attempts to establish an accurate geochronology for the Miocene silicic volcanic rocks of the Socorro-Magdalena area have been limited by low precision of dating techniques, particularly conventional potassium-argon (K-Ar) dating and fission-track dating methods. Earlier geochronologic work was not able to distinguish between closely spaced episodes of volcanism. In a study of the Socorro-Magdalena area volcanics, Bobrow (1984) cited examples of the K/Ar dates contradicting the stratigraphic record.

The most detailed geochemical and lithologic investigation of the Miocene silicic volcanism in the Socorro-Magdalena area was by Bobrow et al. (1983) and Bobrow (1984). The field area was divided into four informal geographic centers based on clusters of silicic vents. Figure 1.b depicts the approximate aerial extent of the volcanic centers of Squaw Peak, Magdalena Peak, Pound Ranch, and Socorro Peak.

Previous to Bobrow (1984), a series of mapping, geochemical, and petrologic projects characterized the Socorro-Magdalena area. The regions of these studies included the Squaw Peak centers by Osburn (1996), Bowring (1980), and Donze (1980); the Magdalena Peak centers by Bobrow (1984) and Allen (1979); the Pound Ranch centers by Osburn (1978) and Petty (1979); and the Socorro Peak centers by Chamberlin (1980). Allen (1979) provided a detailed historic overview of geologic

studies in the area from 1900 to 1979. The units and stratigraphy of the four volcanic centers are described in detail below.

Squaw Peak centers

The oldest silicic domes of the Socorro-Magdalena area are in the Squaw Peak volcanic center, approximately 20 km south of the town of Magdalena (Fig. 2). The rhyolite of McDaniel Tank covers much of the northern Squaw Peak area and is characterized as a high-K, high-SiO₂, phenocryst poor, finely banded rhyolite lava flow (Donze, 1980). In the northwest of the center area, the rhyolite of Alameda Springs unconformably overlies the rhyolite of McDaniel Tank. The Alameda Springs unit was mapped as a rhyolite of Magdalena Peak by Donze (1980), based on the similar mineralogy and field description to the northern Magdalena Peak rhyolite. Bobrow (1984) found the rhyolites to be geochemically similar, both having high-K and high-SiO₂, but gave the unit the informal name of the rhyolite of Alameda Springs, based in part on the K-Ar age differences between the units.

Other units of the Squaw Peak area include an intrusive dacite in the northeast of the Squaw Peak area near Mill Springs and the rhyolite of Squaw Peak (Fig. 2). Osburn (1996) considered the dacite of Mill Springs to be Miocene in age. The unit consists of topographically subdued,

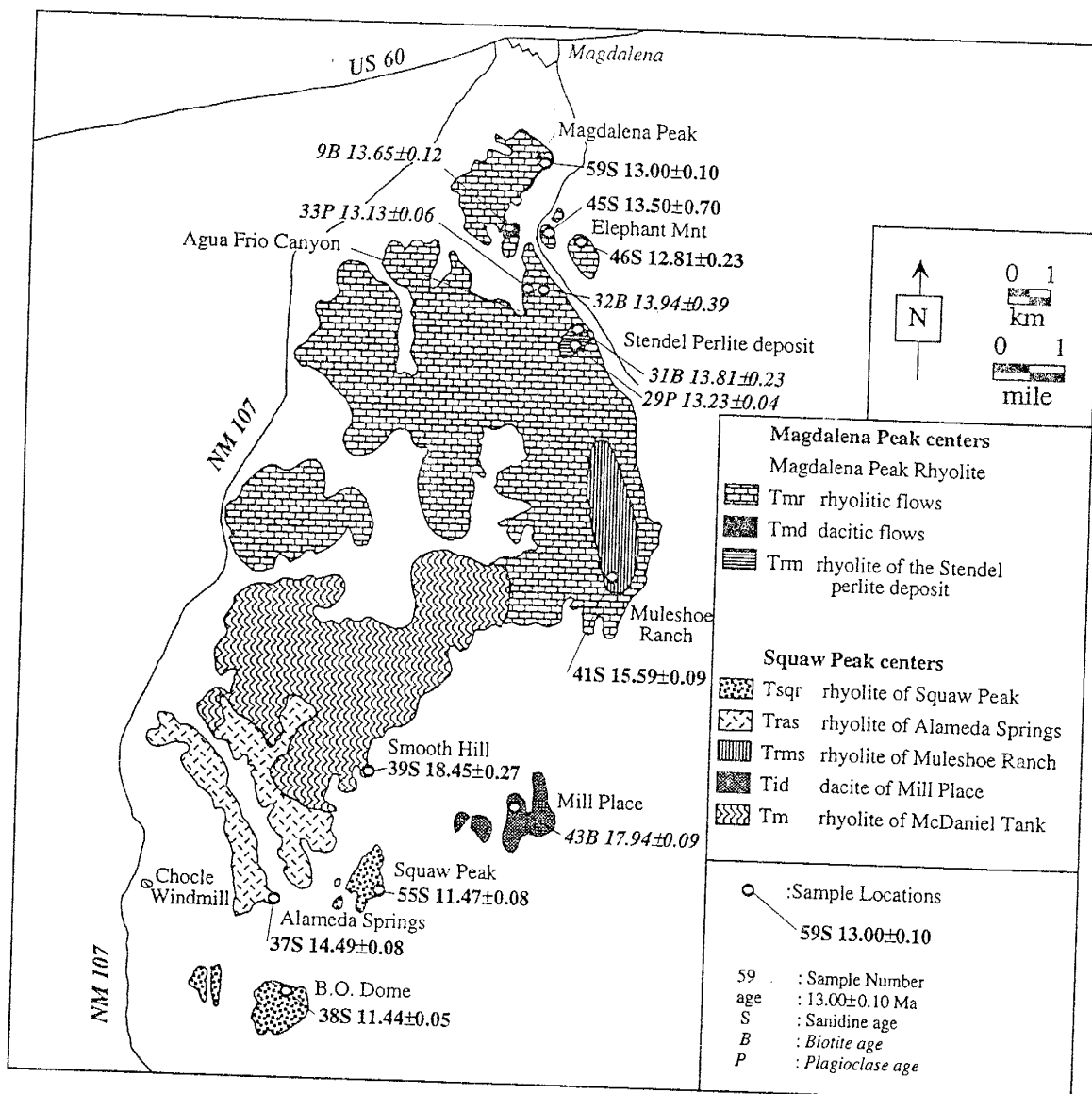


Figure 2. Distribution of Miocene silicic volcanic rocks in the Magdalena and Squaw Peak centers. Compiled from Bobrow (1983) and Osburn (1996)

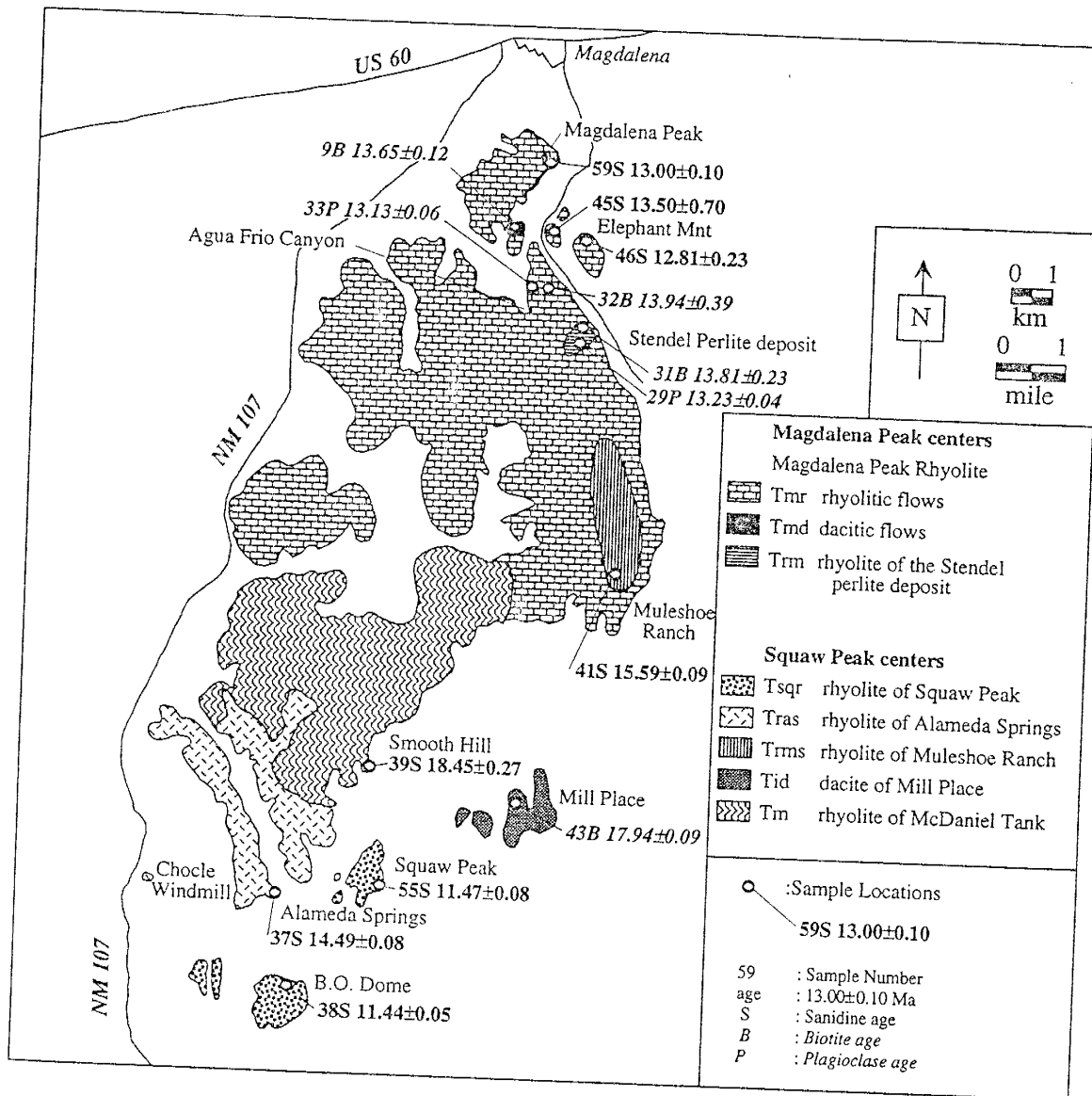


Figure 2. Distribution of Miocene silicic volcanic rocks in the Magdalena and Squaw Peak centers. Compiled from Bobrow (1983) and Osburn (1996)

scattered outcrops with badly altered phenocrysts of plagioclase and biotite. To the south are the youngest domes of the Squaw Peak center, the rhyolites of Squaw Peak and B.O. Ranch. Bobrow et al. (1983) chemically characterized these domes as high-K and high-SiO₂ rhyolites and mapped the phenocryst-poor rhyolite of B.O. Dome and the phenocryst-rich Squaw Peak domes as a single unit, despite mineralogical differences.

Magdalena Peak centers

Miocene domes and flows occur in the vicinity of Magdalena Peak, a prominent volcanic vent located 2 km south of the town of Magdalena (Fig. 2). The stratigraphic chart of Osburn and Chapin (1983) categorizes all of the volcanism of this area as the Magdalena Peak Rhyolite. However, informal names have been assigned to temporally distinct flows. The oldest stratigraphic unit of the Magdalena Peak center area is the rhyolite of the Stendel perlite deposit, first characterized by Weber (1957). The perlite layers were not mapped separately by Allen (1979), and Bobrow et al. (1983) geochemically characterized all of the samples of the unit as high-K and high-SiO₂ rhyolites. No source vent for the Stendel perlite unit was recognized by either study.

In the vicinity of Magdalena Peak, Bobrow (1984) divided the rocks into high-K rhyolite and high-K dacite lava flows. The rhyolitic flows

(Fig. 2), compose the largest unit in the area and are estimated to be 11 to 17 km³ (Bobrow, 1984). The vent for the rhyolite is exposed on the east face of Magdalena Peak and the unit covers steep-sided hills to the south and west of the vent. The rhyolite has phenocrysts of plagioclase, amphibole, and biotite with subordinate sanidine and quartz, and normally includes a vitreous basal layer in outcrop (Bobrow, 1984). The dacitic flow of Magdalena Peak is older than the rhyolite. This unit is poorly exposed on a hill southwest of Magdalena Peak and is estimated to be only 0.01 km³ in volume (Bobrow, 1984).

Pound Ranch centers

The smallest Miocene silicic center is found near Pound Ranch, 3 km south of US highway 60 (Fig. 3), where two closely related rhyolites are exposed. Flows of the lower Pound Ranch rhyolite crop out around vents in the south and north of the area. The older unit is composed of high-K and high-SiO₂ porphyritic rhyolite flows (Bobrow, 1984; Osburn, 1978). Surrounding the lower unit are flows from the upper Pound Ranch rhyolite. The younger high-K, lower SiO₂ unit consists of a black, basal vitrophyre and a finely flow-banded section above, which grades upward into more massive flows (Bobrow, 1984)

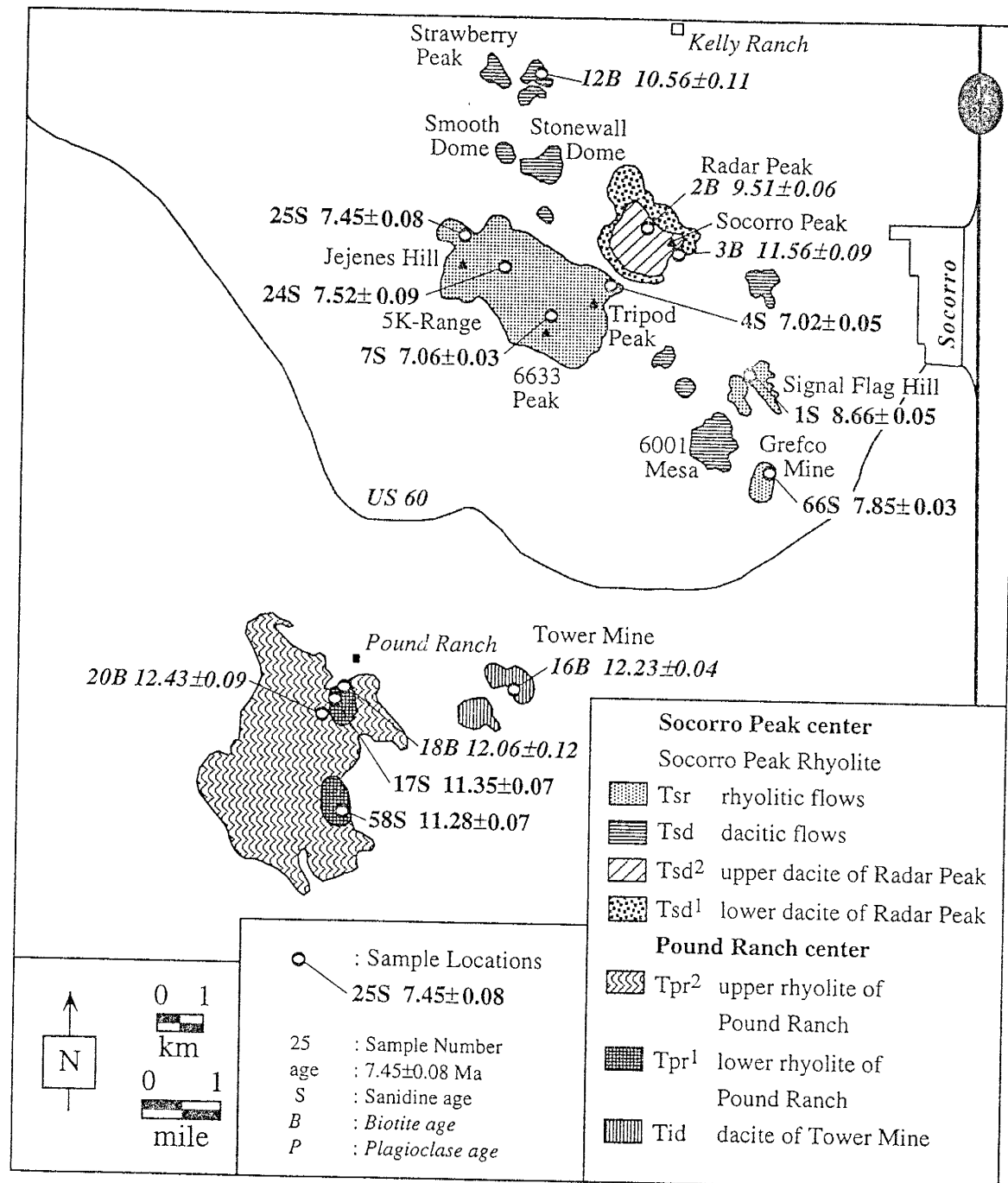


Figure 3. Distribution of Miocene silicic volcanic rocks in the Socorro and Pound Ranch centers. Compiled from Bobrow (1983) and Chamberlin (1980)

Dacitic lavas and a basaltic unit are also exposed in the Pound Ranch area (Fig. 3). The dacite of Tower Mine consists of scattered domes located 2 km to the east of Pound Ranch, near the Tower Mine on the Luis Lopez quad map (Chamberlin, 1980). This strongly altered unit contains phenocrysts of biotite, plagioclase, and hornblende. West of the Pound Ranch center, the basalt of Madera Canyon underlies the upper rhyolite of Pound Ranch (Osburn, 1978).

Socorro Peak centers

The Socorro Peak center includes the youngest silicic domes of the study area (Fig. 3). Osburn and Chapin (1983) formalized the volcanic units of this center as the Socorro Peak Rhyolite. However, informal names have been assigned to separately mapped flows based upon the studies of Chamberlin (1980) and Bobrow (1983). In the north, the prominent dacitic dome of Strawberry Peak stratigraphically overlies eastern outcrops of basaltic andesites, near Kelly Ranch. Two flow units are mapped on the mountain of Socorro Peak. Prominent, columnar-jointed northern cliff on Socorro Peak expose a hornblende rhyodacite, which is termed the lower dacite of Radar Peak, which is also found in smaller domes ranging NW-SE across the Socorro Peak area. The upper unit of Radar Peak, a biotite rhyodacite flow, is mineralogically similar to

Strawberry Peak (Chamberlin, 1980). The unusually glassy Grefco dome hosts an active perlite mine.

Younger rhyolitic flows are found to the west and south of Socorro Peak (Fig 3). Domes of the high-K and high-SiO₂ rhyolitic flows of the Socorro Peak Rhyolite cover much of the western section of the Socorro Peak center and include an exposure south-east of Socorro Peak. Most of the rhyolites have abundant phenocrysts of plagioclase, sanidine, quartz, biotite, and amphibole, except for the nearly aphyric rhyolite of Grefco mine (Bobrow, 1984). Bobrow (1984) identified two possible vents on the Grefco dome.

ANALYTICAL METHODS

Samples for ⁴⁰Ar/³⁹Ar analysis were collected from the unweathered, interior portions of rhyolite and dacite outcrops (Appendix 1 and 2). Crystal-rich, vitrophyric samples with crystals of fresh sanidine and biotite were preferred. Two or more samples of at least 2 kg were collected from each of the previously mapped Miocene silicic units in the study area.

Initially, an attempt was made to separate sanidine and biotite from each rock sample. For samples where those minerals were not present or could not be separated, separation of plagioclase or hornblende was

attempted. Samples were crushed and sieved to between 50 and 100 μm . The magnetic components of the crushed rock were removed using a Frantz magnetic separator. Sanidine was separated from the plagioclase, quartz, and groundmass using lithium metatungstate heavy liquid. Sanidine and plagioclase concentrates were ultrasonically treated in 15% hydrofluoric acid solution for 2-6 minutes to remove any residual groundmass contamination and then rinsed in deionized water. Biotite and hornblende minerals were ultrasonically treated in deionized water to remove groundmass contamination. The purity of mineral separates was evaluated microscopically.

Forty-eight mineral separates were analyzed from thirty different rock samples. Analyses were performed at the New Mexico Geochronology Research Laboratory (NMGRL) at the New Mexico Institute of Mining and Technology. Separates of sanidine, biotite, plagioclase, and hornblende were loaded into 6 to 16 hole machined aluminum disks for irradiation. Disks were stacked and sealed in evacuated Pyrex or quartz tubes. Five sample batches were irradiated at the Nuclear Science Center at Texas A&M University between 7 and 7.6 hours, and one batch was irradiated at the Ford reactor of the University of Michigan for 10 hours. The complete irradiation parameters are in Appendix 3.

Crystals of the flux monitor standard, Fish Canyon Tuff sanidine (FCT-1), were radially interspersed among the mineral separates to monitor

neutron flux. The FCT-1 reference age used for this study was 27.84 Ma (Deino and Potts, 1990) relative to the MMhb-1 age of 520.4 ± 1.7 Ma (Samson and Alexander, 1987). Three to six FCT-1 crystals from each monitor position were fused for 15 seconds at a power setting of 1.6 watts and analyzed, yielding J-values determinations with a precision of $\pm 0.25\%$ (1 sigma).

Samples were heated and fused using furnace and laser heating techniques. The resulting gas was processed by a computer-automated, all-metal argon extraction system. Biotite, hornblende, and plagioclase samples were step-heated in a low-blank, double-vacuum Mo resistance furnace. A SAES AP-10 getter operated simultaneously with the heating, followed by a final 5 minute gas clean-up by a GP-50 getter. Individual sanidine, plagioclase and biotite crystals were fused or step-heated by a 10 watt CO₂ laser system and cleaned of all reactive gases using a GP-50 getter for 2 minutes. After the clean-up procedures, the inert gas was expanded into the Mass Analyzer Products (MAP) 215-50 mass spectrometer operated in the electron multiplier mode with an overall sensitivity of 2.2×10^{-17} moles Ar/pA and a gain of approximately 10,000. The furnace step-heating data was corrected for extraction line blanks ranging from 8×10^{-16} to 3×10^{-15} moles for ⁴⁰Ar and 2×10^{-18} to 8×10^{-18} moles of ³⁶Ar. The extraction line blanks for the laser analyses ranged from 5×10^{-17} to 3×10^{-16} moles of ⁴⁰Ar and 5×10^{-19} to 3×10^{-18} moles of ³⁶Ar. Corrections for interfering reactions

were determined using K-bearing glass and CaF₂. The values used for samples irradiated at the Nuclear Science Center in College Station, TX were (⁴⁰Ar/³⁹Ar)_K = 0.0002±0.0003, (³⁶Ar/³⁷Ar)_{Ca} = 0.00026±0.00002, and (³⁹Ar/³⁷Ar)_{Ca} = 0.00070±0.00005.

Age summary information of all the mineral analyses for the rock samples are listed in Appendix 4, while the detailed numeric data are contained in Appendix 5 according to analytical technique. Sixteen sanidine and three plagioclase mineral samples were analyzed by the single crystal laser fusion method (Appendix 5.a). For the age determinations of each feldspar sample, between 10 and 35 crystals were individually fused in the same manner as described for the FCT-1 crystals.

Twenty-four biotite, two hornblende, and five plagioclase mineral separates were analyzed using the furnace extraction system (Appendix 5.b). Biotite mineral separates weighing 5-10 mg were incrementally heated in nine steps from 600 to 1700 °C. The hornblende separates (15-20 mg) and plagioclase samples (50-60 mg) were heated over ten steps from 750 to 1700 °C. Each heating step was 8 to 10 minutes in length.

The laser system was also employed to analyze fifteen biotite samples. Ten to twelve biotite flakes of each sample were individually heated by laser using a two-step laser heating schedule (Appendix 5.c). During the first step, the CO₂ laser was set at 0.35 watts, to weakly heat biotite, and to cause

slight dewatering and degassing. In the second step, the biotite sample was totally fused at 1.6 watts. The first laser steps yielded gas with higher components of atmospheric argon and higher analytical errors, whereas the gas from the fusion step tended to be more radiogenic and had lower analytical errors.

All ages were determined using the decay constants recommended by Steiger and Jager (1977). Age uncertainties are reported at the one sigma confidence level and include the error in J , isotope measurements, correction factors, and background measurements.

Methods of Evaluation

Data from each Ar isotope analysis was corrected for interfering reactions and extraction line blanks and then assessed with various graphical tools. The furnace data was evaluated using age spectra and inverse isochron plots and the laser data was evaluated by probability distribution diagrams and inverse isochron plots.

The furnace step-heating age-spectra plots (e.g. Fig. 4.a and Appendix 6.a) for the biotite, plagioclase, and hornblende data include the following parameters: apparent Cl/K (a function of measured $^{38}\text{Ar}_{\text{Cl}}/^{39}\text{Ar}_{\text{K}}$), K/Ca (a function of measured $^{39}\text{Ar}_{\text{K}}/^{37}\text{Ar}_{\text{Ca}}$ in log scale), percent radiogenic yield (the measured ^{40}Ar not attributed to argon of atmospheric composition,

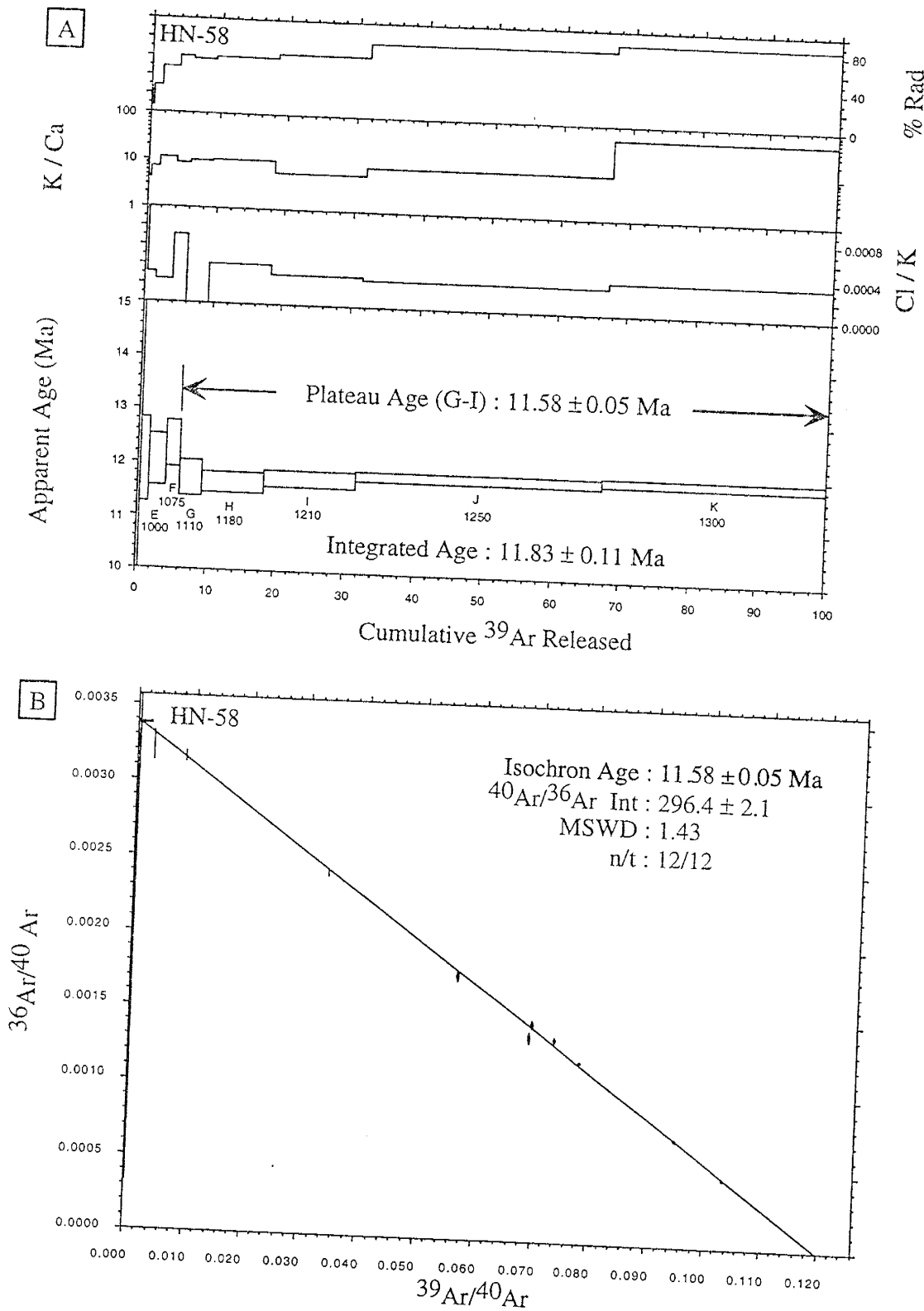


Figure 4.a. Example age spectrum plot of furnace step-heating data from biotite sample HN-58; Figure 4.b. Example isochron plot of furnace step-heating data from sample HN-58.

$[^{40}\text{Ar}/^{36}\text{Ar}]_{\text{atm}}=295.5$), and the apparent age of each temperature step (plotted versus the cumulative percent $^{39}\text{Ar}_K$ released). If the apparent ages of two or more contiguous steps were within two-sigma analytical error and comprised over fifty percent of the total $^{39}\text{Ar}_K$ gas released then a “plateau age” was calculated by weighting those increments by the inverse of variance squared. However, plateau ages can not accurately evaluate ages of mineral samples containing excess or inherited argon, i.e. where the $^{40}\text{Ar}/^{36}\text{Ar}$ intercept of the trapped argon is greater than 295.5 (McDougall and Harrison, 1988).

Inverse isochron plots (e.g. Fig. 4.b and Appendix 6.a and 6.c) depict the $^{39}\text{Ar}_K / ^{40}\text{Ar}$ versus $^{36}\text{Ar} / ^{40}\text{Ar}$ data for biotite and feldspar analyses, with the data points regressed according to York (1969). The inverse of the $^{39}\text{Ar}_K / ^{40}\text{Ar}$ intercept yields the apparent age for the sample and the inverse of the $^{36}\text{Ar} / ^{40}\text{Ar}$ intercept gives the composition of the non-radiogenic argon. A regressed line with a MSWD (Mean Square Weighted Deviation, a measure of a line’s goodness of fit) of 3 or lower was considered statistically acceptable. If the MSWD was not under 3, then heating steps or laser analyses were excluded and the isochron recalculated until the intercepts and errors stabilized (Deino and Potts, 1990).

The sanidine and plagioclase laser data were evaluated by probability distribution plots (e.g. Fig. 5 and 6; Appendix 6.b) versus relative probability for an apparent age. These plots also include auxiliary plots of

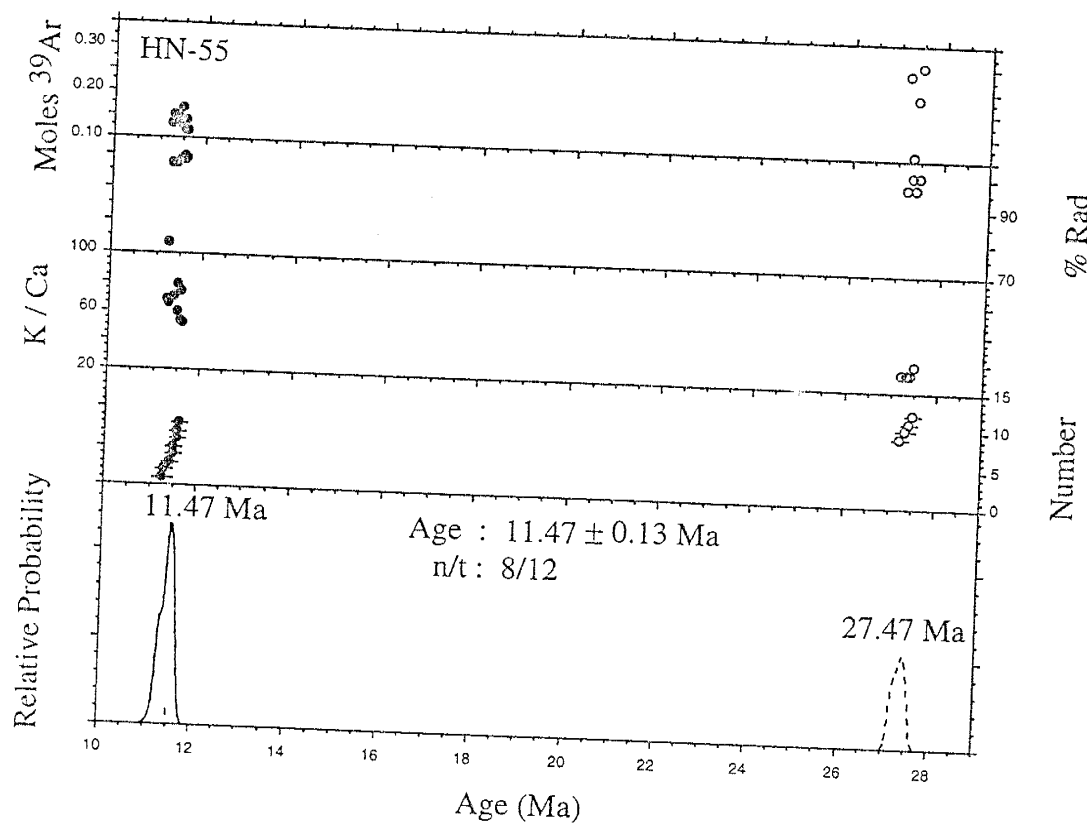


Figure 5. Example probability distribution plot of single crystal laser fusion data from sanidine sample HN-55; Analyses depicted by open circles were considered xenocrystic contaminants and were excluded from the age and error calculations.

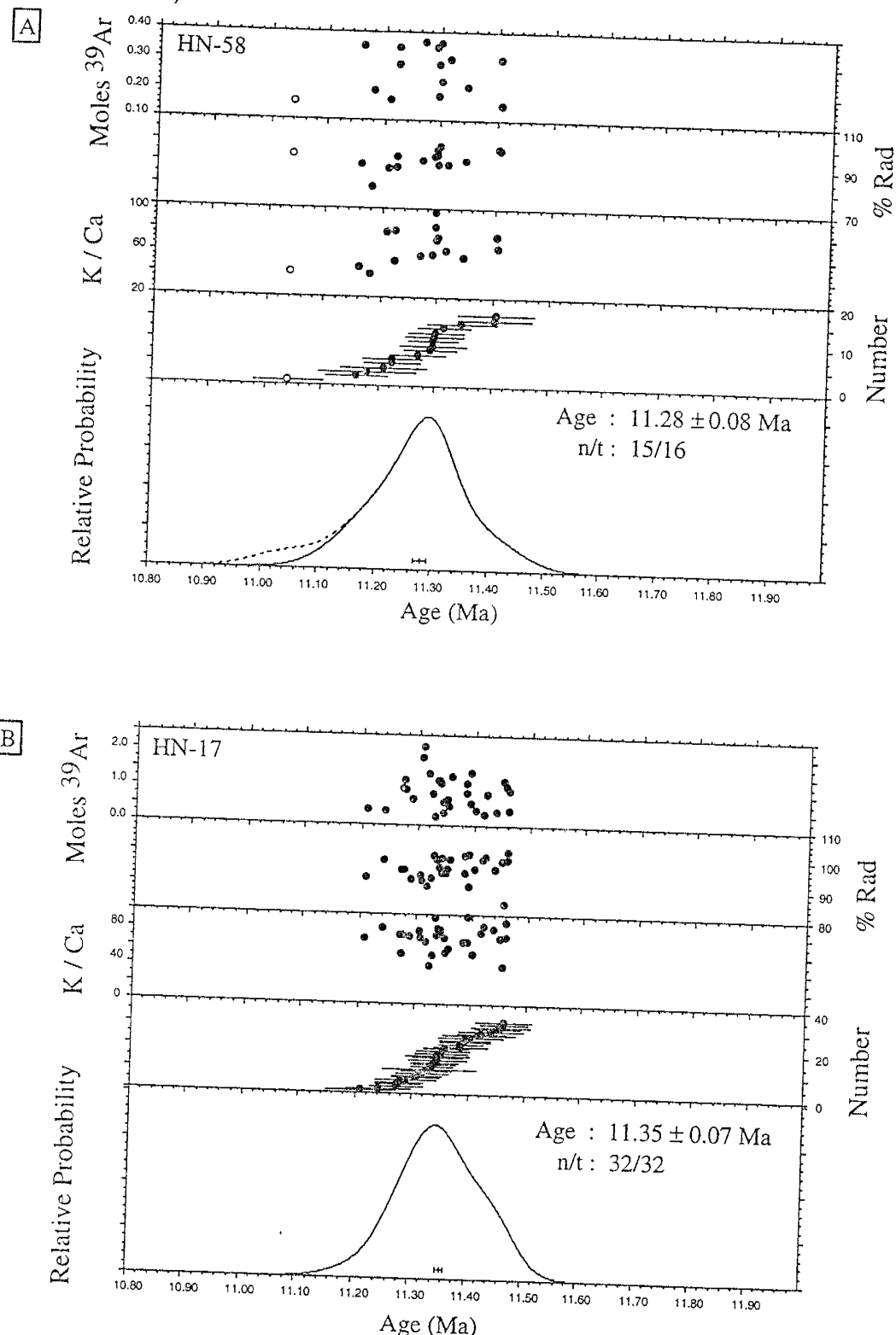


Figure 6.a. Examples of high precision age determinations: probability distribution plot of single crystal laser fusion data from sandine sample HN-58, collected at the south volcanic center of the lower rhyolite of Pound Ranch; Figure 6.b. probability distribution plot of sanidine sample HN-17, from the north center of the lower rhyolite of Pound Ranch

K/Ca (a function of $^{39}\text{Ar}_K / ^{37}\text{Ar}_{\text{Ca}}$), moles of $^{39}\text{Ar}_K$, and percent radiogenic yield. Laser analyses which fell outside of the primary Gaussian age distribution of the probability plot were excluded from age determinations and are depicted by open circles. A dashed line shows the plot before the exclusion of anomalous points. Analyses which comprised well defined Gaussian age probability distributions were averaged to produce each reported sample age. The error reported with the age includes analytical and J-factor errors and was calculated using the following equation:

$$\text{laser fusion error} = \text{sq rt} [(\text{avg analytical error})^2 + (0.25\% * \text{age})^2]$$

Mineral Ages

Commonly the various methods of evaluation produced more than one statistically acceptable age for an analyzed mineral sample. However, each mineral sample was assigned only one age, termed the mineral age (Table 1). Appendix 4 contains the summary information for each $^{40}\text{Ar}/^{39}\text{Ar}$ analysis and the full numeric and graphical data are presented in Appendix 5 and Appendix 6 respectively. The mineral ages were selected using the following criteria.

For biotite and plagioclase furnace step-heating analyses, ages calculated by inverse isochron plots were favored over plateau ages, if the MSWD was less than 3 and the $^{40}\text{Ar}/^{36}\text{Ar}$ intercept was less than 295.5.

TABLE 1. REPORTED MINERAL AGES

Sample	Map	San SXFit	er	Eva ^a	n/t#	Biot Avg**	er	Biot FSHfit	er	Eva ^b	n/t	MSWD	40/36 ± er	Biot LTS ^c	er	Biot LTS ^d	er	MSWD	40/36 ± er	Plag#	er	Type***	n/t	MSWD	40/36 ± er	
(ln-N)	Unit*	(Ma)	(is)	meth	(Ma)	(is)	meth	(Ma)	(is)	meth	(Ma)	(is)	meth	(Ma)	(is)	meth	(Ma)	(is)	(Ma)	(is)	meth					
4	Tsr ^e	7.02	± 0.05	id	9/9			9.20	± 0.30	n/pl	29															
7	Tsr ^e	7.06	± 0.03	id	8/9			8.66	± 0.14	n/pl	5/9															
25	Tsr ^e	7.45	± 0.08	id	9/9																					
24	Tsr ^e	7.52	± 0.09	id	20/20	8.37	± 0.05	8.47	± 0.04	is	11/11	2.31	3/4.5	± 3.0	8.26	± 0.06	is	20/20	2.99	312.7	± 1.4					
66	Tsr ^e	7.85	± 0.03	id	11/11			10.21	± 0.05	8.82	± 0.12	is	7/9	2.59	320.8	± 2.1										
1	Tsr ^e	8.66	± 0.05	id	6/8			11.69	± 0.14	10.91	± 0.03	n/pl	1/9				9.51	± 0.06	is	11/10	2.66	291.3	± 2.3			
2	Tsd ^f							11.82	± 0.18	n/pl	2/9					11.56	± 0.09	is	16/20	2.24	297.8	± 0.8				
3	Tsd ^f							10.56	± 0.11	10.36	± 0.08	is	11/12	1.90	309.7	± 0.7						9.76	± 0.25	SXF-is	6/9	1.28
12	Tsd ^f															10.76	± 0.14	is	20/20	0.87	309.9	± 0.7	SXF-is	8/10	2.71	
Round Ranch Center																										
20	Tpr ^g							12.43	± 0.14	12.34	± 0.05	is	8/11	1.63	311.4	± 2.8										
58	Tpr ^g	11.28	± 0.08	id	15/16	11.78	± 0.05	11.85	± 0.05	is	12/12	1.43	296.4	± 2.1												
17	Tpr ^g	11.35	± 0.07	id	32/33			12.06	± 0.09	12.06	± 0.06	is	8/9	2.06	307.4	± 2.1										
18	Tpr ^g															12.23	± 0.04	is	12/12	2.35	297.1	± 1.1				
16	Tsd ^g																									
Mardalena Peak Center																										
59	Tmr	13.00	± 0.10	id	10/16	13.38	± 0.06	13.46	± 0.06	pl	5/12					13.29	± 0.06	is	20/20	2.05	293.8	± 0.8				
46	Tmr	12.81	± 0.23	id	11/15	14.44	± 0.06	14.43	± 0.05	is	11/12	2.06	296.1	± 1.5												
45	Tmr	13.50	± 0.70	id	3/3	14.41	± 0.08	14.69	± 0.06	pl	4/12					14.45	± 0.06	is	18/20	2.19	300.9	± 1.4				
9	Tmd ^h							13.65	± 0.12	14.06	± 0.09	is	12/12	0.52	299.2	± 1.7										
33	Trm ⁱ							14.13	± 0.31	14.31	± 0.22	is	11/11	0.46	314.2	± 1.4										
32	Trm ⁱ							14.26	± 0.15	14.70	± 0.07	is	9/11	2.10	315.5	± 1.6										
29	Trm ⁱ															13.81	± 0.23	is	16/16	1.80	310.2	± 3.3				
31	Trm ⁱ																									
Saway Peak Center																										
38	Tsq ^j	11.44	± 0.05	id	6/12																					
55	Tsq ^j	11.47	± 0.08	id	8/12	12.02	± 0.12	11.99	± 0.09	pl	7/12					12.05	± 0.14	is	19/20	2.50	292.9	± 1.4				
37	Trs ^k	14.49	± 0.08	id	15/15	14.87	± 0.08	14.54	± 0.10	is	7/11	2.70	310.0	± 1.1												
41	Trs ^k	15.59	± 0.09	id	10/14	17.44	± 0.06	17.43	± 0.06	is	12/12	1.87	295.3	± 2.7												
43	Tid ^l							17.94	± 0.09	pl	5/12					17.44	± 0.06	is	17/20	2.77	299.6	± 1.4				
39	Tid ^l	18.45	± 0.27	id	11/11																					

^aSee unit key of Figures 2 and 3^b Sandine analysis by Single Crystal Laser Fusion
Graphical method of age evaluation
id: ideogram
is: isochron^c pl: plateau^d n/pl: near plateau^e Biotite analysis by Furnace Step-Heating^f Biotite analysis by Laser Two-Step heating^g Analysis of plagioclase^h Type of heating and method of evaluationⁱ Apparent Emplacement Age of Sample^j Preferred Age of Biotite

When the isochron results did not meet those parameters, the plateau age was reported as the mineral age. In the case of an analyses that produced no acceptable plateau or isochron ages, a "near plateau" age was reported if the step-heating spectrum nearly met plateau criteria (e.g. the age data results in a three-step plateau, but comprises only 48% of the total ^{39}Ar released). All mineral ages reported for biotite two-step laser heating were determined using isochron analysis.

Sanidine and plagioclase laser analyses were assessed by both probability distribution and isochron plots. However, all reported sanidine mineral ages were determined using probability distribution analyses. Typically the sanidine analyses had high radiogenic yields (95-99% $^{40}\text{Ar}^*$), which produces tight clusters near the $^{39}\text{Ar}_\text{K}/^{40}\text{Ar}$ axis of isochron plots and does not allow accurate estimates of the $^{40}\text{Ar}/^{36}\text{Ar}$ intercept. For plagioclase analyses, isochron plots were favored due to low radiogenic yields (3-30% $^{40}\text{Ar}^*$) and excess argon ($[^{40}\text{Ar}/^{36}\text{Ar}]$ intercept > 295.5) in the mineral samples.

Selected biotite samples were analyzed by both laser and furnace heating methods. For most of these samples, a preferred mineral age was determined by averaging the two biotite mineral ages (Table 1). However, for two biotite samples, HN-2 and 3, the mineral ages of the laser analyses were preferred over the "near plateau" ages of the furnace analyses.

In addition to the selection of ages for the analyzed minerals, apparent eruption ages were selected for each rock sample (Table 2). When possible, sanidine mineral ages were taken as the apparent age of eruption. However, biotite mineral ages were selected if no sanidine was present. The determinations of apparent eruption ages are explained further in the discussion section.

$^{40}\text{Ar}/^{39}\text{Ar}$ RESULTS

Thirty rock samples were analyzed for this study (Appendix 4), and at least one mineral age is reported for twenty-eight of those samples (Table 1). Twenty of the rock samples have two or more mineral ages. This section compares the mineral ages, and examines the precision and reliability of the results.

A quantitative assessment of the precision and resolution of the $^{40}\text{Ar}/^{39}\text{Ar}$ results must consider many levels of error. Fundamentally, the determination of an accurate age depends upon the structure of the mineral grain and the unique post-crystallization history of a mineral sample. Additionally, the processing of the sample during irradiation and analysis contributes to age uncertainties.

TABLE 2. APPARENT ERUPTION AGE OF SAMPLES AND UNITS

Sample (HN-)	Sample location	Informal Unit* Name	Map* unit	Best age (Ma)	error (ls)	Mineral dated	Lat/Long N/W
<u>Socorro Peak centers</u>							
4	Tripod Pk	rhyolite of Tripod Pk	Tsr ^d	7.02	± 0.05	san	34.06/106.98
7	6633 Pk	rhyolite of Tripod Pk	Tsr ^d	7.06	± 0.03	san	34.05/106.99
		rhyolite of Tripod Pk	Tsr ^d	7.04	± 0.04		
25	Jejenes Hill	rhyolite of Jejenes Hill	Tsr ^d	7.45	± 0.08	san	34.07/107.01
24	5k-Range	rhyolite of Jejenes Hill	Tsr ^d	7.52	± 0.09	san	34.06/107.00
		rhyolite of Jejenes Hill	Tsr ^d	7.49	± 0.09		
66	Grefco MIne	rhyolite of Grefco Mine	Tsr ^d	7.85	± 0.03	san	34.03/106.94
1	Signal Flag	rhyolite of Signal Flag	Tsr ^d	8.66	± 0.05	san	34.04/106.95
2	Radar Pk	upper dacite of Radar Pk	Tsd ^d	9.51	± 0.06	biot	34.08/106.97
3	SW Socorro Pk	lower dacite of Radar Pk	Tsd ^d	11.56	± 0.09	biot	34.07/106.97
12	Strawberry Pk	dacite of Stawberry Peak	Tsd	10.56	± 0.11	biot	34.10/107.99
<u>Pound Ranch centers</u>							
20	Pound Ranch	upper rhyolite of Pound Ranch	Tpr ^d	12.43	± 0.14	biot	33.99/107.04
18	North Center	lower rhyolite of Pound Ranch	Tpr ^d	12.06	± 0.09	biot	33.99/107.04
58	South Center	lower rhyolite of Pound Ranch	Tpr ^d	11.28	± 0.08	san	33.98/107.04
17	North Center	lower rhyolite of Pound Ranch	Tpr ^d	11.35	± 0.07	san	33.99/107.04
		lower rhyolite of Pound Ranch	Avg Tpr ^d	11.32	± 0.07		
16	Tower Mine	dacite of Tower Mine	Tsd	12.23	± 0.04	biot	33.99/107.00
<u>Magdalena Peak centers</u>							
59	Magdalena Pk	rhyolitic flow of Magdalena Peak	Tmr	13.00	± 0.10	san	34.08/107.24
46	Elephant Mnt	rhyolitic flow of Magdalena Peak	Tmr	12.81	± 0.23	san	34.07/107.23
45	S Magdalena Pk	rhyolitic flow of Magdalena Peak	Tmr	13.50	± 0.70	san	34.07/107.24
		rhyolitic flow of Magdalena Peak	Avg Tmr	13.10	± 0.34		
9	SW Magdalena Pk	dacitic flow of Magdalena Peak	Tmd	13.65	± 0.12	biot	34.07/107.25
33	Agua Frio	rhyolite of Agua Frio Canyon	Trm ^d	13.13	± 0.06	plag	34.05/107.24
32	Agua Frio	rhyolite of Agua Frio Canyon	Trm ^d	14.13	± 0.31	biot	34.05/107.24
		rhyolite of Agua Frio Canyon	Avg Trm ^d	13.63	± 0.19		
29	Stendel	rhyolite of the Stendel Perlite dep.	Trm ^d	13.23	± 0.04	plag	34.04/107.23
31	Stendel	rhyolite of the Stendel Perlite dep.	Trm ^d	14.26	± 0.15	biot	34.05/107.23
		rhyolite of the Stendel Perlite dep.	Avg Trm ^d	13.75	± 0.10		
<u>Squaw Peak centers</u>							
38	B.O. Dome	rhyolite of Squaw Peak	Tsqr	11.44	± 0.05	san	33.91/107.30
55	Squaw Pk	rhyolite of Squaw Peak	Tsqr	11.47	± 0.08	san	33.94/107.28
		rhyolite of Squaw Peak	Avg Tsqr	11.45	± 0.06		
37	Alameda Springs	rhyolite of Alameda Springs	Tras	14.49	± 0.08	san	33.93/107.30
41	Muleshoe Ranch	rhyolite of Muleshoe Ranch	Trms	15.59	± 0.09	san	34.00/107.22
43	Mill Place	dacite of Mill Place	Tid	17.94	± 0.09	biot	33.96/107.24
39	Smooth Hill	rhyolite of McDaniel Tank	Tm	18.45	± 0.27	san	33.96/107.28

*See unit keys of Figures 2 &3
Apparent Eruption Age of Unit

Analytical Errors

All $^{40}\text{Ar}/^{39}\text{Ar}$ age analyses are inherently limited by the uncertainty in the age assigned to the radiation flux monitor, which are typically computed using a set of conventional K/Ar age determinations with uncertainties approximately equal to 0.5-1.0% of the monitor age (Samson and Alexander, 1987). The error of the K/Ar monitor age uniformly impacts all mineral analyses of this study and is not computed into the reported error of mineral ages. The extremely homogenous crystals of the Fish Canyon Tuff (FCT-1) sanidine used to monitor the irradiation flux gradient, also provides a measure of analytical uncertainties inherent to the extraction system. The laser analyses of the FCT-1 sanidine samples are reproducible within $\pm 0.25\%$. The J-factors for unknown mineral samples are determined from adjacent FCT-1 aliquots. The reported errors of the mineral ages include the uncertainty of the J-factor.

The largest sources of error for individual ages are uncertainties on the ^{36}Ar measurement and in the J-factor (McIntosh et al., 1990). The reported errors of the sanidine and biotite analyses (Table 1) for this study are within the same order of magnitude. The sanidine errors (1σ) are typically less than $\pm 1\%$ of the age and ranged from 0.4% to 1.8% (Table 1), thus displaying the high crystal to crystal precision (e.g. Fig. 6). One sample, HN-45, has an exceptionally large error of 5.2%, but this determination is based on the analysis of only three crystals and reflects the

scatter of the individual age determinations. The analytical uncertainties of the biotites are somewhat larger, generally ranging from 0.3% to 3.2% of the age (Table 1). However, they still exhibit high step to step and crystal to crystal precision.

The analytical errors of the plagioclase and hornblende separates are larger than most of the sanidine and biotite errors. Two plagioclase samples have single-crystal laser results with errors of 5.4% and 2.6% of the age (Table 1). Five plagioclase samples were analyzed by furnace step-heating, and the four reported mineral ages have low analytical errors from 0.4% to 1.7% (Table 1). The two hornblende samples analyzed by the furnace display very poor step to step precision. Early heating steps of sample HN-5 recorded old ages up to 230 Ma, before dropping to 11 Ma at higher temperatures. Anomalously old ages are also seen in sample HN-6 (Fig. 7), which peaked at 50 Ma, before dropping to an apparent age of 13 Ma. None of the hornblende data met the plateau or isochron age criteria, therefore, no ages are reported.

Mineral to Mineral Comparisons

All phenocrysts within the rhyolitic and dacitic domes sampled in this study effectively cooled simultaneously, therefore all minerals from the same rock sample should have recorded the same eruption age (McDougall and Harrison, 1988). Based upon this principle, mineral to mineral

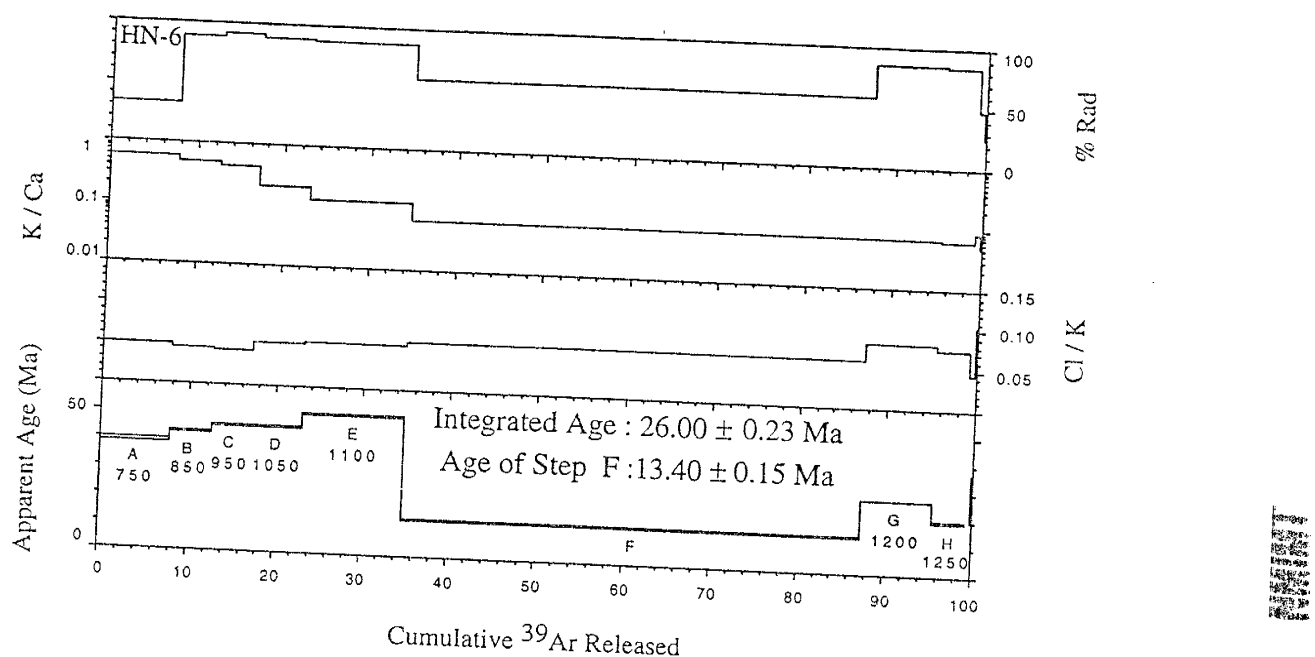


Figure 7. Age spectrum plot of furnace step-heating data from hornblende sample, HN-6

comparisons are invaluable for assessing the accuracy and precision of the different methods and types of minerals dated.

Sixteen biotite samples were analyzed by both furnace step-heating and two-step laser fusion methods. The mineral ages of nine of the biotite sample pairs agree within two sigma analytical error (Table 1). Figure 8 compares the mean ages of furnace and laser biotite analyses. Sample pairs, agreeing within two sigma error, intersect the "ideal line" that bisects the graph. Lines representing 5 and 10% of the mineral age are also included to illustrate any age discordance between the two methods. The age of the biotite furnace analyses tend to be older than the laser samples, which is represented by the ten mean biotite ages significantly below the ideal line of Figure 8. However, there are no clear differences in precision between the two methods. Possible explanations for the biotite age discrepancies are explored in the discussion section.

Twelve analyzed rock samples produced acceptable mineral ages from both sanidine and biotite phenocrysts. Two types of mineral pairs are plotted on Figure 9, one is the mean of a sanidine mineral age and a biotite furnace step heating mineral age, and the second type is the mean age of a sanidine and a biotite two-step laser-fusion pair. Three of the eleven biotite mineral ages determined by furnace step heating agree within two sigma error to the mineral age determined on the sanidine, and three of the nine ages of biotite samples analyzed by two step-laser fusion agree

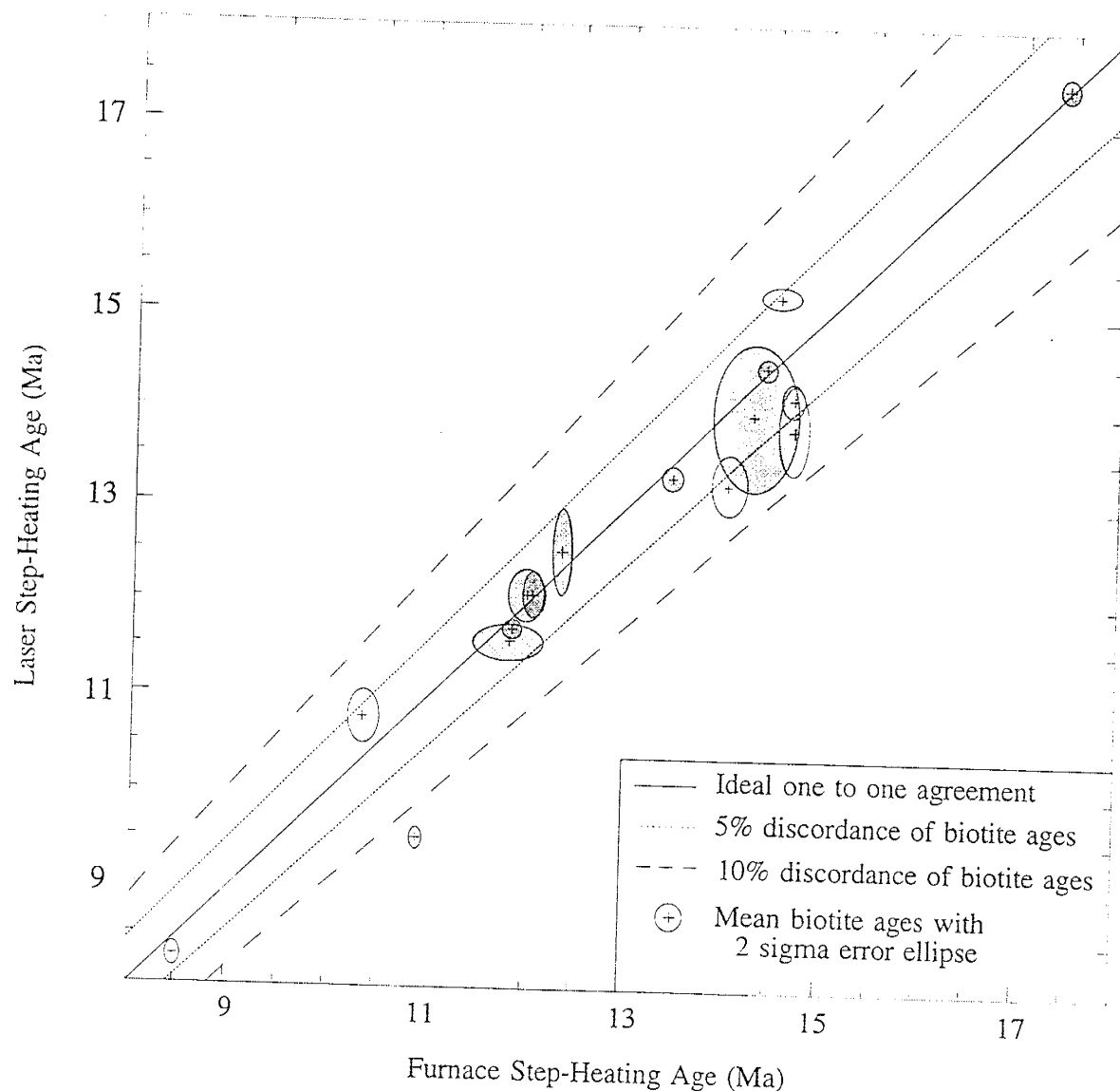


Figure 8. Plot of furnace step-heating ages versus laser step-heating analyses of biotite samples, see Table 1 for values;
Shaded ellipses are within 2 sigma error of ideal line

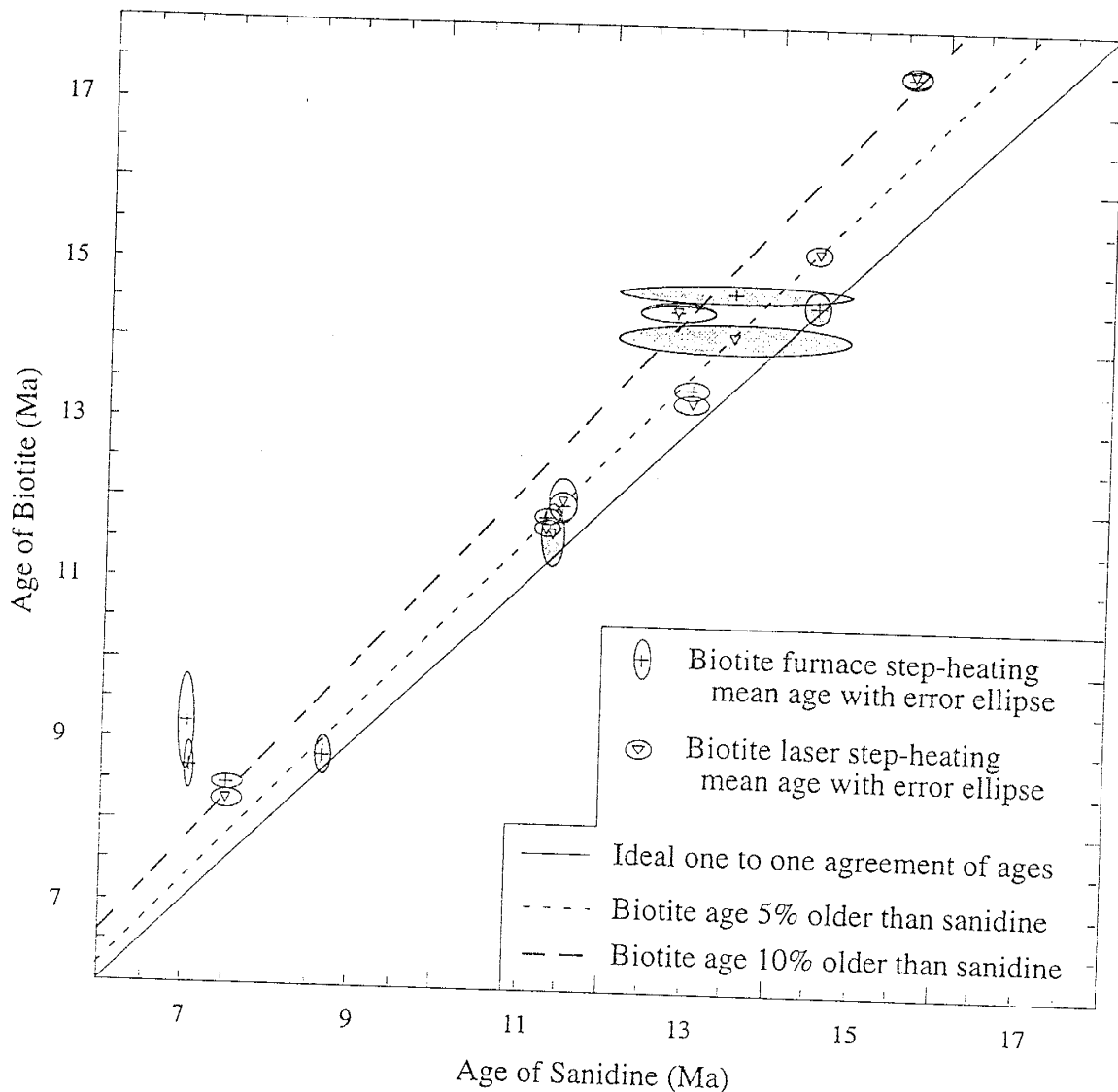


Figure 9. Sanidine ages plotted against biotite ages (furnace and laser) for minerals separated from the same sample, see Table 1 for values; Greyed ellipses are within 2 sigma error of ideal line.

with the age of the corresponding sanidine analysis. Overall, out of the twelve rock samples with sanidine and biotite mineral pairs, four have a biotite analysis within two sigma error of the sanidine mineral age and only one rock sample has both the laser and furnace biotite analysis within error of the sanidine. As Figure 9 clearly illustrates, all of the mean ages of the biotites are older than equivalent sanidine analysis. Possible causes of the poor within sample agreement between sanidine and biotite analyses are evaluated in the discussion section.

Unit Ages

The $^{40}\text{Ar}/^{39}\text{Ar}$ ages are further assessed by comparing mineral ages within stratigraphic units. Apparent age discrepancies of samples from the same map units suggests either errors in the age analyses or incorrect stratigraphic assignment of the flows. Table 1 lists the mineral ages and the apparent eruption age of each sample and Table 2 lists the apparent eruption ages of the units. The justifications for preferring sanidine mineral ages over other minerals follows in the discussion section.

The precise mineral ages for sanidine samples greatly improved the resolution of the stratigraphy of eruptive units. The maps of Chamberlin (1980) and Bobrow et al. (1983) subdivided the flows of the Socorro Peak Rhyolite into four units (Fig. 3). However, the precise sanidine ages of this study allows for the revaluation of these flow units. Ages from the

rhyolitic flows of Socorro Peak Rhyolite allow four separate eruptive units to be distinguished, Tripod Peak (two sanidine mineral ages), Jejenes Hill (two sanidine mineral ages), Grefco Mine, and Signal Flag Hill. The precision of sanidine mineral ages also definitively linked spatially distinct domes, which were correctly mapped together, such as the lower rhyolite of Pound Ranch (Fig. 6.a and 6.b; Fig. 3) and the rhyolite of Squaw Peak (Fig. 2).

Ages of multiple mineral samples within an eruptive unit allowed for the identification of inaccurate apparent ages, as well. The biotite mineral age of sample HN-18 from the lower rhyolite of Pound Ranch is stratigraphically discordant when compared to sanidine mineral ages, therefore it was not included in the calculation of the flow's apparent eruption age (Table 2). The three rock samples from the rhyolitic flows of the Magdalena Peak Rhyolite have six mineral ages, which range from 13.0 to 14.4 Ma (Fig. 2; Table 1). Three of these ages are sanidines analyses and agree within two sigma error (Table 2). However due to the poor age precision of samples HN-45 (13.50 ± 0.70 Ma) and HN-46 (12.81 ± 0.23 Ma), the flow was assigned an apparent eruption age based only on sample HN-59 (13.00 ± 0.10 Ma), the most precise age which was collected from a sample nearest to the apparent vent on Magdalena Peak. The two ages of rhyolitic flows to the south near Agua Frio Canyon are based on a biotite and plagioclase analyses from samples HN-32 (14.13 ± 0.31 Ma) and

HN-33 (13.13 ± 0.06 Ma), respectively. The plagioclase analysis has a high individual precision. However, when the two mineral ages are considered together, the result is a relatively imprecise age for the rhyolitic flow of Agua Frio Canyon. The apparent eruption age of the rhyolite of the Stendel Perlite deposit resulted from similar imprecision of plagioclase and biotite mineral ages.

The apparent eruption ages and error of each unit or clearly independent flow (Table 2) were plotted on a probability distribution plot (Fig. 10). To limit possible sampling bias and allow the ideogram to highlight age distribution trends, every mineral age was not included. The apparent eruption ages range from 18.5 to 7.0 Ma with only minor gaps in recorded volcanism. The four volcanic centers show a peak in activity between 14.5 and 11.3 Ma. An additional plot, Figure 11, highlights the peak in volcanism with apparent eruption ages versus distance from the modern rift axis, approximated by the Rio Grande river. Figure 11 also illustrates a broad age trend of younger apparent eruptive ages closer to the rift axis. The Squaw Peak centers, approximately 40 km from the rift axis, have the oldest ages, while the youngest samples are from the Socorro Peak centers only 8 km from the rift axis. However, within the four volcanic centers, the east-west trend does not apply to individual mineral ages.

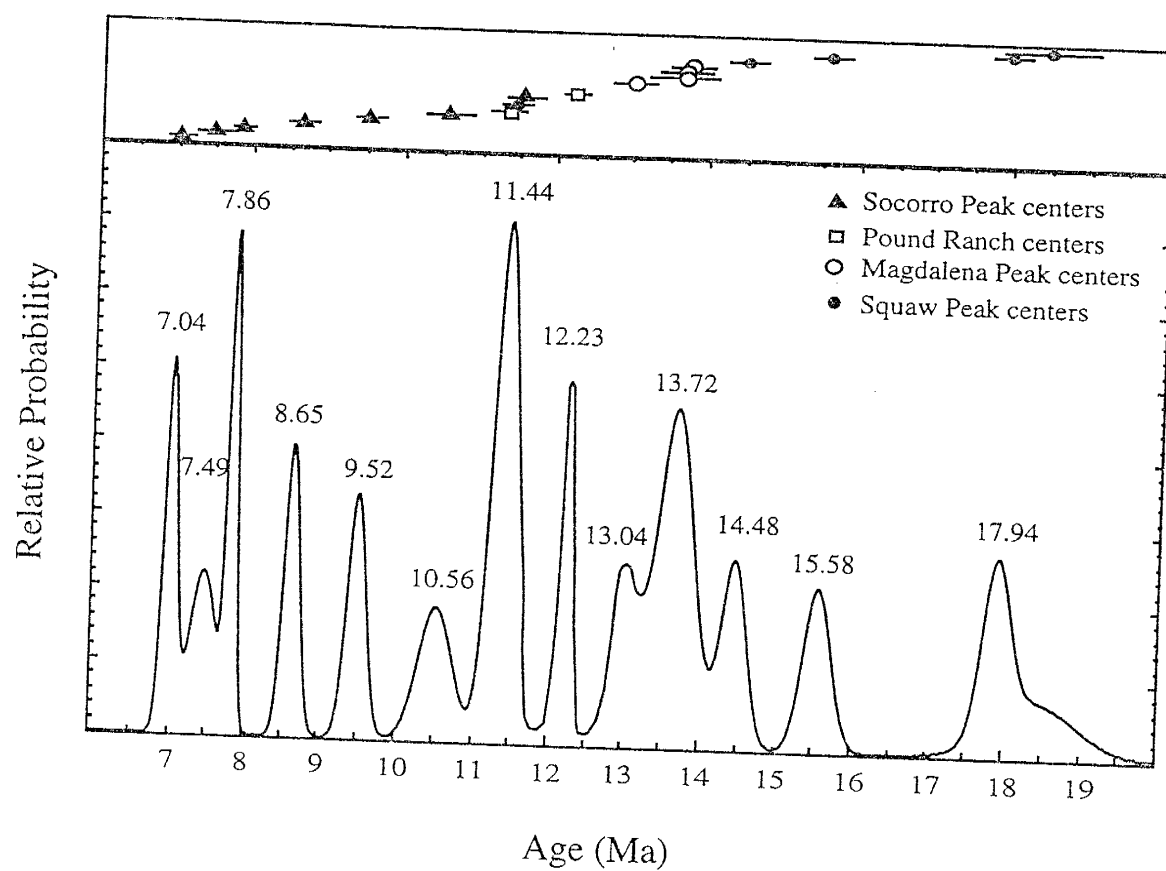


Figure 10. Relative probability distribution of apparent eruption ages (Table 2) for the Miocene silicic centers of the Socorro-Magdalena area. Peaks of volcanism are labeled in millions of years.

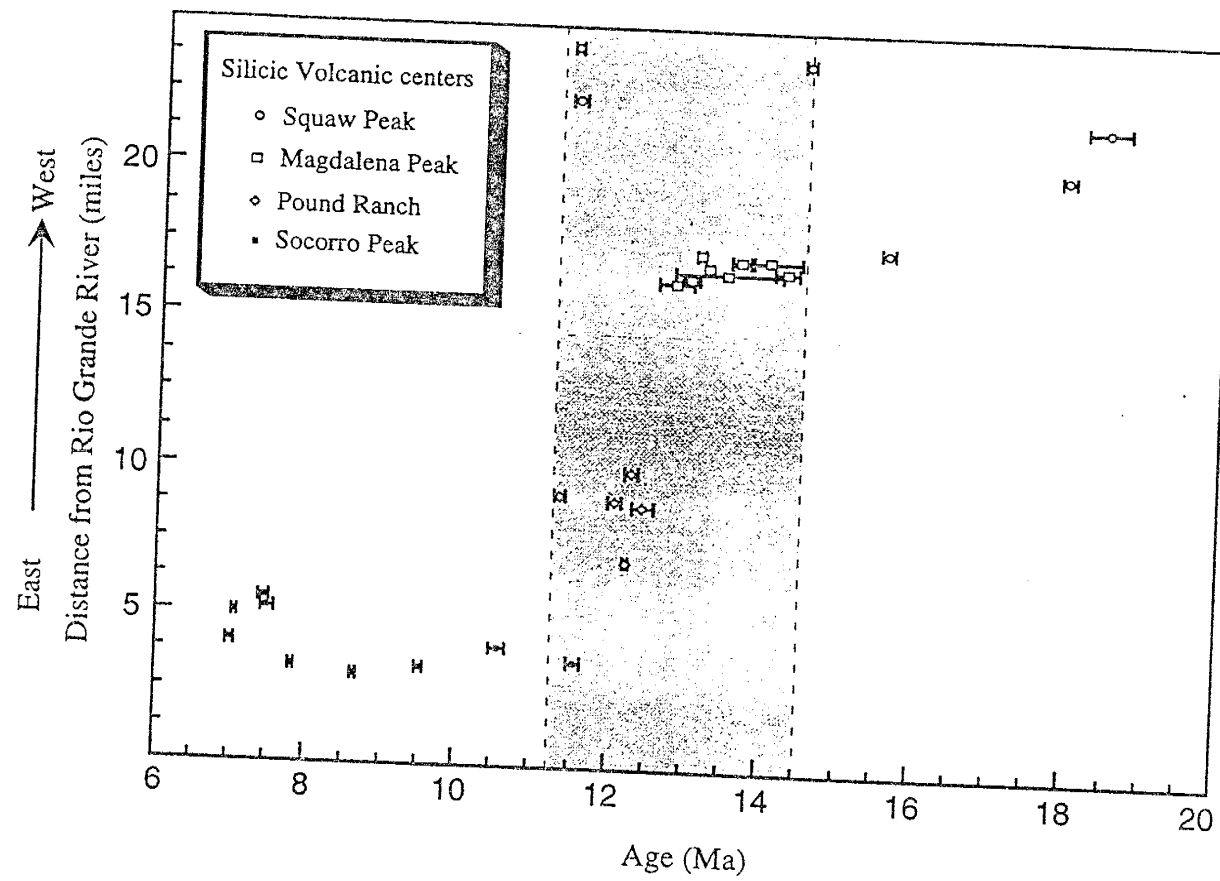


Figure 11. Plot of the sample ages (Table 1) against distance from the Rio Grande river, approximating the intersection of the modern day rift axis and the Socorro accommodation zone. The grey area represents an apparent pulse of volcanism from 14.5 to 11.3 Ma.

DISCUSSION OF MINERAL AGES

Sanidine phenocrysts analyzed by single-crystal laser fusion produced the most reliable ages of the silicic volcanic rocks from the Socorro-Magdalena area. Nearly all of the biotite analyses met the statistical guidelines of an acceptable age. However, the tendency of ages for all biotite samples to be older than the associated sanidine requires that the reliability all of biotite ages to be questioned. For this study the low-K minerals plagioclase and hornblende did not provide accurate ages.

Sanidine Ages

Sanidine, a K-rich, Ar-retentive, anhydrous mineral, has provided highly accurate and precise ages when used with the $^{40}\text{Ar}/^{39}\text{Ar}$ dating method (e.g. McIntosh et al., 1992; Spell and Harrison, 1993), assuming no thermal disruption of the sanidine after eruption. The mineral structure of sanidine does not allow for the complete extraction of argon which resulted in chronic problems for conventional K-Ar dating of sanidines (McDowell, 1983; Turrin et al., 1994). The $^{40}\text{Ar}/^{39}\text{Ar}$ method simultaneously measures the ratio of radiogenic $^{40}\text{Ar}^*$ and ^{40}K , as reactor produced ^{39}Ar , and does not require the extraction of all the $^{40}\text{Ar}^*$.

The total laser fusion of sanidine crystals is a quick and accurate method for obtaining $^{40}\text{Ar}/^{39}\text{Ar}$ ages. The laser fusion method allows for the identification of xenocrystic contamination and altered crystals. Xenocrystic sanidines, if not equilibrated during eruption, will plot older

than primary crystals on ideogram probability diagrams and may be recognized on isochron plots due to variations in isotopic composition (Bogaard, 1995). Altered crystals of sanidine may have older or younger apparent ages than pristine samples, and ideally, should be readily identifiable as outliers based on lower radiogenic yields or discordant K/Ca ratios (Spell and Harrison, 1993).

For this study, the typical sanidine analysis recorded high yields of $^{40}\text{Ar}^*$ of 95-99%, an average K/Ca ratio of approximately 80, and reproducible, high-precision ages (e.g. Fig. 6; Appendix 5.a). In only a few sanidine samples, xenocryst were identified by their significantly older age and eliminated from age calculations. (e.g. Fig 5).

The scatter of the sanidine analyses for samples HN-38, 39, 45, 46, 55, and 59 was much larger than the typical range of sanidine apparent ages (Table 1; Appendix 5.a and 6.a). The radiogenic yields for these analyses were high, and isochron plots of the data showed no evidence of excess argon (e.g. Fig 12). However, the K/Ca ratios were considerably lower (53 to 65) than the typical values of the study (≈ 80). Also, the less precise sanidine analyses recorded about 0.1×10^{-14} moles of ^{39}Ar released per crystal, compared to 0.4×10^{-14} moles produced by a typical sanidine. Alteration of the crystals may have resulted in K loss and produced the low K/Ca ratios of these samples. However, examination under a binocular microscope alteration did not reveal alteration in the samples. The

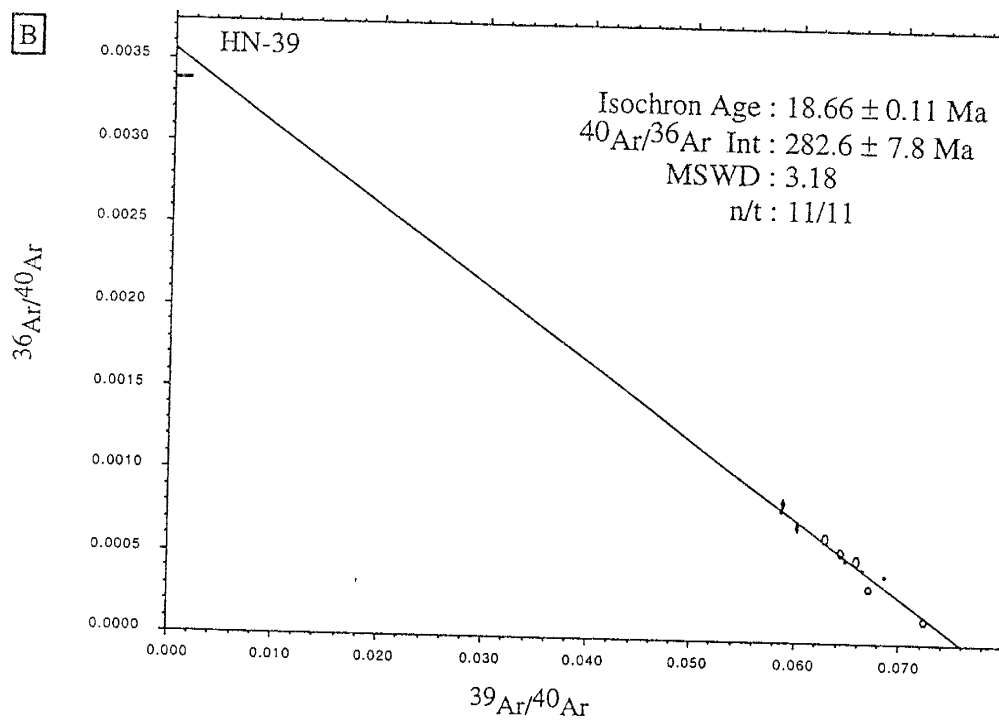
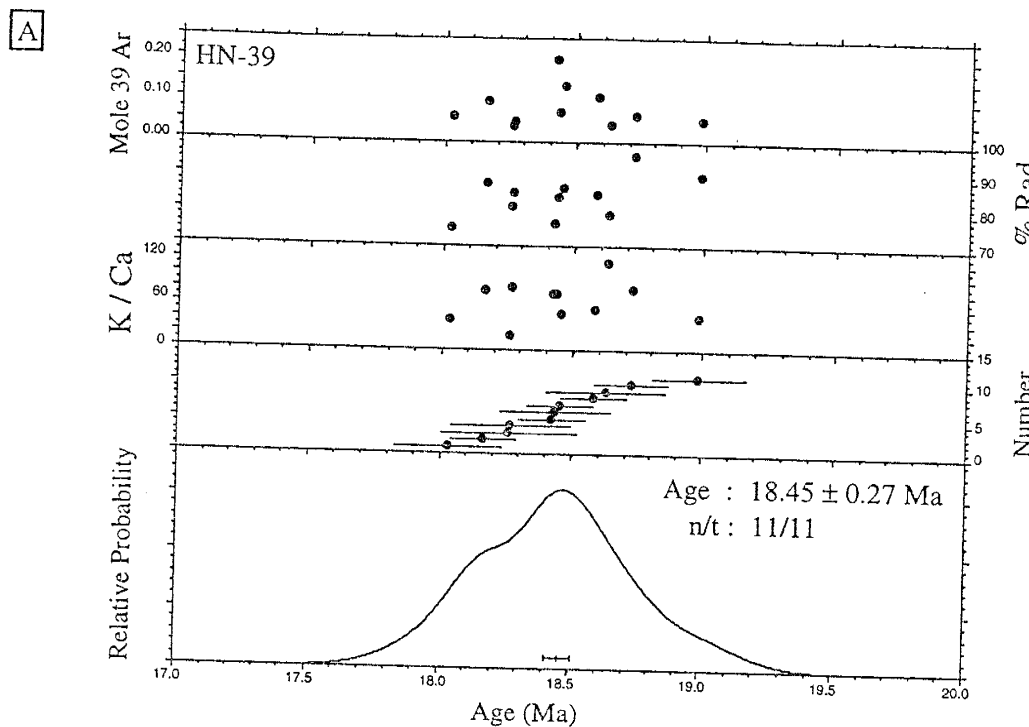


Figure 12.a. Probability distribution plot of single crystal laser fusion data from sandine sample HN-39; Figure 12.b. Isochron diagram of sanidine sample HN-39

phenocryst size did tend to be smaller than average for these sanidines, due in part to the limited number of sanidine minerals present in the rock samples. The small crystal size is reflected in the low amount of ^{39}Ar released and the reduced precision of individual measurements. Both small crystal size and a limited number of measurements resulted in the large uncertainty of sample HN-45 (Table 1), which is based on the analysis of three small sanidine crystals that released approximately 0.04×10^{-14} moles ^{39}Ar each. Despite the six cases of relatively imprecise sanidine mineral ages, none of the sanidine mineral ages contradicted stratigraphic order, therefore all were taken as the apparent eruption age for the rock sample.

Biotite Age Interpretations

Volcanic biotite can produce precise and reliable K-Ar and ^{40}Ar - ^{39}Ar dates when unaffected by post-crystallization heating, alteration, or weathering (Lanphere, 1988). However, the K-Ar method can not detect the presence of excess argon or show evidence of argon loss. In contrast, the $^{40}\text{Ar}/^{39}\text{Ar}$ dating method analyses can identify, and in some cases correct, complexities in the argon systematics.

Typically, an anomalous biotite mineral age results from the combined complications of natural and analytical sources. A volcanic biotite may have natural inhomogeneities introduced by unequilibrated fluid inclusions, xenocrysts, or secondary alteration. An inhomogeneous

biotite will not behave in the same manner as a pristine biotites during irradiation and in vacuo step-heating (McDougall and Harrison, 1988). A general discussion follows, reviewing some of the possible sources of error in the $^{40}\text{Ar}/^{39}\text{Ar}$ age analysis of biotites, and then a discussion concerning the biotites of this study concludes the section.

During in vacuo furnace-step heating, a biotite may lose argon from any point within the grain because the degassing behavior results in the rapid loss of hydrous volatiles and contraction along the cleavage planes (Gaber et al., 1988). Therefore, any interpretation of a discordant or even plateau spectrum of a biotite can not be modeled on the simple diffusive loss of argon . However, useful information still may be gained from biotite step-heating data, provided the possible homogenizing effect of in vacuo heating is recognized (McDougall and Harrison, 1988).

Complex $^{40}\text{Ar}/^{39}\text{Ar}$ release patterns have been observed in apparently pure biotite separates. Hess et al. (1987) studied optically pure biotites and found extensive chlorite inter-growths between the biotite sheets using a transmission electron microscope (TEM) and estimated that 1% of the biotite was secondary chlorite. Hess et al. (1987) recommended that biotite separates with K contents below the stoichiometric K concentration of low-Mg biotites (<8% K) be considered a multiphase systems and stated that the geological significance of $^{40}\text{Ar}/^{39}\text{Ar}$ spectra from low-K biotites must be suspect.

The effect of chloritization upon the release spectra depends on the degree of alteration. Lo (1989) recorded the outgassing of biotite's chlorite phases and reasoned that the effects of minor chloritization should only be seen in the early steps of an age spectrum. However, as the amount of chlorite contamination in biotites increased, the spectra became more disturbed throughout the heating process with increased scatter and $^{40}\text{Ar}/^{36}\text{Ar}$ intercept values greater than 295.5.

Lo (1989) proposed that recoil caused the escalating age spectra discordance in the chloritized biotites. Recoil occurs during sample irradiation when a proton is emitted from the ^{39}K nucleus to produce $^{39}\text{Ar}_\text{K}$, and the released proton may "recoil" the newly formed argon isotope out of the original potassium site. Turner and Cadogan (1974) calculated that recoil can deplete argon from a grain boundary to a mean depth of 0.08 μm . As a consequence of recoil, $^{39}\text{Ar}_\text{K}$ can be redistributed within a grain, ejected into proximal grains, or lost completely. When a biotite sample has intimately intergrown chlorite, the chlorite phase can gain significant $^{39}\text{Ar}_\text{K}$ through recoil. The redistribution of argon into the chlorite phases will produce a disturbed biotite spectrum. The K-poor chlorite will release $^{39}\text{Ar}_\text{K}$ gained from recoil early in the heating steps and reduce the amount of $^{39}\text{Ar}_\text{K}$ released in the later K-rich biotite steps, resulting in increased $^{40}\text{Ar}^*/^{39}\text{Ar}_\text{K}$ ratios and a higher apparent age

during the biotite release steps (Hess et al., 1987). The integrated age of a biotite can also be increased if diffusive loss of $^{39}\text{Ar}_\text{K}$ in the chlorite layers occurs due to elevated temperature during irradiation and/or bakeout in the extraction line (Spell and Harrison, 1993).

In addition to problems with recoil and chloritization, xenocrysts and fluid inclusions contribute extraneous argon in some biotites (McDougall and Harrison, 1988). Variably equilibrated xenocrysts can increase the apparent age of furnace step-heated biotites, and the source would be difficult to detect. However, Spell and Harrison (1993) determined that significant xenocystic biotite contamination in rhyolitic rocks would be unlikely due to the short time required for a biotite to equilibrate within the magma chamber or even within a flow after eruption. Additionally, excess argon can be gained through magmatic fluids incorporated or trapped in the biotites after crystallization and not equilibrated to atmospheric compositions upon eruption (Renne, 1995).

The Ar isotope analysis of biotites from the Socorro-Magdalena area provides a great deal of information needed to assess the samples. The data allow for the evaluation of apparent eruption age, trapped component, approximate %K content, and K/Ca and Cl/K ratios. Consideration of the many aspects of the biotite data provide insights into the cause of the anomalous ages.

Isochron plots indicate that the 22 biotites analyzed had somewhat elevated levels of trapped argon, typically, with $^{40}\text{Ar}/^{36}\text{Ar}$ intercepts of 298 to 310 (e.g. Fig. 4; Table 1; Appendix 4). As stated earlier, the age of all biotite furnace step-heating samples that produced $^{40}\text{Ar}/^{36}\text{Ar}$ ratios greater than 295.5 were evaluated by isochron plots, and all mineral ages of the laser step-heating analyses were produced from isochron evaluation (Table 1). The isochron plots should exclude the influence of excess argon upon the age, since the trapped argon component is not assumed to be atmospheric, unlike a step-heating age spectrum. However, the biotite isochron analyses did not eliminate the age discrepancies with the sanidine mineral ages.

Early in the study, the furnace step-heating analysis of biotites (e.g. sample HN-2, Fig. 13.a) produced complex and discordant age spectra. Therefore, single-crystal laser analysis of biotites was used to investigate possible xenocrystic contamination and excess argon. Individual biotites were heated in two-steps (e.g. Fig. 13.b) in an attempt to separate the radiogenic and excess argon components that might be homogenized in bulk step-heating or total laser fusion. The results did not show xenocrystic contamination by of older biotite flakes. The laser analyses excluded from the age determinations typically had large analytical errors and high trapped argon components (Appendix 5.c). Therefore, undetected variations of secondary alteration or trapped components within

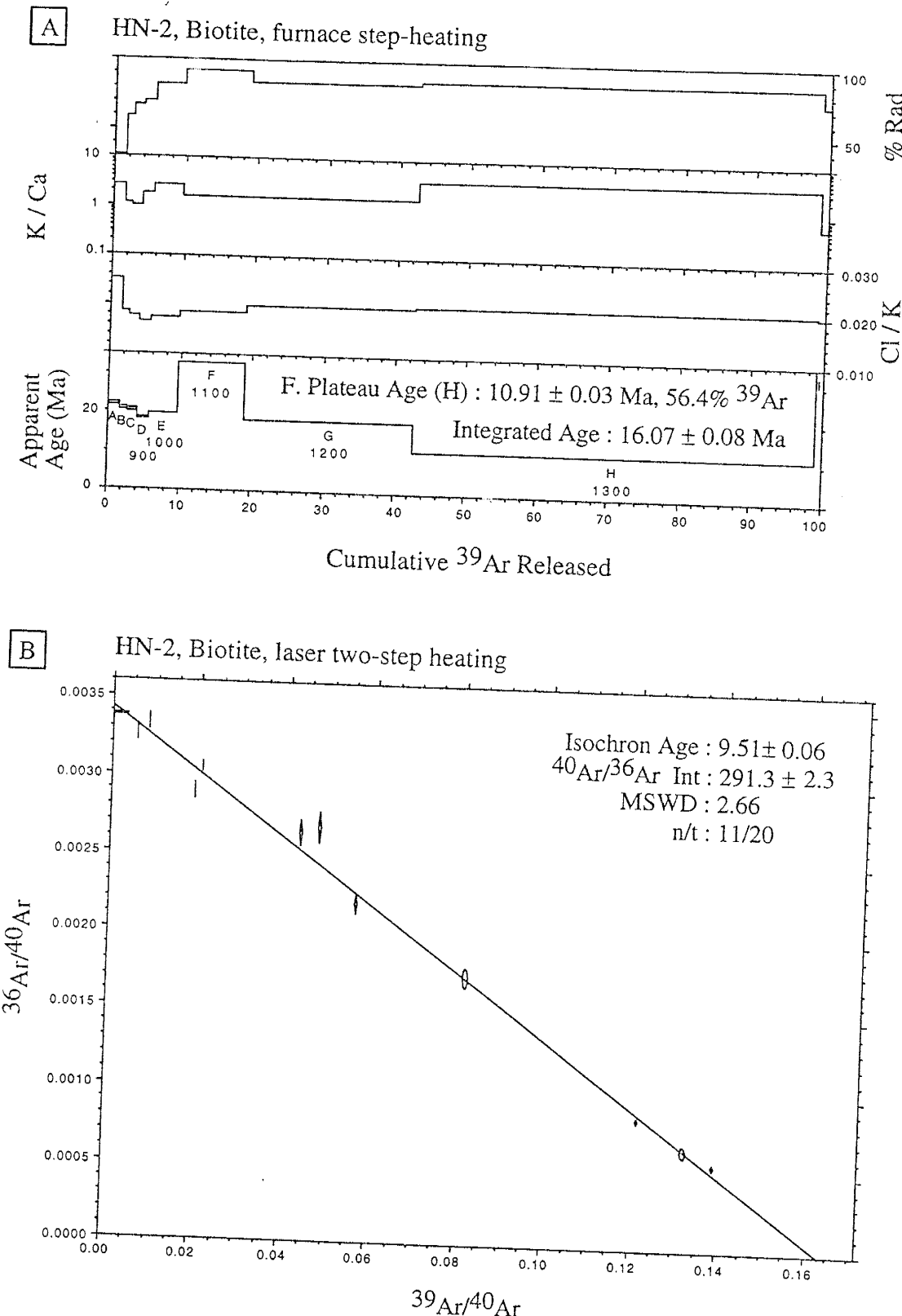


Figure 13.a. Age spectra plot of furnace step-heating data of biotite sample HN-2; Figure 13.b. Inverse isochron plot of two-step laser step-heating data of sample HN-2.

the biotite samples are the most probable sources of the furnace and laser age discrepancies discussed in the results section.

Examination of K/Cl and K/Ca ratios from the furnace heating of the biotites found no correlation between these factors and the amount of discrepancy between biotite ages and sanidine ages. K/Cl ratios were typically higher in the early heating steps, presumably influenced by chlorite. Lanphere (1988) determined the ages of biotites with K/Ca ratios less than 40 tended to be difficult to interpret. A cutoff value of 40-50 for the K/Ca ratio was suggested for biotites to yield reliable age data.. The K/Ca ratios of this study were all lower than Lanphere's cutoff value; typically they were less than 30 (Appendix 5.b). However, the samples showed no pattern between decreasing K/Ca ratios and increasing discordance with the sanidine age.

An attempt was made to estimate the potassium content of the biotites with measurement of $^{39}\text{Ar}_\text{K}$ and the sample weight of the furnace step-heating analyses. However, no systematic trend was found between the estimated K content of the biotites and degree of discordance with the sanidine ages. Beyond this study, an electron microprobe analysis of the biotite samples would provide a more accurate measurements of the biotite compositions, in order to better address how the problems of alteration and chloritization contribute to the age complexities.

The results of the biotite analyses are the most difficult part of this study to interpret. Comparison of the furnace and laser biotite pairs reveals significant inhomogeneities within biotite samples (Fig. 8). In light of the apparent accuracy of the sanidine results and the consistent trend of biotite ages being older than the corresponding sanidine mineral age (Fig. 9), all of the biotite mineral ages should be considered maximum ages. Therefore, the geologic uncertainties of the biotite ages are greater than indicated by the analytical errors. The maximum 2 sigma discordance between the mineral ages of the biotite and sanidine pairs range from 4.7 to 31.3% of the biotite age (Fig. 9) and the mean discordance was 12.4% of the biotite age with a standard deviation of 8.2. However, no systematic trends in the biotite and sanidine age discrepancies are apparent, and it is not possible to determine a standard "geologic correction factor" for all the mineral ages of the biotites.

Plagioclase and Hornblende Age Analyses

Plagioclase and hornblende minerals contain less than 1% K, but accurate $^{40}\text{Ar}/^{39}\text{Ar}$ ages can in many cases be determined from these minerals (McDougall and Harrison, 1988). For this study, the ages produced by laser analyses of plagioclase vary widely (Appendix 5.a). The large sample size of furnace analyses produced a small analytical error in the plagioclase ages (Table 1), however, the geologic significance of the

data is suspect. The age of plagioclase sample HN-20 was more than 5 million years older than the mineral age of the biotite, whereas the age of plagioclase sample HN-32 was almost 1 million years younger than the age of the biotite. Unfortunately, the improved analytical uncertainty of the plagioclase furnace analyses did not produce more accurate ages.

Analyses of two hornblende mineral samples did not produce acceptable mineral ages, due to widely varied ages recorded in the furnace steps (Appendix 5.b). Hornblende samples from HN-5 and 6, two dacitic flows of the Socorro Peak Rhyolite, produced clearly anomalous total gas ages of 26 and 29 Ma. Based upon biotite analyses from Socorro Peak, these samples should be no older than 11.6 Ma and all apparent eruption ages of the Socorro Peak flows are between 11.6 and 7.0 Ma (Table 2). The anomalously old hornblende data is not readily explained. However, fluid inclusions or xenocrystics with a large trapped component of unequilibrated radiogenic argon could have influenced the ages.

GEOCHRONOLOGY OF MIocene SILICIC UNITS

The final phase of this study involved evaluating and appreciating the various $^{40}\text{Ar}/^{39}\text{Ar}$ mineral ages, in order to produce a geochronology for the units of the Socorro-Magdalena Miocene silicic centers. The apparent eruption ages of the units (Table 2) were determined by the type of mineral dated, the precision of the mineral age, and known stratigraphic

constraints. The volcanic chronology of each volcanic center is outlined below.

Squaw Peak centers

The new $^{40}\text{Ar}/^{39}\text{Ar}$ ages (Table 1) of the units in the Squaw Peak center are consistent with reported stratigraphic relationships (Fig. 2; Bobrow, 1984; Osburn, 1996). The volcanic activity of the center ranged from 18.5 to 11.5 Ma. The two oldest units, the rhyolite of McDaniel Tank (18.45 ± 0.27 Ma; sanidine) and the dacite of Mill Place (17.94 ± 0.09 Ma; biotite) are chemically and chronologically distinct from each other. Based on the geochemical and mineralogical compositions, Donze (1980) speculated the rhyolites of Muleshoe Ranch (15.59 ± 0.09 Ma; sanidine) and Alameda Springs (14.49 ± 0.08 Ma; sanidine) were derived from the Magdalena Peak center. However, these flows clearly pre-date the 13.0 Ma rhyolitic lava flow at the apparent vent exposed on Magdalena Peak. The youngest samples were from Squaw Peak (11.47 ± 0.08 Ma; sanidine) and the B.O. Dome (11.44 ± 0.05 Ma; sanidine). Based on the similar chemical compositions, Bobrow (1983) informally grouped these proximal intrusive domes as the rhyolite of Squaw Peak and the map unit is supported by the nearly identical mineral ages. The apparent eruption age of the rhyolite of Squaw Peak (11.45 ± 0.06 Ma; sanidine) was calculated from the two sanidine mineral ages of the domes.

Magdalena Peak centers

Volcanism in the Magdalena Peak centers was restricted to a short interval between 13.8 and 13.0 Ma (Fig. 2). Stratigraphically, the oldest map unit is the Stendel Perlite deposit (Bobrow, 1983) with an average age of 13.75 ± 0.10 Ma (plagioclase and biotite; Table 2). For this study, the overlying rhyolitic flow unit of Magdalena Peak was informally termed the rhyolite of Agua Frio Canyon. Unlike the rhyolitic flows in the vicinity of Magdalena Peak, the rocks samples of Agua Frio Canyon, HN-32 and 33, yielded no sanidine for age analysis and apparent eruption age of 13.63 ± 0.19 Ma was derived from a plagioclase and biotite mineral age. The similar mineralogy and analytically indistinguishable apparent eruption ages presents the possibility the Stendel Perlite and Agua Frio flow units are cogenetic, however, the age analyses are too imprecise to clearly define the eruptive history. The areas south and west of the rhyolite of Agua Frio Canyon extending to the Muleshoe Ranch have not been mapped as thoroughly as other areas of this study, and future investigators would benefit from more detailed mapping and dating.

Three sanidine ages were obtained from samples of the rhyolitic flows directly around of the Magdalena Peak (Fig. 2 and Table 2). The most pristine sample (HN-59: 13.00 ± 0.10 Ma; sanidine) was collected directly below the apparent intrusive neck on Magdalena Peak. The other samples are from the more weathered outcrops around Elephant Peak and

were dated 12.81 ± 0.23 Ma (sanidine) and 13.50 ± 0.70 Ma (sanidine).

Due to the imprecise ages and the apparent alteration of the sanidines, the 13.00 ± 0.10 Ma age of sample HN-59 was used to define the eruption age of the rhyolitic flows. Dacitic flows of the Magdalena Peak Rhyolite underlie the rhyolitic flows (Bobrow, 1983), and the apparent eruption age of the biotite sample (13.65 ± 0.12 Ma) agree with the stratigraphy.

Pound Ranch centers

The eruption age of the oldest unit of the Pound Ranch center (Fig. 3), the lower rhyolite of Pound Ranch, was determined to be 11.35 ± 0.07 Ma by averaging two sanidine mineral ages from the north and south centers (Table 2). However, no sanidine phenocrysts were present in samples of the younger unit, and the biotite age of 12.43 ± 0.14 Ma contradicts the mapped stratigraphic relationship. Based on the sanidine analyses of the lower rhyolite of Pound Ranch, the apparent age of the biotite mineral sample HN-20 from the upper flow is at least 1.1 m.y. too old and was rejected as the apparent eruption age of the unit. Osburn (1978) interpreted the rhyolitic eruptions of Pound Ranch to be close temporally and the age data do not contradict this view.

To the east of Pound Ranch, another center was active near the Tower Mine (Fig. 3). The dacitic sample, HN-16, yielded a biotite mineral age of 12.23 ± 0.04 Ma. However, due to the uncertainty of the biotite mineral ages in this study and the lack of stratigraphic continuity with the

rhyolites of Pound Ranch, the apparent eruption age of HN-16 can only be considered a maximum age for the dacite of Tower Mine.

Socorro Peak centers

The Socorro Peak centers were active from 11.6 to 7.0 Ma and are comprised of more eruptive units than recognized by previous mapping (Fig. 3; Table 2). Based on biotite analyses, this study has identified at least three dacitic flows of the Socorro Peak Rhyolite. The oldest sample was from the lower dacite of Radar Peak, dated 11.56 ± 0.11 Ma, which underlies the upper dacite of Radar Peak, 9.51 ± 0.09 Ma. To the north, the analysis of a biotite sample from Strawberry Peak yielded an age of 10.56 ± 0.11 Ma. Samples from 6001 Mesa and the Stonewall Dome were evaluated but did not produce acceptable mineral ages. However, the undated dacitic domes of the Socorro Peak Rhyolite are believed to be coeval with the upper and lower flows (Bobrow, 1983).

At least four separate flow units were identified within the rhyolitic flows of the Socorro Peak Rhyolite on the basis of sanidine analyses. The oldest rhyolite sample was collected from Signal Flag hill (8.66 Ma ± 0.05 Ma), and to the south the phenocryst poor dome of Grefco Mine was dated at 7.85 ± 0.03 Ma (Table 2; Fig. 3). To west of Socorro Peak, the youngest samples compose at least two chronologically distinct flows. The oldest flow was sampled at two locations, Jejenes Hill (7.45 ± 0.08 Ma) and

Sk-Range (7.52 ± 0.09 Ma), and the average apparent eruption age of 7.49 ± 0.09 Ma was computed for the informal flow unit termed the rhyolite of Jejenes Hill. Samples were also collected and analyzed from the Tripod Peak (7.02 ± 0.05 Ma) and 6633 Mesa (7.06 ± 0.03 Ma) domes. The average of these two mineral ages (7.04 ± 0.04 Ma) yields the apparent eruption age of the flow unit called the rhyolite of Tripod Peak, the youngest documented silicic eruption within the Socorro-Magdalena area.

Geochemical Modeling and Timing of the SAZ

As discussed in the introduction, the silicic volcanism of the Socorro-Magdalena area is attributed to a Rio Grande rift accommodation zone, a domain boundary that was initiated at the inception of rifting (Fig. 1; Chapin, 1989). In a previous geochemical investigation, Bobrow (1984) proposed a petrogenetic origin for the Miocene high-silica rocks of the Socorro-Magdalena area. Based on continuous chemical trends and the modeling of major, trace, and REE elements, the dominant process producing the rhyolitic magmas was interpreted to be crystal fractionation with minor magma mixing. The origin of the dacitic rocks was not as clear from Bobrow's data, but he speculated the dacitic domes resulted from a combination of processes including mixing of a mafic magma with a partial melt of lower-crustal rocks, upper crustal contamination, and fractional crystallization. In thin section analyses, Bobrow found no

mineralogical evidence for crustal contamination. However, the Sr and Pb isotopic data suggested lower and/or upper-crustal contamination.

The $^{40}\text{Ar}/^{39}\text{Ar}$ ages of this study provide further constraints on the model for the silicic volcanism in the Socorro-Magdalena area. Recorded over a nearly 12 million year period, silicic lavas erupted from 18.5 million years ago until the activity abruptly ceased at 7.0 Ma (Table 2). Broad trends are apparent over field area, such as, between 14.5 and 11.3 Ma, all of the volcanic centers were active (Fig. 10 and 11), and no other Miocene period records such a wide range of activity. The pulse of volcanism was most likely triggered by significant tectonic movement along the Rio Grande rift. An additional broad spatial trend, is apparent, with eruption ages generally decreasing from west to east across the Socorro accommodation zone (Fig. 2 and 3). The apparent migration of volcanism may mark the relative movement of the rift axis in this area of the Rio Grande rift.

Mineral ages within individual volcanic centers do not display a west to east migration of volcanism, although, there are compositional trends for some centers. The Magdalena Peak and Pound Ranch centers erupted over short 1 to 2 Ma intervals, resulting in only minor compositional variation. The geochemical composition of the rocks in the Squaw Peak and Socorro Peak volcanic centers do vary systematically from more dacitic to rhyolitic flows over time. In the Squaw Peak center, the rhyolite

of McDaniel Tanks (18.45 ± 0.27 Ma) is 73.9% SiO₂ and the rhyolite of Alameda Springs (11.45 ± 0.27 Ma) is 77.5% SiO₂, while in the Socorro Peak centers, an average dacite from Radar Peak is 69.6% SiO₂ and an average rhyolite of the Socorro Peak Rhyolite is 72.8% SiO₂. These geochemical trends support a crystal fractionation model (Bobrow, 1984) for the evolution of the magmas within the volcanic centers.

Other Rio Grande Rift Related Rhyolite Volcanism

In addition to the Socorro accommodation zone, other volcanic fields related to formation of the Rio Grande rift also produced silicic magmas. At least five volcanoes in the western Mogollon-Datil volcanic field were active during the same period as the Miocene volcanism of the Socorro-Magdalena area. Eagle Peak (Fig. 1.a), Apache Peak, Legget Peak, John Kerr Peak, and Horse Mountain have K-Ar ages between 14 and 12 Ma (Marvin et al., 1987) and are all approximately aligned with the Morenci lineament. A detailed study by Bove et al. (1995) of the Eagle Peak volcano, andesitic to dacitic in composition, determined eruptive ages from 12.1 to 11.4 Ma, which coincides with the 14.5 to 11.3 Ma major pulse volcanism in the Socorro-Magdalena area. Bove et al. favored an eruptive model with significant crustal contamination and an extension related, lithospheric mantle source.

In northern New Mexico at the junction of the Jemez Lineament and the Rio Grande rift (Fig. 1.a), volcanism commenced around 16 Ma in the Jemez area and has been nearly continuous since 13 Ma (Gardner et al., 1986). The Jemez field recorded rhyolitic volcanism from about 13 to 6 Ma, followed by major rhyolitic tuffs erupted from 4 to 3 Ma (Gardner et al, 1986). The latest phase of volcanism has produced major silicic eruptions from 1.78 Ma until about 60 Ma (Spell et al., 1993).

Shorter lived fields with rift related rhyolitic volcanism, include the Taos Plateau Volcanic Field (TPVF) and the Mt. Taylor area (Fig. 1.a). Mt. Taylor, a latitic to rhyolitic volcano, was active from 3.3 to 1.5 Ma and geographically coincides with the Jemez lineament, a line of volcanism trending south-west from the Jemez volcanic field (Perry et al., 1990). In contrast to the Squaw Peak and Socorro Peak centers, the lavas of Mt. Taylor became increasingly mafic over time. Perry et al. (1990) believed the compositional trend to indicate a common control on the magmatic evolution of the multiple chambers over the duration of the field. The composition of the TPVF, located in the far northern section of the NM rift, is primarily basaltic, but rhyolitic volcanism was active at approximately 4 Ma (Appelt, 1997). Lipman and Mehnert (1979) speculated that a high heat source was needed to produce the voluminous basalts of the field, and that limited crystal-fractionation and magma mixing produced the silicic to intermediate lavas.

CONCLUSIONS

The $^{40}\text{Ar}/^{39}\text{Ar}$ geochronologic investigation of the Socorro-Magdalena area provides a clearer and more precise eruptive sequence of the Miocene silicic volcanism. Many of the distinct eruptive flows of this study were not identified by previous field mapping and geochemical studies which were limited by imprecise dates.

Single-crystal laser fusion analysis of sanidine phenocrysts resulted in highly accurate and precise mineral and apparent eruption ages, based upon comparisons of reproducibility within samples and units. Biotite sample pairs displayed variable accuracy from furnace to laser analyses, and biotite apparent ages were systematically older than the ages of sanidine from the same samplers. This study was not able to determine the exact cause of the inhomogeneities and complexities in the biotite samples . The mineral ages of the sanidines were taken as the apparent eruption age for the rock sample, while all biotite age determinations were considered a maximum eruption age. Plagioclase and hornblende ages were found to be inaccurate and of questionable geologic significance.

Silicic lavas began to erupt in the Socorro-Magdalena area at 18.5 Ma and abruptly ceased at 7.0 Ma. Chronological trends found by this study include a pulse of volcanism between 14.5 and 11.3 Ma recorded in all four volcanic centers. Also a general decrease in age of rhyolite volcanism is apparent from the west to the east across the field area, with volcanic

activity ending at 7 Ma near the intersection of the Socorro accommodation zone and the margin of the Rio Grande rift.

REFERENCES

- Allen, P. G., 1979, Geology of the west flank of the Magdalena Mountains south of the Kelly Mining District, Socorro County, New Mexico: M.S. thesis, New Mexico Institute of Mining and Technology, Socorro, 161 p.
- Appelt, R. M., 1997, $^{40}\text{Ar}/^{39}\text{Ar}$ dating of the Taos Plateau volcanic field, Taos, New Mexico and southern Colorado: M.S. thesis, New Mexico Institute of Mining and Technology, Socorro.
- Baldridge, W. S., F. V. Perry, D. T. Vaniman, and others, 1991, Middle to Late Cenozoic magmatism of the southeastern Colorado Plateau and central Rio Grande rift (New Mexico and Arizona, U.S.A.): a model for continental rifting: *Tectonophysics*, v. 197, p. 327-354.
- Bobrow, D. J., P. R. Kyle, and G. R. Osburn, 1983, Miocene Rhyolitic Volcanism in the Socorro Area of New Mexico: 34th Field Conference, Socorro Region II, p. 211-217.
- Bobrow, D. J., 1984, Geochemistry and petrology of Miocene silicic lavas in the Socorro-Magdalena area of New Mexico: M.S. thesis, New Mexico Institute of Mining and Technology, Socorro, 145 p.
- Bogaard, P. v. d., 1995, $^{40}\text{Ar}/^{39}\text{Ar}$ ages of sanidine phenocrysts from Laacher See Tephra (12,900 yr. BP): Chronostratigraphic and petrologic significance: *Earth and Planetary Science Letters*, v. 133, p. 163-174.
- Bosworth, W., 1985, Geometry of propagating continental rifts: *Nature*, v. 316, p. 625-627.
- Bosworth, W., 1986, Comment on "Detachment faulting and the evolution of passive continental margins": *Geology*, v. 14, p. 890-891.
- Bove, D. J., J. C. Ratte, W. C. McIntosh, L. W. Snee, and K. Futa, 1995, The evolution of the Eagle Peak volcano- a distinctive phase of Middle Miocene volcanism in the western Mogollon-Datil volcanic field, New Mexico: *Journal of Volcanology and Geothermal Research*, v. 69, p. 159-186.
- Bowring, S. A., 1980, The geology of the west-central Magdalena Mountains, Socorro County, New Mexico: M.S. thesis, New Mexico Institute of Mining and Technology, Socorro, 135 p.
- Brocher, T. M., 1981, Geometry and physical properties of the Socorro, New Mexico, magma bodies: *Journal of Geophysical Research*, v. 86, p. 9620-9432.
- Cather, S. M., C. E. Chapin, W. C. McIntosh and R. M. Chamberlin, Tectonic and stratigraphic consequences of episodic extension in the central and northern Rio Grande Rift (Abstract): Abstracts with Program- Geological Society of America, v. 26, n.7, p. 132.
- Chamberlin, R. M., 1980, Cenozoic stratigraphy and structure of the Socorro Peak volcanic center, central New Mexico: Ph.D. thesis, Colorado School of Mines, Golden, 532 p.

- Chamberlin, R. M., 1983, Cenozoic domino-style crustal extension in the Lemitar Mountains, New Mexico: a summary: New Mexico Geological Society 34th Annual Field Conference, p. 111-118.
- Chapin, C. E., 1989, Volcanism along the Socorro accommodation zone, Rio Grande rift, New Mexico, in C. E. Chapin, and J. Zidek, eds., Field excursions to volcanic terranes in the Western U.S., Socorro, NM, New Mexico Bureau of Mines and Mineral Resources Memoir 46, p. 46-57.
- Chapin, C. E., and S. M. Cather, 1994, Tectonic setting of the axial basins of the northern and central Rio Grande rift, in G. R. Keller, and S. M. Cather, eds., Basins of the Rio Grande Rift: Structure, Stratigraphy, and Tectonic Setting, Boulder, Colorado, Geological Society of America Special Paper 291, p. 304.
- Deino, A., and R. Potts, 1990, Single-Crystal 40/39 Dating of the Olorgesailie Formation, Southern Kenya Rift: Journal of Geophysical Research, v. 95, p. 8453-8470.
- Donze, M. A., 1980, Geology of Squaw Peak area, Magdalena Mountains, Socorro County, New Mexico: M.S. thesis, New Mexico Institute of Mining and Technology, Socorro, 131 p.
- Dunbar, N. W., S. Kelley, and D. Miggins, 1996, Chronology and thermal history of potassium metasomatism in the Socorro, NM, area: Evidence from $40\text{Ar}/39\text{Ar}$ dating and fission track analysis (Abstract): New Mexico Geological Society Spring Meeting, p. 70.
- Faulds, J. E., J. W. Geissman, and C. K. Mawer, 1990, Structural development of a major extensional accommodation zone in the Basin and Range province, northwestern Arizona and southern Nevada: Implications for kinematic models for continental extension, in B. Wernicke, ed., Basin and Range extensional tectonics near the latitude of Las Vegas, Nevada, Geological Society of America Memoir 176, p. 37-76.
- Gaber, L. J., K. A. Foland, and C. E. Corbato, 1988, On the significance of argon release from biotite and amphibole during $40\text{Ar}/39\text{Ar}$ vacuum heating: *Geochemica et Cosmochimica Acta*, v. 52, p. 2457-2465.
- Gardner, J. N., F. Goff, S. Garcia, and R. C. Hagan, 1986, Stratigraphic relationships and lithologic variations in the Jemez volcanic field, New Mexico: *Journal of Geophysical Research*, v. 91, p. 1763-1778.
- Gibbs, A. D., 1984, Structural evolution of extensional basin margins: *Journal of the Geological Society of London*, v. 141, p. 609-620.
- Hess, J. C., H. J. Lippolt, and R. Wirth, 1987, Interpretation of $40\text{Ar}/39\text{Ar}$ Spectra of Biotites: Evidence from Hydrothermal Degassing Experiments and TEM Studies: *Chemical Geology (Isotope Geoscience Section)*, v. 66, p. 137-149.
- Keller, G. R., M. A. Khan, P. Morgan, and others, 1991, A comparative study of the Rio Grande and Kenya rifts: *Tectonophysics*, v. 197, p. 355-371.
- Lanphere, M. A., 1988, High-resolution $40\text{Ar}/39\text{Ar}$ chronology of Oligocene volcanic rocks, San Juan Mountains, Colorado: *Geochemica et Cosmochimica Acta*, v. 52, p. 1425-1434.

- Lipman, P. W., and H. H. Mehnert, 1979, The Taos Plateau volcanic field, northern Rio Grande rift, New Mexico, Rio Grande Rift: Tectonics and Magmatism, Washington D.C., American Geophysical Union, p. 289-311.
- Lo, C-H., and T. C. Onstott, 1989, ^{39}Ar recoil artifacts in chloritized biotite: *Geochemistry et Cosmochimica Acta*, v. 53, p. 2697-2711.
- Marvin, R. F., C. W. Naeser, M. Bikerman, H. H. Mehnert, and J. C. Ratte, 1987, Isotopic ages of post-Paleocene igneous rocks within and bordering the Clifton $1^{\circ} \times 2^{\circ}$ quadrangle, Arizona-New Mexico, Socorro, NM, New Mexico Bureau of Mines and Mineral Resources Bulletin 118, p. 63.
- McDougall, I., and T. M. Harrison, 1988, *Geochronology and Thermochronology by the $^{40}\text{Ar}/^{39}\text{Ar}$ Method*: New York, Oxford University Press, 212 p.
- McDowell, F. W., 1983, K-Ar dating: Incomplete extraction of radiogenic argon from alkali feldspar: *Chemical Geology*, v. 41, p. 119-126.
- McIntosh, W. C., J. F. Sutter, C. E. Chapin, and L. L. Kedzie, 1990, High-precision $^{40}\text{Ar}/^{39}\text{Ar}$ sanidine geochronology of ignimbrites in the Mogollon-Datil volcanic field, southwestern New Mexico: *Bulletin of Volcanology*, v. 215, p. 1-18.
- McIntosh, W. C., C. E. Chapin, J. C. Ratte, and J. F. Sutter, 1992, Time-stratigraphic framework for the Eocene-Oligocene Mogollon-Datil volcanic field, southwest New Mexico: *Geological Society of America Bulletin*, v. 104, p. 851-871.
- Olsen, K. H., W. S. Baldridge, and T. F. Callender, 1987, Rio Grande rift: an overview: *Tectonophysics*, v. 143, p. 119-139.
- Osburn, G. R., 1978, Geology of the eastern Magdalena Mountains, Water Canyon to Pound Ranch, Socorro County, New Mexico: M.S. thesis, New Mexico Institute of Mining and Technology, Socorro, 160 p.
- Osburn, G. R., and C. E. Chapin, 1983, Nomenclature for Cenozoic rocks of northeast Mogollon-Datil volcanic field, New Mexico, Socorro, New Mexico Bureau of Mines and Mineral Resources, Stratigraphic Chart 1.
- Osburn, G. R., 1996, Geologic map of Squaw Peak Quadrangle, Socorro, NM, New Mexico Bureau of Mines and Mineral Resources Open File Report.
- Perry, F. V., W. S. Baldridge, D. J. DePaolo, and M. Shafiqullah, 1990, Evolution of a magmatic system during continental extension: the Mount Taylor volcanic field, New Mexico: *Journal of Geophysical Research*, v. 95, p. 19327-19348.
- Petty, D. M., 1979, Geology of the southeastern Magdalena Mountains, Socorro County, New Mexico: M.S. thesis, New Mexico Institute of Mining and Technology, Socorro, 174 p.
- Renne, P. R., 1995, Excess ^{40}Ar in biotite and hornblende from the Noril'sk 1 intrusion, Siberia: implications for the age of the Siberian Traps: *Earth and Planetary Science Letters*, v. 131, p. 165-176.

- Samson, S. D., and J. E. C. Alexander, 1987, Calibration of the interlaboratory $^{40}\text{Ar}/^{39}\text{Ar}$ dating standard, MMhb-1: Chemical Geology (Isotope Geoscience Section), v. 66, p. 27-34.
- Sanford, A. R., R. P. Mott, P. J. Shuleski and others, 1977, Geophysical evidence for a magma body in the vicinity of Socorro, New Mexico, in J. P. Heacock, ed., The Earth's Crust: Its Nature and Physical Properties, Washington, D.C., AGU, p. 385-404.
- Sanford, A. R., R. S. Balch, and K. W. Lin, 1995, A seismic anomaly in the Rio Grande rift near Socorro, New Mexico, Socorro, NM: Geophysical Research Center, open file report, New Mexico Institute of Mining and Technology.
- Sanford, A. R., K. W. Lin, I. C. Tsai, and L. H. Jaksha, 1996, Seismicity along a segment of a prominent ENE trending topographic lineament in New Mexico and west Texas, Socorro, NM: Geophysical Research Center open file report, New Mexico Institute of Mining and Technology.
- Spell, T. L., and T. M. Harrison, 1993, $^{40}\text{Ar}/^{39}\text{Ar}$ Geochronology of Post-Valles Caldera Rhyolites Jemez Volcanic Field, New Mexico: Journal of Geophysical Research, v. 98, p. 8031-8051.
- Spell, T. L., P. R. Kyle, M. F. Thirlwall, and A. R. Campbell, 1993, Isotopic and Geochemical Constraints on the Origin and Evolution of Postcollapse Rhyolites in the Valles Caldera, New Mexico: Journal of Geophysical Research, v. 98, p. 19723-19739.
- Steiger, R. H., and E. Jager, 1977, Subcommission on geochronology: Convention on the use of decay constants in geo- and cosmochronology: Earth and Planetary Science Letters, v. 36, p. 359-362.
- Stewart, J. H., 1980, Regional tilt patterns of late Cenozoic basin-range fault blocks, western United States: Geological Society of America Bulletin, v. 91, p. 460-464.
- Thelin, G. P., and R. J. Pike, 1991, Landforms of the conterminous United States- a digital shaded-reflect portrayal: U.S.G.S., U.S. Department of the Interior.
- Turner, G., and P. H. Cadogan, 1974, Possible effects of ^{39}Ar recoil in $^{40}\text{Ar}/^{39}\text{Ar}$ dating: *Geochemica et Cosmochimica Acta*, v. 2, p. 1601-1615.
- Turpin, B. D., J. M. Donnelly-Nolan, and B. C. Hearn Jr., 1994, $^{40}\text{Ar}/^{39}\text{Ar}$ ages from the rhyolite of Alder Creek, California: Age of the Cobb Mountain Normal-Polarity Subchron revisited: *Geology*, v. 22, p. 251-254.
- Weber, R. H., 1957, Geology and petrography of the Stendel perlite deposit, Socorro County, New Mexico, Socorro, New Mexico Bureau of Mines and Mineral Resources.
- York, D., 1969, Least squares fitting of a straight line with correlated errors: *Earth and Planetary Science Letters*, v. 5, p. 320-324.

Appendix 1

Sample Locations

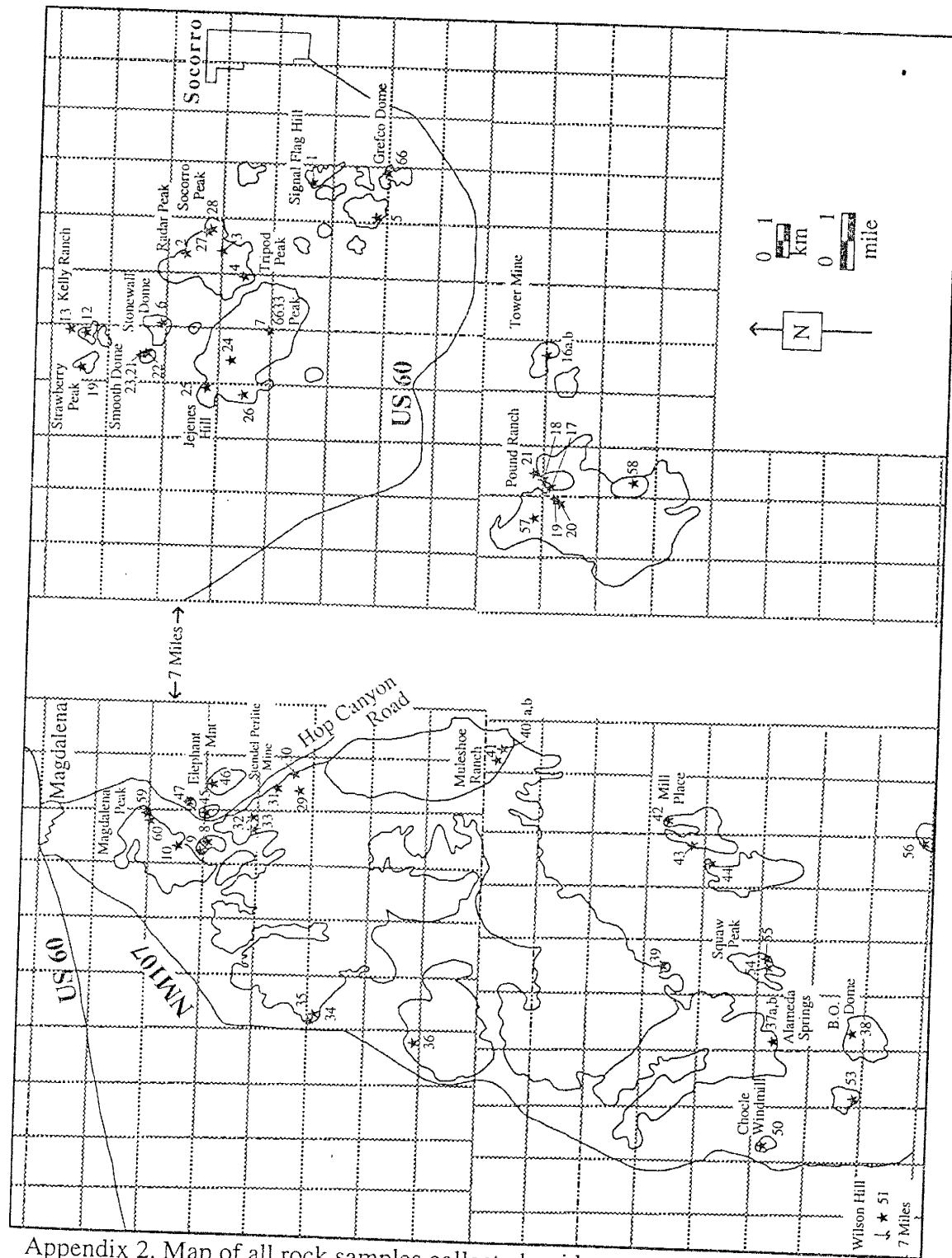
latitude north and longitude west locations of all analyzed samples

SAMPLE LOCATIONS	
HN#	Lat N /Long W
1	34.04/107.23
2	34.08/106.97
3	34.07/106.97
4	34.06/106.98
5	34.03/106.96
6	34.08/106.99
7	34.05/106.99
9	34.07/107.25
12	34.10/107.99
16	33.99/107.00
17	33.99/107.04
18	33.99/107.04
19	33.99/107.04
20	33.99/107.04
24	34.06/107.00
25	34.07/107.01
29	34.04/107.23
31	34.05/107.23
32	34.05/107.24
33	34.05/107.24
37	33.93/107.30
38	33.91/107.30
39	33.96/107.28
41	34.00/107.22
42	33.96/107.24
43	33.96/107.24
45	34.07/107.24
46	34.07/107.23
50	33.94/107.33
51	33.83/107.35
53	33.91/107.32
55	33.94/107.28
58	33.98/107.04
59	34.08/107.24
60	34.08/107.24
66	34.03/106.94

Appendix 2

Sample Map

map locations of all samples collected



Appendix 2. Map of all rock samples collected, grid represents township and range boundaries, and outlines approximate the arial extent of Miocene volcanic outcrops after Osburn, 1984

Appendix 3

Irradiation Information

table listing available information concerning the irradiation
of the mineral samples, see endnotes concerning column headings

L#	HN-95-#	Mineral	Irradiation:date	Tray:hole	Furnace	J-factor	Reactor
2778	1	Biotite	NM-30:3/13/95	M:1	NA	0.001528451	Ford Reactor
2814	1	Sanidine	NM-30:3/13/95	M:2	ND	0.001538546	Location, L67
2779	2	Biotite	NM-30:3/13/95	M:4	NA	0.001534302	Irradiated
2815	2	Plagioclase	NM-30:3/13/95	M:5	ND	0.001531597	for 10 hours
2780	3	Biotite	NM-30:3/13/95	M:7	NA	0.001538949	
2816	3	Plagioclase	NM-30:3/13/95	M:8	ND	0.001528854	
2792	6	Hnbl	NM-30:3/13/95	M:10	NA	0.001533098	
2817	6	Plagioclase	NM-30:3/13/95	M:11	ND	0.001535803	
2781	4	Biotite	NM-30:3/13/95	N:1	NA	0.00152562	
2811	4	Sanidine	NM-30:3/13/95	N:2	ND	0.001524026	
2782	7	Biotite	NM-30:3/13/95	N:4	NA	0.001519856	
2812	7	Sanidine	NM-30:3/13/95	N:5	ND	0.001518397	
2812	7	Sanidine	NM-30:3/13/95	N:7	ND	0.001518397	
2793	5	Hnbl	NM-30:3/13/95	N:8	NA	0.001520174	
5844	32	Plagioclase	NM-41:10/23/95	N:1	60 mg	0.001418949	Texas A&M
5845	33	Plagioclase	NM-41:10/23/95	N:2	52	0.001417564	Location, D-3
5846	31	Plagioclase	NM-41:10/23/95	N:3	57	0.001416915	
5847	29	Plagioclase	NM-41:10/23/95	N:4	50	0.001417651	
5848	20	Plagioclase	NM-41:10/23/95	N:5	54	0.001419036	
5782	18	Biotite	NM-41:10/23/95	J:1	not run	tray spilled	Texas A&M
5786	37b	Biotite	NM-41:10/23/95	J:5	not run	tray spilled	Location, D-3
5788	17	Sanidine	NM-41:10/23/95	J:7	ND	0.0014271089	
5792	37b	Sanidine	NM-41:10/23/95	J:11	ND	0.0014301435	
5796	25	Sanidine	NM-41:10/23/95	J:15	ND	0.0014282911	
5799	24	Sanidine	NM-41:10/23/95	K:2	ND	0.0014573637	
6027	12	Biotite	NM-43:12/20/95	N:1	7.2 mg	0.0007015265	Texas A&M
6028	37b	Sanidine	NM-43:12/20/95	N:2	ND	0.0007006935	Location, L67
6029	17	Biotite	NM-43:12/20/95	N:3	not run	0.0006991532	Irradiated
6030	18	Biotite	NM-43:12/20/95	N:4	3.3	0.0006970915	for 7 hours
6031	20	Biotite	NM-43:12/20/95	N:5	10	0.0006935751	
6032	25	Sanidine	NM-43:12/20/95	N:6	ND	0.0006913604	
6033	24	Biotite	NM-43:12/20/95	N:7	6.2	0.0006895642	
6034	25	Biotite	NM-43:12/20/95	N:8	not run	0.0006884032	
6035	29	Biotite	NM-43:12/20/95	N:9	NA	0.0006881335	
6036	17	Sanidine	NM-43:12/20/95	N:10	ND	0.0006889665	
6037	24	Biotite	NM-43:12/20/95	N:11	6.2	0.0006905068	
6038	33	Biotite	NM-43:12/20/95	N:12	not run	0.0006925685	
6039	32	Biotite	NM-43:12/20/95	N:13	5	0.0006960849	
6040	31	Biotite	NM-43:12/20/95	N:14	5.8	0.0006982996	
6041	37b	Biotite	NM-43:12/20/95	N:15	12	0.0007000958	
6351	38	Sanidine	NM-47:4/16/96	D:1	ND	0.0007902139	Texas A&M
6352	53	Sanidine	NM-47:4/16/96	D:2	ND	0.0007899275	Irradiated
6353	55	Sanidine	NM-47:4/16/96	D:3	ND	0.0007896136	for 7.183 hrs
6354	51	Sanidine	NM-47:4/16/96	D:4	ND	0.0007893101	
6355	45	Sanidine	NM-47:4/16/96	D:5	ND	0.0007889531	
6356	59	Sanidine	NM-47:4/16/96	D:6	ND	0.0007888224	
6357	39	Sanidine	NM-47:4/16/96	D:7	ND	0.0007887975	
6358	50	Sanidine	NM-47:4/16/96	D:8	ND	0.0007888815	
6359	46	Sanidine	NM-47:4/16/96	D:9	ND	0.0007891861	
6360	58	Sanidine	NM-47:4/16/96	D:10	ND	0.0007894725	
6361	45	Biotite	NM-47:4/16/96	D:11	8.8 mg	0.0007897864	
6362	9	Biotite	NM-47:4/16/96	D:12	7.9	0.0007900899	

L#	HN-95-#	Mineral	Irradiation:date	Tray:hole	Furnace	J-factor	Reactor
6363	46	Biotite	NM-47:4/16/96	D:13	6.9	0.0007904469	Texas A&M
6364	41	Biotite	NM-47:4/16/96	D:14	5	0.0007905776	
6365	58	Biotite	NM-47:4/16/96	D:15	6.8	0.0007906025	
6366	51	Biotite	NM-47:4/16/96	D:16	7.1	0.0007905185	
6367	59	Biotite	NM-47:4/16/96	E:1	8 mg	0.0007861621	
6368	53	Biotite	NM-47:4/16/96	E:2	2.5	0.0007867261	
6369	55	Biotite	NM-47:4/16/96	E:3	3.9	0.0007871458	
6370	9	Hnbl	NM-47:4/16/96	E:4	not run	0.0007873706	
6575	50	Biotite	NM-49:5/9/96	K:1	not run	0.0008639013	Texas A&M
6576	41	Sanidine	NM-49:5/9/96	K2	NA	0.0008641341	Irradiated
6577	43	Biotite	NM-49:5/9/96	K:3	ran	0.0008642253	for 7.6 hrs
6578	3	Biotite	NM-49:5/9/96	K:4	ran	0.0008641638	
6579	2	Biotite	NM-49:5/9/96	K:5	ran	0.0008638066	
6580	16B	Biotite	NM-49:5/9/96	K:6	ran	0.0008634336	
6945	61	Sanidine	NM-54:8/7/96	D:15	NA	NA	Texas A&M
6946	61	Biotite	NM-54:8/7/96	D:16	NA	NA	

ENDNOTES:

Column Headings

L#: Lab number, unique designation for each sample packet within a tray
 HN-95-#: Field number designating a rock sample

Tray:hole: designated letter for aluminum irradiation tray, and hole number machined for sample packet
 Furnace: weight in milligrams of sample analyzed by furnace step-heating;

"NA" if sample not analyzed by furnace;

"not run" if sample not analyzed by any means;

"ND" furnace heating not done

Reactor: Applicable information concerning research reactor

Appendix 4

Age Summary for all $^{40}\text{Ar}/^{39}\text{Ar}$ Analyses

table summarizing all relevant information for each age analysis,
see endnotes concerning column headings and abbreviations

Appendix 5.a

Laser Fusion Numeric Data

sanidine and plagioclase samples
see Notes concerning column headings and abbreviations

Notes

Column Headings

Run ID#: Lists lab number (i.e. 2814), the unique designation for each sample packet within an irradiation tray; and the chronological number assigned to the mass spectrometer analysis (i.e. 04)

40/39: ratio of the measured $^{40}\text{Ar}/^{39}\text{Ar}$

37/39: ratio of the measured $^{37}\text{Ar}/^{39}\text{Ar}$

36/39: ratio of the measured $^{36}\text{Ar}/^{39}\text{Ar}$

39K moles: total moles of gas, determined from the measurement of $^{39}\text{Ar}_K$

K/Ca: a function of measured $^{39}\text{Ar}_K/^{37}\text{Ar}_{\text{Ca}}$

%40*: radiogenic ^{40}Ar , not attributed to atmospheric composition

Age: apparent age determined for analysis in millions of years

$\pm\text{Err}$: 1 sigma analytical error of age determination

SEM: standard error of the mean

General Heading

Lists mineral analyzed (i.e. Sanidine, Biotite); field number of rock sample (i.e. HN-95-1); irradiation tray designation (i.e. M), tray hole number (i.e. 2), irradiation number (i.e. 30); project name (i.e. Socorro Peak); and J factor, unique correction factor for extent of irradiation, determined through monitor mineral age analysis

Additional Information

The analytical data in italics were not used in the age determinations, either the geochemical or apparent age values of those analyses were determined to be outside the typical analytical distribution.

mean: this line includes the mean age and error of the acceptable analyses, as well as the number of analyses utilized in the mean age, i.e. n=6

Age corrected for J: error produced by irradiation inequalities added to analytical error

Run ID#	40/39	37/39	36/39	39K moles	K/Ca	%40*	Age	\pm Err	SEM
Sanidine									
HN-95-1, M2:30, SOCORRO PEAK, J=0.001538546+1.690297									
2814-04	5.84	2.53E-02	9.40E-03	1.3E-14	20.2	52.1	8.43	0.07	
2814-07	5.20	1.77E-02	7.16E-03	8.7E-15	28.9	58.9	8.47	0.07	
2814-03	3.79	6.12E-03	2.20E-03	2.1E-14	83.4	82.3	8.63	0.04	
2814-02	6.35	6.00E-03	1.09E-02	1.3E-14	85.1	49.0	8.63	0.08	
2814-06	4.74	3.35E-02	5.42E-03	1.5E-14	15.2	65.8	8.64	0.06	
2814-08	4.89	2.20E-02	5.92E-03	4.2E-15	23.2	63.8	8.65	0.09	
2814-09	5.89	1.63E-02	9.23E-03	6.6E-15	31.4	53.3	8.69	0.09	
2814-10	5.11	1.59E-02	6.55E-03	5.1E-15	32.2	61.7	8.73	0.10	
mean	n=6				45.1	31.0	8.66	0.04	0.02
				Error Corrected for J:	8.66	0.05	0.03		
<i>Plagioclase</i>									
HN-95-2, M5:30, SOCORRO PEAK, J=0.001531597+1.68625									
2815-06	26.67	1.51E+00	7.98E-02	5.1E-16	0.3	11.9	8.77	1.10	
2815-10	11.84	1.13E+00	2.84E-02	6.5E-16	0.5	29.6	9.67	0.48	
2815-07	31.45	3.62E+00	9.50E-02	3.5E-16	0.1	11.6	10.04	1.53	
2815-09	148.97	1.59E+00	4.92E-01	6.9E-16	0.3	2.4	10.05	2.75	
2815-05	45.95	2.21E+00	1.41E-01	1.0E-15	0.2	9.6	12.19	1.11	
2815-03	119.48	4.49E+00	3.87E-01	1.2E-16	0.1	4.6	15.05	5.37	
2815-02	33.15	3.30E-01	9.20E-02	1.9E-16	1.5	18.0	16.38	1.84	
2815-04	40.51	4.51E+00	1.14E-01	3.3E-16	0.1	17.4	19.46	1.47	
2815-01	33.68	4.80E+00	7.74E-02	2.5E-16	0.1	33.1	30.66	1.36	
mean	n=4				0.3	0.1	9.63	0.60	0.30
				Error Corrected for J:	9.63	0.60	0.30		
<i>Plagioclase</i>									
HN-95-3, M8:30, SOCORRO PEAK, J=0.001528854+0.04132605									
2816-10	8.30	3.46E+00	1.76E-02	1.1E-15	0.1	40.2	9.19	0.34	
2816-07	5.37	2.62E+00	7.37E-03	6.3E-16	0.2	62.8	9.30	0.50	
2816-03	42.13	2.83E+00	1.31E-01	1.2E-15	0.2	8.4	9.76	0.94	
2816-04	6.75	3.21E+00	1.12E-02	7.3E-16	0.2	54.1	10.06	0.47	

Run ID#	40/39	37/39	36/39	39K moles	K/Ca	%40*	Age	\pm Err	SEM
2816-02	19.71	3.60E+00	5.52E-02	7.1E-16	0.1	18.5	10.07	0.61	
2816-08	7.88	3.94E+00	1.48E-02	1.0E-15	0.1	48.0	10.43	0.37	
2816-06	16.76	3.42E+00	4.44E-02	1.2E-15	0.1	23.2	10.72	0.44	
2816-01	16.53	3.48E+00	4.36E-02	1.8E-15	0.1	23.6	10.74	0.36	
2816-05	7.77	4.83E+00	6.99E-03	6.1E-16	0.1	77.9	16.68	0.50	
2816-09	17.85	4.43E+00	4.09E-02	7.6E-16	0.1	34.1	16.74	0.59	
mean		n=6			0.0	10.30	0.40	0.16	
			Error Corrected for J:		0.2	10.30	0.40	0.16	
						0.0	0.40	0.16	

Sanidine

HN-95-4, N2:30, SOCORRO PEAK, J=0.001524026+1.694386	2.69	8.11E-03	4.64E-04	4.2E-15	62.9	94.1	6.95	0.06
2811-03	2.67	1.47E-02	3.40E-04	1.3E-14	34.7	95.4	6.99	0.03
2811-02	2.69	1.24E-02	4.05E-04	2.0E-14	41.2	94.8	7.00	0.03
2811-01	2.64	8.05E-03	2.09E-04	1.5E-14	63.3	96.8	7.01	0.03
2811-04	2.63	7.76E-03	1.74E-04	9.1E-15	65.8	97.2	7.02	0.04
2811-07	2.61	7.53E-03	1.20E-04	2.0E-14	67.7	97.8	7.02	0.02
2811-06	2.61	8.21E-03	8.90E-05	2.7E-14	62.2	98.2	7.02	0.02
2811-08	2.64	1.00E-02	1.50E-04	8.4E-15	50.8	97.5	7.05	0.04
2811-10	2.65	1.45E-02	1.11E-04	5.9E-15	35.1	98.0	7.13	0.05
mean		n=9			53.7	13.5	7.02	0.05
			Error Corrected for J:		0.0	0.05	0.02	0.02
					0.1	0.0	0.32	0.18

Plagioclase

HN-95-6, M11:30, SOCORRO PEAK, J=0.001535803+1.642304	22.18	2.18E+01	6.52E-02	1.0E-16	0.0	20.6	12.81	3.46
2817-07	68.72	5.39E+00	2.18E-01	3.7E-16	0.1	7.0	13.28	2.07
2817-01	229.25	2.31E+01	7.60E-01	1.2E-16	0.0	2.8	18.03	9.03
2817-05	27.40	6.78E+00	7.10E-02	4.6E-16	0.1	25.3	19.16	0.94
2817-02	25.63	6.39E+00	6.01E-02	3.3E-16	0.1	32.6	23.09	1.14
2817-03	22.90	6.96E+00	5.04E-02	5.8E-16	0.1	37.2	23.54	0.74
2817-06	28.53	6.54E+00	6.92E-02	2.7E-16	0.1	30.1	23.71	1.52
mean		n=3			0.1	0.0	23.45	0.32
			Error Corrected for J:		0.0	0.05	0.32	0.19
					0.1	0.0	0.32	0.18

Run ID#	40/39	37/39	36/39	39K moles	K/Ca	%40*	Age	$\pm \text{Err}$	SEM
Sanidine									
HN-95-7, N5:30, SOCORRO PEAK, J=0.001518397+1.694506									
2812-09	2.93	1.84E-02	1.13E-03	2.2E-14	27.7	87.9	7.04	0.03	
2812-08	2.62	7.79E-03	6.82E-05	4.4E-14	65.5	98.4	7.05	0.02	
2812-02	2.65	1.30E-02	1.81E-04	3.1E-14	39.1	97.2	7.05	0.02	
2812-06	2.72	8.35E-03	3.90E-04	2.8E-14	61.1	95.0	7.05	0.02	
2812-10	2.93	2.92E-02	1.12E-03	2.5E-14	17.5	88.1	7.06	0.02	
2812-05	3.04	9.28E-03	1.46E-03	2.9E-14	55.0	85.1	7.06	0.02	
2812-04	3.00	4.51E-02	1.34E-03	2.8E-14	11.3	86.2	7.09	0.02	
2812-07	2.90	1.26E-02	9.55E-04	3.5E-14	40.4	89.5	7.09	0.02	
2812-03	2.68	7.96E-03	1.62E-04	2.4E-14	64.1	97.4	7.14	0.02	
mean			n=8	39.7	20.0	7.06	0.02	0.01	
Sanidine-reported									
HN-95-17, J7:41, RPE, J=0.001427109+0.000002									
5788-28	4.73	7.11E-03	1.23E-03	4.2E-15	71.7	92.3	11.21	0.05	
5788-27	4.47	6.07E-03	3.23E-04	3.6E-15	84.0	97.9	11.24	0.05	
5788-08	4.63	6.73E-03	8.10E-04	9.9E-15	75.8	94.8	11.27	0.04	
5788-07	4.63	9.29E-03	8.20E-04	1.2E-14	54.9	94.8	11.27	0.03	
5788-29	4.63	6.74E-03	7.98E-04	9.8E-15	75.7	94.9	11.28	0.04	
5788-19	4.81	6.90E-03	1.39E-03	7.2E-15	73.9	91.5	11.29	0.05	
5788-05	4.74	6.30E-03	1.12E-03	1.9E-14	81.0	93.0	11.31	0.04	
5788-18	4.83	6.92E-03	1.44E-03	2.2E-14	73.7	91.2	11.31	0.04	
5788-06	4.92	7.45E-03	1.74E-03	1.4E-14	68.5	89.6	11.32	0.04	
5788-33	4.79	1.22E-02	1.29E-03	8.4E-15	41.8	92.0	11.33	0.04	
5788-17	4.43	9.48E-03	4.99E-05	2.2E-15	53.8	99.7	11.33	0.08	
5788-21	4.49	5.35E-03	2.55E-04	1.2E-14	95.3	98.3	11.34	0.03	
5788-24	4.50	6.65E-03	2.62E-04	1.2E-14	76.8	98.3	11.34	0.03	
5788-23	4.62	6.10E-03	6.97E-04	1.2E-14	83.7	95.6	11.34	0.04	
5788-26	4.71	6.28E-03	9.85E-04	6.2E-15	81.2	93.8	11.34	0.04	
5788-13	4.47	6.39E-03	1.61E-04	6.4E-15	79.9	98.9	11.35	0.04	
5788-25	4.47	6.19E-03	1.75E-04	3.4E-15	82.4	98.8	11.35	0.05	
5788-22	4.71	7.05E-03	9.71E-04	6.9E-15	72.4	93.9	11.35	0.04	

Run ID#	40/39	37/39	36/39	39K moles	K/Ca	%40*	Age	\pm Err	SEM
5788-34	4.64	9.11E-03	7.24E-04	5.4E-15	56.0	95.4	11.35	0.04	
5788-14	4.49	8.32E-03	2.21E-04	1.3E-14	61.3	98.6	11.36	0.03	
5788-10	4.72	7.41E-03	9.56E-04	8.8E-15	68.9	94.0	11.39	0.04	
5788-01	4.46	7.47E-03	7.60E-05	1.1E-14	68.3	99.5	11.39	0.03	
5788-15	4.43	5.28E-03	-1.35E-05	6.1E-15	96.6	100.1	11.39	0.04	
5788-03	4.96	7.50E-03	1.77E-03	1.4E-14	68.0	89.5	11.39	0.04	
5788-09	4.67	9.22E-03	7.71E-04	4.2E-15	55.3	95.1	11.40	0.05	
5788-32	4.53	6.40E-03	2.68E-04	3.0E-15	79.7	98.3	11.42	0.06	
5788-11	4.48	5.91E-03	8.80E-05	8.5E-15	86.3	99.4	11.42	0.04	
5788-04	4.69	6.09E-03	7.86E-04	3.8E-15	83.8	95.1	11.44	0.05	
5788-30	4.57	7.00E-03	3.58E-04	1.2E-14	72.9	97.7	11.45	0.03	
5788-31	5.33	1.23E-02	2.94E-03	1.1E-14	41.5	83.7	11.46	0.04	
5788-02	4.55	6.80E-03	2.80E-04	9.6E-15	75.0	98.2	11.46	0.04	
5788-16	4.42	5.61E-03	-1.47E-04	4.0E-15	90.9	101.0	11.46	0.04	
mean		n=32		72.8	13.6	11.36	0.06	0.01	
Age Corrected for J:									
11.36									
0.07									
0.03									
Sanidine-unreported									
HN-95-17, N10:43, HN,									
J=0.00068889665+0.0000002									
6036-12	9.37	5.66E-03	1.08E-03	3.9E-15	90.1	96.6	11.21	0.04	
6036-07	9.15	7.35E-03	2.92E-04	2.6E-15	69.4	99.1	11.23	0.05	
6036-11	9.43	8.91E-03	1.18E-03	3.4E-15	57.3	96.3	11.25	0.05	
6036-10	9.34	6.56E-03	8.26E-04	7.6E-15	77.7	97.4	11.26	0.04	
6036-14	10.14	9.29E-03	3.53E-03	1.0E-14	54.9	89.7	11.27	0.04	
6036-04	10.06	1.94E-02	3.25E-03	1.2E-14	26.3	90.5	11.27	0.04	
6036-05	10.21	9.87E-03	3.75E-03	5.6E-15	51.7	89.2	11.28	0.04	
6036-13	9.16	6.32E-03	1.56E-04	6.5E-15	80.7	99.5	11.29	0.03	
6036-01	9.56	6.79E-03	1.48E-03	1.1E-14	75.1	95.4	11.30	0.04	
6036-03	9.57	1.39E-02	1.49E-03	3.0E-15	36.6	95.4	11.31	0.06	
6036-15	9.22	6.82E-03	3.04E-04	5.4E-15	74.8	99.0	11.31	0.04	
6036-06	9.42	8.01E-03	9.41E-04	5.6E-15	63.7	97.0	11.32	0.04	
6036-08	9.75	6.46E-03	2.03E-03	3.6E-15	78.9	93.9	11.34	0.05	

Run ID#	40/39	37/39	36/39	39K moles	K/Ca	%40*	Age	\pm Err	SEM
6036-09	9.45	5.48E-03	9.19E-04	2.3E-15	93.2	97.1	11.38	0.06	
6036-02	9.62	1.24E-02	1.37E-03	4.0E-15	41.1	95.8	11.42	0.04	
					n=15	64.8	19.7	11.30	0.05
					Age Corrected for J:	11.30	0.06	0.01	0.03
Sanidine									
HN-95-24, K2:41, RPE, J=0.001457364+0.000002									
5799-09	2.87	6.14E-03	2.11E-04	5.7E-15	83.1	97.8	7.37	0.03	
5799-05	2.87	6.22E-03	1.75E-04	4.6E-15	82.0	98.2	7.41	0.03	
5799-17	2.88	5.47E-03	1.66E-04	5.4E-15	93.2	98.3	7.43	0.04	
5799-20	2.87	4.77E-03	1.19E-04	6.4E-15	106.9	98.8	7.43	0.03	
5799-12	2.85	9.51E-03	4.90E-05	8.8E-15	53.6	99.5	7.45	0.03	
5799-07	2.93	5.39E-03	2.62E-04	6.9E-15	94.6	97.4	7.48	0.03	
5799-15	2.90	5.89E-03	1.68E-04	5.2E-15	86.7	98.3	7.48	0.04	
5799-04	2.88	5.86E-03	7.86E-05	6.5E-15	87.0	99.2	7.49	0.03	
5799-01	2.89	5.29E-03	1.22E-04	7.1E-15	96.5	98.8	7.49	0.03	
5799-10	2.91	5.31E-03	1.77E-04	4.6E-15	96.1	98.2	7.51	0.04	
5799-19	2.85	5.36E-03	-6.55E-05	3.6E-15	95.3	100.7	7.52	0.05	
5799-16	2.91	3.06E-02	1.23E-04	7.5E-15	16.7	98.8	7.54	0.03	
5799-18	2.92	5.41E-03	1.74E-04	8.6E-15	94.3	98.2	7.54	0.03	
5799-06	2.86	6.52E-03	-4.06E-05	3.3E-15	78.3	100.4	7.54	0.03	
5799-03	2.89	5.82E-03	4.30E-05	4.3E-15	87.7	99.6	7.56	0.05	
5799-11	2.95	5.77E-03	2.00E-04	3.5E-15	88.5	97.9	7.58	0.05	
5799-02	2.89	5.65E-03	-2.22E-05	7.4E-15	90.2	100.2	7.59	0.03	
5799-14	2.89	4.57E-03	-1.06E-04	3.9E-15	111.6	101.1	7.65	0.04	
5799-13	2.90	5.41E-03	-1.02E-04	2.5E-15	94.2	101.0	7.69	0.07	
5799-08	2.99	5.80E-03	1.77E-04	4.5E-15	88.0	98.3	7.71	0.04	
					n=20	86.2	20.0	7.52	0.09
					Age Corrected for J:	7.52	0.09	0.02	0.03
Sanidine									
HN-95-25, N6:43, HN, J=0.0006913604+0.000002									
6032-13	6.05	6.12E-03	5.09E-04	3.3E-15	83.3	97.5	7.34	0.04	
6032-12	6.05	6.72E-03	4.82E-04	2.8E-15	75.9	97.6	7.35	0.04	

Run ID#	40/39	37/39	36/39	39K moles	K/Ca	%40*	Age	\pm Err	SEM
6351-09	8.18	5.47E-03	4.64E-04	1.0E-15	93.3	98.3	11.43	0.09	
6351-23	8.19	7.96E-03	4.21E-04	6.7E-16	64.1	98.5	11.46	0.11	
6351-04	8.14	6.17E-03	2.45E-04	1.5E-15	82.7	99.1	11.47	0.07	
6351-07	8.48	7.54E-03	1.37E-03	6.4E-16	67.6	95.2	11.48	0.11	
6351-22	8.28	6.22E-03	2.55E-04	1.0E-15	82.0	99.1	11.66	0.08	
6351-15	8.24	5.82E-03	4.91E-04	5.3E-16	87.7	101.8	11.91	0.14	
6351-14	8.21	3.92E-03	-1.26E-03	4.7E-16	130.1	104.6	12.19	0.15	
6351-20	17.92	1.63E-02	2.93E-03	2.6E-15	31.2	95.2	24.15	0.07	
6351-08	17.93	1.55E-02	2.46E-03	3.8E-15	33.0	96.0	24.37	0.08	
6351-01	17.30	1.34E-02	2.85E-04	2.6E-15	38.0	99.5	24.37	0.07	
mean					n=6	82.3	14.4	0.05	0.02
				Age Corrected for J:		11.44	0.05	0.03	
Sanidine									
HN-39, O7:47, HN,				J=0.0007887975+0.000002					
6357-11	17.00	1.27E-02	1.44E-02	6.0E-16	40.3	74.9	18.03	0.19	
6357-10	14.59	6.46E-03	5.95E-03	9.9E-16	79.0	88.0	18.17	0.11	
6357-13	15.92	2.77E-02	1.03E-02	3.9E-16	18.4	81.0	18.26	0.24	
6357-08	15.17	6.18E-03	7.68E-03	4.7E-16	82.6	85.0	18.27	0.21	
6357-12	17.05	6.84E-03	1.37E-02	2.0E-15	74.6	76.3	18.42	0.11	
6357-15	15.55	6.80E-03	8.57E-03	6.9E-16	75.1	83.7	18.44	0.19	
6357-09	15.04	1.05E-02	6.79E-03	1.4E-15	48.5	86.7	18.46	0.11	
6357-01	15.44	9.48E-03	7.84E-03	1.1E-15	53.8	85.0	18.58	0.11	
6357-07	16.65	4.37E-03	1.18E-02	4.1E-16	116.7	79.0	18.63	0.21	
6357-03	13.80	6.28E-03	1.96E-03	6.3E-16	81.2	95.8	18.72	0.12	
6357-06	14.90	1.15E-02	5.04E-03	5.2E-16	44.6	90.0	18.98	0.17	
mean					n=11	65.0	26.9	0.27	0.08
				Age Corrected for J:		18.45	0.27	0.09	
Sanidine									
HN-41, K2:49, HN,				J=0.0008602+0.000002					
6586-08	10.86	8.63E-04	4.11E-03	2.5E-16	591.2	88.8	14.91	0.49	
6586-09	12.92	7.58E-03	1.09E-02	5.3E-16	67.3	75.1	14.99	0.26	
6586-13	11.32	4.87E-03	5.27E-03	3.3E-16	104.9	86.3	15.09	0.38	
6586-07	12.97	2.41E-02	1.07E-02	1.4E-15	21.2	75.6	15.15	0.13	

Run ID#	40/39	37/39	36/39	39K moles	K/Ca	%40*	Age	\pm Err	SEM
6586-14	12.37	6.57E-03	8.05E-03	1.4E-15	77.6	80.8	15.44	0.11	
6586-01	10.85	6.68E-03	2.83E-03	1.7E-15	76.4	92.3	15.48	0.11	
6586-11	10.80	5.97E-03	2.49E-03	1.5E-15	85.5	93.2	15.55	0.10	
6586-15	10.85	4.87E-03	2.63E-03	1.9E-15	104.8	92.8	15.56	0.07	
6586-12	12.58	7.20E-03	8.43E-03	1.3E-15	70.8	80.2	15.60	0.16	
6586-03	11.10	8.86E-03	3.34E-03	1.2E-15	57.6	91.1	15.63	0.13	
6586-06	12.17	9.24E-03	6.96E-03	1.5E-15	55.2	83.1	15.63	0.12	
6586-02	10.81	6.44E-03	2.29E-03	2.2E-15	79.2	93.8	15.66	0.07	
6586-04	11.76	5.41E-03	5.46E-03	7.5E-16	94.4	86.3	15.67	0.20	
6586-05	10.84	7.32E-03	2.30E-03	6.1E-16	69.7	93.7	15.71	0.21	
mean		n=10		77.1	15.3	15.59	0.09	0.03	
Age Corrected for J:				15.59	0.09	0.05			
Sanidine									
HN-45, O5:47, HN,									
6355-06	9.23	6.30E-03	9.36E-04	5.5E-16	80.9	97.0	12.70	0.15	
6355-09	9.64	2.08E-02	-3.24E-04	3.3E-16	24.6	101.0	13.80	0.17	
6355-07	9.30	1.17E-02	-1.92E-03	2.6E-16	43.7	106.1	13.99	0.26	
mean		n=3		49.7	28.7	13.50	0.70	0.40	
Age Corrected for J:				13.50	0.70	0.70	0.40		
Sanidine									
HN-46, O9:47, HN,									
6359-03	9.28	1.22E-02	1.97E-03	4.1E-16	41.7	93.7	12.34	0.17	
6359-13	9.45	1.23E-02	2.04E-03	7.1E-16	41.4	93.6	12.55	0.12	
6359-11	9.28	8.44E-03	1.03E-03	3.6E-16	60.5	96.7	12.73	0.20	
6359-14	9.41	9.93E-03	1.41E-03	7.6E-16	51.4	95.6	12.77	0.13	
6359-04	9.42	8.54E-03	1.41E-03	6.1E-16	59.8	95.6	12.77	0.14	
6359-06	9.91	1.02E-02	2.97E-03	2.6E-16	50.1	91.2	12.81	0.30	
6359-07	9.53	2.50E-02	1.70E-03	6.4E-16	20.4	94.8	12.82	0.12	
6359-12	9.86	1.03E-02	2.68E-03	8.0E-16	49.5	92.0	12.86	0.11	
6359-02	9.49	7.60E-03	1.04E-03	3.7E-16	67.2	96.8	13.02	0.19	
6359-05	9.25	7.85E-03	3.93E-05	8.0E-16	65.0	99.9	13.11	0.11	
6359-01	9.46	6.50E-03	7.53E-04	3.5E-16	78.5	97.7	13.11	0.20	
6359-09	9.22	6.43E-03	-7.15E-04	5.9E-16	79.3	102.3	13.38	0.12	

Run ID#	40/39	37/39	36/39	39K moles	K/Ca	%40*	Age	\pm Err	SEM
6359-10	9.51	8.58E-03	2.38E-04	8.8E-16	59.5	99.3	13.40	0.10	
6359-08	9.48	8.37E-03	9.62E-05	4.4E-16	60.9	99.7	13.41	0.16	
Sanidine									
HN-55, O3:47, HN, J=0.00007896136+0.0000002									
6353-10	10.84	7.47E-03	9.82E-03	1.3E-15	68.3	73.3	11.28	0.11	
6353-08	8.21	7.86E-03	8.58E-04	1.5E-15	64.9	96.9	11.30	0.06	
6353-14	8.28	7.31E-03	8.26E-04	1.4E-15	69.8	97.1	11.41	0.07	
6353-05	8.22	6.48E-03	4.67E-04	1.7E-15	78.8	68.3	11.47	0.06	
6353-06	8.23	8.59E-03	4.73E-04	1.3E-15	59.4	98.3	11.49	0.07	
6353-12	8.31	9.64E-03	5.57E-04	1.4E-15	52.9	98.0	11.57	0.07	
6353-03	8.21	6.91E-03	1.83E-04	1.2E-15	73.9	99.3	11.58	0.07	
6353-09	8.27	9.75E-03	2.98E-04	1.2E-15	52.3	98.9	11.62	0.07	
6353-04	20.07	1.58E-02	2.75E-03	2.8E-15	32.2	96.0	27.24	0.08	
6353-01	19.42	1.58E-02	2.41E-04	1.1E-15	32.3	99.6	27.35	0.11	
6353-11	20.15	1.58E-02	2.55E-03	2.3E-15	32.4	96.3	27.43	0.09	
6353-02	19.51	1.36E-02	1.61E-04	3.0E-15	37.5	99.8	27.51	0.08	
Sanidine									
HN-58, O10:47, HN, J=0.00007894725+0.0000002									
6360-13	8.28	1.24E-02	1.69E-03	1.6E-15	41.1	94.0	11.04	0.06	
6360-16	8.76	1.11E-02	3.03E-03	3.5E-15	45.9	89.8	11.16	0.05	
6360-15	9.92	1.27E-02	6.93E-03	2.0E-15	40.2	79.4	11.18	0.08	
6360-12	8.96	6.55E-03	3.61E-03	1.7E-15	78.0	88.1	11.21	0.07	
6360-08	8.47	6.38E-03	1.91E-03	3.5E-15	79.9	93.3	11.22	0.04	
6360-05	8.94	9.77E-03	3.49E-03	2.9E-15	52.2	88.5	11.23	0.05	
6360-04	8.66	9.04E-03	2.44E-03	3.7E-15	56.4	91.7	11.27	0.04	
6360-06	8.51	8.69E-03	1.89E-03	3.5E-15	58.7	93.4	11.29	0.04	
6360-03	8.46	6.15E-03	1.70E-03	1.8E-15	82.9	94.1	11.30	0.05	
6360-10	8.25	5.31E-03	9.79E-04	2.9E-15	96.0	96.5	11.30	0.04	
6360-02	8.89	7.17E-03	3.16E-03	3.6E-15	71.1	89.5	11.30	0.05	

Run ID#	40/39	37/39	36/39	39K moles	K/Ca	%40*	Age	± Err	SEM
6360-01	8.12	6.95E-03	5.45E-04	2.3E-15	73.4	98.0	11.30	0.04	
6360-09	8.87	8.27E-03	3.05E-03	3.1E-15	61.7	89.9	11.32	0.04	
6360-07	8.72	9.24E-03	2.47E-03	2.1E-15	55.2	91.6	11.35	0.06	
6360-14	8.29	6.81E-03	8.66E-04	3.0E-15	75.0	96.9	11.41	0.06	
6360-11	8.33	8.02E-03	1.01E-03	1.5E-15	63.6	96.4	11.41	0.06	
	mean	n=15		66.0	15.2	11.28	0.07	0.02	
			Age Corrected for J:		11.28	0.08	0.03		
Sanidine									
HN-59, O6:47, HN,		J=0.00078882+0.000002							
6356-17	9.22	7.88E-03	4.48E-04	2.0E-15	64.7	98.6	12.88	0.05	
6356-13	9.24	6.36E-03	4.73E-04	4.3E-16	80.2	98.5	12.90	0.18	
6356-16	9.29	7.32E-03	6.20E-04	1.2E-15	69.7	98.0	12.91	0.07	
6356-18	9.35	7.94E-03	8.13E-04	8.2E-16	64.3	97.4	12.91	0.09	
6356-01	9.73	8.28E-03	2.01E-03	1.9E-15	61.6	93.9	12.96	0.06	
6356-02	9.38	8.58E-03	5.33E-04	1.4E-15	59.4	98.3	13.08	0.07	
6356-23	9.32	6.72E-03	3.37E-04	1.3E-15	75.9	98.9	13.08	0.07	
6356-22	9.36	8.72E-03	4.24E-04	6.4E-16	58.5	98.7	13.09	0.14	
6356-19	9.39	1.39E-02	5.14E-04	1.5E-15	36.8	98.4	13.10	0.06	
6356-20	9.55	7.28E-03	1.04E-03	1.1E-15	70.1	96.8	13.10	0.08	
6356-03	9.64	7.67E-03	1.05E-03	1.3E-15	66.5	96.8	13.23	0.07	
6356-14	9.38	7.52E-03	1.66E-04	1.4E-15	67.8	99.5	13.24	0.07	
6356-12	9.34	7.83E-03	-1.08E-04	9.7E-16	65.2	100.3	13.29	0.09	
6356-24	9.29	4.54E-02	-5.73E-04	6.3E-16	11.2	101.9	13.42	0.14	
6356-25	9.48	7.60E-03	-1.11E-04	8.5E-16	67.1	100.4	13.48	0.10	
6356-21	9.57	5.24E-03	1.05E-05	8.5E-16	97.4	100.0	13.56	0.10	
	mean	n=10		64.1	11.9	13.00	0.10	0.03	
			Age Corrected for J:		13.00	0.10	0.04		

Appendix 5.b

Furnace Step-Heating Numeric Data

biotite, hornblende, and plagioclase samples
see Notes concerning column headings and abbreviations

Notes

Column Headings

Run ID#: Lists lab number (i.e. 2814), the unique designation for each sample packet within an irradiation tray; and the chronological number assigned to the mass spectrometer analysis (i.e. 04)

Temp: furnace temperature in Celsius

40/39: ratio of the measured $^{40}\text{Ar}/^{39}\text{Ar}$

37/39: ratio of the measured $^{37}\text{Ar}/^{39}\text{Ar}$

36/39: ratio of the measured $^{36}\text{Ar}/^{39}\text{Ar}$

39K moles: total moles of gas, determined from the measurement of $^{39}\text{Ar}_\text{K}$

K/Ca: a function of measured $^{39}\text{Ar}_\text{K}/^{37}\text{Ar}_\text{Ca}$

Cl/K: a function of measured $^{36}\text{Ar}_\text{Cl}/^{39}\text{Ar}_\text{K}$

%40*: radiogenic ^{40}Ar , not attributed to atmospheric composition

Age: apparent age determined for analysis in millions of years

$\pm\text{Err}$: 1 sigma analytical error of age determination

General Heading

field number of rock sample (i.e. HN-95-1);
 irradiation tray designation (i.e. M), tray hole number (i.e. 2), and
 J factor, unique correction factor for extent of irradiation,
 determined through monitor mineral age analysis

Additional Information

Lists mineral analyzed (i.e. Biotite, Plagioclase)

total gas age: this line includes the mean age all heating steps and error of the analyses, as well as the total number of analyses, i.e. n=9

Error corrected for J: error produced by irradiation inequalities added to analytical error

If multiple apparent ages were determined for the mineral separate, all are listed below the total gas age.

The "mineral age" for the mineral separate is enclosed by a box.
 The graphically determined "plateau age" is included if available.
 The "isochron age" includes the 40/36 Ar intercept and MSWD of the analyses used in the calculation.

Run ID#	Temp	J=0.001538949±600	40/39	37/39	36/39	39K moles	K/Ca	Cl/K	%40*	%39Ar	Age	± Err
HN-95-1,												
2778-01A	3	3.68E+01	3.87E-02	1.10E-01	3.6E-15	1.3E+01	2.0E-02	1.1.8	3.2	12.04	0.64	
2778-01B	3	1.86E+01	3.88E-02	4.66E-02	1.4E-15	1.3E+01	6.9E-03	25.7	4.4	13.18	0.49	
2778-01C	3	1.55E+01	3.59E-02	3.94E-02	1.1E-15	1.4E+01	1.3E-02	24.7	5.4	10.58	0.51	
2778-01D	3	9.25E+00	1.98E-02	1.86E-02	2.8E-15	2.6E+01	1.4E-02	40.4	7.8	10.36	0.20	
2778-01E	3	6.31E+00	1.08E-02	9.75E-03	7.7E-15	4.7E+01	1.3E-02	54.0	14.7	9.45	0.10	
2778-01F	3	5.27E+00	1.22E-02	6.47E-03	1.6E-14	4.2E+01	1.2E-02	63.3	28.6	9.25	0.06	
2778-01G	3	4.02E+00	2.32E-02	2.59E-03	4.2E-14	2.2E+01	1.3E-02	80.4	65.5	8.96	0.03	
2778-01H	3	3.56E+00	1.69E-02	1.08E-03	3.8E-14	3.0E+01	1.3E-02	90.4	100.0	8.93	0.03	
total gas age		n=9				1.1E-13	2.9E+01	1.5E+01				

Biotite FSH

Biotite ECH

$n/t = 1/9$	1.2×10^{-3}	2.9×10^{-3}	$1.0 \times 10^{+00}$	Error Corrected for J:	16.07	0.07
				F. Plateau Age of sample HN-2:	16.07	0.08
				% ^{39}Ar :	10.91	0.03

Run ID#	Temp	J=0.001528451±600	37/39	36/39	39K moles	K/Ca	C/K	%40*	%39Ar	Age	± Err
HN-95-3,											
2780-01A	3	8.59E+01	4.78E-02	2.83E-01	1.1E+15	2.0E-02	2.1E-02	2.8	3.1	6.71	1.58
2780-01B	3	1.89E+01	3.68E-02	5.41E-02	1.5E-15	1.4E+01	2.0E-02	15.1	5.5	7.86	0.54
2780-01C	3	1.08E+01	2.19E-02	2.41E-02	4.3E-15	2.3E+01	2.1E-02	33.9	12.2	10.05	0.24
2780-01D	3	6.91E+00	1.20E-02	8.41E-03	1.4E-14	4.3E+01	2.0E-02	63.7	33.8	12.09	0.08
2780-01E	3	6.46E+00	1.13E-02	7.18E-03	1.6E-14	4.5E+01	2.0E-02	66.8	59.0	11.87	0.07
2780-01F	3	6.89E+00	2.24E-02	8.82E-03	1.1E-14	2.3E+01	2.1E-02	61.9	75.6	11.73	0.09
2780-01G	3	5.87E+00	3.41E-01	6.26E-03	8.8E-15	1.5E+00	2.8E-02	68.6	89.4	11.06	0.08
2780-01H	3	5.15E+00	1.43E-01	3.41E-03	6.6E-15	3.6E+00	2.6E-02	80.2	99.7	11.35	0.08
2780-01I	3	2.31E+01	1.27E+00	4.55E-02	1.6E-16	4.0E-01	2.5E-02	42.0	100.0	26.57	2.27
total gas age	n=9		6.4E-14	2.7E+01	1.7E+01					11.39	0.15

Biotite FSH

Run ID#	Temp	J=0.00152562±600	37/39	36/39	39K moles	K/Ca	C/K	%40*	%39Ar	Age	± Err
HN-95-4,											
2781-01A	3	4.67E+01	7.51E-02	1.54E-01	1.8E-15	6.8E+00	2.9E-02	2.5	0.9	3.26	0.91
2781-01B	3	2.25E+01	6.18E-02	6.69E-02	1.2E-15	8.3E+00	3.0E-02	12.1	1.5	7.46	0.52
2781-01C	3	1.36E+01	3.77E-02	3.49E-02	2.5E-15	1.4E+01	2.9E-02	23.8	2.7	8.88	0.30
2781-01D	3	6.32E+00	2.58E-02	1.01E-02	7.2E-15	2.0E+01	2.7E-02	52.3	6.2	9.07	0.10
2781-01E	3	5.21E+00	2.99E-02	6.23E-03	1.8E-14	1.7E+01	2.7E-02	64.3	14.9	9.19	0.05
2781-01F	3	5.56E+00	1.40E-01	4.25E-03	3.3E-14	3.7E+00	4.8E-02	77.2	30.8	11.77	0.04
2781-01G	3	4.10E+00	8.85E-02	2.12E-03	8.7E-14	5.8E+00	3.2E-02	84.4	73.1	9.51	0.03
2781-01H	3	3.54E+00	2.63E-02	8.99E-04	5.5E-14	1.9E+01	2.5E-02	91.9	99.9	8.92	0.02
2781-01I	3	4.15E+01	3.96E+00	8.88E-02	1.5E-16	1.3E-01	2.2E-01	37.5	100.0	42.44	2.48
total gas age	n=9		2.1E-13	1.1E+01	7.2E+00					9.62	0.05

Biotite FSH

n/t=2/9	F. Plateau Age of sample HN-3:	11.82	0.18
% ³⁹ Ar:		41.80	

Error Corrected for J:

69.10

Error Corrected for J:

9.20

Error Corrected for J:

9.62

Error Corrected for J:

0.30

Run ID#	Temp	J=0.001520174±749	40/39	37/39	36/39	39K moles	K/Ca	Cl/K	%40*	%39Ar	Age	± Err
HN-95-5,												
2793-01A	3	8.28E+01	9.58E-01	2.28E-01	1.1E-15	5.3E-01	2.1E-02	18.8	3.6	42.21	1.47	
2793-01B	3	6.47E+01	1.88E+00	3.90E-02	3.1E-16	2.7E-01	2.0E-02	82.3	4.6	140.58	1.66	
2793-01C	3	9.77E+01	3.18E+00	3.69E-02	2.9E-16	1.6E-01	3.1E-02	89.1	5.5	224.63	1.87	
2793-01D	3	8.22E+01	6.17E+00	3.32E-02	1.1E-15	8.3E-02	5.6E-02	88.6	8.9	190.11	0.79	
2793-01E	3	1.48E+01	8.20E+00	1.66E-02	7.8E-15	6.2E-02	6.5E-02	71.0	33.7	28.75	0.17	
2793-01F	3	6.03E+00	8.30E+00	8.23E-03	1.2E-14	6.1E-02	6.1E-02	69.9	71.3	11.58	0.10	
2793-01G	3	9.44E+00	9.02E+00	9.96E-03	6.4E-15	5.7E-02	8.0E-02	75.9	91.5	19.68	0.14	
2793-01H	3	1.04E+01	9.47E+00	8.04E-03	2.4E-15	5.4E-02	8.9E-02	83.9	99.2	23.96	0.23	
2793-01I	3	2.31E+01	1.12E+01	4.20E-02	1.3E-16	4.5E-02	1.3E-01	49.9	99.6	31.54	3.06	
2793-01J	3	2.74E+01	7.94E+00	4.40E-02	1.2E-16	6.4E-02	8.6E-02	54.8	100.0	41.00	3.43	
total gas age	n=10				3.1E-14	8.1E-02	1.6E-01			28.98	0.26	

Hornblende FSH

Run ID#	Temp	J=0.001533098±749	40/39	37/39	36/39	39K moles	K/Ca	Cl/K	%40*	%39Ar	Age	± Err
HN-95-6,												
2792-01A	3	4.40E+01	8.85E-01	1.00E-01	2.4E-15	5.8E-01	4.9E-02	32.8	7.8	39.59	0.66	
2792-01B	3	1.75E+01	1.02E+00	6.66E-03	1.6E-15	5.0E-01	4.4E-02	89.1	12.8	42.58	0.32	
2792-01C	3	1.81E+01	1.21E+00	5.22E-03	1.4E-15	4.2E-01	4.3E-02	91.9	17.2	45.40	0.28	
2792-01D	3	1.87E+01	2.52E+00	8.16E-03	1.8E-15	2.0E-01	5.4E-02	88.1	23.0	45.17	0.25	
2792-01E	3	2.12E+01	3.93E+00	1.06E-02	3.7E-15	1.3E-01	5.7E-02	86.6	34.9	50.17	0.19	
2792-01F	3	8.22E+00	7.55E+00	1.33E-02	1.6E-14	6.8E-02	6.1E-02	58.9	87.4	13.40	0.09	
2792-01G	3	1.13E+01	7.34E+00	7.19E-03	2.5E-15	7.0E-02	8.2E-02	86.0	95.4	26.92	0.21	
2792-01H	3	8.40E+00	8.30E+00	6.69E-03	1.2E-15	6.1E-02	7.5E-02	83.8	99.2	19.46	0.32	
2792-01I	3	2.52E+01	5.77E+00	4.53E-02	1.8E-16	8.8E-02	4.4E-02	48.5	99.8	33.64	2.00	
2792-01J	3	4.36E+01	1.01E+01	1.12E-01	7.4E-17	5.1E-02	1.0E-01	26.1	100.0	31.45	5.41	
total gas age	n=10				3.1E-14	1.6E-01	2.0E-01			26.00	0.22	

Hornblende FSH

Run ID#	Temp	J=0.001533098±749	40/39	37/39	36/39	39K moles	K/Ca	Cl/K	%40*	%39Ar	Age	± Err
HN-95-6,												
2792-01A	3	3.1E-14	1.6E-01	2.0E-01	3.1E-14	1.6E-01	2.0E-01	32.8	7.8	39.59	0.66	

Run ID#	Temp	$J=0.001519856 \pm 599$	40/39	37/39	36/39	39K moles	K/Ca	C/I/K	%40*	%39Ar	Age	$\pm Err$
HN-95-7,												
2782-01A	3	2.80E+01	8.74E-02	8.92E-02	3.5E-15	5.8E+00	1.7E-02	5.9	1.4	4.51	0.52	
2782-01B	3	9.79E+00	5.17E-02	2.53E-02	2.8E-15	9.9E+00	2.2E-02	23.5	2.6	6.29	0.24	
2782-01C	3	7.35E+00	4.84E-02	1.54E-02	4.6E-15	1.1E+01	2.6E-02	37.8	4.5	7.60	0.14	
2782-01D	3	5.07E+00	3.43E-02	6.55E-03	1.1E-14	1.5E+01	2.6E-02	61.4	9.0	8.51	0.07	
2782-01E	3	4.47E+00	2.91E-02	4.56E-03	2.5E-14	1.8E+01	2.5E-02	69.4	19.3	8.48	0.04	
2782-01F	3	4.33E+00	9.55E-02	4.14E-03	3.8E-14	5.3E+00	2.7E-02	71.5	34.8	8.47	0.03	
2782-01G	3	3.93E+00	2.26E-01	2.56E-03	1.1E-13	2.3E+00	3.0E-02	80.7	79.0	8.68	0.03	
2782-01H	3	3.65E+00	1.17E-01	1.39E-03	5.1E-14	4.4E+00	2.8E-02	88.4	99.9	8.83	0.02	
2782-01I	3	4.39E+01	7.91E+00	1.04E-01	1.2E-16	6.5E-02	2.3E-01	31.1	100.0	37.29	3.27	
total gas age	n=9				2.4E-13	5.6E+00	5.8E+00			8.56	0.04	
Biotite FSH												
HN-9,	D12:47,	$J=0.00079009 \pm 0.000002$										
6362-01A	650	5.30E+03	2.76E-02	1.79E+01	9.8E-17	1.8E+01	-2.3E-02	0.4	0.2	29.29	122.54	
6362-01B	750	9.19E+02	1.05E-02	2.99E+00	1.0E-17	4.9E+01	2.7E-02	3.7	0.3	48.44	95.18	
6362-01C	850	1.07E+03	1.29E-01	4.04E+00	2.9E-15	4.0E+00	8.5E-02	-11.1	7.3	0.00	0.00	
6362-01D	920	6.95E+01	2.10E-02	2.01E-01	7.6E-15	2.4E+01	4.3E-04	14.7	26.1	14.51	0.59	
6362-01E	1000	2.95E+01	2.00E-02	6.53E-02	1.2E-14	2.5E+01	3.9E-04	34.6	56.0	14.48	0.22	
6362-01F	1075	2.07E+01	2.30E-02	3.66E-02	8.2E-15	2.2E+01	2.6E-04	47.9	76.2	14.10	0.13	
6362-01G	1110	1.91E+01	3.55E-02	3.10E-02	3.5E-15	1.4E+01	1.8E-04	52.0	84.8	14.10	0.15	
6362-01H	1180	1.74E+01	1.23E-01	2.56E-02	2.5E-15	4.1E+00	2.7E-04	56.6	90.8	14.02	0.14	
6362-01I	1210	1.48E+01	2.48E-01	1.67E-02	1.9E-15	2.1E+00	3.1E-04	66.7	95.5	14.05	0.11	
6362-01J	1250	1.31E+01	3.29E-01	1.06E-02	1.5E-15	1.6E+00	6.1E-04	76.2	99.0	14.13	0.11	
6362-01K	1300	1.68E+01	1.67E-01	2.29E-02	3.6E-16	3.1E+00	-2.5E-04	59.8	99.9	14.25	0.35	
6362-01L	1650	4.27E+02	1.50E+00	1.43E+00	2.3E-17	3.4E-01	6.0E-03	1.3	100.0	8.17	22.41	
total gas age	n=12				4.1E-14	1.9E+01	1.5E+01			13.33	0.57	
F. Plateau Age of sample HN-7:								8.66	0.14			
n/t=5/9								90.90				
% ^{39}Ar :												
Error Corrected for J:								8.56	0.05			

Run ID#	Temp	40/39	37/39	36/39	39K moles	K/Ca	Cl/K	%40*	%39Ar	Age	\pm Err
Biotite FSH					n/t=9/12	Plateau Age of sample HN-9:		14.20	0.08		
					% ³⁹ Ar:	92.70					
							Isochron analysis:	14.06	0.09		
							⁴⁰ Ar/ ³⁶ Ar Intercept:	299.20	1.70		
							MSWD:	0.52			
HN-95-12, N1:43,											
	J=0.00007015265±0.0000002										
6027-01A	550	1.84E+04	2.06E-01	5.91E+01	2.1E-16	2.5E+00	8.7E-02	5.2	0.7	921.07	406.82
6027-01B	650	2.16E+03	2.43E-02	6.97E+00	1.3E-16	2.1E+01	7.6E-03	4.8	1.2	126.63	38.04
6027-01C	750	1.60E+03	4.40E-02	5.15E+00	2.8E-16	1.2E+01	1.2E-02	5.0	2.2	99.52	21.77
6027-01D	850	6.50E+02	2.64E-02	2.05E+00	1.9E-15	1.9E+01	5.6E-03	6.7	8.9	54.20	5.35
6027-01E	950	1.21E+02	1.55E-02	3.54E-01	7.0E-15	3.3E+01	1.2E-03	13.5	33.9	20.55	0.95
6027-01F	1050	3.76E+01	1.59E-02	9.31E-02	8.0E-15	3.2E+01	3.9E-04	26.8	62.0	12.69	0.26
6027-01G	1150	2.26E+01	2.83E-02	4.57E-02	4.7E-15	1.8E+01	6.6E-04	40.1	78.8	11.41	0.16
6027-01H	1250	1.64E+01	1.11E-01	2.66E-02	3.1E-15	4.6E+00	5.4E-04	52.2	89.9	10.82	0.11
6027-01I	1350	1.28E+01	1.64E-01	1.46E-02	2.8E-15	3.1E+00	7.4E-04	66.5	99.9	10.77	0.09
6027-01J	1450	1.13E+01	2.85E-01	-5.36E-03	4.9E-17	1.8E+00	1.1E-03	114.2	100.0	16.30	2.24
6027-01K	1650	6.23E+01	0.00E+00	1.34E-01	-7.2E-18	0.0E+00	-4.7E-02	36.3	100.0	28.39	19.16
					n=11	2.8E-14	2.3E+01	1.2E+01		24.92	4.11
							F. Plateau Age of sample HN-12:	10.89	0.18		
							% ³⁹ Ar:	45.00			
							Isochron analysis:	10.36	0.04		
							⁴⁰ Ar/ ³⁶ Ar Intercept:	309.70	0.70		
							MSWD:	1.90			
Biotite											
HN-16B, K6:50, RPE,											
	J=0.000086343±0.0000002										
6580-01A	650	2.75E+02	3.07E-02	8.99E-01	9.4E-16	1.7E+01	9.1E-04	3.4	1.9	14.30	2.78
6580-01B	750	9.27E+01	2.20E-02	2.88E-01	7.0E-16	2.3E+01	2.1E-04	8.2	3.3	11.87	0.96
6580-01C	850	6.43E+01	8.92E-03	1.94E-01	7.2E-16	5.7E+01	-2.7E-04	10.9	4.8	10.93	0.83
6580-01D	920	2.66E+01	5.72E-03	6.25E-02	1.4E-15	8.9E+01	3.9E-04	30.5	7.7	12.58	0.24
6580-01E	1000	1.96E+01	9.15E-03	3.98E-02	2.8E-15	5.6E+01	3.6E-04	40.0	13.3	12.19	0.15

Run ID#	Temp	40/39	37/39	36/39	39K moles	K/Ca	C/K	%40*	%39Ar	Age	\pm Err
6580-01F	1075	1.68E+01	1.59E-02	2.92E-02	6.5E-15	3.2E+01	3.2E-04	48.7	26.4	12.70	0.12
6580-01G	1110	1.29E+01	2.19E-02	1.70E-02	4.5E-15	2.3E+01	3.0E-04	61.1	35.6	12.23	0.09
6580-01H	1180	1.19E+01	4.13E-02	1.35E-02	1.2E-14	1.2E+01	3.8E-04	66.5	60.6	12.32	0.06
6580-01I	1210	9.77E+00	3.35E-02	6.47E-03	1.9E-14	1.5E+01	2.2E-04	80.4	98.7	12.20	0.04
6580-01J	1250	1.07E+01	9.03E-02	9.75E-03	5.8E-16	5.6E+00	9.4E-05	73.2	99.8	12.18	0.18
6580-01K	1300	1.02E+02	1.07E+00	3.41E-01	8.7E-18	4.8E-01	-6.6E-04	1.6	99.9	2.58	17.13
6580-01L	1650	5.17E+01	5.15E-01	1.45E-01	7.0E-17	9.9E-01	-1.6E-03	17.3	100.0	13.93	1.94
total gas age		n=12	5.0E-14	2.3E+01	2.7E+01	Plateau Age of sample HN-16:		13.23	12.32	0.16	
Biotite FSH		n/t=6/12	% ³⁹ Ar:			% ³⁹ Ar:		0.05	0.05		
n/t=12/12						73.60	Isochron analysis:	12.23	0.04		
							⁴⁰ Ar/ ³⁶ Ar Intercept:	297.10	1.10		
							MSWD:	2.35			
Biotite											
HN-95-18,	N4.43,	J=0.0006970915±0.000002									
6030-01A	700	8.65E+02	1.36E-01	2.80E+00	8.7E-17	3.8E+00	8.9E-03	4.3	0.6	45.88	14.53
6030-01B	850	3.30E+02	5.29E-02	1.04E+00	2.5E-16	9.6E+00	2.0E-03	7.2	2.2	29.75	4.37
6030-01C	950	4.19E+01	2.05E-02	1.06E-01	3.7E-16	2.5E+01	3.9E-04	25.4	4.6	13.31	0.57
6030-01D	1050	2.36E+01	1.17E-02	4.51E-02	7.4E-16	4.4E+01	2.0E-04	43.6	9.4	12.90	0.25
6030-01E	1150	1.49E+01	2.21E-02	1.83E-02	2.2E-15	2.3E+01	3.9E-04	63.8	24.0	11.94	0.11
6030-01F	1250	1.17E+01	2.24E-02	7.53E-03	1.0E-14	2.3E+01	2.7E-04	80.9	90.2	11.83	0.05
6030-01G	1350	1.11E+01	8.47E-03	5.70E-03	1.5E-15	6.0E+01	2.7E-04	84.8	99.9	11.75	0.10
6030-01H	1450	1.78E+01	0.00E+00	8.89E-02	1.2E-17	0.0E+00	3.5E-03	-47.5	100.0	-10.67	7.99
6030-01I	1650	6.49E+01	0.00E+00	4.65E-02	7.5E-18	0.0E+00	-9.9E-03	78.8	100.0	63.16	12.84
total gas age		n=9	1.5E-14	2.7E+01	2.1E+01	Plateau Age of sample HN-18:		12.42	0.25		
Biotite FSH		n/t=2/9	% ³⁹ Ar:			% ³⁹ Ar:		11.20	0.06		
n/t=8/9						76.10	Isochron analysis:	12.06	0.06		
							⁴⁰ Ar/ ³⁶ Ar Intercept:	307.40	2.10		
							MSWD:	2.06			

Run ID#	Temp	40/39	37/39	36/39	39K moles	K/Ca	Ci/K	%40*	%39Ar	Age	± Err
Plag FSH		n/t=2/11	Plateau Age of sample HN-20:			% ³⁹ Ar:				17.50	0.30
						% ³⁹ Ar:					
Biotite											
HN-95-24, N11:43,		J=0.0006905068±0.000002									
6037-01A	650	7.72E+02	1.55E-01	2.44E+00	1.8E-16	3.3E+00	7.1E-03	6.5	0.7	61.40	10.44
6037-01A	650	7.72E+02	1.55E-01	2.44E+00	1.8E-16	3.3E+00	7.1E-03	6.5	1.3	61.40	10.44
6037-01B	800	6.44E+01	4.55E-02	1.87E-01	4.7E-16	1.1E+01	1.6E-03	14.3	3.0	11.44	0.78
6037-01C	850	1.80E+01	2.14E-02	3.45E-02	4.2E-16	2.4E+01	2.9E-04	43.3	4.5	9.65	0.37
6037-01D	950	1.26E+01	1.85E-02	1.81E-02	1.4E-15	2.8E+01	4.1E-04	57.6	9.5	9.01	0.11
6037-01E	1050	9.32E+00	9.65E-03	8.33E-03	4.2E-15	5.3E+01	6.1E-04	73.6	24.6	8.53	0.05
6037-01F	1150	8.10E+00	2.36E-02	4.53E-03	6.4E-15	2.2E+01	3.2E-04	83.5	47.7	8.41	0.04
6037-01G	1200	8.02E+00	4.70E-02	3.89E-03	5.6E-15	1.1E+01	3.6E-04	85.7	67.8	8.55	0.03
6037-01H	1250	7.70E+00	3.13E-02	2.74E-03	6.9E-15	1.6E+01	3.4E-04	89.5	92.8	8.57	0.03
6037-01I	1350	7.58E+00	1.03E-02	1.85E-03	2.0E-15	4.9E+01	3.4E-04	92.8	100.1	8.74	0.05
6037-01J	1450	-5.60E+01	4.37E-01	-1.71E-01	-7.7E-18	1.2E+00	3.2E-02	9.5	100.1	-6.62	12.81
6037-01K	1650	-1.16E+01	0.00E+00	-5.37E-02	-1.4E-17	0.0E+00	-7.2E-03	-37.1	100.0	5.34	5.27
total gas age		n=12		2.8E-14		2.5E+01	1.8E+01			9.31	0.19
Biotite FSH											
Plagioclase											
HN-95-29, N4:41,		J=0.001417651±0.000002									
5847-01A	550	-3.79E+02	5.53E-01	-7.44E-01	-8.5E-19	9.2E-01	-1.3E-01	42.0	0.0	0.00	0.00
5847-01B	650	1.45E+03	0.00E+00	3.83E+00	1.4E-18	0.0E+00	-9.4E-02	21.8	0.0	667.38	1401.92
5847-01C	750	8.07E+01	3.35E+00	2.46E-01	1.0E-16	1.5E-01	1.8E-03	10.2	0.4	21.00	3.88
5847-01D	825	1.47E+01	4.48E+00	3.41E-02	4.8E-16	1.1E-01	5.8E-04	33.9	2.1	12.77	0.66
5847-01E	900	8.13E+00	5.60E+00	1.25E-02	7.5E-16	9.1E-02	5.4E-04	59.8	4.8	12.44	0.31
5847-01F	1000	6.06E+00	6.41E+00	4.75E-03	1.9E-15	8.0E-02	2.5E-04	84.9	11.5	13.17	0.16
5847-01G	1100	5.57E+00	6.55E+00	3.53E-03	2.6E-15	7.8E-02	3.3E-04	90.3	20.9	12.87	0.09
Isochron analysis:											
n/t=11/11			40Ar/ ³⁶ Ar Intercept:			MSWD:			8.47		
n/t=3/11			Plateau Age of sample HN-24:			58.60			58.60		
n/t=11/11			Isochron analysis:			314.50			3.00		
			MSWD:			2.31					

Run ID#	Temp	40/39	37/39	36/39	39K moles	K/Ca	C/K	%40*	%39Ar	Age	± Err
5847-01H	1250	5.43E+00	6.06E+00	2.41E-03	7.9E-15	8.4E-02	3.1E-04	95.5	49.4	13.26	0.06
5847-01I	1450	7.18E+00	5.72E+00	5.44E-03	5.3E-15	8.9E-02	1.1E-04	83.7	68.3	15.38	0.09
5847-01J	1650	7.60E+00	6.48E+00	6.02E-03	7.9E-15	7.9E-02	3.5E-04	83.1	96.6	16.15	0.08
5847-01K	1750	1.23E+01	5.89E+00	2.32E-02	9.6E-16	8.7E-02	5.7E-04	48.0	100.0	15.14	0.33
Plag FSH		total gas age		n=11	2.8E-14	8.4E-02	2.6E-01			14.53	0.19
n/t=6/11		n/t=3/11		F. Plateau Age of sample HN-29:		% ³⁹ Ar:		Isochron analysis:		13.13	0.11
n/t=9/11		n/t=3/11		Isochron analysis:		% ³⁹ Ar:		13.23		49.00	0.04
Biotite		40Ar/ ³⁶ Ar Intercept:		MSWD:		40Ar/ ³⁶ Ar Intercept:		13.23		49.00	0.04
HN-95-31, N1443,		J=0.0006982996±0.000002		MSWD:		MSWD:		1.53		4.60	
6040-01A	700	4.33E+03	9.82E-02	1.38E+01	2.9E-16	5.2E+00	2.2E-02	6.1		305.39	54.86
6040-01B	800	3.00E+02	1.62E-02	9.21E-01	6.6E-16	3.1E+01	3.0E-03	9.3		3.9	34.84
6040-01C	850	5.31E+01	8.86E-03	1.30E-01	9.4E-16	5.8E+01	9.9E-04	27.8		7.8	2.65
6040-01D	950	2.76E+01	6.86E-03	5.06E-02	3.3E-15	7.4E+01	3.5E-04	45.7		21.3	0.46
6040-01E	1050	1.86E+01	6.81E-03	2.25E-02	5.8E-15	7.5E+01	3.1E-04	64.2		15.81	0.18
6040-01F	1150	1.86E+01	4.24E-02	2.37E-02	3.7E-15	1.2E+01	4.4E-04	62.4		45.2	14.94
6040-01G	1200	1.75E+01	6.13E-02	1.89E-02	3.8E-15	8.3E+00	2.8E-04	68.1		60.4	14.56
6040-01H	1250	1.45E+01	2.03E-02	1.03E-02	4.8E-15	2.5E+01	1.9E-04	79.2		76.2	14.93
6040-01I	1350	1.40E+01	3.32E-03	7.84E-03	9.1E-16	1.5E+02	6.1E-04	83.4		95.8	14.45
6040-01J	1450	1.30E+01	0.00E+00	-9.03E-03	1.0E-16	0.0E+00	-1.7E-03	120.5		100.0	0.06
6040-01K	1650	2.29E+01	4.12E+00	-1.53E-01	-7.7E-19	1.2E-01	-3.9E-01	298.9		100.0	0.14
total gas age		n=11		Plateau Age of sample HN-31:		4.5E+01		4.7E+01		84.34	129.25
Biotite FSH		n/t=3/11		Isochron analysis:		% ³⁹ Ar:		14.66		19.08	0.84
n/t=9/11		Isochron analysis:		% ³⁹ Ar:		14.70		54.90		1.60	

Run ID#	Temp	40/39	37/39	36/39	39K moles	K/Ca	C/K	%40*	%39Ar	Age	± Err
Plagioclase											
HN-95-31, N3:41,		J=0.001416915±0.0000002									
5846-01A	550	1.43E+03	4.25E+00	4.44E+00	4.7E-18	1.2E-01	0.0E+00	8.0	0.0	272.90	490.02
5846-01B	650	7.72E+03	7.09E+00	2.48E+01	1.6E-18	7.2E-02	0.0E+00	5.0	0.0	792.30	7645.58
5846-01C	750	1.40E+02	4.49E+00	4.41E-01	2.1E-16	1.1E-01	0.0E+00	7.2	0.6	25.55	4.43
5846-01D	825	1.55E+01	5.50E+00	3.37E-02	5.5E-16	9.3E-02	1.9E-04	38.3	2.3	15.15	0.60
5846-01E	900	8.75E+00	6.09E+00	1.56E-02	4.6E-16	8.4E-02	1.2E-03	52.6	3.6	11.77	0.62
5846-01F	1000	7.66E+00	6.78E+00	9.78E-03	3.4E-15	7.5E-02	3.9E-04	69.1	13.7	13.54	0.14
5846-01G	1100	5.62E+00	6.58E+00	3.51E-03	5.2E-15	7.8E-02	2.6E-04	90.5	29.0	13.03	0.08
5846-01H	1250	5.91E+00	5.89E+00	3.85E-03	9.0E-15	8.7E-02	4.5E-04	88.4	55.4	13.37	0.07
5846-01I	1450	8.25E+00	5.09E+00	9.05E-03	7.7E-15	1.0E-01	2.6E-04	72.3	78.1	15.24	0.09
5846-01J	1650	8.86E+00	6.08E+00	9.51E-03	7.4E-15	8.4E-02	2.7E-04	73.6	100.0	16.66	0.09
total gas age											
	n=10			3.4E-14	8.7E-02	1.6E-02			14.64	0.56	

Biotite

HN-95-32, N13:43,		J=0.00069608±0.0000002									
6039-01A	700	2.56E+04	3.72E-01	8.22E+01	2.7E-16	1.4E+00	1.2E-01	5.3	1.4	1194.63	1186.37
6039-01B	800	6.47E+03	6.62E-02	2.09E+01	2.6E-16	7.7E+00	2.1E-02	4.5	2.8	333.88	114.74
6039-01C	850	1.45E+03	3.43E-02	4.62E+00	1.1E-15	1.5E+01	8.1E-03	5.8	8.6	102.22	12.75
6039-01D	950	3.51E+02	2.02E-02	1.08E+00	2.6E-15	2.5E+01	2.1E-03	8.7	22.0	37.95	2.75
6039-01E	1050	1.19E+02	1.45E-02	3.42E-01	6.0E-15	3.5E+01	8.9E-04	15.2	52.9	22.60	0.95
6039-01F	1150	5.09E+01	2.74E-02	1.27E-01	4.7E-15	1.9E+01	1.8E-04	26.4	77.3	16.79	0.37
6039-01G	1200	4.69E+01	1.16E-01	1.15E-01	1.5E-15	4.4E+00	-7.0E-05	27.6	85.1	16.21	0.39
6039-01H	1250	3.43E+01	1.24E-01	7.31E-02	1.5E-15	4.1E+00	-2.5E-04	37.1	92.7	15.92	0.28
6039-01I	1350	2.68E+01	1.67E-01	4.91E-02	1.4E-15	3.1E+00	4.1E-04	46.0	100.0	15.41	0.24
6039-01J	1450	-2.24E+02	0.00E+00	-1.39E+00	-8.5E-19	0.0E+00	6.5E-02	-83.6	100.0	221.39	703.79
6039-01K	1650	-7.86E+01	0.00E+00	-3.78E-01	-1.5E-18	0.0E+00	9.0E-02	-42.3	100.0	41.26	163.51
total gas age											
	n=11			1.9E-14	2.1E+01	1.2E+01			47.02	19.74	

Biotite FSH

n/t=4/11	F. Plateau Age of sample HN-32:	16.10	0.40
	% ³⁹ Ar:	47.10	
	⁴⁰ Ar/ ³⁶ Ar Intercept:	14.31	0.22
	MSWD:	314.20	1.40
		0.46	

6500, 6000, 4000, 1000,

Plagioclase	HN-95-33, N2	Plagioclase
5845-01A		
5845-01B		
5845-01C		
5845-01D		
5845-01E		
5845-01F		
5845-01G		
5845-01H		
5845-01I		
5845-01J		

$n/t = 3/10$	Plateau Age of sample HN-33:	14.27	0.12
	$\%^{39}\text{Ar}$:	13.13	0.06
		54.50	

Run ID#	Temp	40/39	37/39	36/39	39K moles	K/Ca	C/K	%40*	%39Ar	Age	\pm Err
Biotite FSH						n/t=5/12	Plateau % ³⁹ Ar:			17.46	0.06
						n/t=12/12	Isochron analysis:			70.90	
							⁴⁰ Ar/ ³⁶ Ar	Intercept:		17.43	0.05
								MSWD:		295.30	2.70
										1.87	
Biotite											
HN-43, K3.50, RPE,		J=0.00086423±0.000002									
6577-01A	650	2.55E+02	2.48E-02	8.45E-01	6.3E-16	2.1E+01	1.1E-03	2.0	2.8	7.79	2.63
6577-01B	750	1.44E+02	1.48E-02	4.52E-01	8.1E-16	3.4E+01	6.9E-04	7.0	6.3	15.67	1.47
6577-01C	850	4.22E+01	9.40E-03	1.09E-01	5.4E-16	5.4E+01	1.8E-04	23.9	8.7	15.69	0.53
6577-01D	920	2.98E+01	6.37E-03	6.01E-02	3.3E-15	8.0E+01	2.5E-04	40.4	23.1	18.64	0.22
6577-01E	1000	3.90E+01	8.75E-03	9.18E-02	3.3E-15	5.8E+01	6.6E-04	30.5	37.6	18.45	0.33
6577-01F	1075	2.17E+01	7.49E-03	3.41E-02	3.8E-15	6.8E+01	2.6E-04	53.5	54.4	18.02	0.14
6577-01G	1110	1.69E+01	1.42E-02	1.81E-02	1.9E-15	3.6E+01	3.2E-04	68.4	62.8	17.95	0.13
6577-01H	1180	1.44E+01	2.71E-02	9.69E-03	5.3E-15	1.9E+01	2.4E-04	80.1	85.8	17.88	0.07
6577-01I	1210	1.37E+01	1.18E-02	5.92E-03	2.9E-15	4.3E+01	7.1E-04	87.2	93.5	18.50	0.07
6577-01J	1250	1.62E+01	1.97E-02	1.10E-02	2.4E-16	2.6E+01	1.6E-03	79.9	99.5	20.08	0.37
6577-01K	1300	3.69E+01	2.30E-01	8.61E-02	2.8E-17	2.2E+00	-4.1E-03	31.1	99.6	17.80	3.02
6577-01L	1650	4.75E+01	3.23E-01	1.20E-01	8.2E-17	1.6E+00	7.4E-04	25.3	100.0	18.69	1.58
total gas age											
						n=12	2.3E-14	4.8E+01	2.5E+01	17.80	0.29
						n/t=5/12	Plateau % ³⁹ Ar:			17.94	0.09
Biotite FSH											
HN-45, D11:47,		J=0.00078979±0.000002									
6361-01A	650	8.82E+02	5.97E+00	5.24E+00	1.3E-19	8.5E-02	4.0E-01	-75.5	0.0	0.00	0.00
6361-01B	750	6.08E+03	0.00E+00	2.07E+01	3.6E-18	0.0E+00	4.5E-03	-0.5	0.0	0.00	0.00
6361-01C	850	1.75E+02	7.42E-02	5.73E-01	4.6E-16	6.9E+00	1.1E-03	3.0	0.9	7.39	2.12
Biotite											
HN-45, D11:47,		J=0.00078979±0.000002									
6361-01A	650	8.82E+02	5.97E+00	5.24E+00	1.3E-19	8.5E-02	4.0E-01	-75.5	0.0	0.00	0.00
6361-01B	750	6.08E+03	0.00E+00	2.07E+01	3.6E-18	0.0E+00	4.5E-03	-0.5	0.0	0.00	0.00
6361-01C	850	1.75E+02	7.42E-02	5.73E-01	4.6E-16	6.9E+00	1.1E-03	3.0	0.9	7.39	2.12

Run ID#	Temp	40/39	37/39	36/39	39K moles	K/Ca	Cl/K	%40*	%39Ar	Age	$\pm E_{rr}$
6361-01D	920	2.38E+01	2.66E-02	4.48E-02	1.7E-15	1.9E+01	7.6E-04	44.4	4.0	15.02	0.22
6361-01E	1000	1.39E+01	1.37E-02	1.19E-02	5.0E-15	3.7E+01	2.1E-04	74.9	13.3	14.81	0.07
6361-01F	1075	1.24E+01	9.99E-03	7.19E-03	6.9E-15	5.1E+01	3.5E-04	82.9	26.3	14.65	0.06
6361-01G	1110	1.21E+01	1.56E-02	6.18E-03	6.6E-15	3.3E+01	1.1E-04	85.0	38.6	14.63	0.05
6361-01H	1180	1.29E+01	6.76E-02	8.44E-03	6.8E-15	7.5E+00	3.7E-04	80.6	51.3	14.72	0.06
6361-01I	1210	1.24E+01	8.17E-02	6.90E-03	8.5E-15	6.2E+00	3.2E-04	83.6	67.2	14.77	0.06
6361-01J	1250	1.18E+01	4.29E-02	4.54E-03	1.3E-14	1.2E+01	3.0E-04	88.7	91.9	14.86	0.05
6361-01K	1300	1.18E+01	2.11E-02	4.35E-03	4.3E-15	2.4E+01	4.0E-04	89.1	99.9	14.94	0.05
6361-01L	1650	2.08E+02	9.03E-01	6.63E-01	4.8E-17	5.7E-01	-4.1E-04	6.0	100.0	17.68	6.37
total gas age		n=12	5.3E-14	2.2E+01	1.7E+01					14.72	0.09
Biotite FSH		n/t=4/12	Plateau Age of sample HN-45:							14.69	0.06
			% ³⁹ Ar:							53.90	
			n/t=10/12							14.82	0.05
			Isochron analysis:							290.70	2.00
			⁴⁰ Ar/ ³⁶ Ar Intercept:							4.60	
			MSWD:								
Biotite											
HN-46, D13:47, J=0.00079045±0.000002											
6363-01A	650	2.10E+04	3.17E-01	7.06E+01	6.6E-18	1.6E+00	3.6E-02	0.6	0.0	182.33	4553.17
6363-01B	750	1.43E+03	1.21E-01	5.18E+00	1.9E-18	4.2E+00	1.1E-01	-7.2	0.0	0.00	0.00
6363-01C	850	9.38E+02	4.12E-02	3.14E+00	8.8E-16	1.2E+01	7.0E-04	1.0	2.2	13.81	9.38
6363-01D	920	4.07E+01	1.80E-02	1.05E-01	1.9E-15	2.8E+01	6.8E-04	24.1	7.1	13.93	0.38
6363-01E	1000	1.79E+01	1.20E-02	2.55E-02	6.4E-15	4.3E+01	4.1E-04	58.0	23.3	14.78	0.11
6363-01F	1075	1.39E+01	1.25E-02	1.28E-02	5.0E-15	4.1E+01	3.8E-04	72.8	36.1	14.42	0.07
6363-01G	1110	1.24E+01	2.13E-02	7.94E-03	3.5E-15	2.4E+01	3.9E-04	81.2	45.1	14.35	0.07
6363-01H	1180	1.22E+01	8.96E-02	8.31E-03	5.6E-15	5.7E+00	3.8E-04	79.9	59.2	13.85	0.06
6363-01I	1210	1.15E+01	8.79E-02	4.83E-03	6.7E-15	5.8E+00	3.4E-04	87.7	76.3	14.34	0.06
6363-01J	1250	1.11E+01	5.84E-02	3.09E-03	8.0E-15	8.7E+00	2.0E-04	91.8	96.6	14.47	0.05
6363-01K	1300	1.18E+01	1.62E-01	5.55E-03	1.3E-15	3.2E+00	3.0E-04	86.2	100.0	14.46	0.10
6363-01L	1650	2.88E+03	6.93E+00	9.90E+00	2.5E-18	7.4E-02	1.3E-02	-1.6	100.0	0.00	0.00
total gas age		n=12	3.9E-14	2.0E+01	1.5E+01					14.38	1.05

Run ID#	Temp	40/39	37/39	36/39	39K moles	K/Ca	Cl/K	%40*	%39Ar	Age	± Err
Biotite											
HN-58, D15:47,											
6365-01A	65.0	-2.09E+03	3.22E-03	-7.09E+00	-4.1E-18	1.6E+02	-1.0E-02	-0.2	0.0	4.53	401.25
6365-01B	75.0	2.85E+03	0.00E+00	9.70E+00	6.9E-19	0.0E+00	-2.7E-01	-0.8	0.0	0.00	0.00
6365-01C	85.0	1.21E+02	1.18E-01	3.82E-01	1.7E-16	4.3E+00	2.3E-03	6.5	0.4	11.07	1.97
6365-01D	92.0	2.96E+01	6.93E-02	7.16E-02	5.3E-16	7.4E+00	3.2E-04	28.6	1.6	12.04	0.40
6365-01E	100.0	1.77E+01	4.46E-02	3.12E-02	1.1E-15	1.1E+01	2.5E-04	47.9	4.1	12.05	0.25
6365-01F	107.5	1.45E+01	5.91E-02	1.97E-02	8.7E-16	8.6E+00	7.2E-04	59.9	6.1	12.35	0.21
6365-01G	111.0	1.44E+01	4.97E-02	2.08E-02	1.4E-15	1.0E+01	3.5E-07	57.2	9.3	11.71	0.16
6365-01H	118.0	1.36E+01	4.72E-02	1.83E-02	3.9E-15	1.1E+01	4.1E-04	60.2	18.2	11.65	0.10
6365-01I	121.0	1.28E+01	8.41E-02	1.55E-02	5.9E-15	6.1E+00	3.1E-04	64.4	31.7	11.74	0.07
6365-01J	125.0	1.05E+01	5.79E-02	7.53E-03	1.6E-14	8.8E+00	2.9E-04	78.9	67.3	11.83	0.04
6365-01K	130.0	9.67E+00	9.82E-03	4.49E-03	1.4E-14	5.2E+01	3.5E-04	86.3	99.9	11.86	0.04
6365-01L	165.0	3.51E+02	2.29E-01	1.13E+00	2.8E-17	2.2E+00	1.6E-02	4.6	100.0	22.67	15.59
total gas age											
n=12											
biotite FSH											
n/t=12/12											
n/t=6/12											
Plateau Age of sample HN-58:											
n=12/12											
Isochron analysis:											
$^{40}\text{Ar}/^{36}\text{Ar}$ Intercept:											
MSWD:											
1.43											
93.90											
1.1.85 0.05											
296.40 2.10											
1.43											
iolite											
N-59, E1:47,											
367-01A	65.0	6.49E+03	0.00E+00	2.21E+01	1.1E-17	0.0E+00	-6.5E-02	-0.8	0.0	0.00	0.00
367-01B	75.0	6.19E+02	1.18E-01	2.41E+00	2.5E-18	4.3E+00	-5.5E-02	-14.9	0.0	0.00	0.00
367-01C	85.0	4.16E+02	7.19E-02	1.38E+00	7.8E-16	7.1E+00	2.5E-03	2.1	1.6	12.58	4.27
367-01D	92.0	2.00E+01	2.22E-02	3.62E-02	4.2E-15	2.3E+01	4.1E-04	46.6	10.3	13.17	0.14
367-01E	100.0	1.19E+01	1.25E-02	7.66E-03	8.2E-15	4.1E+01	4.1E-04	80.9	27.1	13.58	0.05
367-01F	107.5	1.13E+01	1.44E-02	6.31E-03	6.2E-15	3.5E+01	2.9E-04	83.6	39.9	13.40	0.05
367-01G	111.0	1.13E+01	2.52E-02	6.04E-03	3.9E-15	2.0E+01	1.6E-04	84.1	47.9	13.38	0.06
367-01H	118.0	1.16E+01	8.66E-02	7.37E-03	4.4E-15	5.9E+00	2.7E-04	81.3	56.9	13.33	0.06

Run ID#	Temp	40/39	37/39	36/39	39K moles	K/Ca	Cl/K	%40*	%39Ar	Age	± Err
6367-01I	1210	1.12E+01	1.11E-01	5.78E-03	5.2E-15	4.6E+00	5.2E-04	84.9	67.5	13.45	0.05
6367-01J	1250	1.07E+01	6.71E-02	3.75E-03	9.7E-15	7.6E+00	2.9E-04	89.7	87.4	13.55	0.04
6367-01K	1300	1.05E+01	1.77E-02	3.03E-03	6.1E-15	2.9E+01	3.1E-04	91.5	99.9	13.60	0.05
6367-01L	1650	1.77E+02	1.46E-01	5.41E-01	3.7E-17	3.5E+00	1.1E-02	9.7	100.0	24.29	6.41
total gas age		n=12		4.9E-14	2.1E+01	1.4E+01				13.45	0.13
n/t=5/12		Plateau Age of sample HN-59:								13.46	0.06
		% ³⁹ Ar:									
		Isochron analysis:									
		⁴⁰ Ar/ ³⁶ Ar Intercept:									
		MSWD:									
		3.17									

n/t=11/12

⁴⁰Ar/³⁶Ar Intercept:
MSWD:
3.17

³⁹Ar:⁴⁰Ar/³⁶Ar Intercept:
MSWD:
3.17

Biotite FSH

SCHAFER

Appendix 5.c

Two-Step Laser Fusion Numeric Data

biotite samples

see Notes concerning column headings and abbreviations

Notes

Column Headings

Run ID#: Lists lab number (i.e. 2814), the unique designation for each sample packet within an irradiation tray; and the chronological number assigned to the mass spectrometer analysis (i.e. 04)

Temp: heating step

40/39: ratio of the measured $^{40}\text{Ar}/^{39}\text{Ar}$

37/39: ratio of the measured $^{37}\text{Ar}/^{39}\text{Ar}$

36/39: ratio of the measured $^{36}\text{Ar}/^{39}\text{Ar}$

39K moles: total moles of gas, determined from the measurement of $^{39}\text{Ar}_K$

K/Ca: a function of measured $^{39}\text{Ar}_K/^{37}\text{Ar}_{\text{Ca}}$

Cl/K: a function of measured $^{36}\text{Ar}_{\text{Cl}}/^{39}\text{Ar}_K$

%40*: radiogenic ^{40}Ar , not attributed to atmospheric composition

Age: apparent age determined for analysis in millions of years

$\pm\text{Err}$: 1 sigma analytical error of age determination

General Heading

Total number of biotite analyses

field number of rock sample (i.e. HN-2);

irradiation tray designation (i.e. M), tray hole number (i.e. 2), and J factor, unique correction factor for extent of irradiation, determined through monitor mineral age analysis

Additional Information

total gas age: this line includes the mean age the two heating steps and error of the analyses, as well as the number of analyses, i.e. $n=2$

Error corrected for J: error produced by irradiation inequalities added to analytical error

Isochron analysis includes the number of analyses used in graphical evaluation versus the total number of analyses (i.e. $n/t=11/20$), as well as, the 40/36 Ar intercept and the MSWD of the graphical analysis

Run ID#	Temp	40/39	37/39	36/39	39K moles	K/Ca	Cl/K	%40*	%39Ar	Age	± Err
Two-step laser heating of 10 biotite flakes, sample HN-2											
HN-2, K5:49, RPE,	J=0.00086381±0.000002										
11-01A	0	1.23E+01	1.41E-02	2.11E-02	2.2E-16	3.6E+01	-4.1E-04	49.2	46.7	9.39	0.39
11-01B	2	8.25E+00	2.45E-02	4.28E-03	2.5E-16	2.1E+01	7.7E-04	84.7	100.0	10.85	0.27
HN-2, K5:49, RPE,	J=0.00086381±0.000002	n=2			4.7E-16	2.8E+01	1.1E+01			10.17	0.33
12-02A	0	4.89E+01	3.59E-02	1.49E-01	2.2E-16	1.4E+01	1.6E-03	9.8	15.8	7.42	0.93
12-02B	2	8.06E+00	2.33E-02	5.87E-03	1.2E-15	2.2E+01	7.6E-04	78.5	100.0	9.83	0.09
HN-2, K5:49, RPE,	J=0.00086381±0.000002	n=2			1.4E-15	2.1E+01	5.4E+00			9.45	0.22
13-03A	0	2.11E+01	5.41E-02	5.64E-02	8.6E-17	9.4E+00	-7.7E-04	21.1	8.3	6.93	1.01
13-03B	2	8.24E+00	1.32E-02	6.88E-03	9.5E-16	3.9E+01	3.8E-04	75.3	100.0	9.64	0.09
HN-2, K5:49, RPE,	J=0.00086381±0.000002	n=2			1.0E-15	3.6E+01	2.1E+01			9.41	0.17
14-04A	0	1.79E+01	4.22E-02	3.92E-02	1.7E-16	1.2E+01	6.9E-04	35.3	14.5	9.83	0.57
14-04B	2	7.19E+00	2.76E-02	3.97E-03	9.8E-16	1.9E+01	1.8E-04	83.7	100.0	9.36	0.08
HN-2, K5:49, RPE,	J=0.00086381±0.000002	n=2			1.1E-15	1.8E+01	4.5E+00			9.43	0.15
15-05A	0	1.09E+01	1.85E-02	1.82E-02	2.8E-16	2.8E+01	6.0E-04	51.0	45.3	8.67	0.27
15-05B	2	7.05E+00	3.13E-02	5.70E-03	3.3E-16	1.6E+01	3.6E-04	76.1	100.0	8.34	0.20
HN-2, K5:49, RPE,	J=0.00086381±0.000002	n=2			6.1E-16	2.1E+01	8.0E+00			8.49	0.23
16-06A	0	1.86E+02	3.38E-02	6.08E-01	6.5E-17	1.5E+01	4.4E-03	3.5	6.2	10.00	5.13
16-06B	2	7.06E+00	2.36E-02	5.72E-03	9.7E-16	2.2E+01	1.8E-04	76.1	100.0	8.35	0.09
total gas age		n=2			1.0E-15	2.1E+01	4.6E+00			8.45	0.41

Run ID#	Temp	RPE,	J=0.00086381±0.000002	40/39	37/39	36/39	39K moles	K/Ca	C/K	%40*	%39Ar	Age	± Err
17-07A	0	2.32E+01	1.21E-02	6.12E-02	1.1E-16	4.2E+01	2.5E-03	22.2	19.1	8.04	0.94		
17-07B	2	6.89E+00	1.47E-02	4.96E-03	4.9E-16	3.5E+01	1.3E-04	78.8	100.0	8.44	0.15		
	total gas age	n=2			6.0E-16	3.6E+01	5.1E+00			8.36	0.30		

HN-2, K5:49, RPE, J=0.00086381±0.000002

18-08A	0	1.24E+02	4.79E-02	4.14E-01	6.4E-17	1.1E+01	-3.2E-03	1.5	2.6	2.87	3.29
18-08B	2	8.96E+00	3.09E-02	7.62E-03	2.4E-15	1.6E+01	4.7E-04	74.9	100.0	10.43	0.06
	total gas age	n=2			2.5E-15	1.6E+01	4.1E+00			10.23	0.15

HN-2, K5:49, RPE, J=0.00086381±0.000002

19-09A	0	5.26E+01	0.00E+00	1.52E-01	1.2E-16	0.0E+00	-1.9E-03	14.4	16.7	11.76	1.40
19-09B	2	7.56E+00	2.02E-02	4.90E-03	5.7E-16	2.5E+01	3.9E-04	80.9	100.0	9.50	0.14
	total gas age	n=2			6.9E-16	0.0E+00	0.0E+00			9.88	0.35

HN-2, K5:49, RPE, J=0.00086381±0.000002

20-10A	0	3.15E+01	7.11E-02	9.89E-02	9.9E-17	7.2E+00	1.9E-03	7.2	7.4	3.52	1.12
20-10B	2	6.55E+00	4.76E-02	4.00E-03	1.2E-15	1.1E+01	5.3E-04	82.0	100.0	8.36	0.09
	total gas age	n=2			1.3E-15	1.0E+01	2.5E+00			8.00	0.16

HN-2, K5:49, RPE, J=0.00086381±0.000002

1-01A	0	2.25E+02	5.59E-02	7.45E-01	1.4E-16	9.1E+00	-2.1E-03	2.1	68.4	7.40	3.82
1-01B	2	2.25E+01	3.32E-02	6.02E-02	6.4E-17	1.5E+01	-3.4E-03	21.0	100.0	7.38	1.62
	total gas age	n=2			2.0E-16	1.1E+01	4.4E+00			7.39	3.13

Two-step laser heating of 10 biotite flakes, sample HN-3

HN-3, K4:49, RPE,	J=0.00086416±0.000002	40/39	37/39	36/39	39K moles	K/Ca	C/K	%40*	%39Ar	Age	± Err
1-01A	0	2.25E+02	5.59E-02	7.45E-01	1.4E-16	9.1E+00	-2.1E-03	2.1	68.4	7.40	3.82
1-01B	2	2.25E+01	3.32E-02	6.02E-02	6.4E-17	1.5E+01	-3.4E-03	21.0	100.0	7.38	1.62
	total gas age	n=2			2.0E-16	1.1E+01	4.4E+00			7.39	3.13

isochron analysis of HN-2:

40Ar/36Ar Intercept:

291.30

2.30

2.66

GRANULITE

Run ID#	Temp	40/39	37/39	36/39	39K moles	K/Ca	C/K	%40*	%39Ar	Age	± Err
HN-3, K4:49, RPE, J=0.00086416±0.000002											
2-02A	0	4.90E+02	2.15E-02	1.62E+00	9.3E-16	2.4E+01	-1.1E-04	2.4	49.6	18.63	5.05
2-02B	2	1.53E+01	3.86E-02	2.89E-02	9.5E-16	1.3E+01	6.5E-04	44.3	100.0	10.55	0.21
	total gas age	n=2			1.9E-15	1.8E+01	7.4E+00			14.55	2.61
HN-3, K4:49, RPE, J=0.00086416±0.000002											
3-03A	0	1.82E+02	1.71E-02	5.82E-01	1.0E-15	3.0E+01	2.9E-04	5.5	79.5	15.54	1.94
3-03B	2	1.04E+01	2.01E-02	1.11E-02	2.6E-16	2.5E+01	-2.0E-04	68.6	100.0	11.14	0.35
	total gas age	n=2			1.3E-15	2.9E+01	3.1E+00			14.64	1.61
HN-3, K4:49, RPE, J=0.00086416±0.000002											
4-04A	0	6.72E+02	1.53E-02	2.24E+00	5.6E-16	3.3E+01	-7.2E-04	1.7	61.5	17.47	7.48
4-04B	2	1.57E+01	1.66E-02	2.72E-02	3.5E-16	3.1E+01	8.9E-04	49.0	100.0	11.97	0.35
	total gas age	n=2			9.0E-16	3.2E+01	1.8E+00			15.35	4.74
HN-3, K4:49, RPE, J=0.00086416±0.000002											
5-05A	0	1.19E+02	1.15E-02	3.76E-01	6.7E-16	4.4E+01	9.9E-04	6.6	56.8	12.21	1.33
5-05B	2	1.12E+01	8.94E-02	1.37E-02	5.1E-16	5.7E+00	3.1E-04	64.1	100.0	11.17	0.21
	total gas age	n=2			1.2E-15	2.8E+01	2.7E+01			11.76	0.85
HN-3, K4:49, RPE, J=0.00086416±0.000002											
6-06A	0	2.65E+02	1.28E-02	8.55E-01	6.0E-16	4.0E+01	2.9E-04	4.8	34.0	19.53	2.73
6-06B	2	1.76E+01	2.08E-02	3.28E-02	1.2E-15	2.5E+01	5.2E-04	45.0	100.0	12.30	0.17
	total gas age	n=2			1.8E-15	3.0E+01	1.1E+01			14.76	1.04
HN-3, K4:49, RPE, J=0.00086416±0.000002											
7-07A	0	1.21E+02	8.85E-03	3.79E-01	2.6E-16	5.8E+01	1.3E-03	7.4	57.5	13.86	1.69
7-07B	2	1.72E+01	7.59E-03	2.84E-02	1.9E-16	6.7E+01	6.4E-04	51.1	100.0	13.64	0.46
	total gas age	n=2			4.5E-16	6.2E+01	6.8E+00			13.77	1.17
HN-3, K4:49, RPE, J=0.00086416±0.000002											
8-08A	0	1.38E+02	1.99E-02	4.40E-01	1.4E-15	2.6E+01	3.0E-04	6.1	59.8	13.15	1.37
8-08B	2	1.06E+01	7.20E-02	1.03E-02	9.5E-16	7.1E+00	5.1E-04	71.4	100.0	11.78	0.12
	total gas age	n=2			2.4E-15	1.8E+01	1.3E+01			12.60	0.87

Run ID#	Temp	RPE,	J=0.00086416±0.000002
HN-3, K4:49	0	6.47E+01	1.02E-02
	2	9.57E+00	6.35E-02
	total gas age	n=2	7.08E-03
HN-3, K4:49, RPE,	J=0.00086416±0.000002		
10-10A	0	4.28E+01	4.89E-02
	2	6.49E+00	2.85E-02
	total gas age	n=2	4.72E-03
	n/t=16/20		

Two-step laser heating of 10 biotite flakes, sample HN-9
HN-9, D12:47, HN, J=0.00079009±0.000002
 11-01A 0 1.39E+02 2.54E-02 4.30E-01
 11-01B 2 1.69E+01 1.94E-01 2.60E-02
 total gas age n=2
HN-9, D12:47, HN, J=0.00079009±0.000002
 12-02A 0 1.41E+03 4.74E-02 4.61E+00
 12-02B 2 3.78E+01 9.79E-02 9.42E-02
 total gas age n=2
HN-9, D12:47, HN, J=0.00079009±0.000002
 13-03A 0 1.54E+02 2.38E-02 4.78E-01
 13-03B 2 1.64E+01 1.44E-01 2.47E-02
 total gas age n=2
HN-9, D12:47, HN, J=0.00079009±0.000002
 14-04A 0 7.78E+02 3.91E-02 2.56E+00
 14-04B 2 3.29E+01 5.73E-02 1.06E-01
 total gas age n=2

Two-step laser heating of 10 biotite flakes, sample HN-3:
Isochron analysis of HN-3:
 40Ar/36Ar Intercept: 297.80 0.80
 MSWD: 2.24

Run ID#	Temp	40/39	37/39	36/39	39K moles	K/Ca	Cl/K	%40*	%39Ar	Age	± Err
HN-9, D12:47, HN, J=0.00079009±0.000002											
15-05A	0	8.66E+02	3.67E-02	2.84E+00	6.4E-16	1.4E+01	-1.2E-04	3.0	30.4	36.29	9.20
15-05B	2	3.14E+01	8.17E-02	7.49E-02	1.5E-15	6.2E+00	9.8E-04	29.6	100.0	13.22	0.32
total gas age	n=2				2.1E-15	8.6E+00	5.4E+00			20.23	3.02
HN-9, D12:47, HN, J=0.00079009±0.000002											
16-06A	0	3.32E+02	3.75E-02	1.08E+00	6.9E-16	1.4E+01	1.9E-03	3.9	96.9	18.48	3.76
16-06B	2	3.15E+01	4.88E-02	1.40E-01	2.2E-17	1.0E+01	-1.5E-02	-31.4	100.0	-14.12	5.24
total gas age	n=2				7.1E-16	1.4E+01	2.2E+00			17.45	3.81
HN-9, D12:47, HN, J=0.00079009±0.000002											
17-07A	0	4.17E+02	1.48E-02	1.36E+00	1.0E-15	3.4E+01	1.1E-03	3.8	66.2	22.39	4.08
17-07B	2	3.76E+01	1.63E-01	9.22E-02	5.3E-16	3.1E+00	-3.7E-04	27.7	100.0	14.78	0.53
total gas age	n=2				1.6E-15	2.4E+01	2.2E+01			19.82	2.88
HN-9, D12:47, HN, J=0.00079009±0.000002											
18-08A	0	2.70E+02	1.80E-02	8.67E-01	1.1E-15	2.8E+01	3.1E-03	5.1	85.7	19.59	2.90
18-08B	2	1.80E+01	9.64E-02	2.52E-02	1.9E-16	5.3E+00	-1.2E-03	58.7	100.0	14.96	0.78
total gas age	n=2				1.3E-15	2.5E+01	1.6E+01			18.93	2.60
HN-9, D12:47, HN, J=0.00079009±0.000002											
19-09A	0	1.15E+03	2.27E-02	3.78E+00	4.5E-16	2.3E+01	6.7E-04	2.9	30.7	46.47	12.88
19-09B	2	3.31E+01	4.79E-02	7.52E-02	1.0E-15	1.1E+01	7.0E-04	32.9	100.0	15.44	0.37
total gas age	n=2				1.5E-15	1.4E+01	8.4E+00			24.95	4.20
HN-9, D12:47, HN, J=0.00079009±0.000002											
20-10A	0	7.98E+01	1.70E-02	2.34E-01	9.4E-16	3.0E+01	5.4E-04	13.3	40.5	15.03	0.91
20-10B	2	3.64E+01	2.96E-02	8.92E-02	1.4E-15	1.7E+01	1.3E-04	27.6	100.0	14.27	0.38
total gas age	n=2				2.3E-15	2.2E+01	9.0E+00			14.58	0.59
<i>n/t=18/20</i>											

Isochron analysis of HN-9:
 40Ar/36Ar Intercept:
 MSWD:

13.23 0.16
 301.70 0.80
 2.36

Run ID#	Temp	40/39	37/39	36/39	39K moles	K/Ca	Ci/K	%40*	%39Ar	Age	± Err
Two-step laser heating of 10 biotite flakes, sample HN-12											
HN-12, N1:43, sing. flake biotite, J=0.0007015265±0.3											
0-10A	0	1.45E+03	3.55E-02	4.67E+00	5.2E-16	1.4E+01	8.0E-03	4.8	24.5	86.70	14.90
0-10B	2	1.01E+02	5.20E-02	3.07E-01	1.6E-15	9.8E+00	1.4E-03	10.4	100.0	13.35	0.87
total gas age		n=2			2.1E-15	1.1E+01	3.2E+00			31.29	4.30
HN-12, N1:43, sing. flake biotite, J=0.0007015265±0.3											
1-11A	0	1.90E+03	4.14E-02	6.16E+00	4.0E-16	1.2E+01	7.3E-03	4.4	10.8	102.24	21.47
1-11B	2	2.61E+02	8.75E-02	8.19E-01	3.3E-15	5.8E+00	1.2E-03	7.3	100.0	24.01	2.08
total gas age		n=2			3.7E-15	6.5E+00	4.6E+00			32.44	4.17
HN-12, N1:43, sing. flake biotite, J=0.0007015265±0.3											
2-12A	0	1.38E+03	2.74E-02	4.47E+00	3.3E-16	1.9E+01	7.6E-03	4.4	10.2	74.85	16.26
2-12B	0	6.53E+01	6.85E-02	1.85E-01	2.9E-15	7.5E+00	8.9E-04	16.2	100.0	13.32	0.52
total gas age		n=2			3.2E-15	8.6E+00	7.9E+00			19.59	2.13
HN-12, N1:43, sing. flake biotite, J=0.0007015265±0.3											
3-13A	0	1.18E+03	3.92E-02	3.78E+00	3.5E-16	1.3E+01	9.2E-03	5.1	19.6	73.73	15.22
3-13B	0	6.24E+01	6.00E-02	1.74E-01	1.5E-15	8.5E+00	9.1E-04	17.7	100.0	13.91	0.52
total gas age		n=2			1.8E-15	9.4E+00	3.2E+00			25.61	3.39
HN-12, N1:43, sing. flake biotite, J=0.0007015265±0.3											
4-14A	0	2.15E+03	2.91E-02	6.92E+00	3.4E-16	1.8E+01	8.3E-03	4.8	27.5	124.64	30.54
4-14B	2	4.73E+01	1.18E-01	1.27E-01	9.0E-16	4.3E+00	9.6E-04	20.7	100.0	12.33	0.44
total gas age		n=2			1.2E-15	7.9E+00	9.3E+00			43.18	8.71
HN-12, N1:43, sing. flake biotite, J=0.0007015265±0.3											
5-15A	0	8.02E+02	3.10E-02	2.56E+00	4.2E-16	1.6E+01	4.0E-03	5.6	11.3	56.13	8.72
5-15B	2	2.08E+01	8.34E-02	4.01E-02	3.3E-15	6.1E+00	3.7E-04	43.2	100.0	11.37	0.14
total gas age		n=2			3.8E-15	7.3E+00	7.3E+00			16.41	1.10
HN-12, N1:43, sing. flake biotite, J=0.0007015265±0.3											
6-16A	0	1.67E+03	4.34E-02	5.41E+00	5.7E-16	1.2E+01	1.1E-02	4.5	39.2	93.51	17.20
6-16B	2	4.48E+01	6.24E-02	1.15E-01	8.8E-16	8.2E+00	8.6E-04	23.9	100.0	13.48	0.45
total gas age		n=2			1.5E-15	9.6E+00	2.5E+00			44.88	7.02

Run ID#	Temp	40/39	37/39	36/39	39K moles	K/Ca	C/K	%40*	%39Ar	Age	± Err
HN-12, N1:43, sing. flake biotite, J=0.0007015265±0.3											
7-17A	0	4.50E+02	3.26E-02	1.43E+00	9.1E-16	1.6E+01	2.6E-03	6.2	79.2	34.93	3.91
7-17B	2	3.15E+01	8.57E-02	7.52E-02	2.4E-16	6.0E+00	2.9E-03	29.5	100.0	11.71	0.67
total gas age n=2											
HN-12, N1:43, sing. flake biotite, J=0.0007015265±0.3											
8-18A	0	3.13E+03	4.96E-02	1.01E+01	5.7E-16	1.0E+01	1.5E-02	4.9	18.4	183.46	35.91
8-18B	2	1.36E+02	4.43E-02	4.12E-01	2.5E-15	1.2E+01	1.0E-03	10.6	100.0	18.14	1.10
total gas age n=2											
HN-12, N1:43, sing. flake biotite, J=0.0007015265±0.3											
9-19A	0	7.50E+02	2.05E-02	2.43E+00	7.4E-16	2.5E+01	3.5E-03	4.1	44.0	38.88	8.00
9-19B	2	3.08E+02	3.20E-02	9.72E-01	9.4E-16	1.6E+01	2.9E-03	6.8	100.0	26.39	2.84
total gas age n=2											
n/t=20/20											
Isochron analysis of HN-12:											
40Ar/36Ar Intercept:											
MSWD:											
0.87											
Two-step laser heating of 10 biotite flakes, sample HN-17											
HN-17, N3:43, sing. flake biotite, J=0.0006991532±0.3											
10-10A	0	7.43E+02	0.00E+00	2.31E+00	6.7E-17	0.0E+00	2.3E-03	8.3	15.9	75.78	26.55
10-10B	0	2.68E+01	5.90E-04	5.44E-02	3.6E-16	8.7E+02	1.0E-03	39.9	100.0	13.41	0.47
total gas age n=2											
HN-17, N3:43, sing. flake biotite, J=0.0006991532±0.3											
11-11A	0	1.64E+02	0.00E+00	4.92E-01	5.8E-17	0.0E+00	-4.5E-04	11.5	10.6	23.69	7.13
11-11B	2	1.32E+01	1.42E-02	1.15E-02	4.8E-16	3.6E+01	6.3E-04	74.2	100.0	12.32	0.33
total gas age n=2											
HN-17, N3:43, sing. flake biotite, J=0.0006991532±0.3											
12-12A	0	1.92E+02	2.89E-03	5.84E-01	1.3E-16	1.8E+02	-3.0E-03	9.9	37.7	23.87	3.46
12-12B	2	1.78E+01	1.96E-02	2.58E-02	2.1E-16	2.6E+01	3.8E-04	57.1	100.0	12.77	0.60
total gas age n=2											
40Ar/36Ar Intercept:											
MSWD:											
0.87											

Run ID#	Temp	40/39	37/39	36/39	39K moles	K/Ca	Cl/K	%40*	%39Ar	Age	± Err
HN-17, N3:43, sing. flake biotite, J=0.0006991532±0.3											
13-13A	0	7.81E+01	1.02E-02	2.21E-01	2.3E-16	5.0E+01	1.6E-04	16.6	54.5	16.29	1.08
13-13B	0	1.33E+01	0.00E+00	5.72E-03	1.9E-16	0.0E+00	-2.6E-03	87.3	100.0	14.57	0.58
total gas age			n=2		4.2E-16	0.0E+00	0.0E+00			15.51	0.86
HN-17, N3:43, sing. flake biotite, J=0.0006991532±0.3											
14-14A	0	3.61E+02	7.17E-01	1.11E+00	3.9E-17	7.1E-01	9.5E-03	9.5	13.1	42.59	14.66
14-14B	2	1.68E+01	4.60E-01	2.29E-02	2.6E-16	1.1E+00	-1.8E-04	59.8	100.0	12.61	0.47
total gas age			n=2		3.0E-16	1.1E+00	2.8E-01			16.53	2.32
HN-17, N3:43, sing. flake biotite, J=0.0006991532±0.3											
15-15A	0	2.14E+02	0.00E+00	6.48E-01	5.6E-17	0.0E+00	5.1E-03	10.6	10.7	28.40	6.93
15-15B	2	1.43E+01	0.00E+00	1.77E-02	4.6E-16	0.0E+00	1.1E-03	63.4	100.0	11.36	0.28
total gas age			n=2		5.2E-16	0.0E+00	0.0E+00			13.18	0.99
HN-17, N3:43, sing. flake biotite, J=0.0006991532±0.3											
16-16A	0	7.75E+01	0.00E+00	2.03E-01	6.6E-17	0.0E+00	7.5E-03	22.7	41.7	22.09	2.97
16-16B	2	1.63E+01	0.00E+00	2.47E-02	9.2E-17	0.0E+00	3.5E-03	55.3	100.0	11.34	1.16
total gas age			n=2		1.6E-16	0.0E+00	0.0E+00			15.82	1.92
HN-17, N3:43, sing. flake biotite, J=0.0006991532±0.3											
17-17A	0	9.40E+01	0.00E+00	2.81E-01	9.2E-17	0.0E+00	1.7E-03	11.5	36.6	13.63	2.58
17-17B	0	1.57E+01	0.00E+00	2.17E-02	1.6E-16	0.0E+00	4.1E-03	59.2	100.0	11.72	0.69
total gas age			n=2		2.5E-16	0.0E+00	0.0E+00			12.42	1.39
HN-17, N3:43, sing. flake biotite, J=0.0006991532±0.3											
18-18A	0	4.34E+01	0.00E+00	1.01E-01	2.2E-16	0.0E+00	5.1E-04	31.5	62.4	17.13	0.84
18-18B	2	3.04E+01	0.00E+00	6.31E-02	1.4E-16	0.0E+00	-1.5E-04	38.7	100.0	14.79	0.92
total gas age			n=2		3.6E-16	0.0E+00	0.0E+00			16.25	0.87

Run ID#	Temp	40/39	37/39	36/39	39K moles	K/Ca	Cl/K	%40*	%39Ar	Age	± Err
HN-17, N3:43, sing. flake biotite, J=0.0006991532±0.3											
19-19A	0	5.15E+01	0.00E+00	1.27E-01	1.8E-16	0.0E+00	-6.2E-04	27.4	52.0	17.69	0.88
19-19B	0	1.38E+01	0.00E+00	1.25E-02	1.7E-16	0.0E+00	8.0E-04	73.3	100.0	12.73	0.61
total gas age	n=2				3.5E-16	0.0E+00	0.0E+00			15.31	0.75
		n/t=18/20								11.63	0.20
										319.30	2.40
											2.42
Two-step laser heating of 10 biotite flakes, sample HN-18											
HN-18, N4:43, sing. flake biotite, J=0.0006970915±0.3											
20-10A	0	7.47E+01	7.38E-02	2.15E-01	8.4E-17	6.9E+00	1.1E-03	14.9	8.3	13.92	2.09
20-10B	0	1.23E+01	1.40E-02	9.27E-03	9.2E-16	3.6E+01	-1.3E-04	77.8	100.0	12.01	0.17
total gas age	n=2				1.0E-15	3.4E+01	2.1E+01			12.17	0.33
HN-18, N4:43, sing. flake biotite, J=0.0006970915±0.3											
21-11A	0	1.23E+02	1.90E-03	3.74E-01	2.4E-17	2.7E+02	-6.3E-03	10.3	3.0	15.96	7.97
21-11B	0	1.28E+01	1.47E-02	8.95E-03	7.6E-16	3.5E+01	-1.9E-04	79.3	100.0	12.68	0.18
total gas age	n=2				7.8E-16	4.2E+01	1.6E+02			12.78	0.42
HN-18, N4:43, sing. flake biotite, J=0.0006970915±0.3											
22-12A	0	5.57E+01	9.11E-02	1.41E-01	9.4E-17	5.6E+00	-4.8E-03	25.2	18.2	17.57	2.01
22-12B	0	1.22E+01	4.37E-04	6.22E-03	4.2E-16	1.2E+03	-1.1E-03	85.0	100.0	13.04	0.28
total gas age	n=2				5.2E-16	9.6E+02	8.2E+02			13.86	0.59
HN-18, N4:43, sing. flake biotite, J=0.0006970915±0.3											
23-13A	0	4.41E+01	0.00E+00	7.88E-02	3.8E-17	0.0E+00	-1.1E-02	47.2	18.3	26.02	3.30
23-13B	0	1.47E+01	0.00E+00	1.34E-02	1.7E-16	0.0E+00	-3.3E-03	73.0	100.0	13.43	0.60
total gas age	n=2				2.1E-16	0.0E+00	0.0E+00			15.73	1.09
HN-18, N4:43, sing. flake biotite, J=0.0006970915±0.3											
24-14A	0	4.05E+02	0.00E+00	1.00E+00	3.5E-18	0.0E+00	3.8E-02	26.8	1.1	131.42	111.34
24-14B	2	1.35E+01	0.00E+00	1.24E-02	3.2E-16	0.0E+00	1.5E-03	72.7	100.0	12.26	0.32
total gas age	n=2				3.3E-16	0.0E+00	0.0E+00			13.54	1.51

Run ID#	Temp	4.0/3.9	3.7/3.9	3.6/3.9	3.9K moles	K/Ca	Ci/K	%40*	%39Ar	Age	\pm Err
HN-18, N4:43, sing. flake biotite, J=0.0006970915±0.3											
25-15A	0	5.39E+01	0.00E+00	1.44E-01	5.3E-17	0.0E+00	4.2E-03	21.3	9.6	14.42	2.68
25-15B	0	1.22E+01	2.16E-02	8.92E-03	5.0E-16	2.4E+01	1.0E-03	78.4	100.0	11.96	0.20
total gas age		n=2			5.5E-16	0.0E+00	0.0E+00			12.20	0.44
HN-18, N4:43, sing. flake biotite, J=0.0006970915±0.3											
26-16A	0	4.72E+01	2.34E-03	1.31E-01	5.3E-17	2.2E+02	-3.4E-03	18.2	9.7	10.81	2.60
26-16B	2	1.36E+01	1.16E-02	1.35E-02	4.9E-16	4.4E+01	-5.1E-04	70.7	100.0	12.02	0.25
total gas age		n=2			5.4E-16	6.1E+01	1.2E+02			11.90	0.48
HN-18, N4:43, sing. flake biotite, J=0.0006970915±0.3											
27-17A	0	4.57E+01	5.70E-02	1.11E-01	3.4E-17	8.9E+00	3.6E-03	28.0	6.1	16.04	3.23
27-17B	2	1.40E+01	7.50E-03	1.51E-02	5.3E-16	6.8E+01	-2.0E-04	68.2	100.0	11.99	0.21
total gas age		n=2			5.6E-16	6.4E+01	4.2E+01			12.23	0.40
HN-18, N4:43, sing. flake biotite, J=0.0006970915±0.3											
28-18A	0	1.65E+01	0.00E+00	2.32E-02	1.0E-16	0.0E+00	0.0E+00	58.6	45.0	12.16	0.83
28-18B	0	2.54E+01	0.00E+00	5.49E-02	1.2E-16	0.0E+00	1.3E-03	36.2	100.0	11.53	0.97
total gas age		n=2			2.2E-16	0.0E+00	0.0E+00			11.81	0.91
HN-18, N4:43, sing. flake biotite, J=0.0006970915±0.3											
29-19A	0	2.40E+01	0.00E+00	5.13E-02	7.9E-17	0.0E+00	-2.6E-03	36.9	29.4	11.09	1.26
29-19B	2	1.43E+01	0.00E+00	1.71E-02	1.9E-16	0.0E+00	-7.5E-04	64.6	100.0	11.54	0.57
total gas age		n=2			2.7E-16	0.0E+00	0.0E+00			11.41	0.77
n/t=20/20											
Isochron analysis of HN-18:											
40Ar/36Ar Intercept:											
MSWD:											
											2.88
Two-step laser heating of 10 biotite flakes, sample HN-20											
HN-20, N5:43, sing. flake biotite, J=0.0006935751±0.3											
30-01A	0	6.17E+02	2.01E+00	1.2E-17	7.9E+00	1.2E-02	3.7	0.5	28.35	67.70	
30-01B	0	1.40E+01	4.17E-02	1.43E-02	2.3E-15	1.2E+01	5.3E-04	69.8	100.0	12.20	0.09
total gas age		n=2			2.3E-15	1.2E+01	3.1E+00			12.29	0.45

JULY 2004

Run ID#	Temp	40/39	37/39	36/39	39K moles	K/Ca	C/K	%40*	%39Ar	Age	± Err
39-09A	0	1.53E+01	9.17E-03	1.73E-02	2.3E-16	5.6E+01	3.8E-04	66.6	69.2	12.71	0.49
39-09B	0	1.92E+01	1.04E-02	2.35E-02	1.0E-16	4.9E+01	1.1E-03	63.8	100.0	15.22	1.26
HN-20, N5:43, sing. flake biotite,	J=0.0006935751±0.3	n=2		3.4E-16	5.4E+01	4.5E+00				13.48	0.73
40-10A	0	1.47E+01	3.52E-02	1.38E-02	1.3E-16	1.4E+01	1.5E-03	72.3	88.3	13.26	0.93
40-10B	0	1.05E+03	1.79E-01	3.36E+00	1.8E-17	2.9E+00	1.6E-02	5.7	100.0	73.69	72.05
total gas age		n=2		1.5E-16	1.3E+01	8.2E+00				20.32	9.25
total gas age		n/t=19/20								12.51	0.23
										307.70	2.50
										1.17	
Isochron analysis of HN-20:											
40Ar/36Ar Intercept:											
MSWD:											
Two-step laser heating of 10 biotite flakes, sample HN-24											
HN-24, N11:43, sing. flake biotite, J=0.0006905068±0.3											
41-01A	0	2.64E+01	2.82E-02	6.66E-02	2.4E-16	1.8E+01	-2.8E-05	25.5	21.3	8.38	0.55
41-01B	0	1.77E+01	4.85E-02	3.50E-02	8.8E-16	1.1E+01	8.4E-04	41.8	100.0	9.21	0.21
total gas age		n=2		1.1E-15	1.2E+01	5.4E+00				9.03	0.28
HN-24, N11:43, sing. flake biotite, J=0.0006905068±0.3											
42-02A	0	3.98E+01	2.69E-02	1.06E-01	2.2E-16	1.9E+01	2.5E-03	21.6	15.5	10.70	0.73
42-02B	0	1.44E+01	2.69E-02	2.47E-02	1.2E-15	1.9E+01	2.9E-04	49.2	100.0	8.79	0.15
total gas age		n=2		1.4E-15	1.9E+01	1.2E-02				9.09	0.24
HN-24, N11:43, sing. flake biotite, J=0.0006905068±0.3											
43-03A	0	9.28E+01	0.00E+00	2.64E-01	4.6E-17	0.0E+00	-8.8E-03	16.0	4.6	18.45	3.72
43-03B	0	3.98E+01	8.42E-03	1.10E-01	9.6E-16	6.1E+01	3.6E-04	18.4	100.0	9.12	0.37
total gas age		n=2		1.0E-15	0.0E+00	0.0E+00				9.55	0.53
HN-24, N11:43, sing. flake biotite, J=0.0006905068±0.3											
44-04A	0	2.50E+01	3.53E-03	5.80E-02	2.4E-16	1.4E+02	-2.4E-03	31.4	26.3	9.74	0.56
44-04B	2	2.34E+01	7.12E-03	5.32E-02	6.6E-16	7.2E+01	-1.3E-04	32.9	100.0	9.58	0.29
total gas age		n=2		8.9E-16	9.1E+01	5.1E+01				9.62	0.36

Run ID#	Temp	40/39	37/39	J=0.0006905068±0.3	36/39	39K moles	K/Ca	C/K	%40*	%39Ar	Age	± Err
HN-24, N11:43, sing. flake biotite, J=0.0006905068±0.3	0	5.80E+01	2.02E-02	1.57E-01	1.3E-16	2.5E+01	-1.9E-03	19.8	7.8	14.26	1.37	
45-05A	0	8.74E+00	2.56E-02	7.40E-03	1.5E-15	2.0E+01	3.4E-04	75.0	100.0	8.14	0.09	
45-05B	0			n=2	1.6E-15	2.0E+01	3.8E+00			8.62	0.19	
total gas age												
HN-24, N11:43, sing. flake biotite, J=0.0006905068±0.3	0	2.54E+01	2.21E-02	5.67E-02	1.4E-16	2.3E+01	-1.1E-03	34.0	37.9	10.71	0.99	
46-06A	0	1.20E+01	5.13E-03	1.71E-02	2.3E-16	9.9E+01	1.2E-03	57.9	100.0	8.63	0.57	
46-06B	0			n=2	3.7E-16	7.1E+01	5.4E+01			9.42	0.72	
total gas age												
HN-24, N11:43, sing. flake biotite, J=0.0006905068±0.3	0	3.67E+01	2.15E-02	9.97E-02	9.8E-17	2.4E+01	2.5E-04	19.8	14.7	9.05	1.47	
47-07A	2	1.18E+01	1.06E-02	1.73E-02	5.7E-16	4.8E+01	1.2E-03	56.8	100.0	8.33	0.19	
47-07B	2			n=2	6.7E-16	4.4E+01	1.7E+01			8.43	0.38	
total gas age												
HN-24, N11:43, sing. flake biotite, J=0.0006905068±0.3	0	1.12E+02	3.24E-02	3.44E-01	7.2E-17	1.6E+01	4.3E-03	8.9	2.9	12.33	3.06	
48-08A	2	9.72E+00	3.23E-02	9.79E-03	2.4E-15	1.6E+01	4.3E-04	70.3	100.0	8.49	0.07	
48-08B	2			n=2	2.5E-15	1.6E+01	3.5E-02			8.60	0.16	
total gas age												
HN-24, N11:43, sing. flake biotite, J=0.0006905068±0.3	0	7.37E+01	1.81E-03	2.13E-01	4.5E-16	2.8E+02	1.6E-03	14.4	22.7	13.15	0.85	
49-09A	2	1.07E+01	1.60E-02	1.25E-02	1.5E-15	3.2E+01	5.9E-04	65.6	100.0	8.76	0.09	
49-09B	2			n=2	2.0E-15	8.9E+01	1.8E+02			9.75	0.26	
total gas age												
HN-24, N11:43, sing. flake biotite, J=0.0006905068±0.3	0	1.37E+03	0.00E+00	4.39E+00	3.2E-16	0.0E+00	8.8E-03	5.7	9.9	95.45	14.81	
50-10A	2	2.04E+01	1.05E-02	4.31E-02	2.9E-15	4.9E+01	6.1E-04	37.6	100.0	9.55	0.15	
50-10B	2			n=2	3.2E-15	0.0E+00	0.0E+00			18.05	1.60	
total gas age												
<i>n/t=20/20</i>												

123

Isochron analysis of HN-24:
 40Ar/36Ar Intercept:
 MSWD:

8.26 0.06

312.70 1.40

2.99

Run ID#	Temp	40/39	37/39	36/39	39K moles	K/Ca	C/I/K	%40*	%39Ar	Age	± Err
Two-step laser heating of 9 biotite flakes, sample HN-31											
HN-31, N14:43, sing. flake biotite, J=0.0006982996±0.3											
81-01A	0	4.17E+01	0.00E+00	1.01E-01	2.0E-16	0.0E+00	7.7E-04	28.3	48.4	14.84	0.86
81-01B	2	1.49E+01	1.79E-02	5.93E-03	2.1E-16	2.9E+01	1.2E-03	88.3	100.0	16.55	0.54
				n=2	4.0E-16	0.0E+00	0.0E+00			15.72	0.69
HN-31, N14:43, sing. flake biotite, J=0.0006982996±0.3											
82-02A	0	5.61E+01	4.80E-02	1.46E-01	2.7E-16	1.1E+01	1.4E-03	23.1	51.0	16.27	0.80
82-02B	2	1.27E+01	2.06E-02	2.97E-03	2.6E-16	2.5E+01	1.4E-03	93.1	100.0	14.81	0.43
				n=2	5.2E-16	1.8E+01	1.0E+01			15.56	0.62
HN-31, N14:43, sing. flake biotite, J=0.0006982996±0.3											
83-03A	0	6.04E+01	0.00E+00	1.58E-01	9.4E-17	0.0E+00	1.0E-04	22.6	94.3	17.09	1.51
83-03B	2	2.40E+01	3.66E-01	5.27E-02	5.6E-18	1.4E+00	-2.2E-02	35.3	100.0	10.63	18.30
				n=2	9.9E-17	0.0E+00	0.0E+00			16.72	2.46
HN-31, N14:43, sing. flake biotite, J=0.0006982996±0.3											
84-04A	0	3.16E+01	3.58E-02	7.15E-02	3.4E-17	1.4E+01	3.6E-03	33.2	57.3	13.18	3.79
84-04B	2	1.77E+01	3.76E-02	4.24E-02	2.5E-17	1.4E+01	-9.3E-03	29.1	100.0	6.47	4.42
				n=2	5.9E-17	1.4E+01	4.7E-01			10.32	4.06
HN-31, N14:43, sing. flake biotite, J=0.0006982996±0.3											
85-05A	0	6.53E+01	1.48E-02	1.72E-01	1.2E-16	3.4E+01	2.8E-03	22.2	58.0	18.19	1.58
85-05B	2	1.60E+01	0.00E+00	1.87E-02	8.4E-17	0.0E+00	2.2E-03	65.4	100.0	13.12	1.49
				n=2	2.0E-16	0.0E+00	0.0E+00			16.06	1.54
HN-31, N14:43, sing. flake biotite, J=0.0006982996±0.3											
86-06A	0	4.61E+01	4.83E-02	1.20E-01	1.0E-16	1.1E+01	3.4E-04	23.0	45.1	13.34	1.43
86-06B	0	1.43E+01	9.36E-02	1.65E-02	1.3E-16	5.4E+00	6.7E-04	66.1	100.0	11.90	0.87
				n=2	2.3E-16	7.8E+00	3.6E+00			12.55	1.12
HN-31, N14:43, sing. flake biotite, J=0.0006982996±0.3											
87-07A	0	5.58E+01	3.95E-02	1.47E-01	1.6E-16	1.3E+01	1.3E-03	22.3	28.5	15.60	1.33
87-07B	0	1.38E+01	1.86E-02	9.47E-03	4.1E-16	2.7E+01	1.5E-04	79.7	100.0	13.78	0.28
				n=2	5.7E-16	2.3E+01	1.0E+01			14.30	0.58

Run ID#	Temp	40/39	37/39	36/39	39K moles	K/Ca	C/K	%40*	%39Ar	Age	\pm Err
HN-31, N14:43, sing. flake biotite, J=0.0006982996±0.3											
88-08A	0	8.61E+01	0.00E+00	2.27E-01	5.7E-17	0.0E+00	2.6E-03	22.2	21.1	23.95	3.13
88-08B	0	1.53E+01	3.88E-02	1.36E-02	2.1E-16	1.3E+01	-3.5E-04	73.7	100.0	14.17	0.59
				n=2	2.7E-16	0.0E+00	0.0E+00			16.23	1.12
HN-31, N14:43, sing. flake biotite, J=0.0006982996±0.3											
89-09A	0	2.35E+01	1.63E-03	3.70E-02	1.1E-16	3.1E+02	4.0E-03	53.6	52.1	15.84	1.12
89-09B	2	1.30E+01	1.07E-01	3.68E-03	1.0E-16	4.8E+00	2.3E-03	91.7	100.0	15.02	1.14
				n=2	2.1E-16	1.7E+02	2.2E+02			15.44	1.13
				n/t=16/16							
Isochron analysis of HN-31:											
										13.81	0.23
										31.0.20	3.30
MSWD:											
											1.80
Two-step laser heating of 10 biotite flakes, sample HN-32											
HN-32, N13:43, sing. flake biotite, J=0.0006960849±0.3											
51-01A	0	6.09E+02	0.00E+00	1.95E+00	2.0E-16	0.0E+00	3.2E-03	5.2	4.8.9	39.22	8.50
51-01B	2	1.50E+02	7.51E-02	4.50E-01	2.1E-16	6.8E+00	4.7E-04	11.0	100.0	20.57	1.90
				n=2	4.2E-16	0.0E+00	0.0E+00			29.69	5.13
HN-32, N13:43, sing. flake biotite, J=0.0006960849±0.3											
52-02A	0	8.35E+02	3.04E-02	2.69E+00	1.9E-16	1.7E+01	8.1E-03	4.7	92.7	48.37	11.26
52-02B	2	2.83E+01	0.00E+00	4.44E-03	1.5E-17	0.0E+00	9.7E-03	95.4	100.0	33.52	7.33
				n=2	2.0E-16	0.0E+00	0.0E+00			47.28	10.98
HN-32, N13:43, sing. flake biotite, J=0.0006960849±0.3											
53-03A	0	2.88E+02	1.46E-02	9.02E-01	1.7E-16	3.5E+01	-4.2E-03	7.4	36.0	26.47	4.68
53-03B	2	2.35E+01	1.50E-02	4.10E-02	3.0E-16	3.4E+01	6.2E-04	48.5	100.0	14.26	0.46
				n=2	4.7E-16	3.4E+01	6.3E-01			18.66	1.98
HN-32, N13:43, sing. flake biotite, J=0.0006960849±0.3											
54-04A	0	6.36E+01	0.00E+00	1.78E-01	1.0E-16	0.0E+00	-3.1E-03	17.3	51.6	13.74	1.76
54-04B	2	1.98E+01	4.05E-02	3.28E-02	9.3E-17	1.3E+01	1.3E-03	51.0	100.0	12.62	1.27
				n=2	1.9E-16	0.0E+00	0.0E+00			13.19	1.52

Run ID#	Temp	40/39	37/39	J=0.0006960849±0.3	39K moles	K/Ca	C/K	%40*	%39Ar	Age	± Err
HN-32, N13:43, sing. flake biotite,											
55-05A	0	2.61E+03	4.10E-02	8.57E+00	7.4E-17	1.2E+01	1.6E-02	2.9	81.7	91.78	75.29
55-05B	2	3.77E+01	0.00E+00	1.16E-01	1.6E-17	0.0E+00	8.3E-03	9.3	100.0	4.41	7.85
total gas age			n=2		9.0E-17	0.0E+00	0.0E+00			75.78	62.95
HN-32, N13:43, sing. flake biotite,				J=0.0006960849±0.3							
56-06A	0	1.84E+02	3.83E-02	5.64E-01	3.2E-16	1.3E+01	2.6E-03	9.4	100.0	21.51	2.06
total gas age			n=1		3.2E-16	1.3E+01	0.0E+00			21.51	2.06
HN-32, N13:43, sing. flake biotite,				J=0.0006960849±1.6							
66-06B	2	2.18E+01	1.44E-01	4.60E-02	1.7E-17	3.6E+00	2.1E-03	37.6	100.0	10.27	7.25
total gas age			n=1		1.7E-17	3.6E+00	0.0E+00			10.27	7.25
HN-32, N13:43, sing. flake biotite,				J=0.0006960849±0.3							
77-07A	0	3.80E+02	0.00E+00	1.20E+00	2.3E-16	0.0E+00	1.6E-03	6.6	96.4	31.19	4.65
77-07B	0	9.81E+01	0.00E+00	2.83E-01	8.6E-18	0.0E+00	1.8E-02	14.6	100.0	17.86	19.22
total gas age			n=2		2.4E-16	0.0E+00	0.0E+00			30.70	5.18
HN-32, N13:43, sing. flake biotite,				J=0.0006960849±0.3							
78-08A	0	1.95E+03	2.86E-02	6.35E+00	3.8E-16	1.8E+01	1.2E-02	3.9	72.9	93.00	25.12
78-08B	2	3.13E+01	2.91E-01	6.09E-02	1.4E-16	1.8E+00	-1.6E-03	42.6	100.0	16.69	0.97
total gas age			n=2		5.2E-16	1.3E+01	1.1E+01			72.28	18.56
HN-32, N13:43, sing. flake biotite,				J=0.0006960849±0.3							
79-09A	0	2.92E+02	0.00E+00	9.12E-01	1.9E-16	0.0E+00	5.0E-04	7.8	100.0	28.33	4.17
total gas age			n=1		1.9E-16	0.0E+00	0.0E+00			28.33	4.17
HN-32, N13:43, sing. flake biotite,				J=0.0006960849±1.6							
80-09B	2	2.43E+01	2.82E-02	4.10E-02	9.8E-17	1.8E+01	1.0E-03	50.2	100.0	15.28	1.19
total gas age			n=1		9.8E-17	1.8E+01	0.0E+00			15.28	1.19
		n/t=18/20								13.94	0.39
										306.40	1.30
										1.14	
<i>Isochron analysis of HN-32:</i>											
<i>40Ar/36Ar Intercept:</i>											
<i>Mswd:</i>											

Run ID#	Temp	40/39	37/39	36/39	39K moles	K/Ca	C/K	%40*	%39Ar	Age	± Err
Two-step laser heating of 14 biotite flakes, sample HN-37b											
HN-37b, N15:43, sing. flake biot., J=0.0007000958±0.35											
60-25A	0	2.77E+02	6.53E-03	8.33E-01	9.1E-17	7.8E+01	4.6E-03	11.1	2.8	38.41	4.82
60-25B	2	1.67E+01	5.60E-02	1.56E-02	3.2E-15	9.1E+00	3.3E-04	72.5	100.0	15.25	0.09
total gas age	n=2				3.3E-15	1.1E+01	4.9E+01			15.90	0.22
HN-37b, N15:43, sing. flake biot., J=0.0007000958±0.35											
61-26A	0	6.76E+02	3.83E-02	2.15E+00	6.6E-16	1.3E+01	5.3E-03	6.0	53.8	50.41	6.00
61-26B	2	1.39E+03	3.78E-02	4.53E+00	5.7E-16	1.4E+01	4.0E-03	3.4	100.0	59.15	14.29
total gas age	n=2				1.2E-15	1.3E+01	1.4E-01			54.45	9.83
HN-37b, N15:43, sing. flake biot., J=0.0007000958±0.35											
62-27A	0	2.52E+01	8.00E-02	4.17E-02	2.6E-16	6.4E+00	5.1E-04	51.2	83.7	16.22	0.53
62-27B	2	2.25E+02	5.19E-02	7.05E-01	5.1E-17	9.8E+00	5.4E-03	7.3	100.0	20.51	5.16
total gas age	n=2				3.1E-16	6.9E+00	2.4E+00			16.92	1.29
HN-37b, N15:43, sing. flake biot., J=0.0007000958±0.35											
63-28A	0	5.61E+02	4.62E-02	1.79E+00	3.8E-16	1.1E+01	4.3E-03	5.8	78.3	40.61	5.51
63-28B	2	2.45E+03	6.95E-02	7.95E+00	1.1E-16	7.3E+00	2.0E-02	3.9	100.0	117.99	45.77
total gas age	n=2				4.9E-16	1.0E+01	2.6E+00			57.38	14.23
HN-37b, N15:43, sing. flake biot., J=0.0007000958±0.35											
64-29A	0	2.66E+01	5.57E-02	5.00E-02	2.3E-16	9.2E+00	-7.9E-04	44.5	58.5	14.90	0.85
64-29B	2	2.87E+03	2.88E-02	9.35E+00	1.6E-16	1.8E+01	8.9E-03	3.7	100.0	130.13	47.80
total gas age	n=2				4.0E-16	1.3E+01	6.0E+00			62.77	20.35
HN-37b, N15:43, sing. flake biot., J=0.0007000958±0.35											
65-30A	0	9.35E+02	4.03E-02	2.97E+00	7.5E-16	1.3E+01	6.2E-03	6.0	38.2	69.67	7.93
65-30B	2	2.53E+01	9.47E-02	4.73E-02	1.2E-15	5.4E+00	1.6E-05	44.7	100.0	14.23	0.23
total gas age	n=2				2.0E-15	8.2E+00	5.1E+00			35.43	3.17
HN-37b, N15:43, sing. flake biot., J=0.0007000958±0.35											
66-31A	0	3.11E+01	8.59E-02	6.52E-02	2.6E-16	5.9E+00	1.2E-03	38.0	75.4	14.85	0.66
66-31B	2	2.51E+01	7.00E-02	4.20E-02	8.5E-17	7.3E+00	5.2E-03	50.6	100.0	16.00	1.46
total gas age	n=2				3.5E-16	6.3E+00	9.5E-01			15.13	0.86

Run ID#	Temp	40/39	37/39	J=0.0007000958±0.35	36/39	39K moles	K/Ca	Cl/K	%40*	%39Ar	Age	± Err
HN-37b, N15:43, sing. flake biot., J=0.0007000958±0.35												
67-32A	0	3.79E+01	4.39E-02	9.04E-02	4.0E-16	1.2E+01	3.2E-04	29.5	8.5	14.09	0.55	
67-32B	2	1.27E+01	6.03E-02	3.44E-03	4.3E-15	8.5E+00	3.9E-04	92.1	100.0	14.76	0.05	
total gas age			n=2		4.7E-15	8.7E+00	2.2E+00			14.71	0.10	
HN-37b, N15:43, sing. flake biot., J=0.0007000958±0.35												
68-33A	0	2.79E+03	8.35E-02	8.94E+00	8.1E-16	6.1E+00	1.5E-02	5.2	78.2	173.84	27.00	
68-33B	2	5.89E+01	7.48E-02	1.66E-01	2.3E-16	6.8E+00	1.5E-03	16.5	100.0	12.26	1.19	
total gas age			n=2		1.0E-15	6.3E+00	5.1E-01			138.56	21.36	
HN-37b, N15:43, sing. flake biot., J=0.0007000958±0.35												
69-34A	0	2.84E+01	6.00E-02	5.55E-02	4.3E-16	8.5E+00	4.4E-04	42.4	43.4	15.15	0.47	
69-34B	2	1.28E+01	9.72E-03	2.09E-03	5.5E-16	5.2E+01	-1.1E-04	95.2	100.0	15.31	0.21	
total gas age			n=2		9.8E-16	3.3E+01	3.1E+01			15.24	0.32	
HN-37b, N15:43, sing. flake biot., J=0.0007000958±0.35												
70-35A	0	2.06E+03	7.91E-02	6.55E+00	6.6E-16	6.5E+00	8.4E-03	6.0	13.7	149.39	19.94	
70-35B	2	5.61E+01	8.64E-02	1.47E-01	4.1E-15	5.9E+00	7.2E-04	22.5	100.0	15.88	0.41	
total gas age			n=2		4.8E-15	6.0E+00	3.9E-01			34.17	3.09	
HN-37b, N15:43, sing. flake biot., J=0.0007000958±0.35												
71-36A	0	1.10E+03	9.76E-02	3.52E+00	6.1E-16	5.2E+00	6.9E-03	5.7	80.2	77.99	11.08	
71-36B	2	5.14E+01	1.84E-01	1.52E-01	1.5E-16	2.8E+00	-1.4E-03	12.6	100.0	8.18	1.28	
total gas age			n=2		7.6E-16	4.7E+00	1.7E+00			64.19	9.15	
HN-37b, N15:43, sing. flake biot., J=0.0007000958±0.35												
72-37A	0	2.27E+03	1.87E-01	7.28E+00	6.3E-16	2.7E+00	1.2E-02	5.1	90.1	140.09	22.31	
72-37B	2	6.08E+01	2.71E-01	1.83E-01	7.0E-17	1.9E+00	-1.4E-03	11.0	100.0	8.41	2.86	
total gas age			n=2		7.0E-16	2.6E+00	5.9E-01			127.01	20.38	

Run ID#	Temp	40/39	37/39	36/39	39K moles	K/Ca	Cl/K	%40*	%39Ar	Age	± Err
HN-37b, N15:43, sing. flake biot., J=0.0007900958±0.35											
73-38A	0	4.24E+03	1.21E-01	1.37E+01	5.2E-16	4.2E+00	9.7E-03	4.7	74.7	236.33	51.18
73-38B	2	6.27E+01	1.78E-01	1.80E-01	1.8E-16	2.9E+00	5.5E-04	15.4	100.0	12.15	1.68
total gas age		n=2			7.0E-16	3.9E+00	9.4E-01			179.68	38.67
		n/t=21/28								15.20	0.06
										308.10	0.80
											2.92

Two-step laser heating of 10 biotite flakes, sample HN-41

HN-41, D14:47, HN, J=0.00079058±0.000002											
31-01A	0	8.40E+01	2.68E-02	2.39E-01	6.1E-16	1.9E+01	2.1E-03	15.8	43.8	18.79	0.99
31-01B	2	1.36E+01	5.97E-02	2.87E-03	7.9E-16	8.5E+00	-1.8E-04	93.8	100.0	18.11	0.16
total gas age		n=2			1.4E-15	1.3E+01	7.4E+00			18.41	0.52
HN-41, D14:47, HN, J=0.00079058±0.000002											
32-02A	0	2.09E+01	0.00E+00	2.89E-02	4.0E-16	0.0E+00	-5.0E-04	59.1	19.7	17.49	0.48
32-02B	2	1.36E+01	2.66E-02	4.47E-03	1.6E-15	1.9E+01	3.2E-04	90.3	100.0	17.38	0.09
total gas age		n=2			2.0E-15	0.0E+00	0.0E+00			17.40	0.16
HN-41, D14:47, HN, J=0.00079058±0.000002											
33-03A	0	5.92E+01	0.00E+00	1.54E-01	3.5E-16	0.0E+00	-7.5E-04	23.3	24.8	19.58	0.90
33-03B	2	1.35E+01	1.68E-01	4.03E-03	1.0E-15	3.0E+00	6.5E-05	91.3	100.0	17.55	0.14
total gas age		n=2			1.4E-15	0.0E+00	0.0E+00			18.05	0.33
HN-41, D14:47, HN, J=0.00079058±0.000002											
34-04A	0	2.19E+01	0.00E+00	3.15E-02	3.9E-16	0.0E+00	-2.3E-04	57.6	78.4	17.91	0.41
34-04B	2	1.46E+01	0.00E+00	3.68E-03	1.1E-16	0.0E+00	-4.2E-04	92.6	100.0	19.16	1.00
total gas age		n=2			5.0E-16	0.0E+00	0.0E+00			18.18	0.54
HN-41, D14:47, HN, J=0.00079058±0.000002											
35-05A	0	1.11E+02	0.00E+00	3.26E-01	6.4E-16	0.0E+00	9.8E-04	13.3	25.4	20.96	1.46
35-05B	2	1.36E+01	4.49E-02	4.71E-03	1.9E-15	1.1E+01	3.0E-04	89.8	100.0	17.32	0.09
total gas age		n=2			2.5E-15	0.0E+00	0.0E+00			18.24	0.44

Run ID#	Temp	40/39	37/39	36/39	39K moles	K/Ca	Ci/K	%40*	%39Ar	Age	± Err
HN-41, D14:47, HN, J=0.00079058±0.000002											
36-06A	0	2.04E+01	5.20E-03	2.87E-02	2.0E-16	9.8E+01	-2.0E-03	58.5	12.0	16.95	0.48
36-06B	2	1.36E+01	5.26E-02	4.29E-03	1.5E-15	9.7E+00	4.7E-05	90.7	100.0	17.49	0.08
total gas age		n=2			1.6E-15	2.0E+01	6.2E+01			17.43	0.13
HN-41, D14:47, HN, J=0.00079058±0.000002											
37-07A	0	9.04E+01	4.06E-02	2.66E-01	2.5E-16	1.3E+01	-1.5E-04	13.1	72.4	16.80	1.36
37-07B	2	1.73E+01	3.25E-02	2.30E-02	9.6E-17	1.6E+01	-3.3E-03	60.7	100.0	14.90	0.87
total gas age		n=2			3.5E-16	1.3E+01	2.2E+00			16.28	1.23
HN-41, D14:47, HN, J=0.00079058±0.000002											
38-08A	0	2.36E+01	1.67E-02	3.74E-02	3.7E-16	3.1E+01	1.0E-03	53.2	75.8	17.85	0.30
38-08B	2	1.37E+01	8.53E-02	1.17E-03	1.2E-16	6.0E+00	7.9E-04	97.5	100.0	19.03	0.70
total gas age		n=2			4.9E-16	2.5E+01	1.7E+01			18.14	0.40
HN-41, D14:47, HN, J=0.00079058±0.000002											
39-09A	0	1.51E+01	2.59E-02	5.64E-03	2.0E-16	2.0E+01	1.5E-03	89.0	55.4	19.11	0.43
39-09B	2	2.20E+01	1.23E-01	4.58E-02	1.6E-16	4.2E+00	5.4E-03	38.5	100.0	12.05	0.63
total gas age		n=2			3.6E-16	1.3E+01	1.1E+01			15.97	0.52
HN-41, D14:47, HN, J=0.00079058±0.000002											
40-10A	0	9.20E+01	1.07E-02	2.68E-01	4.3E-16	4.8E+01	1.0E-03	13.9	42.2	18.21	1.17
40-10B	2	1.32E+01	4.95E-02	1.95E-03	5.9E-16	1.0E+01	1.7E-04	95.7	100.0	17.96	0.16
total gas age		n=2			1.0E-15	2.6E+01	2.6E+01			18.07	0.59
n/t=17/20											
HN-45, D11:47, HN, J=0.00078979±0.000002											
1-01A	0	1.31E+02	1.94E-02	4.15E-01	4.1E-16	2.6E+01	1.0E-04	6.2	12.8	11.51	1.69
1-01B	2	4.20E+01	5.63E-02	1.08E-01	2.8E-15	9.1E+00	6.5E-04	24.3	100.0	14.48	0.37
total gas age		n=2			3.2E-15	1.1E+01	1.2E+01			14.10	0.54
MSWD:										2.77	
Two-step laser heating of 10 biotite flakes, sample HN-45											
Isochron analysis of HN-41:											
40Ar/36Ar Intercept:										17.44	0.06
299.60											

Run ID#	Temp	40/39	37/39	36/39	39K moles	K/Ca	Ci/K	%40*	%39Ar	Age	± Err
HN-45, D11:47, HN, J=0.00078979±0.000002											
2-02A	0	5.48E+01	3.67E-02	1.54E-01	4.0E-16	1.4E+01	-8.5E-05	17.3	12.1	13.44	0.86
2-02B	2	2.75E+01	5.74E-02	5.87E-02	2.9E-15	8.9E+00	1.9E-04	36.9	100.0	14.43	0.24
	total gas age		n=2		3.3E-15	9.5E+00	3.6E+00			14.31	0.32
HN-45, D11:47, HN, J=0.00078979±0.000002											
3-03A	0	3.74E+01	1.14E-02	8.92E-02	5.5E-16	4.5E+01	1.4E-03	29.6	15.1	15.72	0.56
3-03B	2	1.58E+01	1.22E-02	1.80E-02	3.1E-15	4.2E+01	3.0E-04	66.3	100.0	14.86	0.11
	total gas age		n=2		3.6E-15	4.2E+01	2.3E+00			14.99	0.18
HN-45, D11:47, HN, J=0.00078979±0.000002											
4-04A	0	2.29E+01	4.51E-03	4.30E-02	4.4E-16	1.1E+02	-2.3E-04	44.5	31.4	14.45	0.40
4-04B	2	9.95E+01	2.00E-02	3.03E-01	9.6E-16	2.6E+01	2.1E-03	10.0	100.0	14.12	1.07
	total gas age		n=2		1.4E-15	5.3E+01	6.2E+01			14.22	0.86
HN-45, D11:47, HN, J=0.00078979±0.000002											
5-05A	0	3.72E+01	2.74E-02	9.33E-02	4.2E-16	1.9E+01	-1.7E-04	25.9	36.4	13.68	0.63
5-05B	2	1.32E+02	6.83E-02	4.11E-01	7.4E-16	7.5E+00	-5.2E-04	7.7	100.0	14.32	1.46
	total gas age		n=2		1.2E-15	1.2E+01	7.9E+00			14.09	1.16
HN-45, D11:47, HN, J=0.00078979±0.000002											
6-06A	0	1.77E+02	5.93E-03	5.67E-01	4.2E-16	8.6E+01	-3.6E-04	5.4	11.1	13.70	2.30
6-06B	2	2.51E+01	3.14E-02	4.94E-02	3.4E-15	1.6E+01	5.0E-04	41.9	100.0	14.93	0.19
	total gas age		n=2		3.8E-15	2.4E+01	4.9E+01			14.80	0.42
HN-45, D11:47, HN, J=0.00078979±0.000002											
7-07A	0	8.43E+01	3.82E-02	2.51E-01	1.5E-16	1.3E+01	-1.1E-04	12.2	100.0	14.54	1.88
	total gas age		n=1		1.5E-16	1.3E+01	0.0E+00			14.54	1.88
HN-45, D11:47, HN, J=0.00078979±0.000002											
6-07B	2	2.36E+01	4.94E-02	4.40E-02	3.0E-15	1.0E+01	3.8E-04	44.9	100.0	15.03	0.19
	total gas age		n=1		3.0E-15	1.0E+01	0.0E+00			15.03	0.19

Run ID#	Temp	40/39	37/39	36/39	39K moles	K/Ca	Ci/K	%40*	%39Ar	Age	± Err
HN-45, D11:47, HN,	J=0.00078979±0.000002										
8-08A	0	8.58E+01	0.00E+00	2.29E-01	7.0E-17	0.0E+00	2.2E-03	21.2	3.9	25.80	2.56
8-08B	2	1.80E+02	6.48E-02	5.52E-01	1.7E-15	7.9E+00	1.1E-03	9.3	100.0	23.80	1.67
		total gas age		n=2	1.8E-15	0.0E+00	0.0E+00			23.88	1.71
HN-45, D11:47, HN,	J=0.00078979±0.000002										
9-09A	0	2.17E+02	0.00E+00	6.55E-01	3.4E-17	0.0E+00	1.6E-03	10.7	2.2	32.70	9.57
9-09B	2	3.37E+01	2.75E-02	7.71E-02	1.5E-15	1.9E+01	5.6E-04	32.4	100.0	15.47	0.33
		total gas age		n=2	1.5E-15	0.0E+00	0.0E+00			15.85	0.53
HN-45, D11:47, HN,	J=0.00078979±0.000002										
10-10A	0	7.26E+01	0.00E+00	1.95E-01	1.2E-16	0.0E+00	3.7E-03	20.7	9.9	21.31	1.55
10-10B	2	1.42E+01	3.39E-02	1.16E-02	1.1E-15	1.5E+01	8.1E-04	75.8	100.0	15.22	0.13
		total gas age		n=2	1.3E-15	0.0E+00	0.0E+00			15.82	0.27
				n/t=17/20							
		Isochron analysis of HN-45:									
		40Ar/36Ar Intercept:									
		MSWD:									
										292.90	1.10
											1.94
Two-step laser heating of 10 biotite flakes, sample HN-46											
HN-46, D13:47, HN,	J=0.00079045±0.000002										
21-01A	0	1.26E+02	1.57E-02	3.90E-01	5.5E-16	3.2E+01	7.1E-04	8.6	21.5	15.42	1.54
21-01B	2	1.26E+01	7.38E-02	9.32E-03	2.0E-15	6.9E+00	3.8E-04	78.2	100.0	14.05	0.11
		total gas age		n=2	2.6E-15	1.2E+01	1.8E+01			14.34	0.42
HN-46, D13:47, HN,	J=0.00079045±0.000002										
22-02A	0	7.32E+02	3.10E-02	2.38E+00	4.8E-16	1.6E+01	2.0E-03	3.8	85.9	39.50	9.02
22-02B	2	7.42E+01	2.32E-01	2.70E-01	7.8E-17	2.2E+00	1.8E-03	-7.6	100.0	-8.09	3.12
		total gas age		n=2	5.5E-16	1.4E+01	1.0E+01			32.80	8.19
HN-46, D13:47, HN,	J=0.00079045±0.000002										
23-03A	0	3.31E+02	7.70E-03	1.06E+00	6.2E-16	6.6E+01	1.5E-03	5.3	43.4	24.87	3.75
23-03B	2	1.81E+01	7.03E-02	2.58E-02	8.0E-16	7.3E+00	7.4E-04	57.9	100.0	14.88	0.27
		total gas age		n=2	1.4E-15	3.3E+01	4.2E+01			19.22	1.78

Run ID#	Temp	40/39	37/39	36/39	39K moles	K/Ca	C/K	%40*	%39Ar	Age	± Err
HN-46, D13:47, HN, J=0.00079045±0.000002											
24-04A	0	1.56E+01	2.99E-02	1.49E-02	2.3E-16	1.7E+01	-2.6E-04	71.7	32.4	15.83	0.57
24-04B	2	1.09E+01	4.28E-02	3.24E-03	4.8E-16	1.2E+01	1.4E-03	91.2	100.0	14.10	0.26
HN-46, D13:47, HN, J=0.00079045±0.000002	total gas age	n=2			7.2E-16	1.4E+01	3.7E+00			14.66	0.36
25-05A	0	7.62E+01	2.40E-02	2.21E-01	1.4E-16	2.1E+01	4.4E-03	14.2	5.7	15.33	1.98
25-05B	2	1.37E+01	4.47E-02	1.17E-02	2.4E-15	1.1E+01	4.7E-04	74.8	100.0	14.52	0.10
HN-46, D13:47, HN, J=0.00079045±0.000002	total gas age	n=2			2.5E-15	1.2E+01	6.9E+00			14.56	0.21
26-06A	0	1.66E+01	1.89E-02	2.27E-02	3.3E-16	2.7E+01	1.3E-05	59.6	35.9	14.07	0.45
26-06B	2	1.10E+01	3.03E-02	4.72E-03	5.8E-16	1.7E+01	2.3E-04	87.4	100.0	13.65	0.22
HN-46, D13:47, HN, J=0.00079045±0.000002	total gas age	n=2			9.1E-16	2.0E+01	7.1E+00			13.80	0.30
27-07A	0	5.77E+01	0.00E+00	1.48E-01	5.3E-17	0.0E+00	-8.9E-03	24.5	3.4	20.04	3.56
27-07B	2	1.18E+01	3.56E-02	5.28E-03	1.5E-15	1.4E+01	3.6E-04	86.7	100.0	14.48	0.10
HN-46, D13:47, HN, J=0.00079045±0.000002	total gas age	n=2			1.6E-15	0.0E+00	0.0E+00			14.67	0.22
28-08A	0	1.40E+02	1.54E-01	4.51E-01	6.3E-17	3.3E+00	7.5E-03	4.6	1.9	9.19	6.15
28-08B	2	1.19E+01	3.29E-02	5.58E-03	3.2E-15	1.6E+01	7.1E-05	86.2	100.0	14.60	0.08
HN-46, D13:47, HN, J=0.00079045±0.000002	total gas age	n=2			3.3E-15	1.5E+01	8.6E+00			14.49	0.20
29-09A	0	2.05E+01	4.52E-02	3.53E-02	5.7E-16	1.1E+01	1.3E-03	49.2	51.6	14.32	0.37
29-09B	2	1.21E+01	3.94E-02	6.26E-03	5.3E-16	1.3E+01	1.1E-03	84.7	100.0	14.53	0.28
total gas age		n=2			1.1E-15	1.2E+01	1.2E+00			14.42	0.33

Run ID#	Temp	40/39	37/39	36/39	39K moles	K/Ca	Ci/K	%40*	%39Ar	Age	± Err
HN-55, E3:47, HN, 76-06A	0	2.42E+01	3.28E-02	5.71E-02	3.5E-16	1.6E+01	-2.8E-04	30.4	97.7	10.41	0.58
76-06B	2	1.08E+02	2.22E-01	4.12E-01	8.0E-18	2.3E+00	-2.5E-03	-12.7	100.0	-19.61	20.87
HN-55, E3:47, HN, 77-07A	0	3.70E+01	4.91E-02	1.03E-01	3.6E-16	1.5E+01	9.4E+00			9.73	1.04
77-07B	2	1.36E+02	5.00E-01	4.16E-01	6.0E-18	1.0E+00	-8.3E-03	9.8	100.0	18.79	27.19
HN-55, E3:47, HN, 78-08A	0	8.92E+01	1.24E-01	2.82E-01	7.5E-17	4.1E+00	-2.5E-03	6.6	95.6	9.49	1.32
78-08B	2	1.98E+01	5.86E-02	3.70E-02	1.3E-16	8.7E+00	-1.6E-03	44.7	100.0	12.50	1.05
HN-55, E3:47, HN, 79-09A	0	2.16E+01	1.88E-02	4.25E-02	1.5E-16	2.7E+01	7.8E-04			10.96	1.83
79-09B	2	2.20E+03	7.07E-05	7.48E+00	3.2E-17	7.2E+03	9.6E-03	-0.7	100.0	-20.79	118.33
HN-55, E3:47, HN, 80-10A	0	5.02E+01	1.30E-01	1.75E-01	1.9E-16	1.3E+03	5.1E+03			6.99	21.20
80-10B	2	1.13E+03	5.97E-02	3.83E+00	5.9E-17	3.9E+00	3.3E-03	-2.9	47.5	-2.04	2.85
Two-step laser heating of 10 biotite flakes, sample HN-55											
HN-55, E3:47, HN, 71-01A	0	1.99E+02	2.80E-02	6.47E-01	9.5E-16	1.8E+01	7.4E-04	3.9	39.7	10.98	2.12
71-01B	2	2.00E+01	5.66E-02	3.73E-02	1.4E-15	9.0E+00	1.5E-04	44.9	100.0	12.70	0.22
HN-55, E3:47, HN, 72-02A	0	1.30E+02	8.50E-02	4.08E-01	2.4E-15	1.3E+01	6.5E+00			12.02	0.97
72-02B	2	1.29E+01	2.45E-02	1.50E-02	6.9E-16	2.1E+01	5.5E-04	7.5	33.9	13.75	1.90
total gas age	n=2				1.0E-15	1.6E+01	2.2E-04	65.8	100.0	12.04	0.21
total gas age	n=2						1.0E+01			12.62	0.79

Run ID#	Temp	40/39	37/39	36/39	39K moles	K/Ca	C/K	%40*	%39Ar	Age	± Err
HN-55, E3:47, HN, J=0.00078715±0.000002											
73-03A	0	1.30E+02	3.91E-02	4.17E-01	2.8E-16	1.3E+01	3.3E-04	5.2	25.5	9.49	1.89
73-03B	2	2.94E+01	8.38E-03	7.25E-02	8.1E-16	6.1E+01	4.1E-04	27.2	100.0	11.30	0.35
	total gas age		n=2		1.1E-15	4.9E+01	3.4E+01			10.84	0.74
HN-55, E3:47, HN, J=0.00078715±0.000002											
74-04A	0	4.41E+01	4.01E-02	1.24E-01	4.7E-16	1.3E+01	-2.7E-05	17.1	64.4	10.68	0.75
74-04B	2	1.35E+01	0.00E+00	1.73E-02	2.6E-16	0.0E+00	-1.2E-03	62.2	100.0	11.86	0.49
	total gas age		n=2		7.3E-16	0.0E+00	0.0E+00			11.10	0.66
HN-55, E3:47, HN, J=0.00078715±0.000002											
75-05A	0	7.11E+01	6.67E-02	2.13E-01	4.1E-16	7.6E+00	-2.1E-04	11.2	42.5	11.31	1.05
75-05B	2	1.67E+01	6.10E-04	2.98E-02	5.6E-16	8.4E+02	-1.5E-03	47.3	100.0	11.17	0.29
	total gas age		n=2		9.7E-16	4.8E+02	5.9E+02			11.23	0.62
HN-55, E3:47, HN, J=0.00078715±0.000002											
76-06A	0	2.42E+01	3.28E-02	5.71E-02	3.5E-16	1.6E+01	-2.8E-04	30.4	97.7	10.41	0.58
76-06B	2	1.08E+02	2.22E-01	4.12E-01	8.0E-18	2.3E+00	-2.5E-03	-12.7	100.0	-19.61	20.87
	total gas age		n=2		3.6E-16	1.5E+01	9.4E+00			9.73	1.04
HN-55, E3:47, HN, J=0.00078715±0.000002											
77-07A	0	3.70E+01	4.91E-02	1.03E-01	1.3E-16	1.0E+01	-6.0E-04	18.1	95.6	9.49	1.32
77-07B	2	1.36E+02	5.00E-01	4.16E-01	6.0E-18	1.0E+00	-8.3E-03	9.8	100.0	18.79	27.19
	total gas age		n=2		1.4E-16	1.0E+01	6.6E+00			9.89	2.45
HN-55, E3:47, HN, J=0.00078715±0.000002											
78-08A	0	8.92E+01	1.24E-01	2.82E-01	7.5E-17	4.1E+00	-2.5E-03	6.6	37.4	8.38	3.14
78-08B	2	1.98E+01	5.86E-02	3.70E-02	1.3E-16	8.7E+00	-1.6E-03	44.7	100.0	12.50	1.05
	total gas age		n=2		2.0E-16	7.0E+00	3.2E+00			10.96	1.83
HN-55, E3:47, HN, J=0.00078715±0.000002											
79-09A	0	2.16E+01	1.88E-02	4.25E-02	1.5E-16	2.7E+01	7.8E-04	41.8	82.8	12.76	1.03
79-09B	2	2.20E+03	7.07E-05	7.48E+00	3.2E-17	7.2E+03	9.6E-03	-0.7	100.0	-20.79	118.33
	total gas age		n=2		1.9E-16	1.3E+03	5.1E+03			6.99	21.20

Run ID#	Temp	40/39	37/39	36/39	39K moles	K/Ca	Cl/K	%40*	%39Ar	Age	\pm Err
HN-55, E3:47, HN, J=0.00078715±0.000002											
80-10A	0	5.02E+01	1.30E-01	1.75E-01	5.9E-17	3.9E+00	3.3E-03	-2.9	47.5	-2.04	2.85
80-10B	2	1.13E+03	5.97E-02	3.83E+00	6.5E-17	8.5E+00	5.4E-03	-0.1	100.0	-2.06	40.32
total gas age		n=2			1.2E-16	6.4E+00	3.3E+00			-2.05	22.51
n/t=19/20											
Isochron analysis of HN-55:											
40Ar/36Ar Intercept:											
MSWD:											
2.50											
Two-step laser heating of 10 biotite flakes, sample HN-58											
HN-58, D15:47, HN, J=0.0007906±0.000002											
41-01A	0	6.10E+01	1.99E-02	1.78E-01	9.7E-17	2.6E+01	-1.9E-03	13.5	4.8	11.75	1.50
41-01B	2	1.11E+01	6.24E-02	9.20E-03	1.9E-15	8.2E+00	4.8E-05	75.6	100.0	11.96	0.08
total gas age		n=2			2.0E-15	9.0E+00	1.2E+01			11.95	0.15
HN-58, D15:47, HN, J=0.0007906±0.000002											
42-02A	0	2.48E+01	3.93E-02	5.58E-02	2.6E-16	1.3E+01	7.6E-04	33.6	13.1	11.84	0.48
42-02B	2	9.95E+00	1.28E-02	6.00E-03	1.8E-15	4.0E+01	1.3E-04	82.2	100.0	11.63	0.07
total gas age		n=2			2.0E-15	3.6E+01	1.9E+01			11.66	0.12
HN-58, D15:47, HN, J=0.0007906±0.000002											
43-03A	0	3.58E+01	5.63E-03	9.22E-02	1.5E-16	9.1E+01	-1.7E-03	23.8	7.4	12.11	0.91
43-03B	2	1.19E+01	1.24E-02	1.27E-02	1.9E-15	4.1E+01	3.5E-04	68.5	100.0	11.55	0.09
total gas age		n=2			2.0E-15	4.5E+01	3.5E+01			11.60	0.15
HN-58, D15:47, HN, J=0.0007906±0.000002											
44-04A	0	6.41E+01	2.48E-01	2.15E-01	8.5E-17	2.1E+00	4.0E-03	0.9	4.2	0.85	2.07
44-04B	2	1.65E+01	1.48E-02	2.78E-02	1.9E-15	3.4E+01	2.2E-04	50.3	100.0	11.81	0.12
total gas age		n=2			2.0E-15	3.3E+01	2.3E+01			11.34	0.20
HN-58, D15:47, HN, J=0.0007906±0.000002											
45-05A	0	7.22E+01	1.45E-01	2.10E-01	5.2E-17	3.5E+00	1.5E-04	14.2	1.9	14.56	2.60
45-05B	2	9.86E+00	5.99E-02	5.40E-03	2.7E-15	8.5E+00	9.4E-05	83.8	100.0	11.75	0.05

Run ID#	Temp	40/39	37/39	36/39	39K moles	K/Ca	C/I/K	%40*	%39Ar	Age	± Err
total gas age											
HN-58, D15:47, HN,	J=0.0007906±0.000002			n=2	2.7E-15	8.4E+00	3.5E+00			11.80	0.10
46-06A	0	4.44E+01	4.22E-02	1.14E-01	7.8E-17	1.2E+01	-9.6E-04	24.2	4.7	15.23	1.53
46-06B	2	1.14E+01	2.21E-02	1.08E-02	1.6E-15	2.3E+01	3.6E-04	72.1	100.0	11.65	0.09
total gas age											
HN-58, D15:47, HN,	J=0.0007906±0.000002			n=2	1.7E-15	2.3E+01	7.8E+00			11.82	0.16
47-07A	0	5.45E+01	7.30E-02	1.64E-01	1.6E-16	7.0E+00	1.7E-04	11.3	8.1	8.74	1.22
47-07B	2	1.18E+01	5.33E-02	1.12E-02	1.8E-15	9.6E+00	4.2E-04	72.0	100.0	12.06	0.09
total gas age											
HN-58, D15:47, HN,	J=0.0007906±0.000002			n=2	2.0E-15	9.4E+00	1.8E+00			11.79	0.18
48-08A	0	1.27E+01	0.00E+00	1.71E-02	2.0E-16	0.0E+00	-1.7E-04	60.4	71.1	10.93	0.43
48-08B	2	1.14E+01	0.00E+00	7.67E-03	8.1E-17	0.0E+00	3.2E-03	80.1	100.0	12.98	0.96
total gas age											
HN-58, D15:47, HN,	J=0.0007906±0.000002			n=2	2.8E-16	0.0E+00	0.0E+00			11.52	0.58
49-09A	0	4.40E+01	0.00E+00	1.25E-01	4.3E-17	0.0E+00	-2.9E-03	16.3	4.0	10.21	2.47
49-09B	2	1.06E+01	0.00E+00	7.07E-03	1.0E-15	0.0E+00	4.4E-04	80.3	100.0	12.14	0.12
total gas age											
HN-58, D15:47, HN,	J=0.0007906±0.000002			n=2	1.1E-15	0.0E+00	0.0E+00			12.06	0.21
50-10A	0	3.10E+01	1.31E-02	7.66E-02	1.2E-16	3.9E+01	-2.0E-04	27.1	7.5	11.93	0.92
50-10B	2	1.07E+01	2.62E-02	8.47E-03	1.5E-15	1.9E+01	5.1E-04	76.6	100.0	11.64	0.08
total gas age											
				n=2	1.6E-15	2.1E+01	1.4E+01			11.67	0.14
				n/t=17/20						11.70	0.05
Isochron analysis of HN-58:											
40Ar/36Ar Intercept:											
MSWD:											
										2.40	

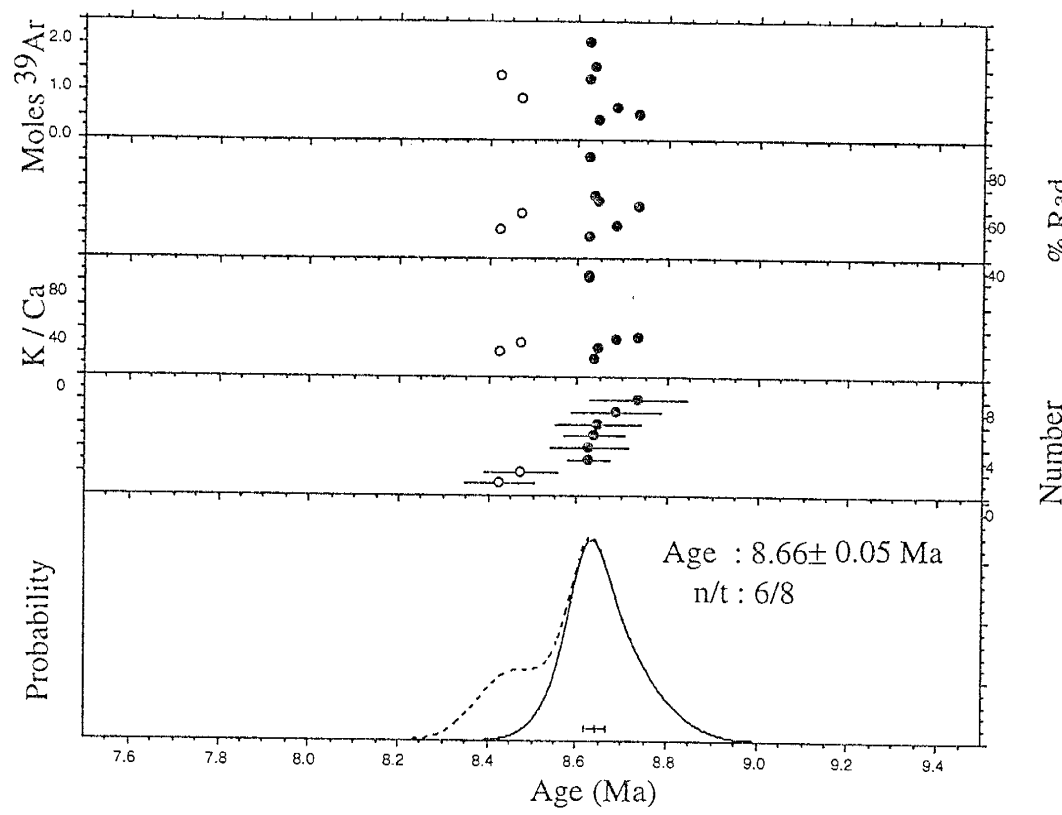
Run ID#	Temp	40/39	37/39	36/39	39K moles	K/Ca	Cl/K	%40*	%39Ar	Age	\pm Err
Two-step laser heating of 10 biotite flakes, sample HN-59											
HN-59, E1:47, HN, J=0.00078616±0.000002	0	2.48E+02	2.53E-02	8.16E-01	9.3E-16	2.0E+01	-6.5E-04	2.7	33.7	9.44	2.61
61-01A	0	1.39E+01	7.42E-02	1.59E-02	1.8E-15	6.9E+00	5.3E-04	66.4	100.0	13.05	0.12
61-01B	2	3.23E-02	8.02E-02	n=2	2.7E-15	1.1E+01	9.4E+00			11.83	0.96
HN-59, E1:47, HN, J=0.00078616±0.000002	0	5.54E+01	2.58E-02	1.58E-01	8.4E-16	2.0E+01	6.2E-04	15.9	40.4	12.43	0.70
62-02A	2	3.32E+01	3.23E-02	n=2	1.2E-15	1.6E+01	7.3E-04	28.7	100.0	13.46	0.34
62-02B	0	3.88E+02	2.90E-02	1.29E+00	1.4E-15	5.0E+00	1.4E-04	18.7	100.0	13.04	0.49
63-03A	2	5.28E+01	1.03E-01	1.45E-01	2.1E-15	1.7E+01	2.8E+00				
HN-59, E1:47, HN, J=0.00078616±0.000002	0	2.99E+01	3.84E-03	6.78E-02	5.8E-16	1.3E+02	2.2E-03	2.0	48.5	10.92	4.13
64-04A	2	6.17E+01	1.73E-02	1.74E-01	7.6E-16	2.9E+01	1.1E-03	16.8	100.0	13.94	0.53
HN-59, E1:47, HN, J=0.00078616±0.000002	0	3.40E+01	2.00E-02	8.43E-02	9.7E-16	2.5E+01	9.1E-04	33.0	43.6	13.94	0.47
65-05A	2	1.15E+01	3.87E-02	7.06E-03	3.0E-15	7.5E+01	7.3E+01			14.33	0.62
HN-59, E1:47, HN, J=0.00078616±0.000002	0	1.03E+02	1.83E-02	3.16E-01	8.7E-16	2.8E+01	5.7E-04	26.6	32.4	12.79	0.37
66-06A	2	1.18E+01	8.13E-02	8.02E-03	1.5E-15	6.3E+00	5.3E-04	81.9	100.0	13.34	0.09
HN-59, E1:47, HN, J=0.00078616±0.000002	0	9.15E+01	1.54E-02	2.84E-01	2.4E-15	1.4E+01	8.7E+00			13.16	0.18
67-07A	2	1.16E+01	2.47E-02	7.58E-03	1.6E-15	2.1E+01	5.2E-04	8.9	37.0	12.94	1.12
67-07B	0	1.16E+01	2.47E-02	n=2	2.4E-15	1.4E+01	1.5E+01			13.36	0.11
total gas age										13.21	0.48
HN-59, E1:47, HN, J=0.00078616±0.000002	0	9.15E+01	1.54E-02	2.84E-01	8.1E-16	3.3E+01	8.5E-04	8.3	34.2	10.70	1.07
total gas age	2	1.16E+01	2.47E-02	n=2	2.4E-15	2.5E+01	6.4E-05	80.8	100.0	13.30	0.12
								8.8E+00		12.41	0.45

Run ID#	Temp	40/39	37/39	36/39	39K moles	K/Ca	Ci/K	%40*	%39Ar	Age	± Err
HN-59, E1:47, HN,	J=0.00078616±0.000002										
68-08A	0	2.40E+01	1.10E-01	5.27E-02	4.1E-16	4.6E+00	1.2E-03	35.2	24.6	11.97	0.44
68-08B	2	1.06E+01	3.52E-02	4.21E-03	1.3E-15	1.4E+01	5.7E-04	88.3	100.0	13.26	0.09
total gas age		n=2		1.7E-15	1.2E+01	7.0E+00				12.94	0.18
HN-59, E1:47, HN,	J=0.00078616±0.000002										
69-09A	0	4.95E+01	2.18E-02	1.38E-01	5.7E-16	2.3E+01	5.7E-04	17.8	46.7	12.47	0.65
69-09B	2	1.14E+01	4.08E-02	7.72E-03	6.5E-16	1.2E+01	8.4E-04	80.1	100.0	12.95	0.21
total gas age		n=2		1.2E-15	1.8E+01	7.7E+00				12.72	0.41
HN-59, E1:47, HN,	J=0.00078616±0.000002										
70-10A	0	1.22E+02	1.80E-02	3.84E-01	1.6E-15	2.8E+01	9.8E-04	6.8	52.3	11.76	1.30
70-10B	2	1.16E+01	8.88E-02	7.13E-03	1.5E-15	5.7E+00	3.3E-05	81.9	100.0	13.43	0.13
total gas age		n=2		3.1E-15	1.8E+01	1.6E+01				12.55	0.74
n/t=20/20											
Isochron analysis of HN-59:								13.29	0.06		
40Ar/36Ar Intercept:								293.80	0.80		
Mswd:								2.05			

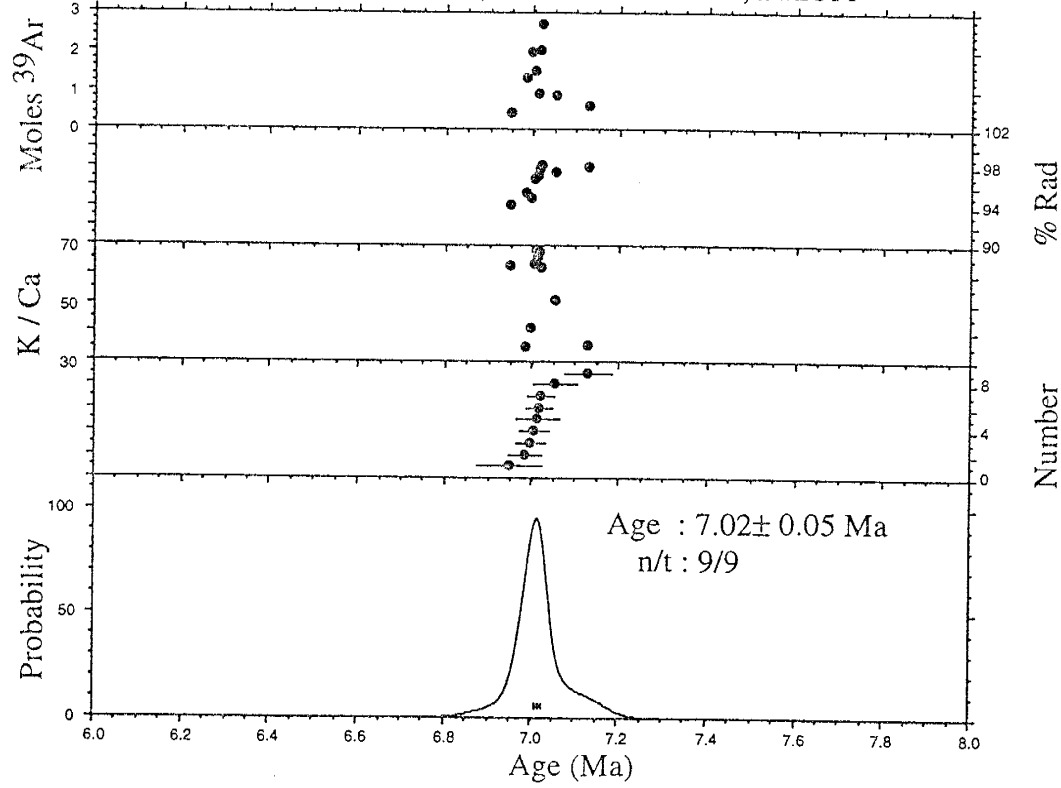
Appendix 6.a

Laser Fusion Graphical Analysis
sanidine and plagioclase samples

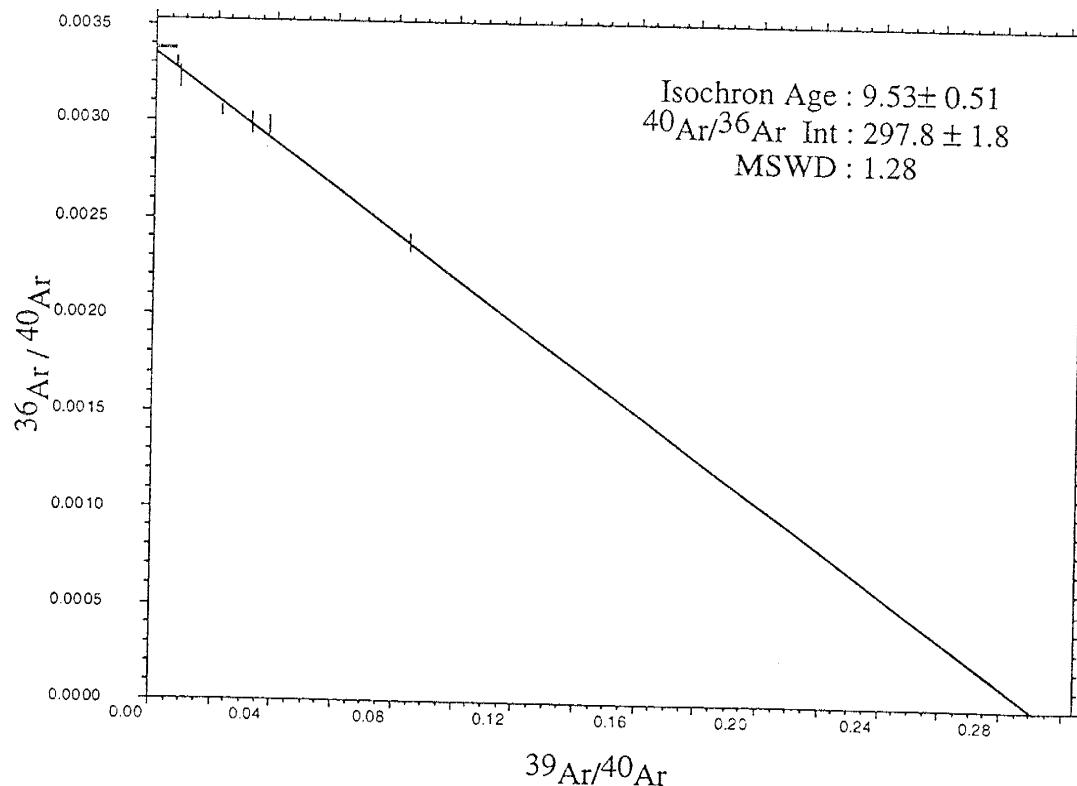
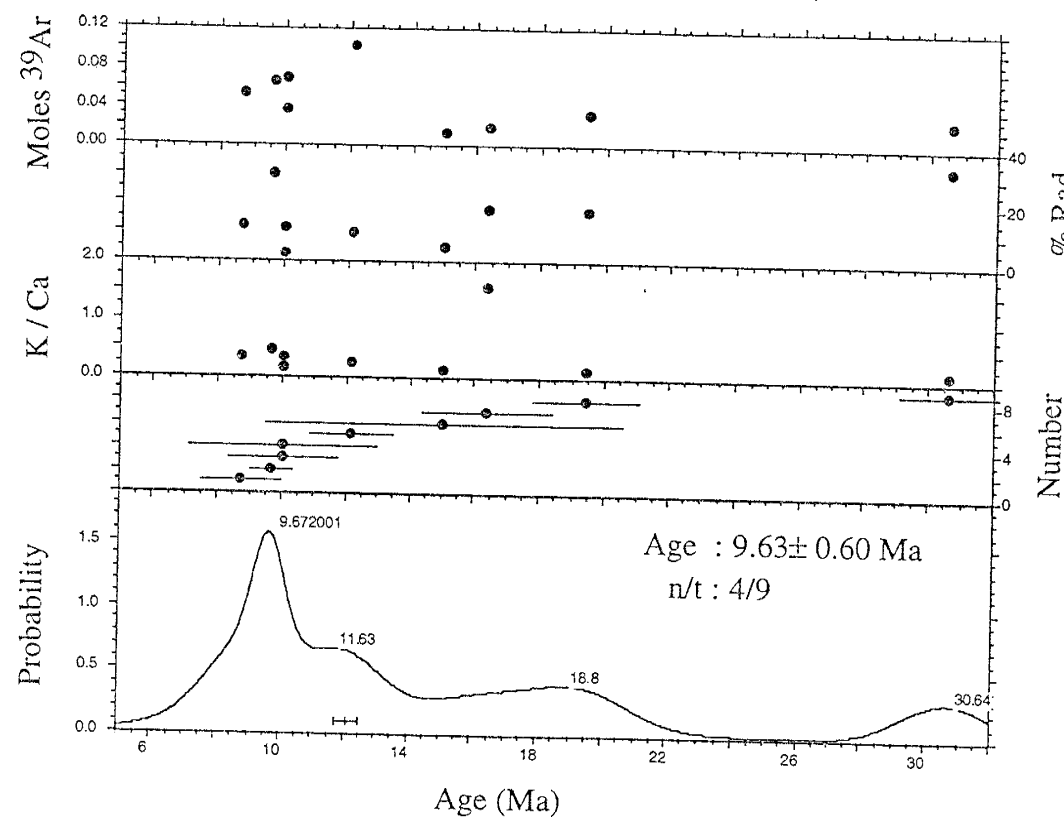
HN-1, Sanidine, Laser Total Fusion, L#2814



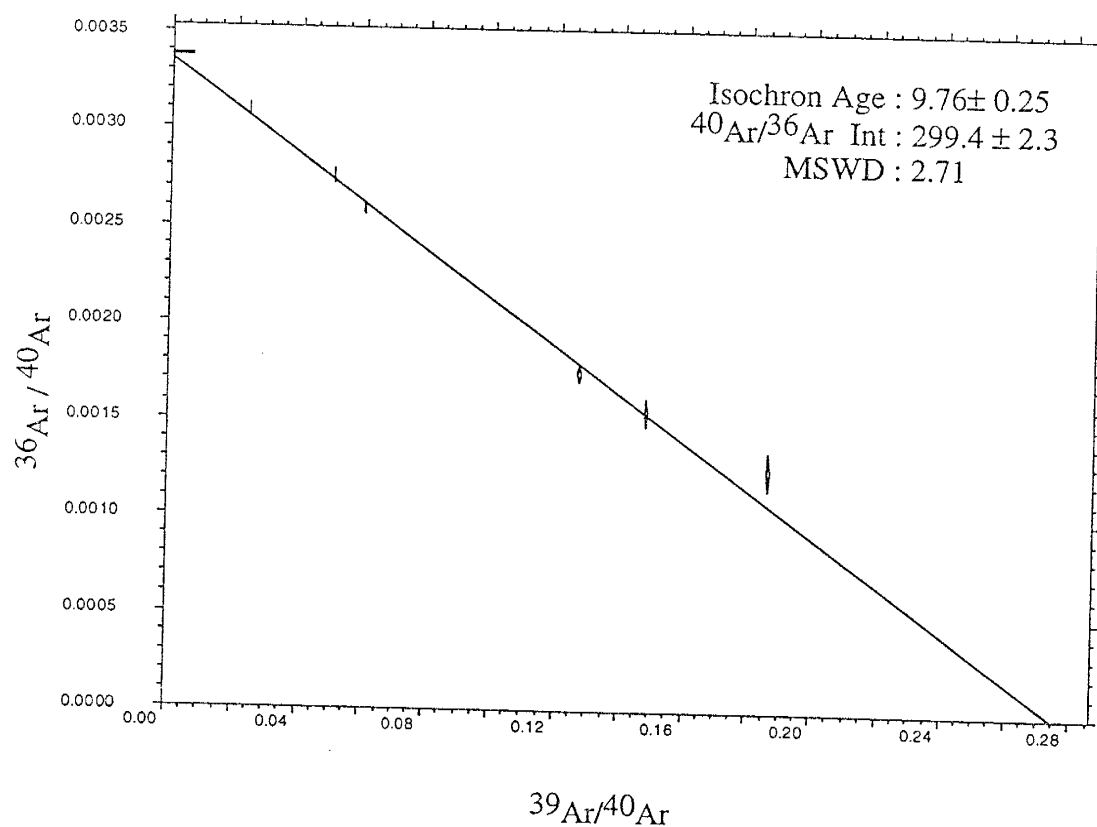
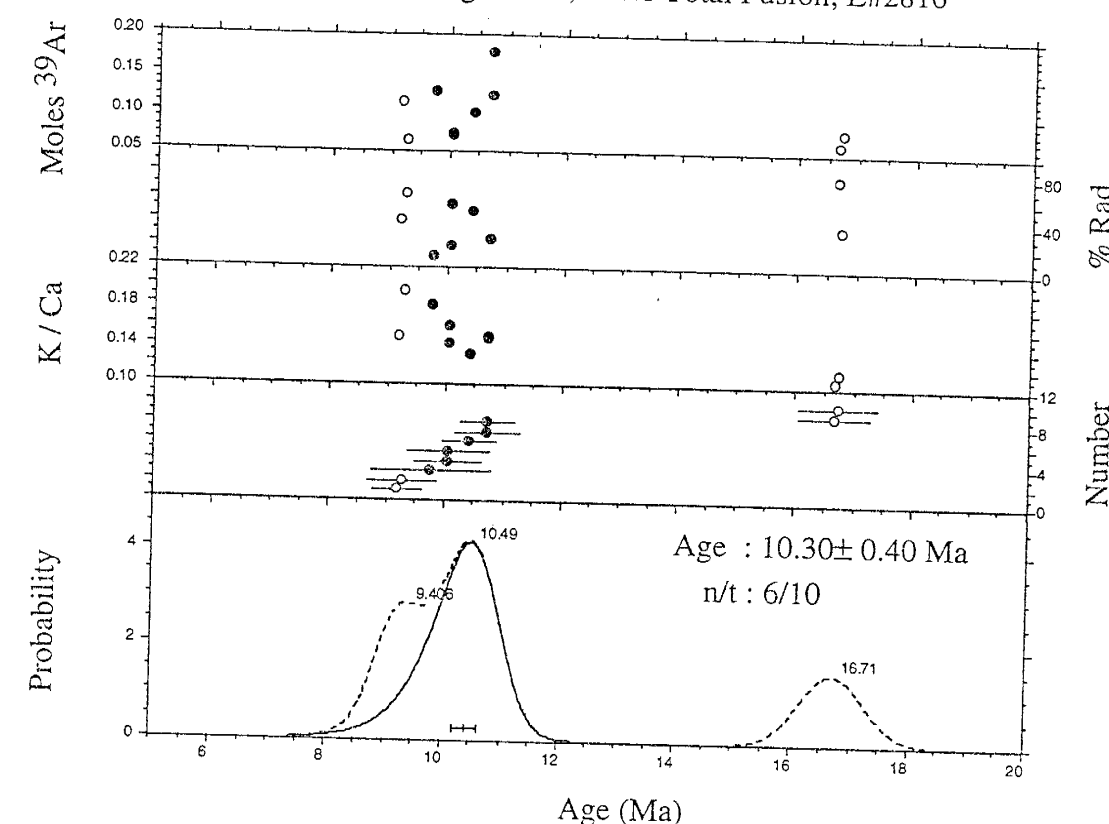
HN-4, Sanidine, Laser Total Fusion, L#2811



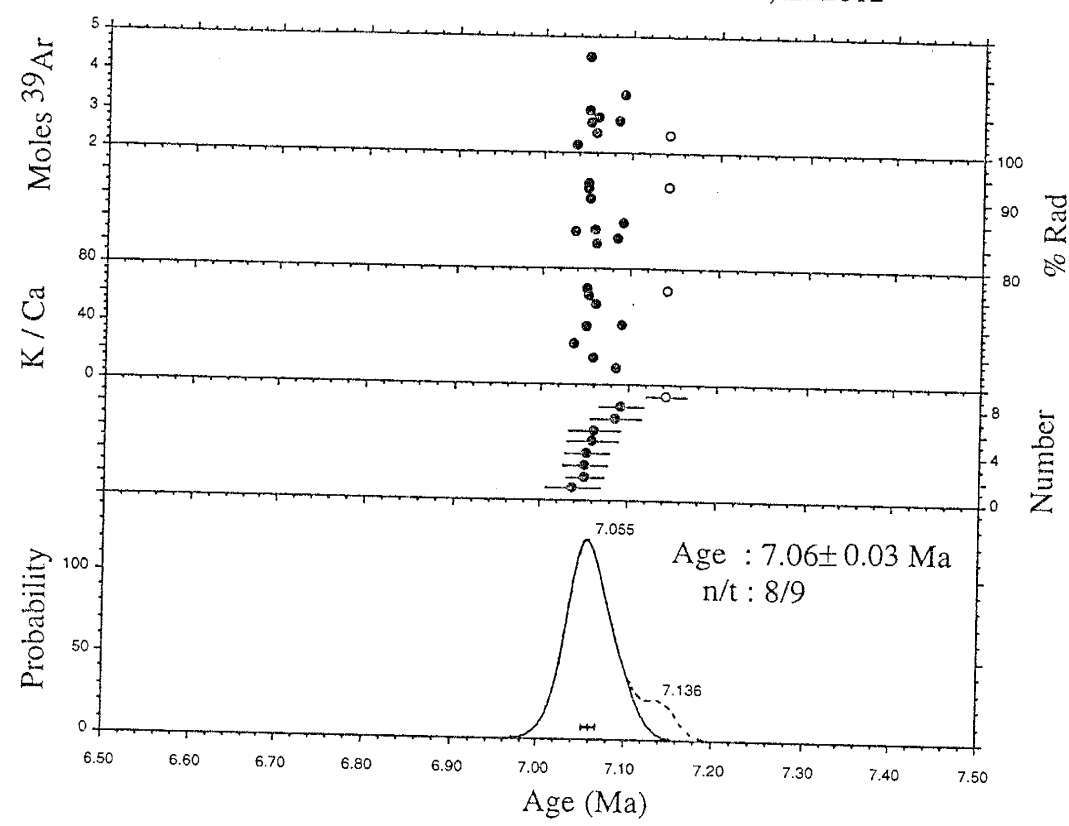
HN-2, Plagioclase, Laser Total Fusion, L#2815



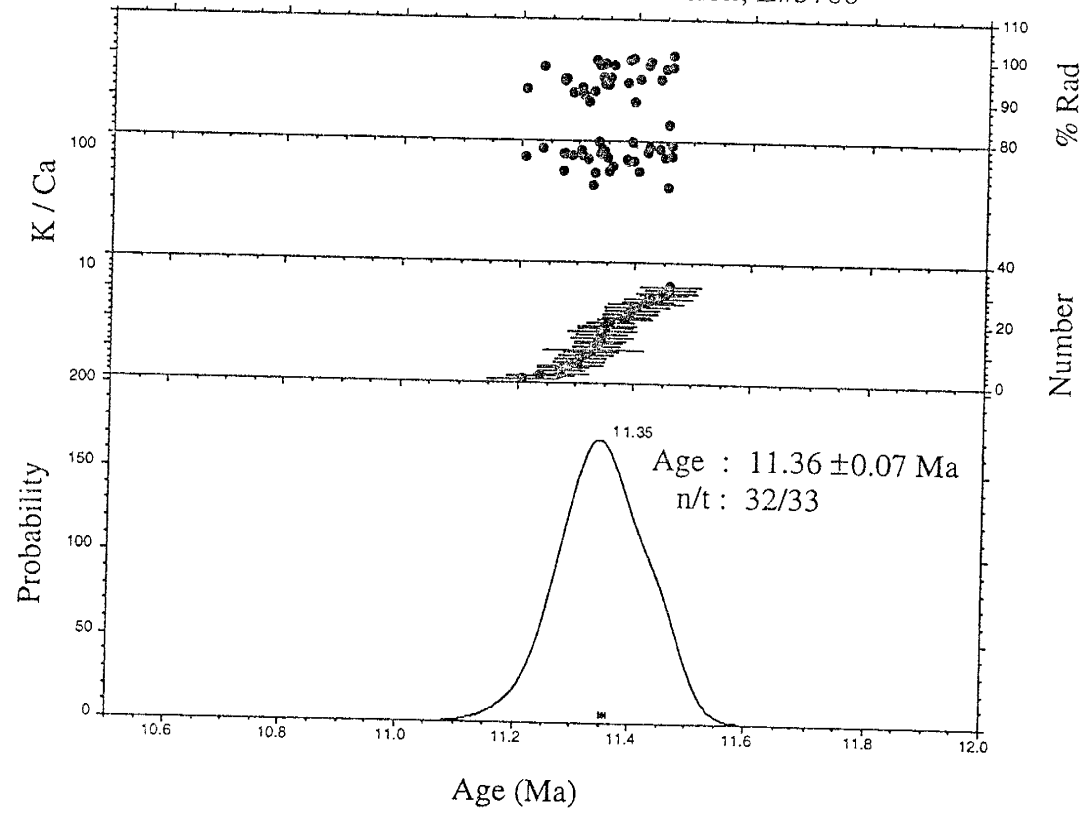
HN-3, Plagioclase, Laser Total Fusion, L#2816

 $^{39}\text{Ar}/^{40}\text{Ar}$

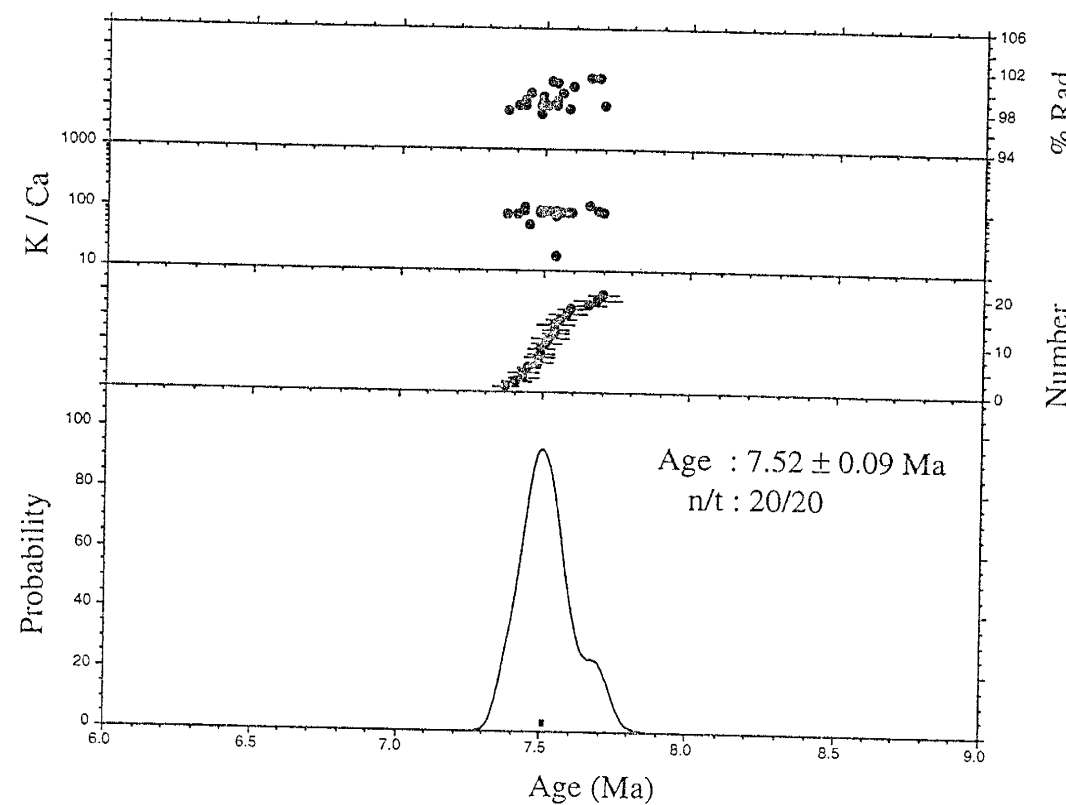
HN-7, Sanidine, Laser Total Fusion, L#2812



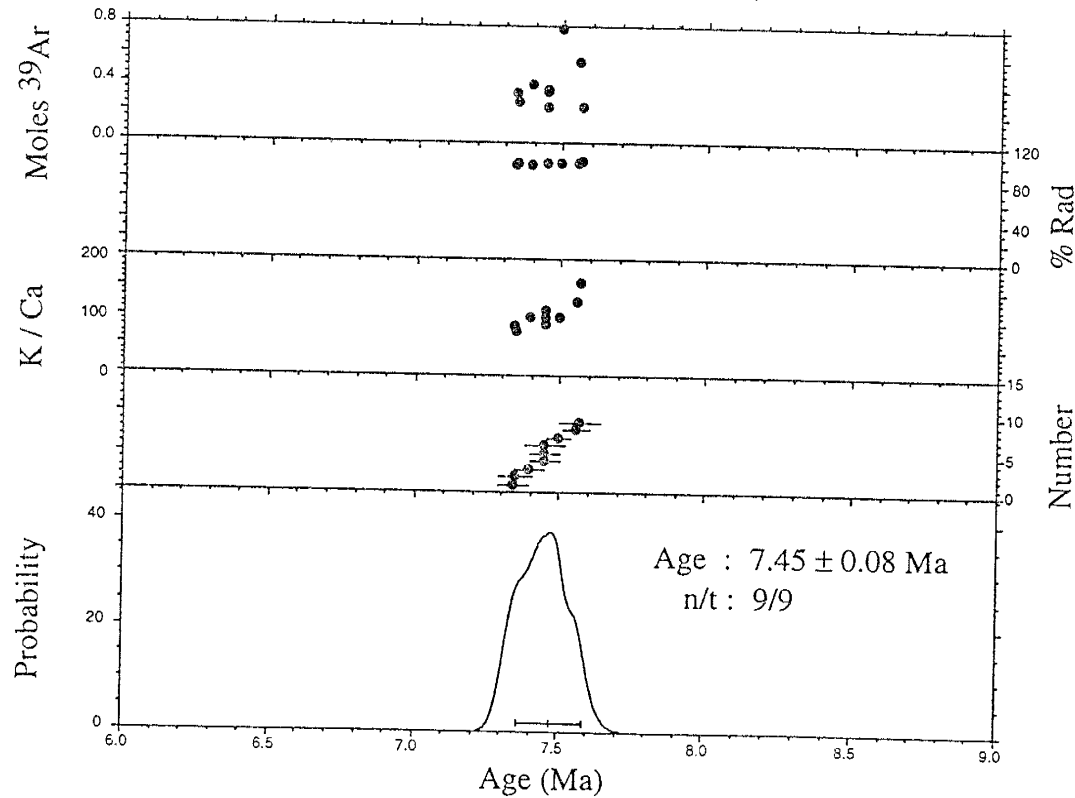
HN-17, Sanidine, Laser Total Fusion, L#5788



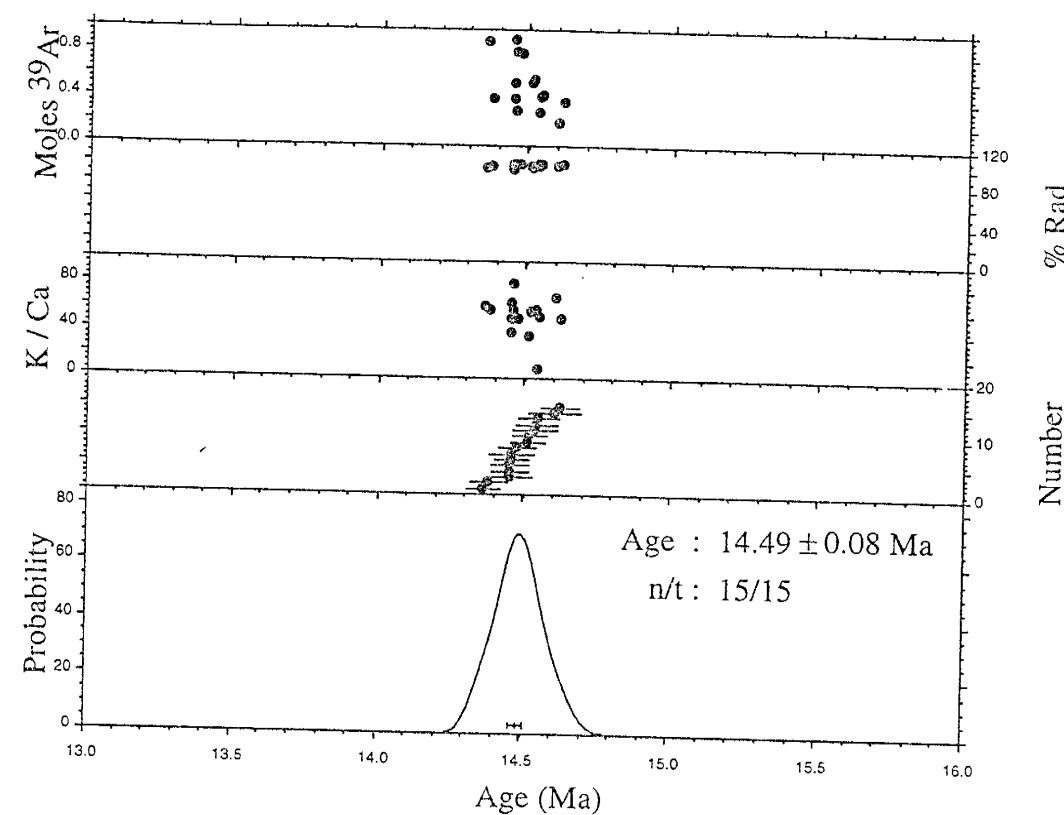
HN-24, Sanidine, Laser Total Fusion, L#5799



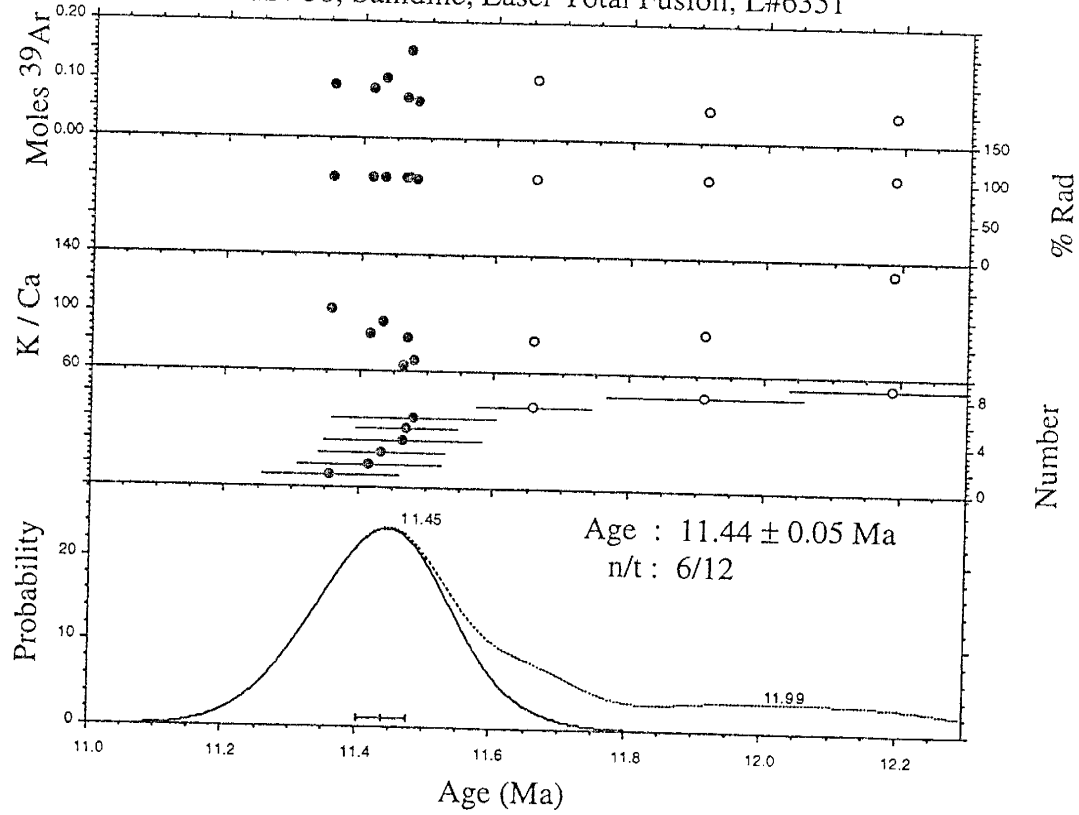
HN-25, Sanidine, Laser Total Fusion, L#6032



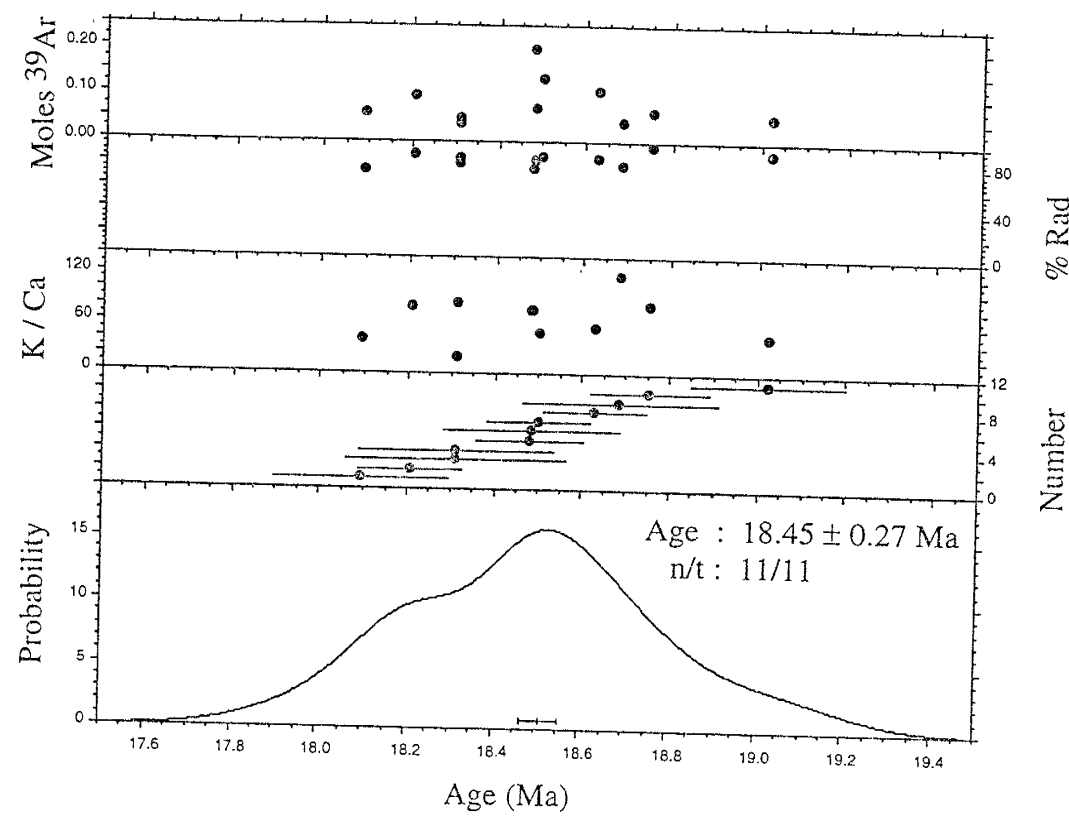
HN-37, Sanidine, Laser Total Fusion, L#6028



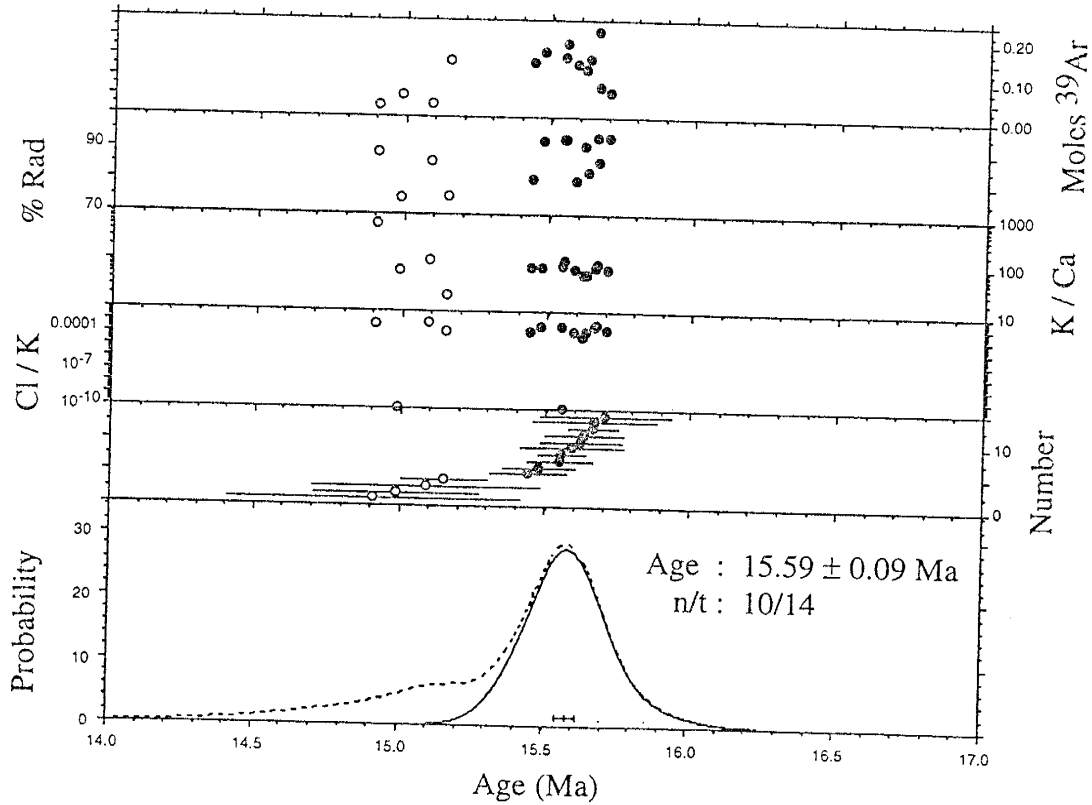
HN-38, Sanidine, Laser Total Fusion, L#6351



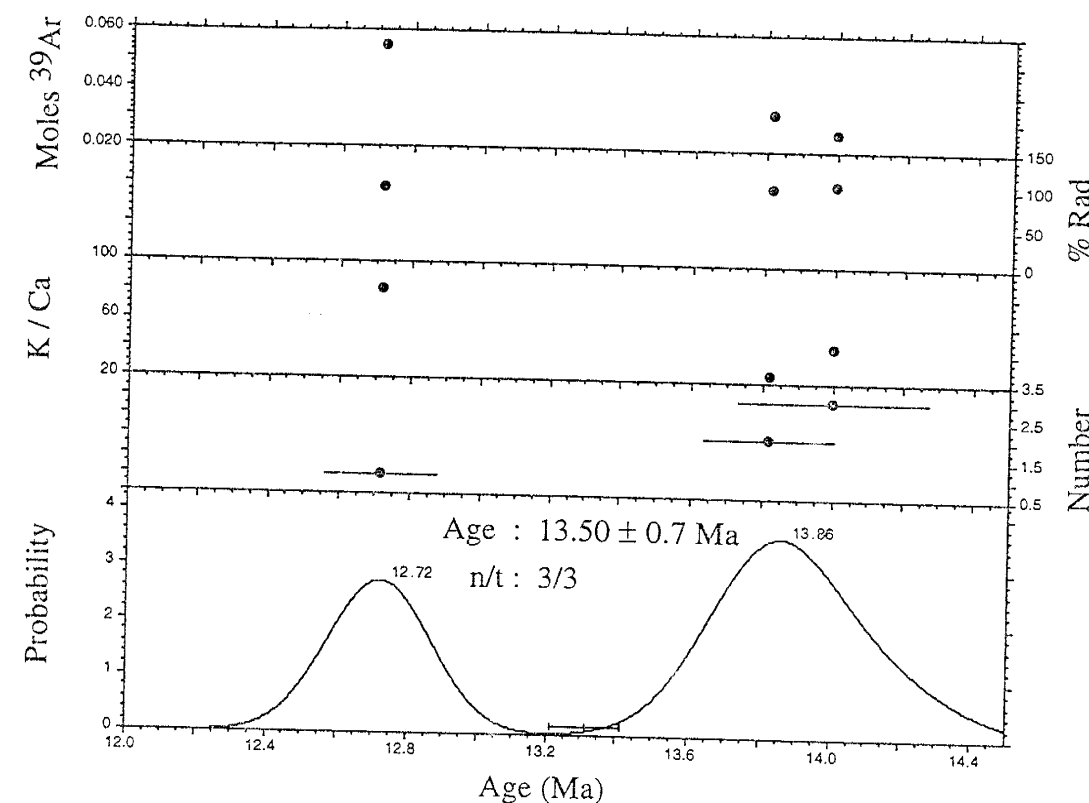
HN-39, Sanidine, Laser Total Fusion, L#6357



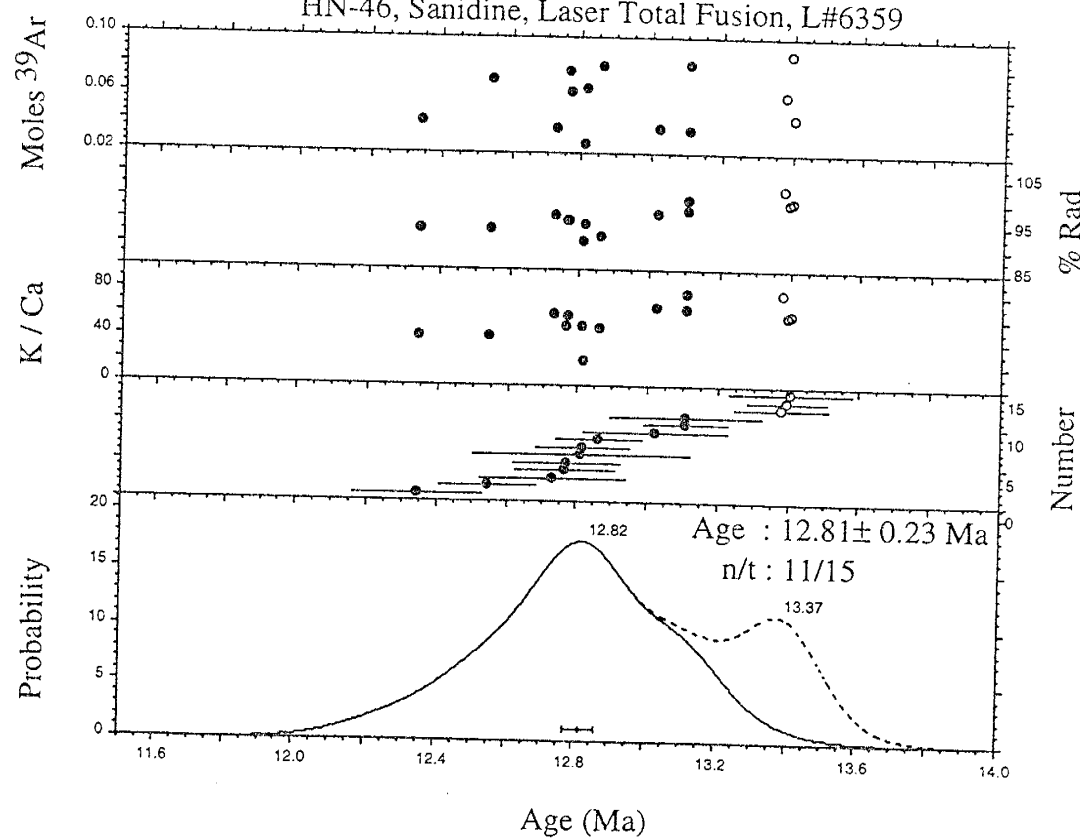
HN-41, Sanidine, Laser Total Fusion, L#6586



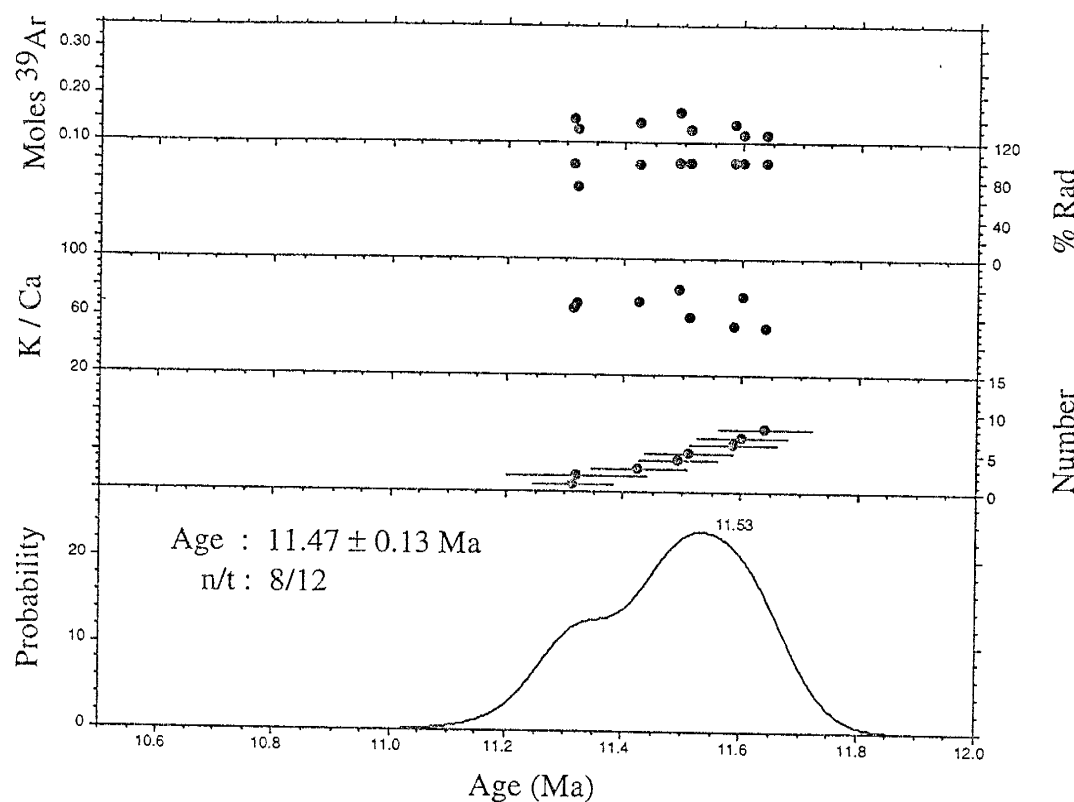
HN-45, Sanidine, Laser Total Fusion, L#6355



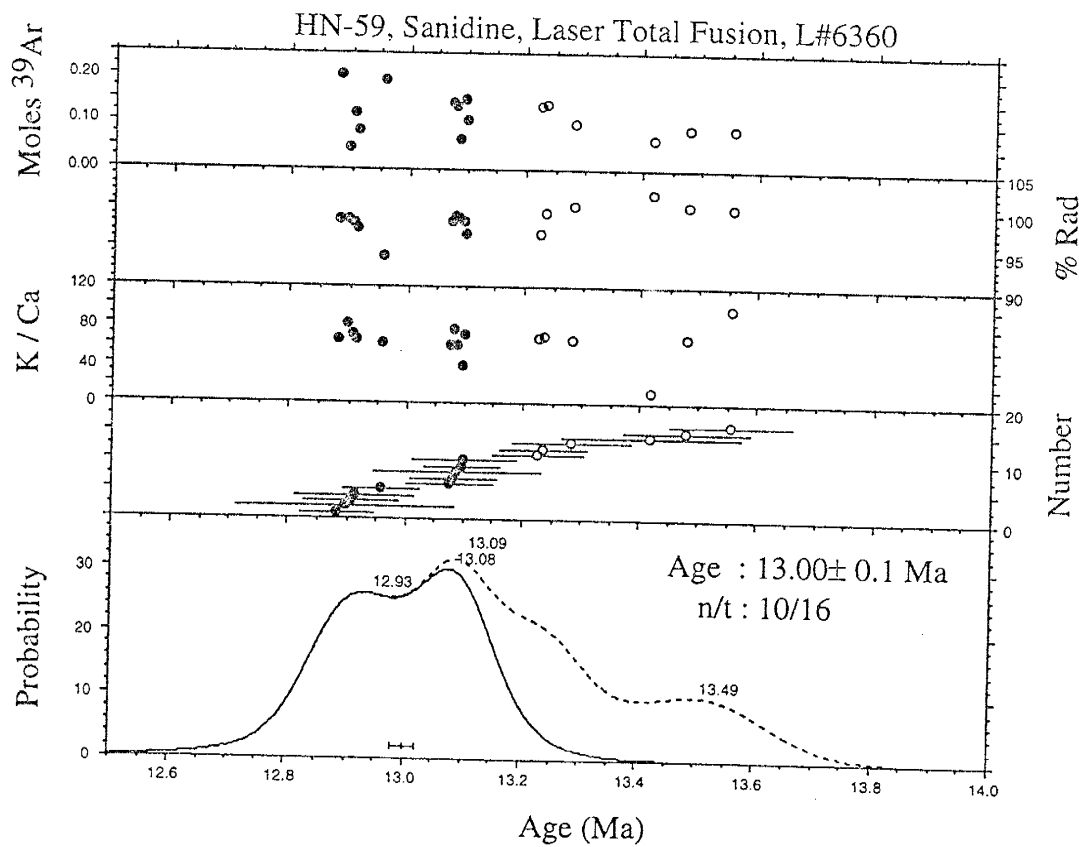
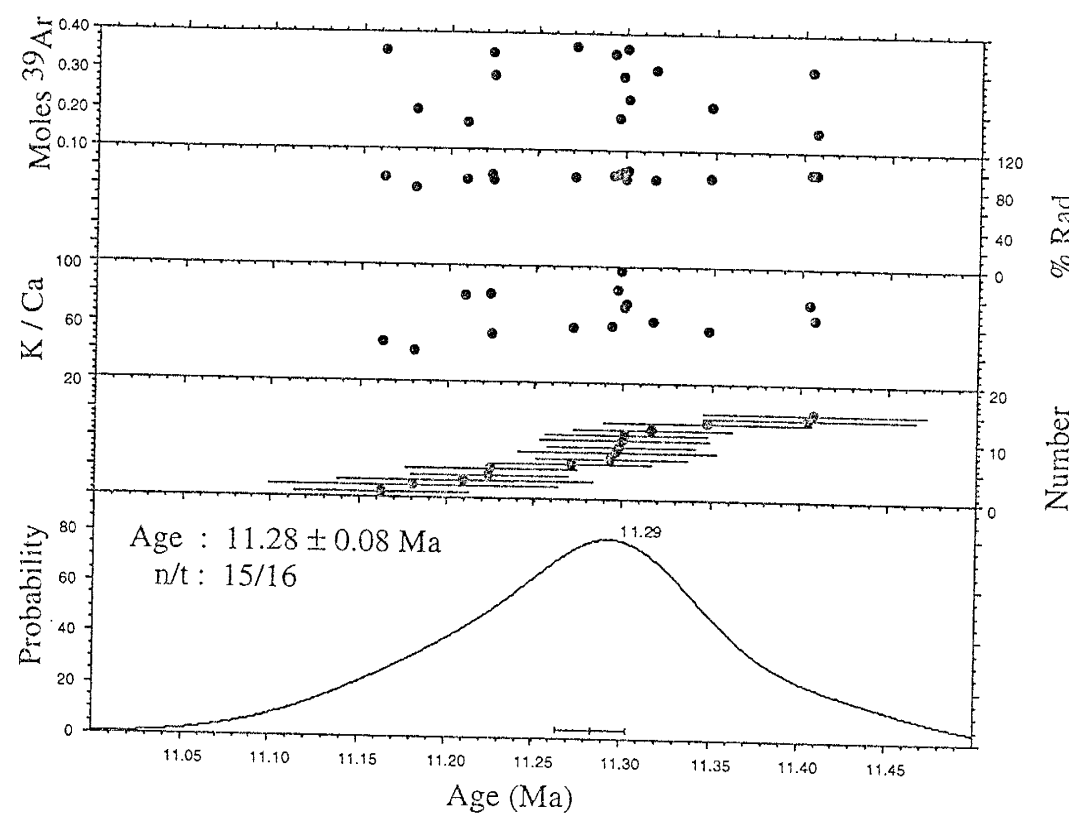
HN-46, Sanidine, Laser Total Fusion, L#6359



HN-55, Sanidine, Laser Total Fusion, L#6353



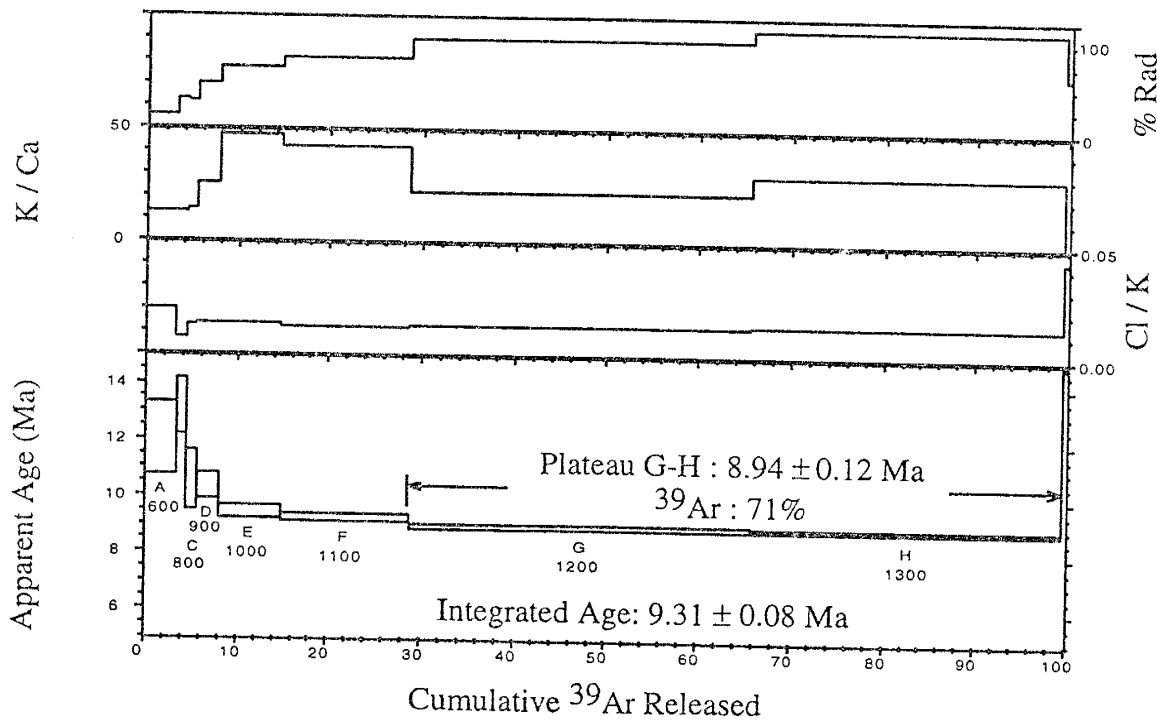
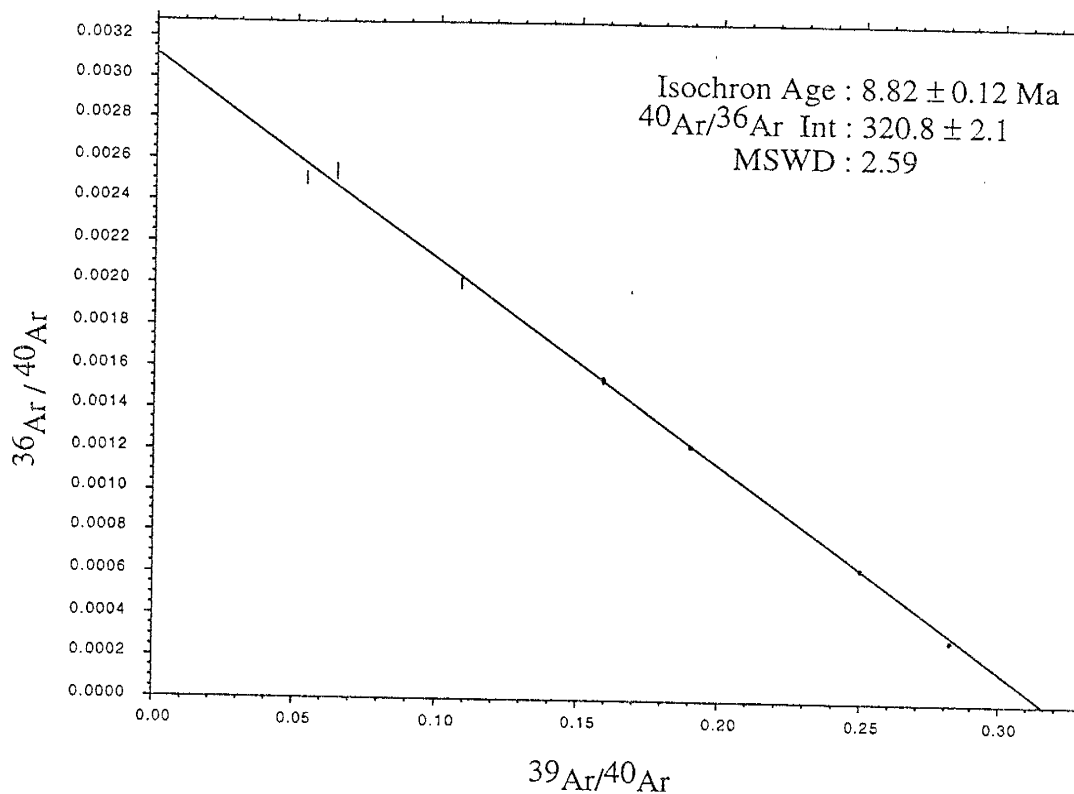
HN-58, Sanidine, Laser Total Fusion, L#6360



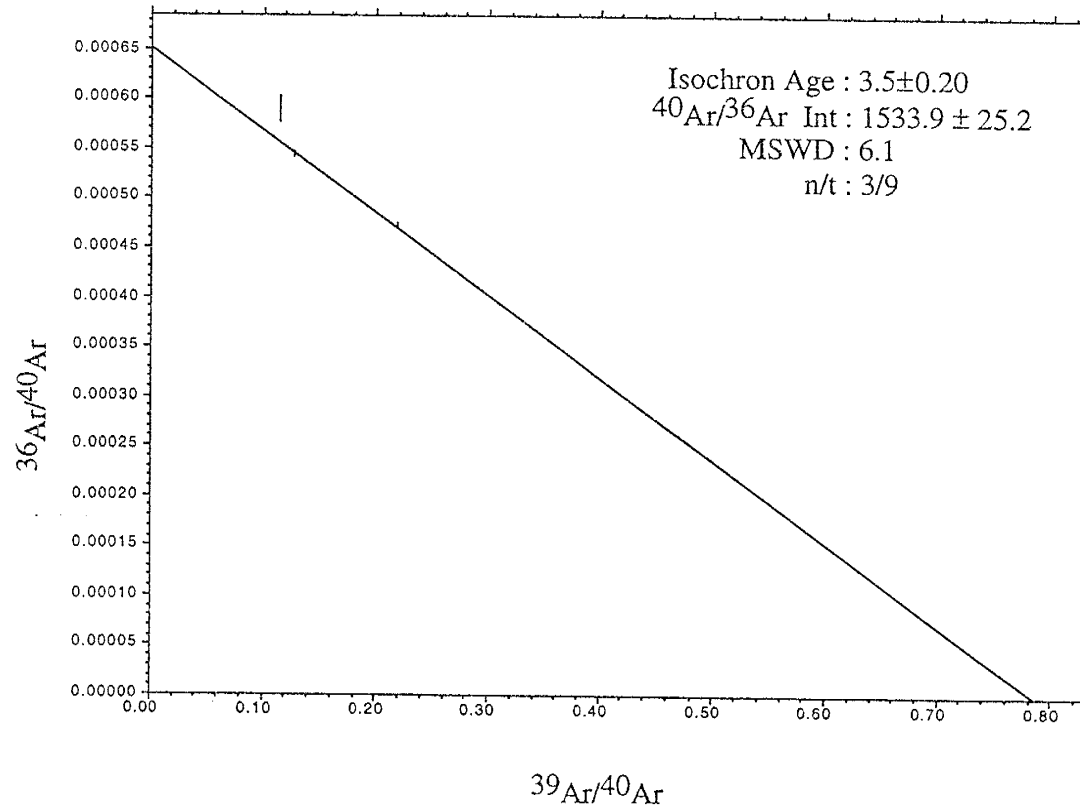
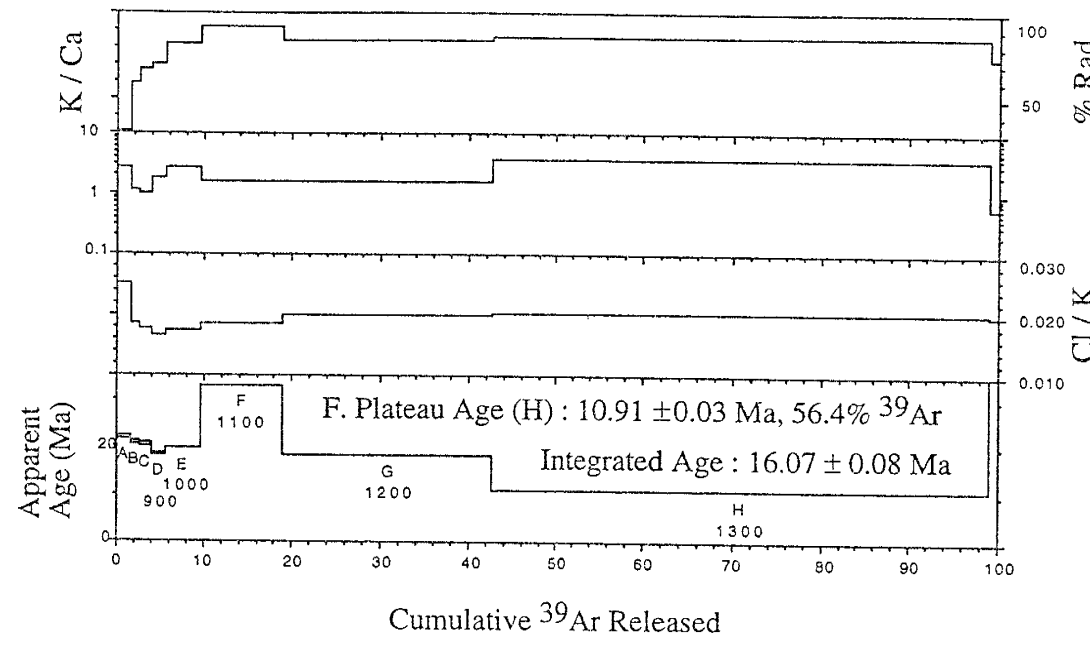
Appendix 6.b

Furnace Step-Heating Graphical Analysis
biotite, hornblende, and plagioclase samples

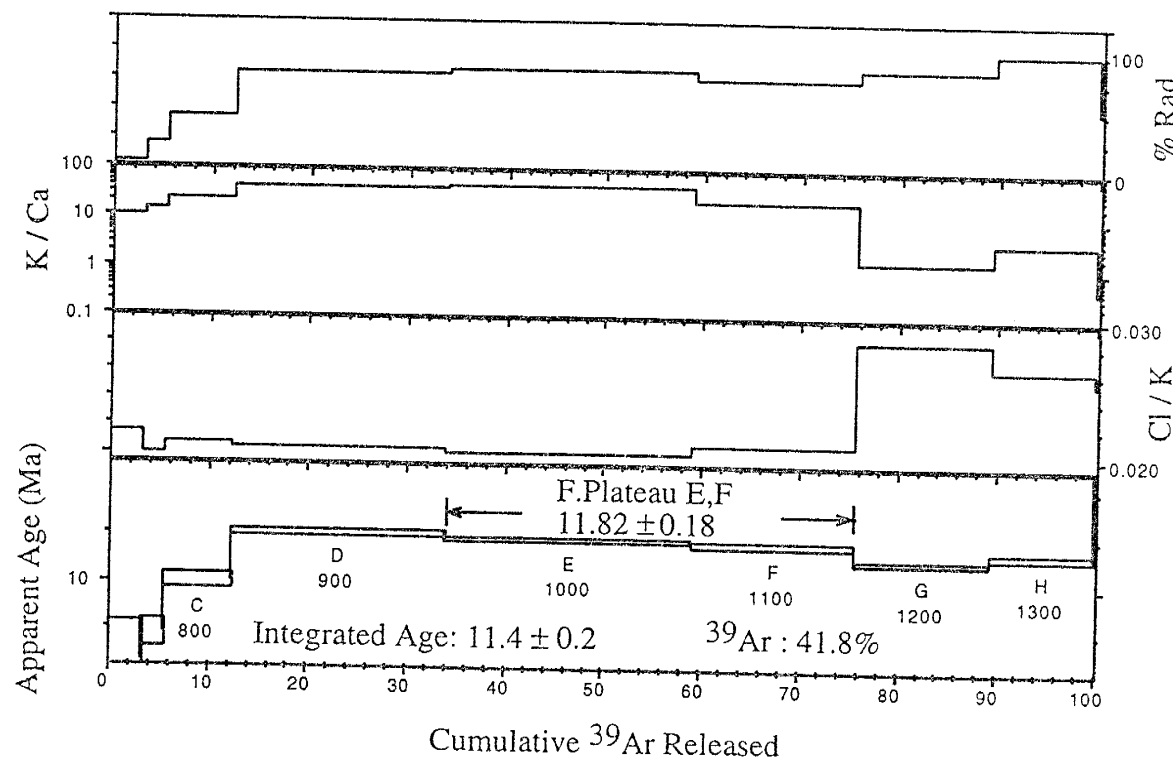
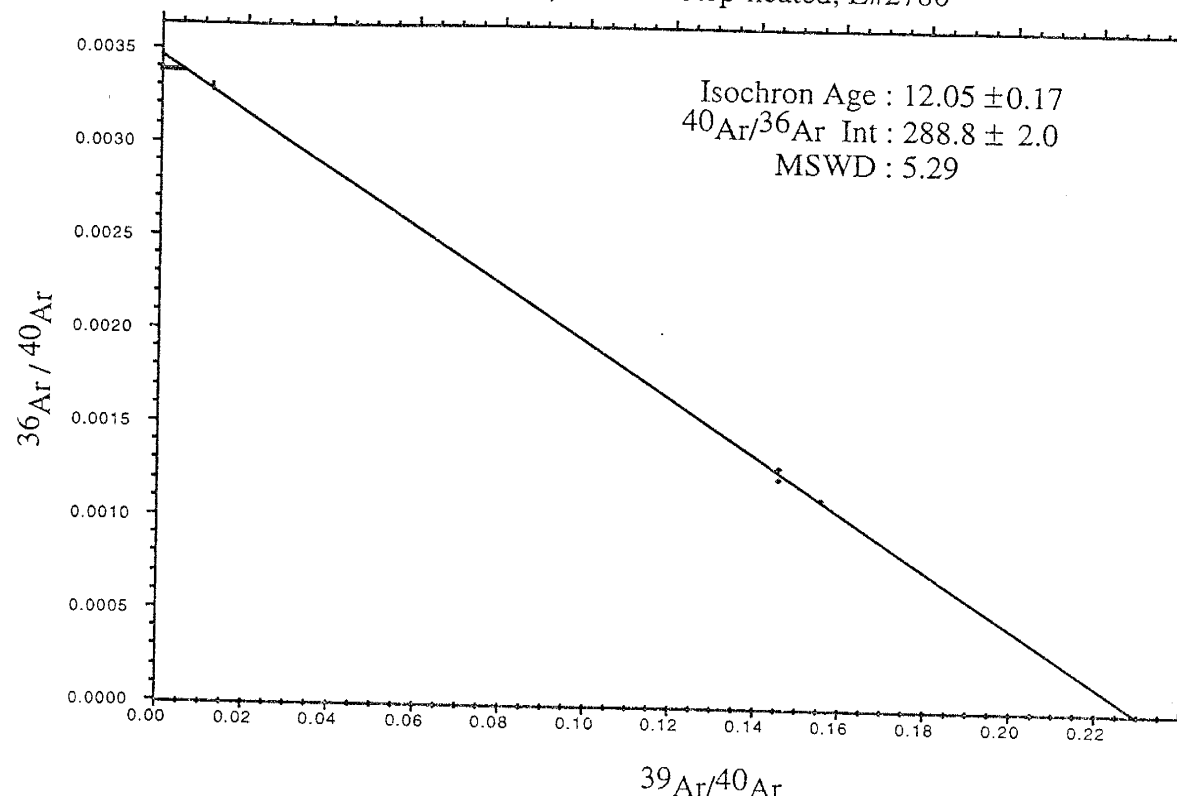
HN-1, Biotite, Furnace Step-heated, L#2778



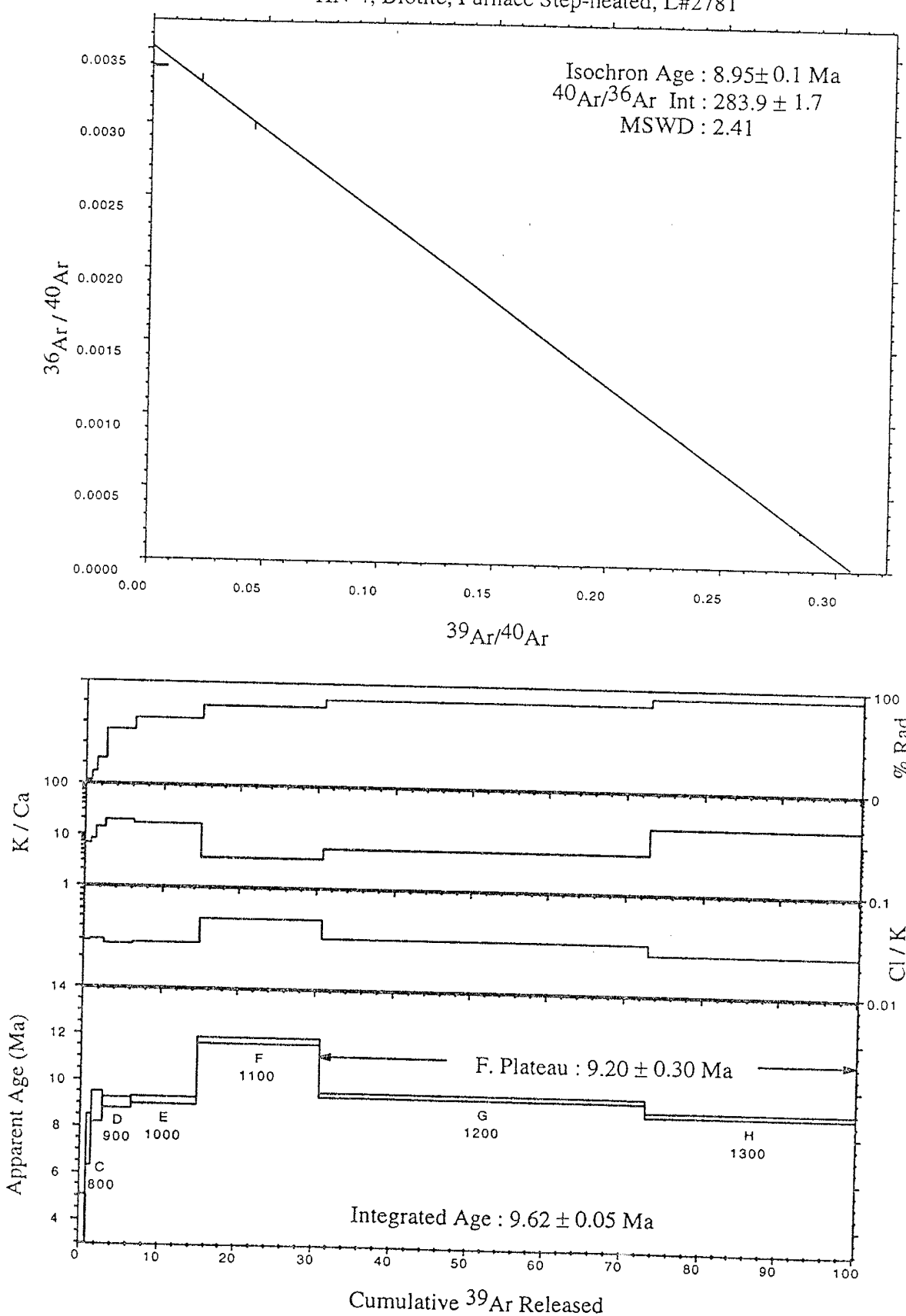
HN-2, Biotite, furnace step-heating



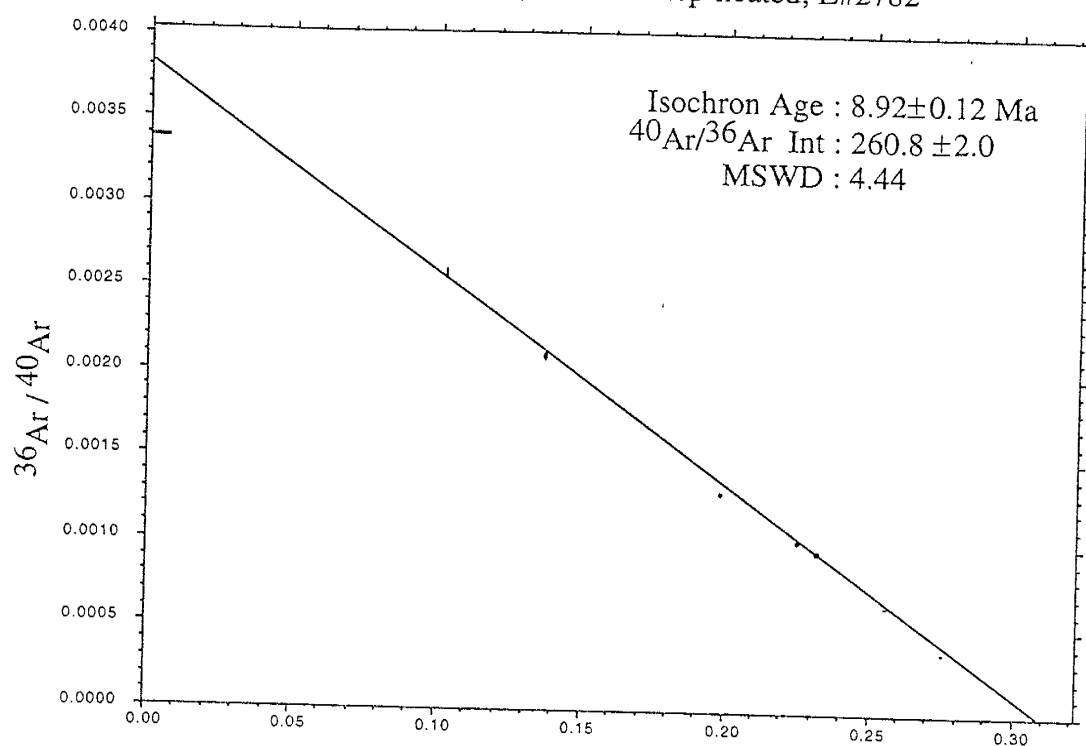
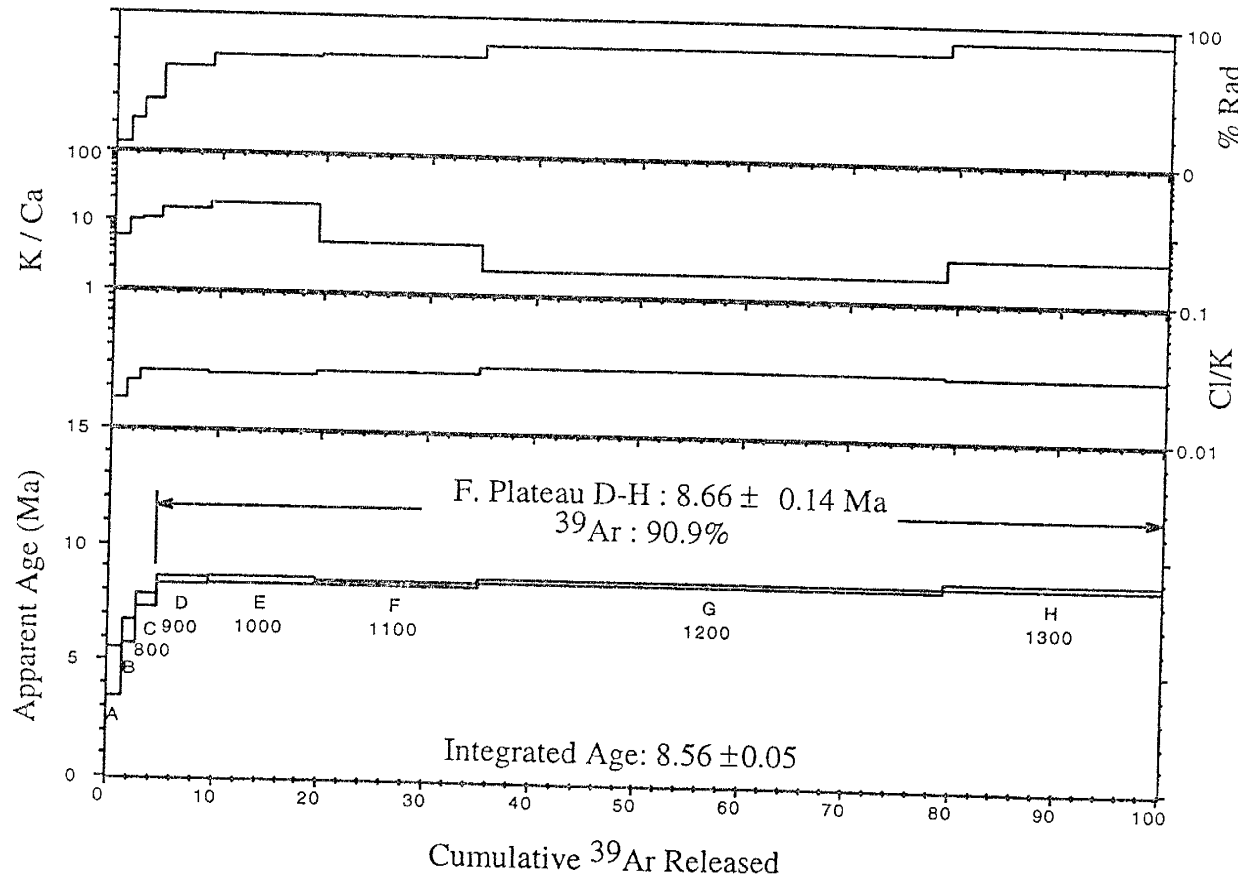
HN-3, Biotite, Furnace Step-heated, L#2780



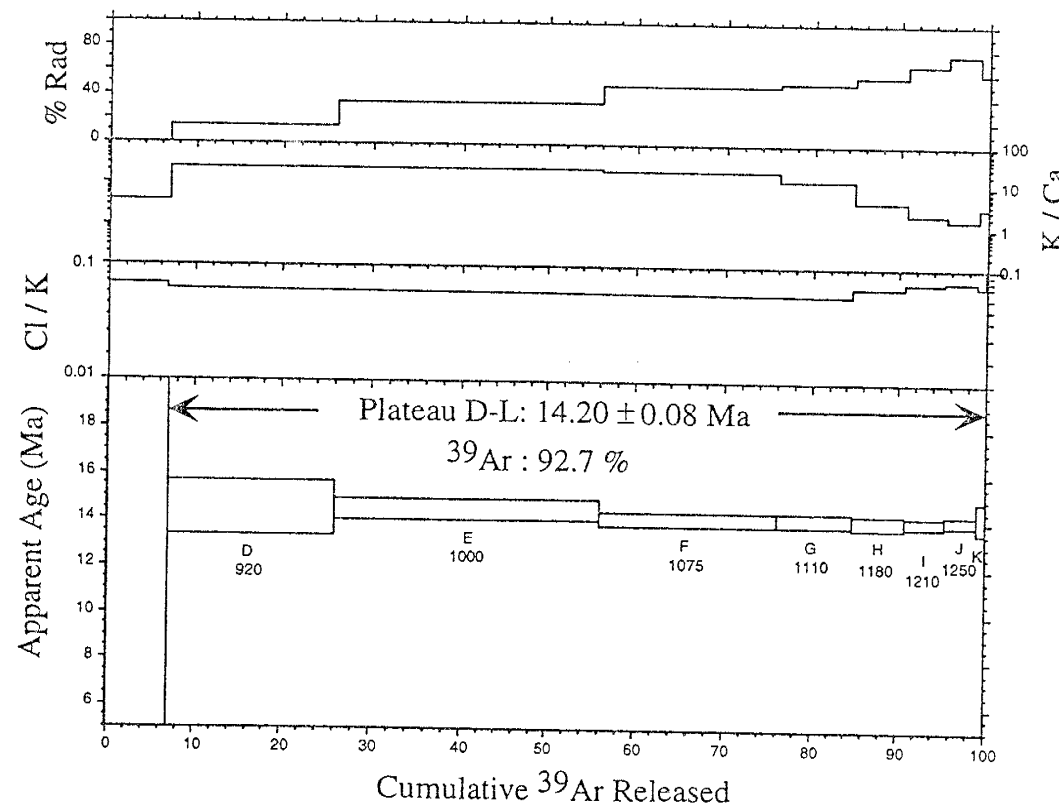
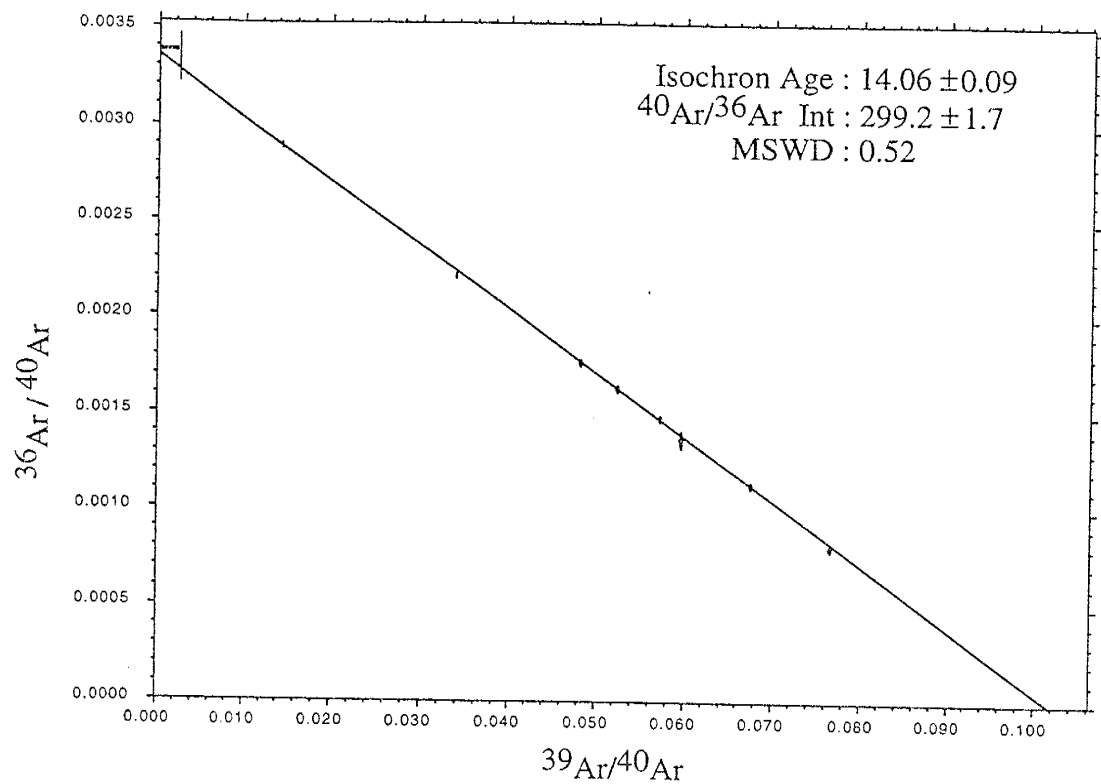
HN-4, Biotite, Furnace Step-heated, L#2781



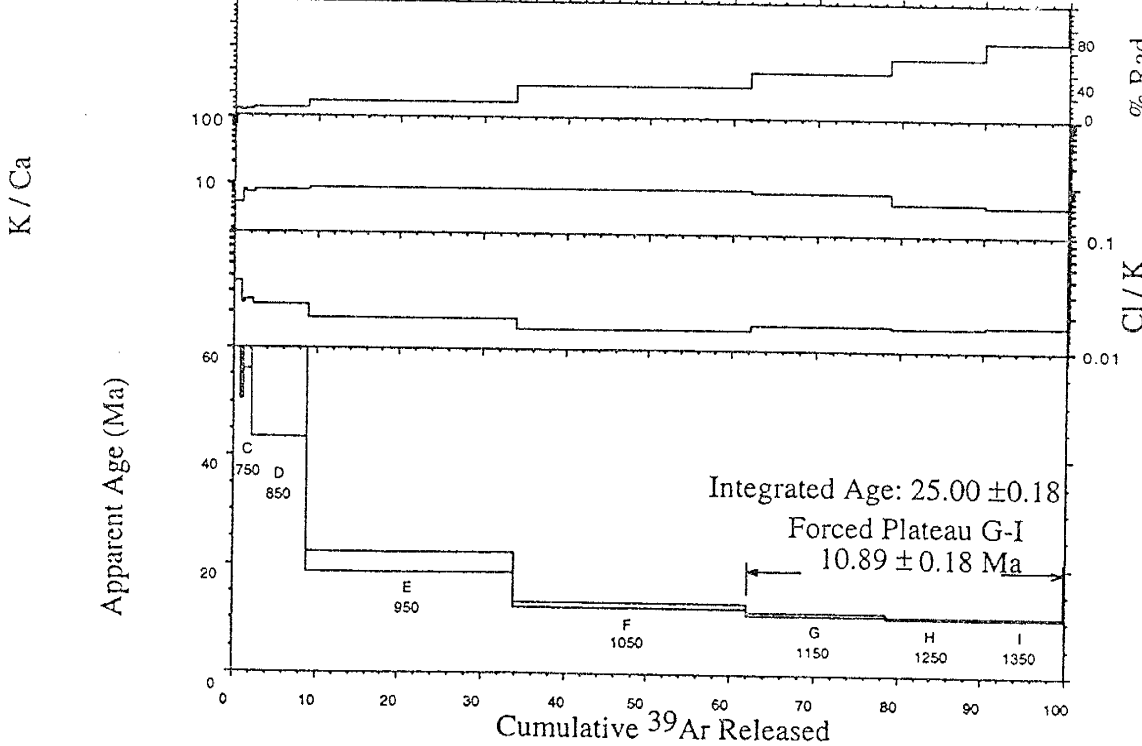
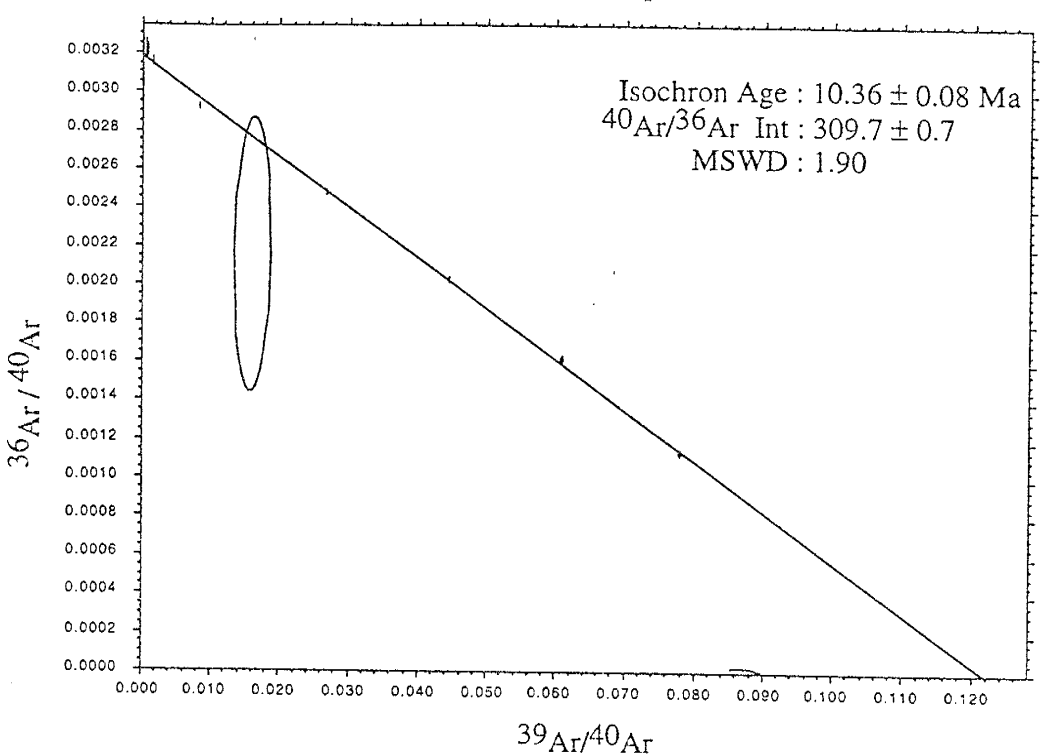
HN-7, Biotite, Furnace Step-heated, L#2782

 $^{39}\text{Ar}/^{40}\text{Ar}$ 

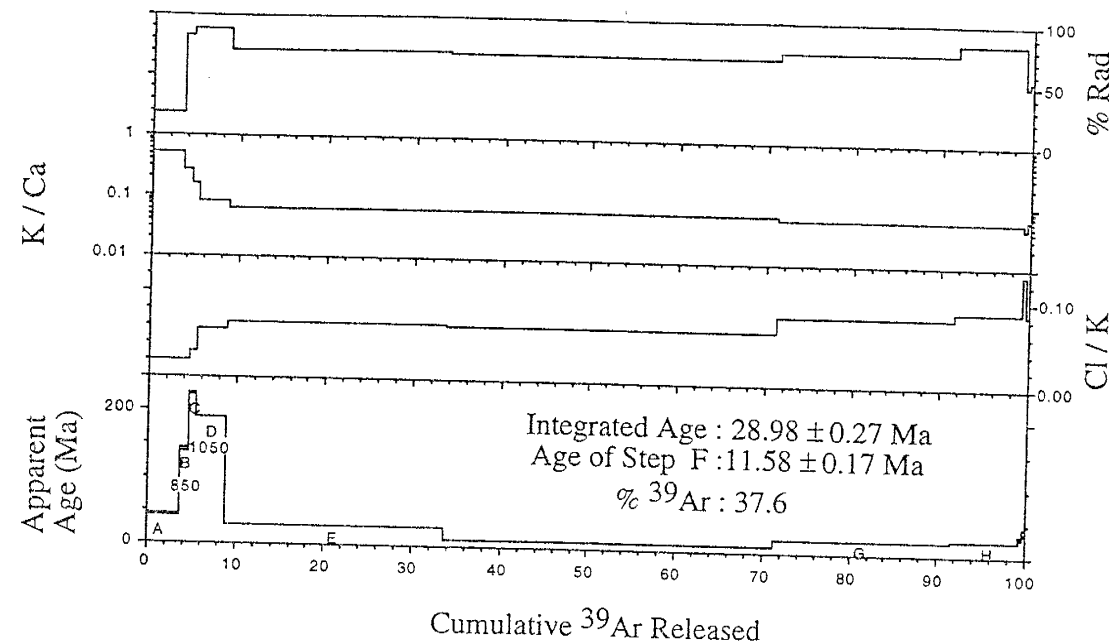
HN-9, Biotite, Furnace Step-heated, L#6362



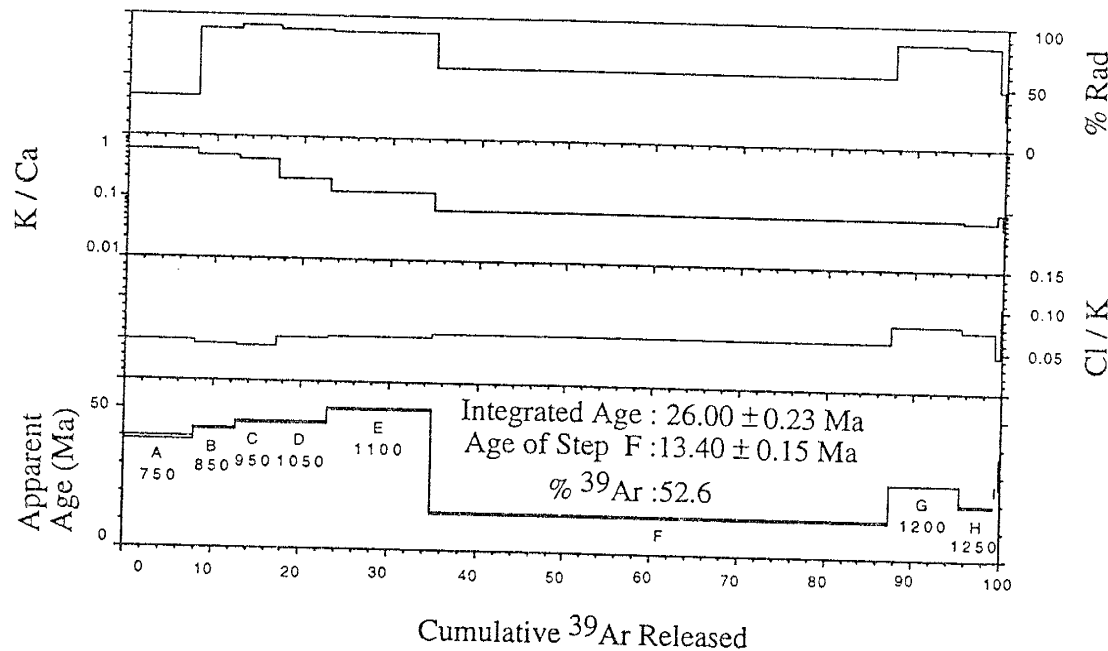
HN-12, Biotite, Furnace Step-heated, L#6027



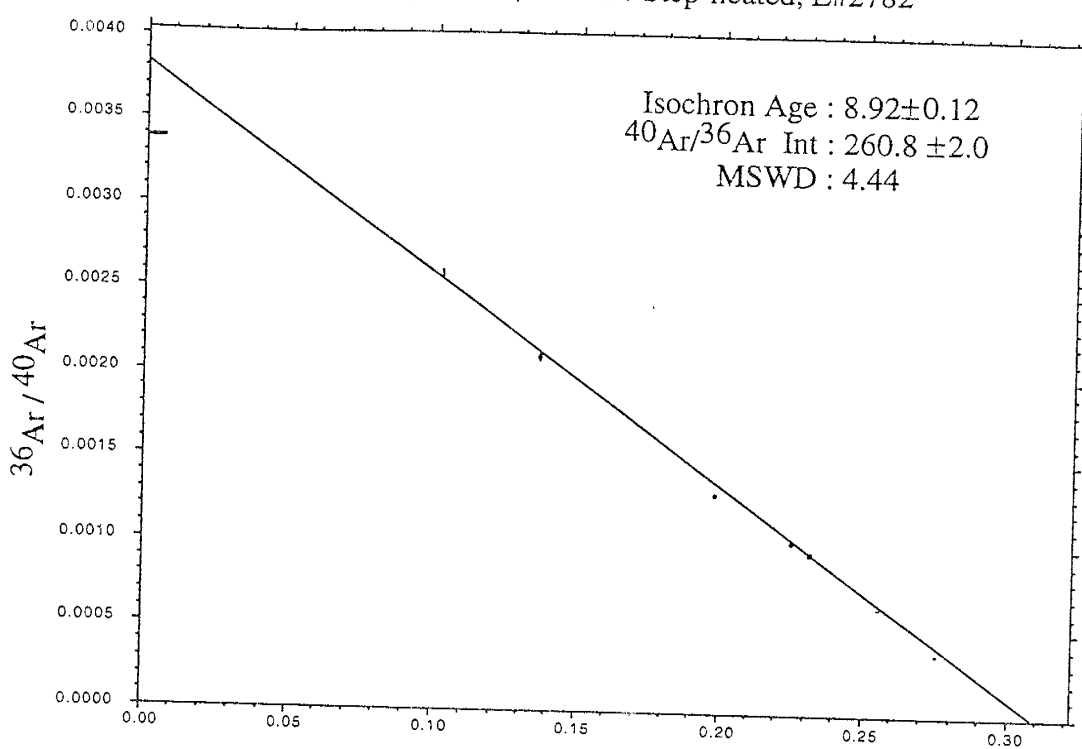
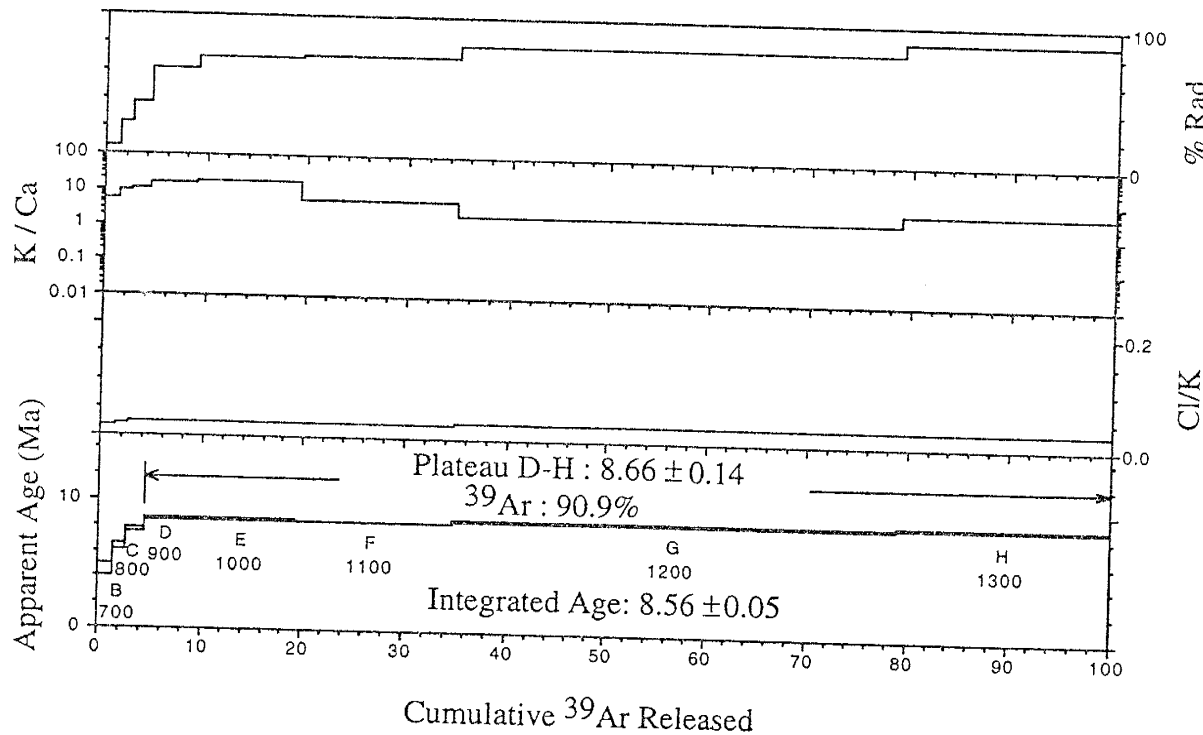
HN-5, hornblende, furnace step-heating, L#2793



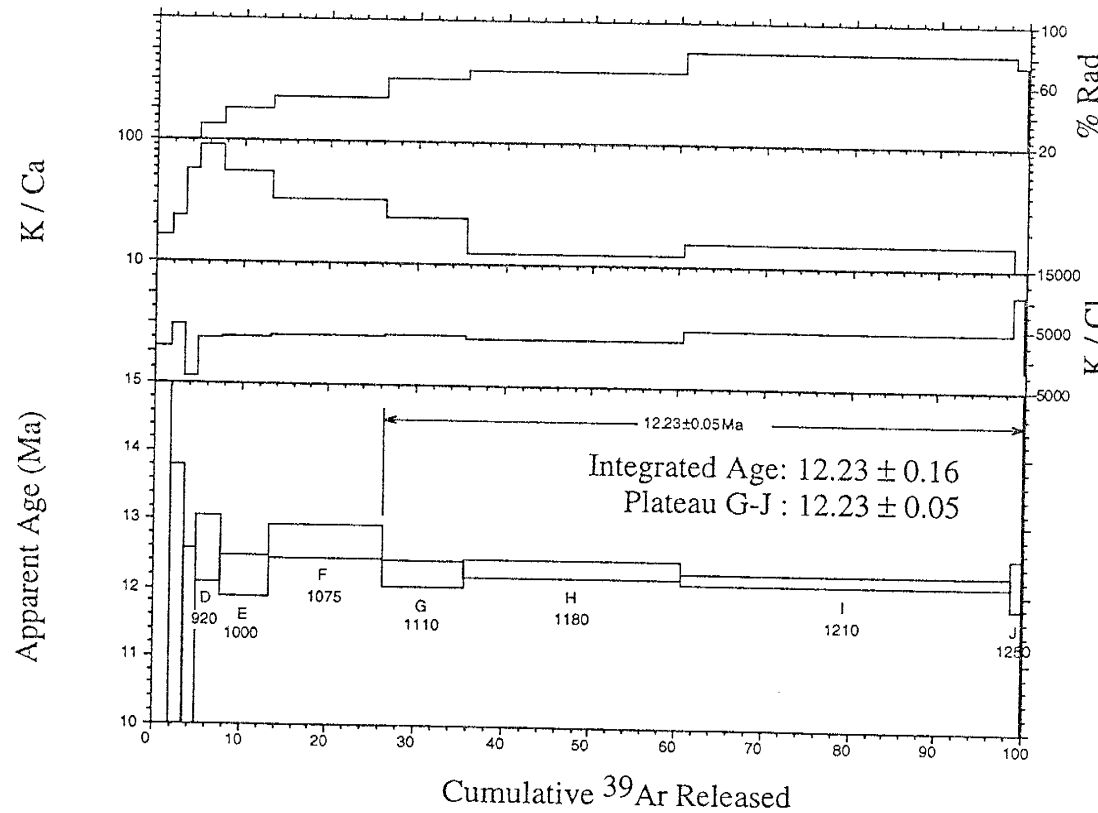
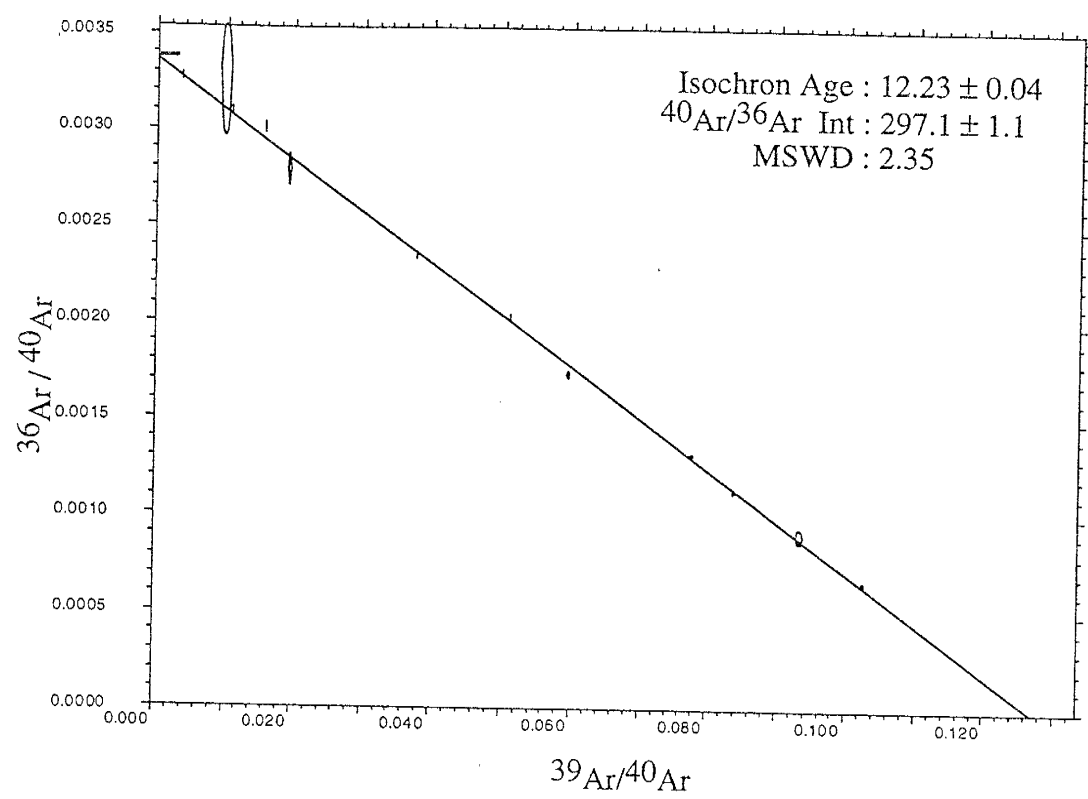
HN-6, hornblende, furnace step-heating, L#2817



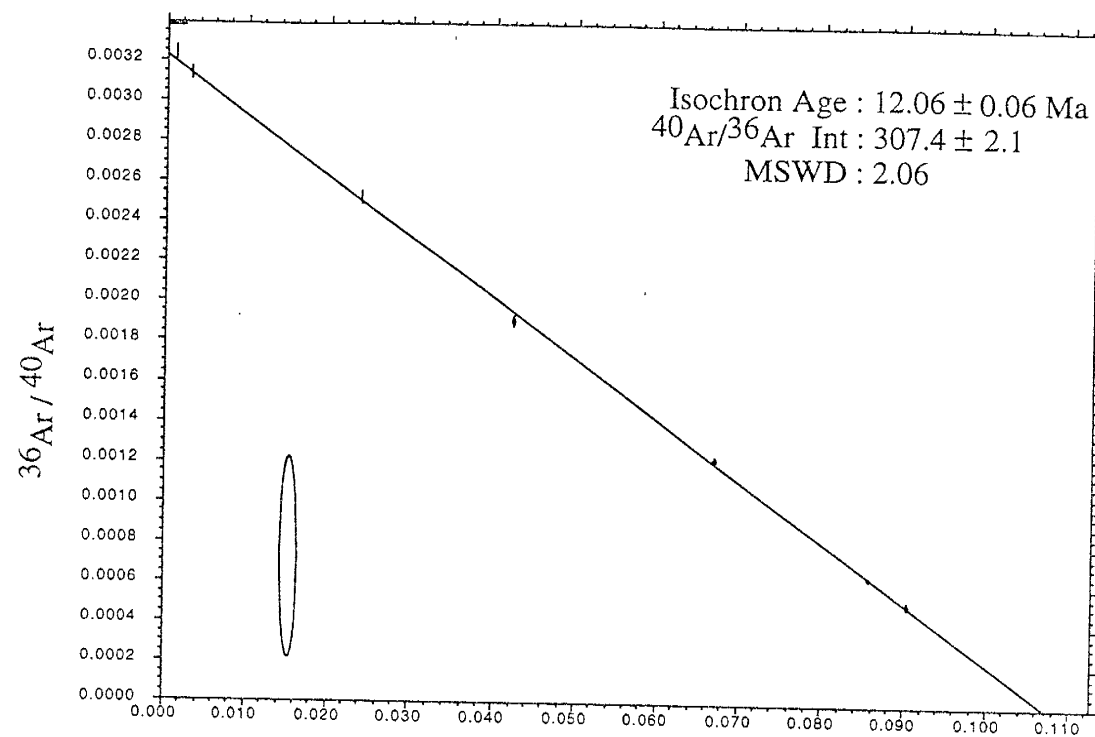
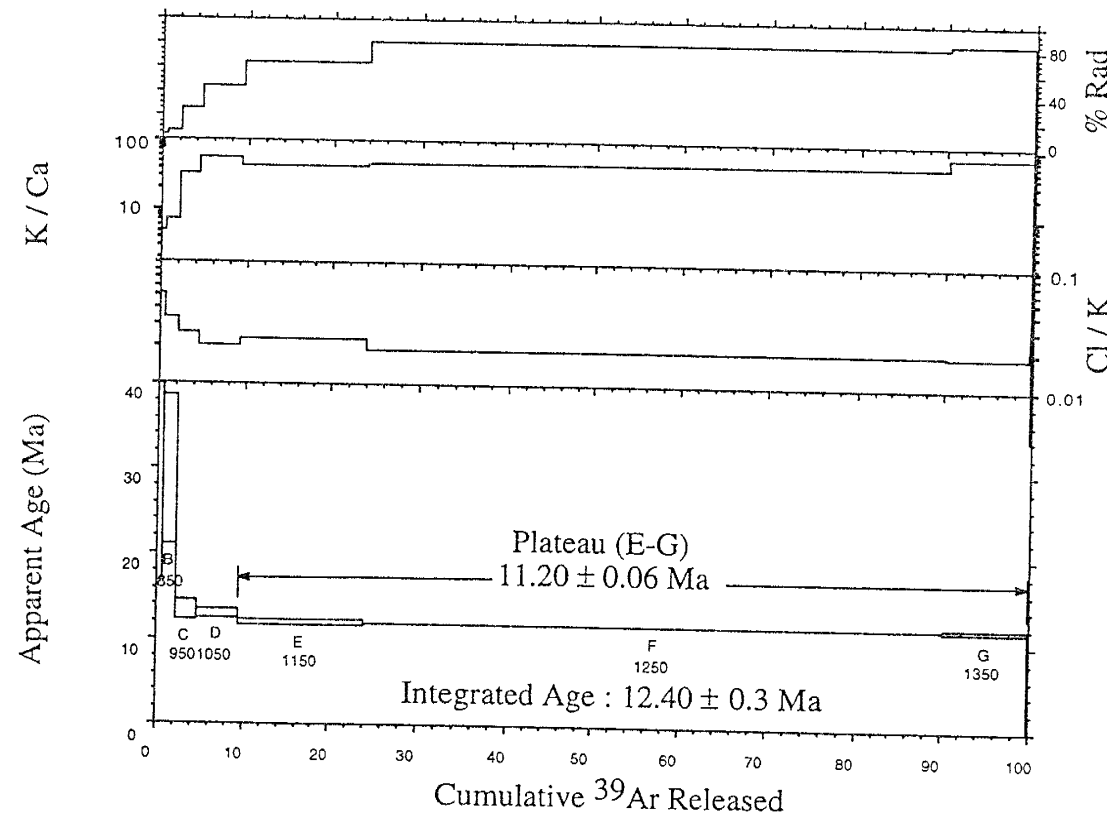
HN-7, Biotite, Furnace Step-heated, L#2782

 $^{39}\text{Ar}/^{40}\text{Ar}$ 

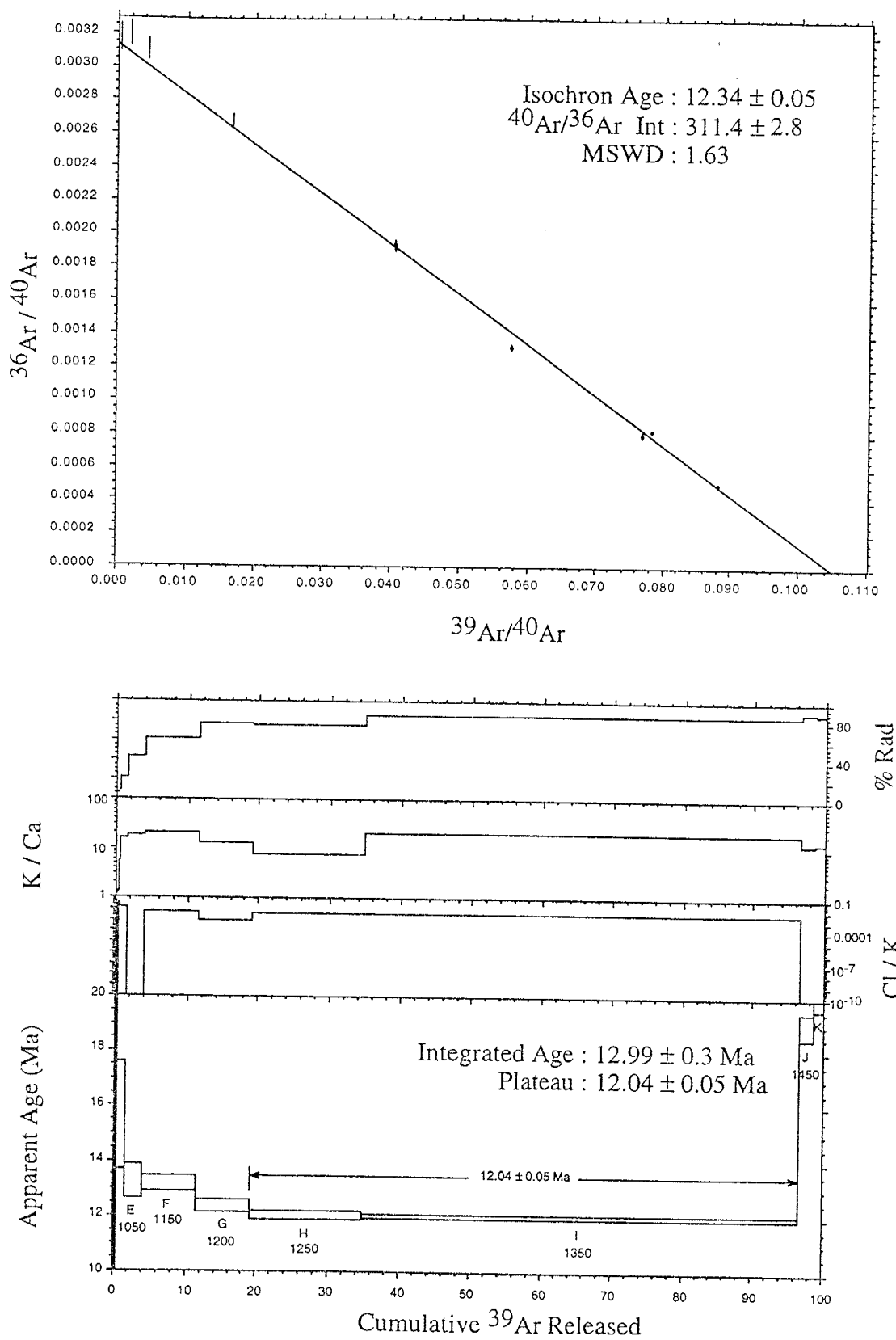
HN-16b, Biotite, Furnace Step-heated, L#6080



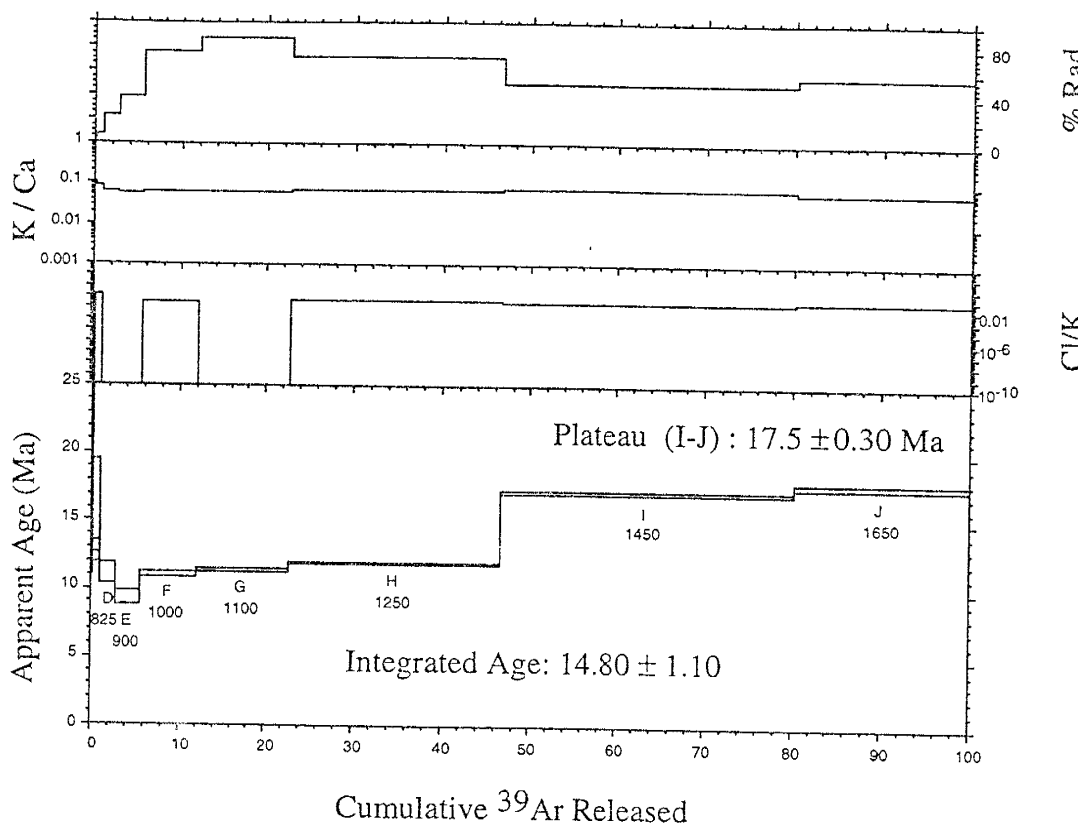
HN-18, Biotite, Furnace Step-heated, L#6030

 $^{39}\text{Ar}/^{40}\text{Ar}$ 

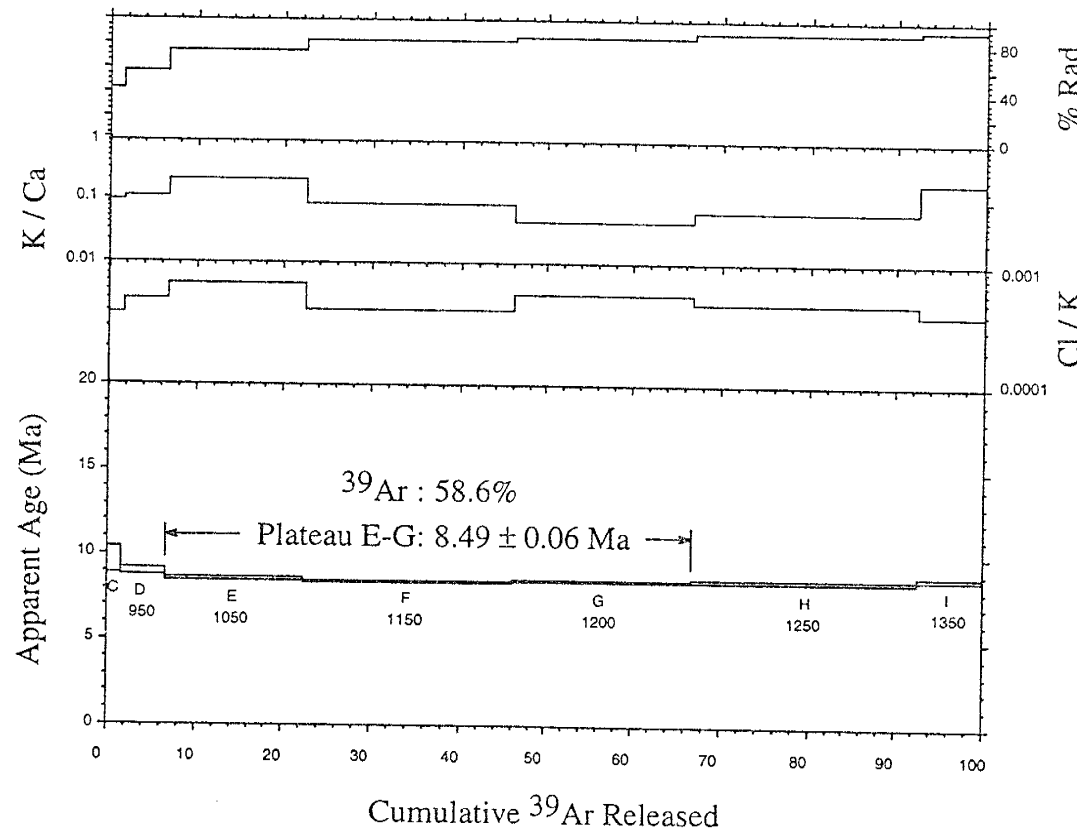
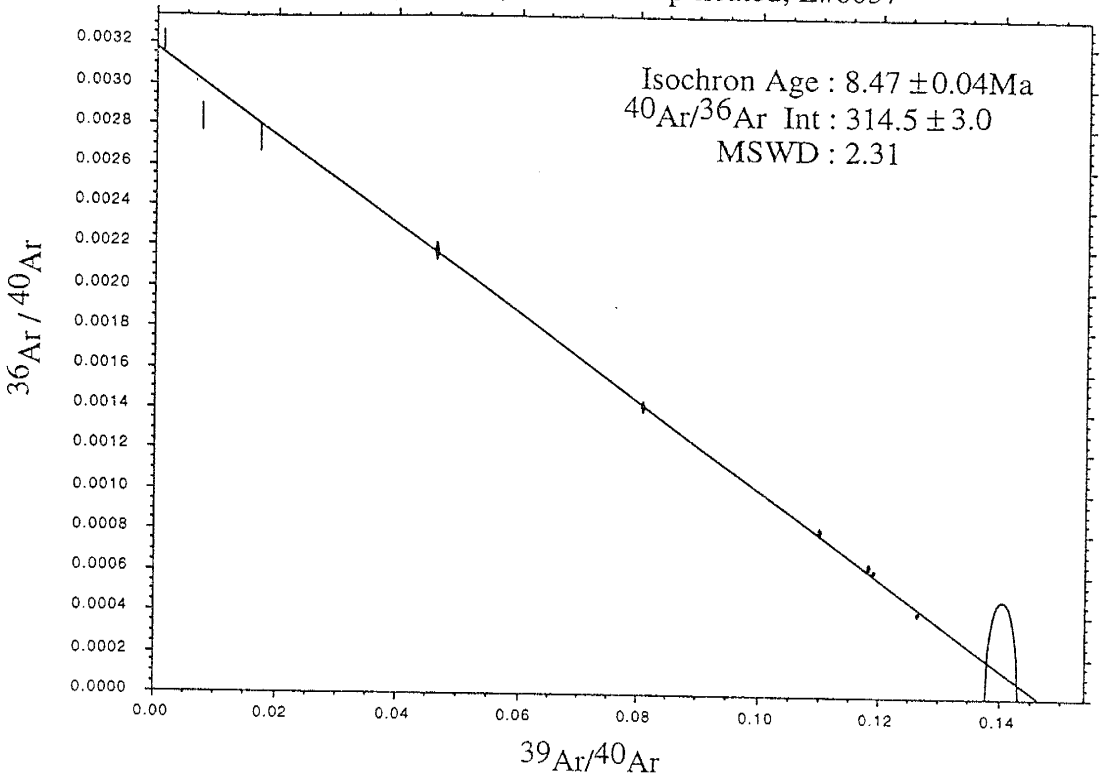
HN-20, Biotite, Furnace Step-heated, L#6031



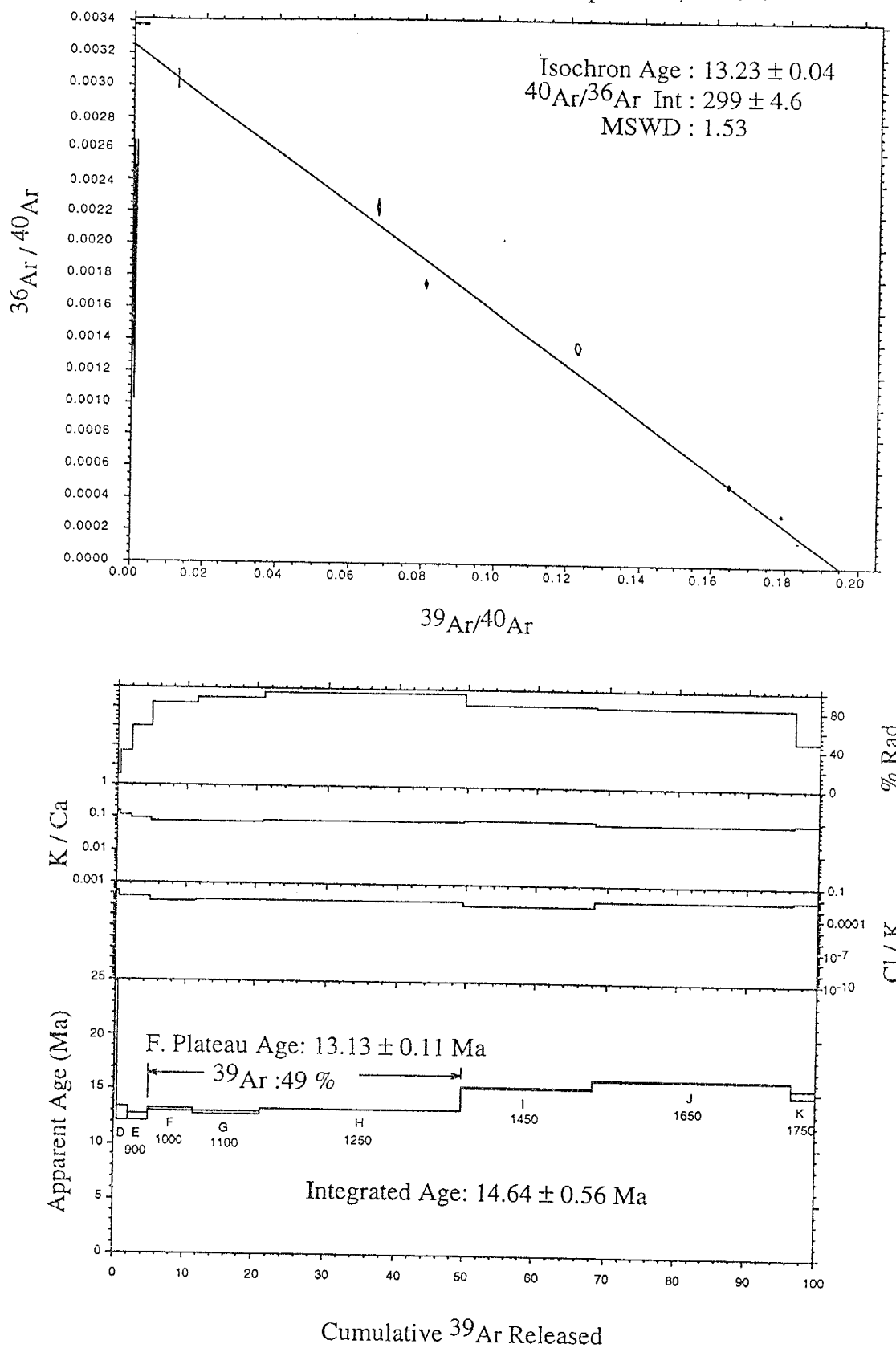
HN-20, Plagioclase, Furnace Step-heated, L#5848



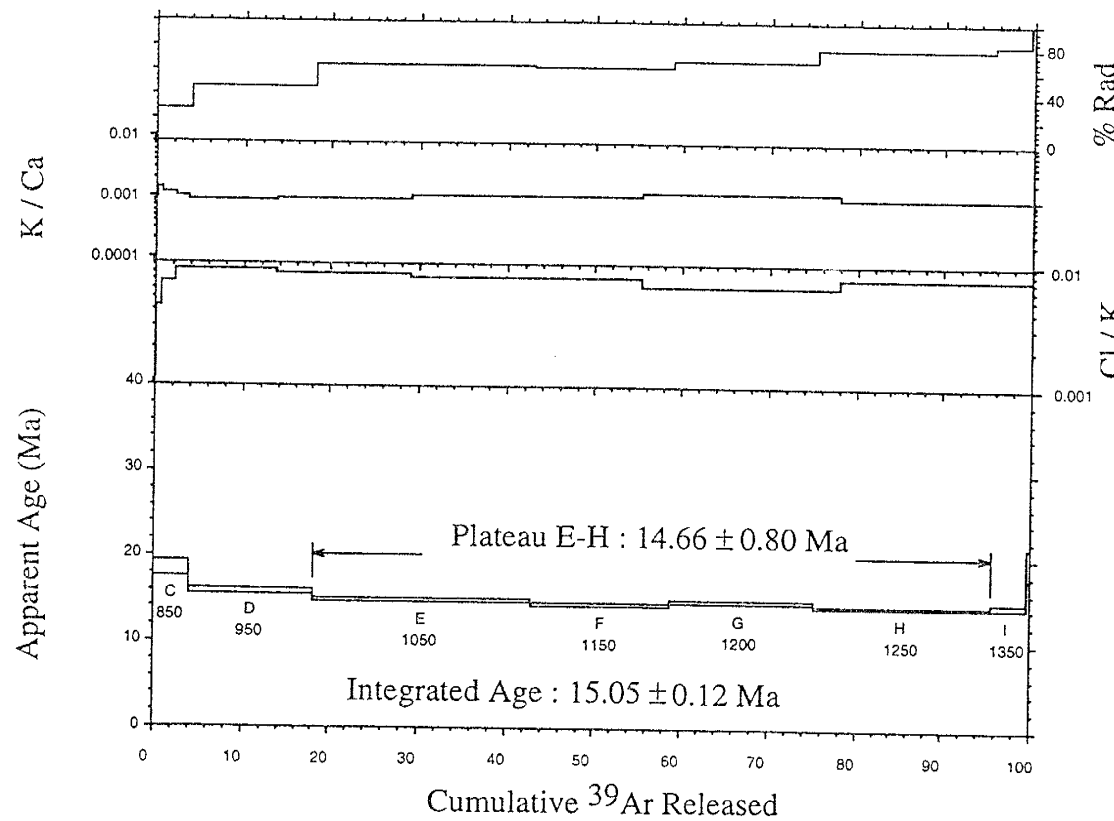
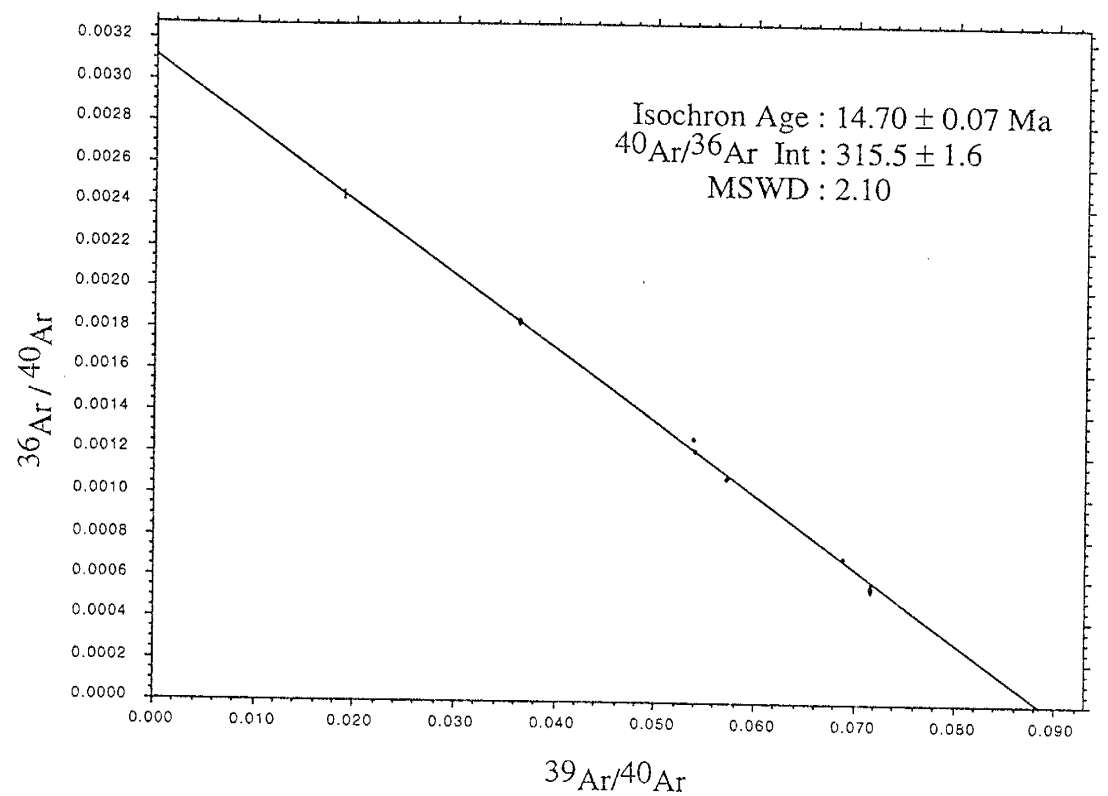
HN-24, Biotite, Furnace Step-heated, L#6037



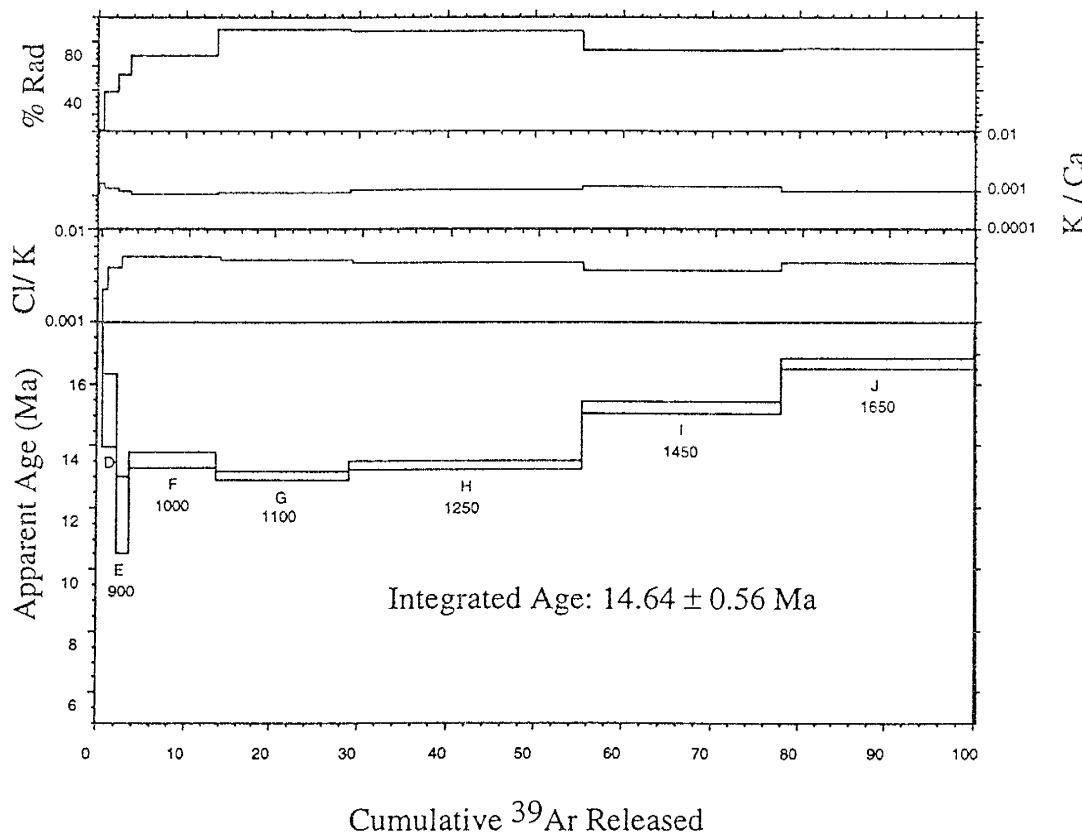
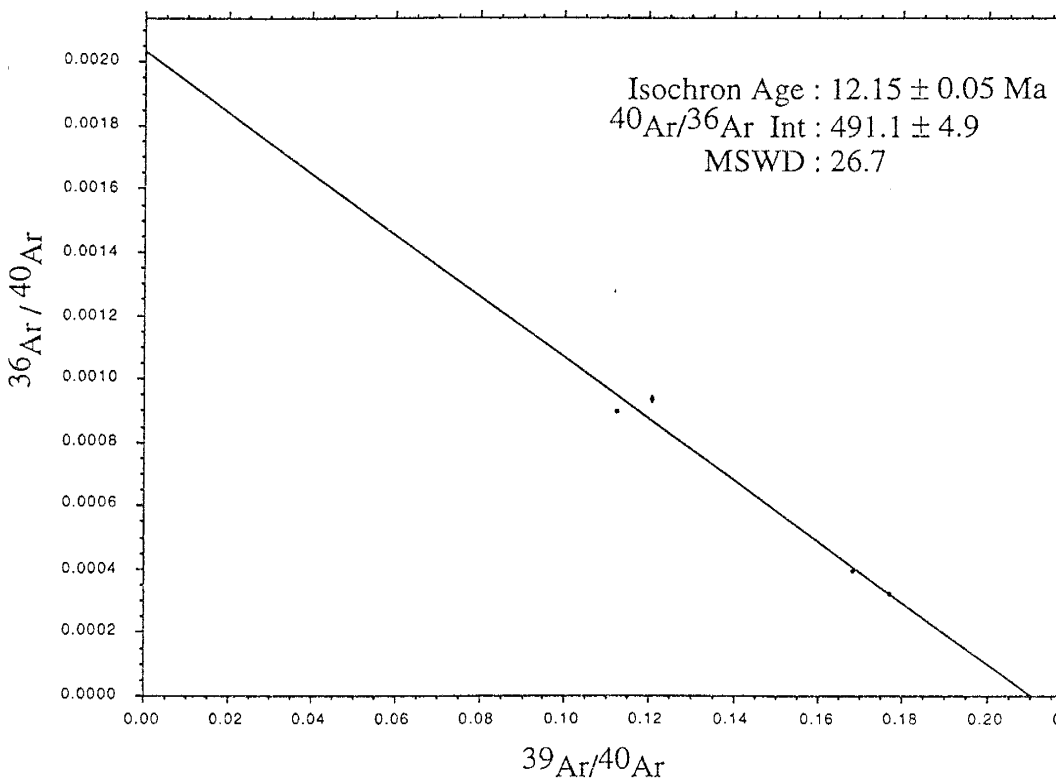
HN-29, Plagioclase, Furnace Step-heated, L#5847



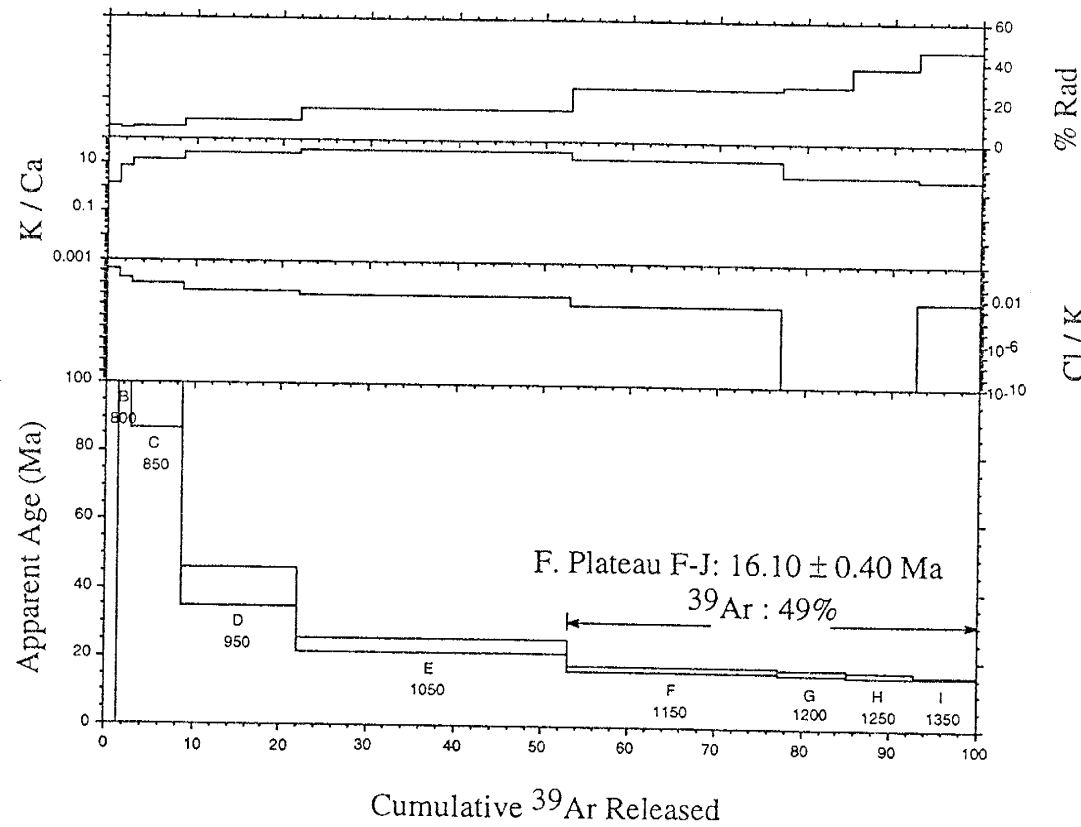
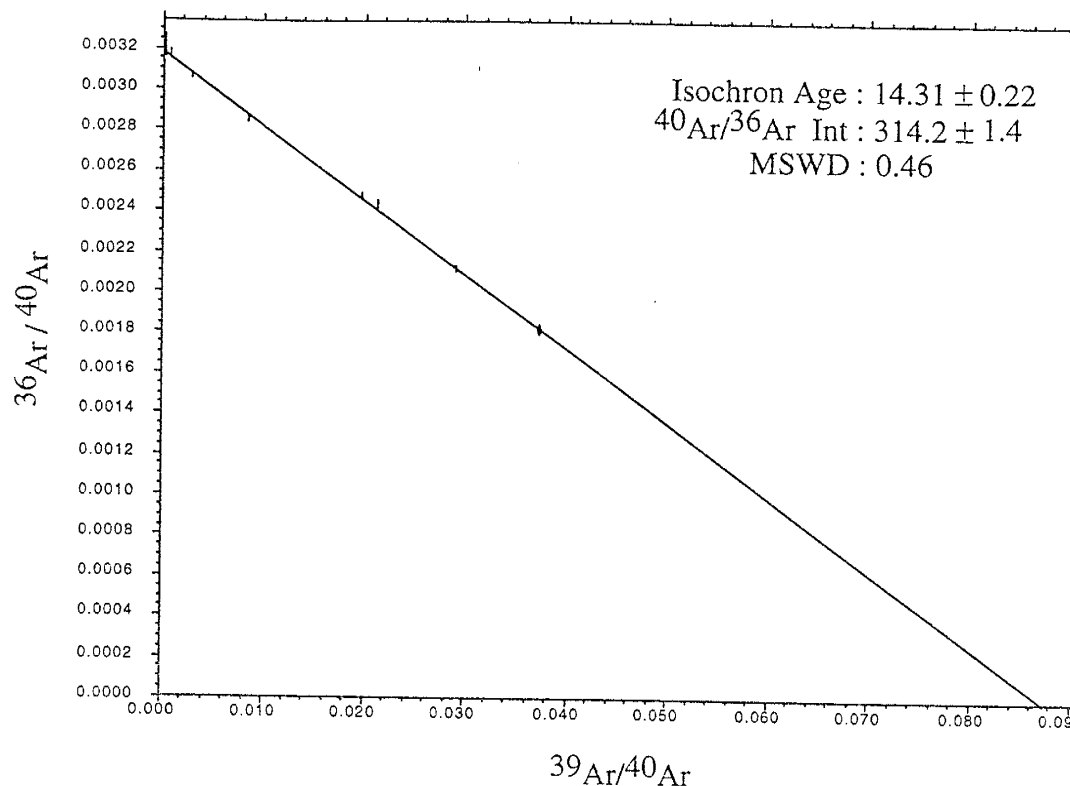
HN-31, Biotite, Furnace Step-heated, L#6040



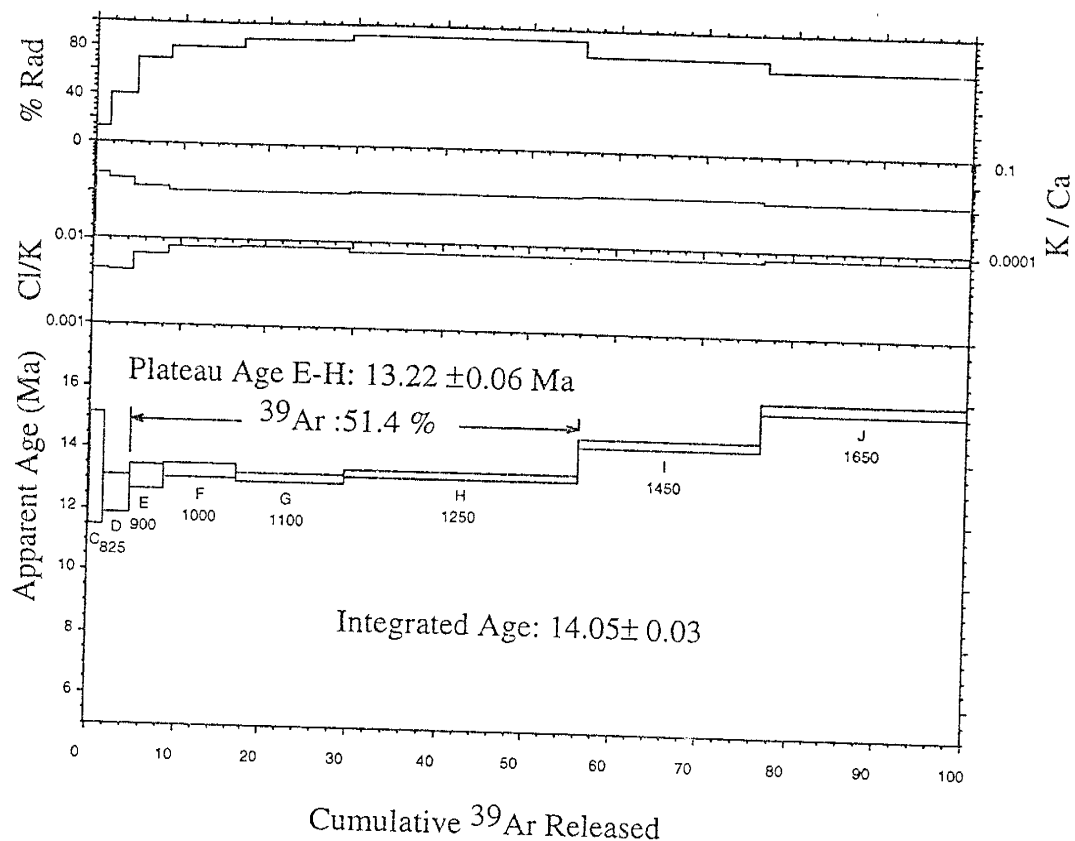
HN-31, Plagioclase, Furnace Step-heated, L#5846



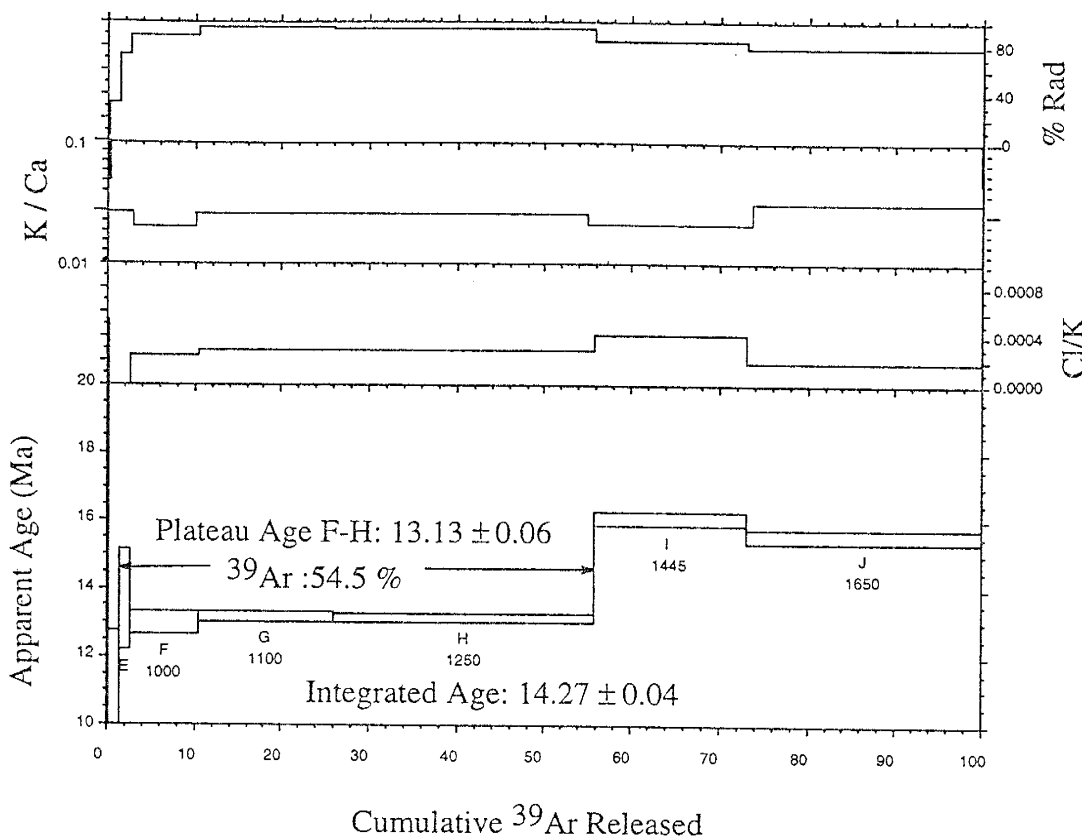
HN-32, Biotite, Furnace Step-heated, L#6039



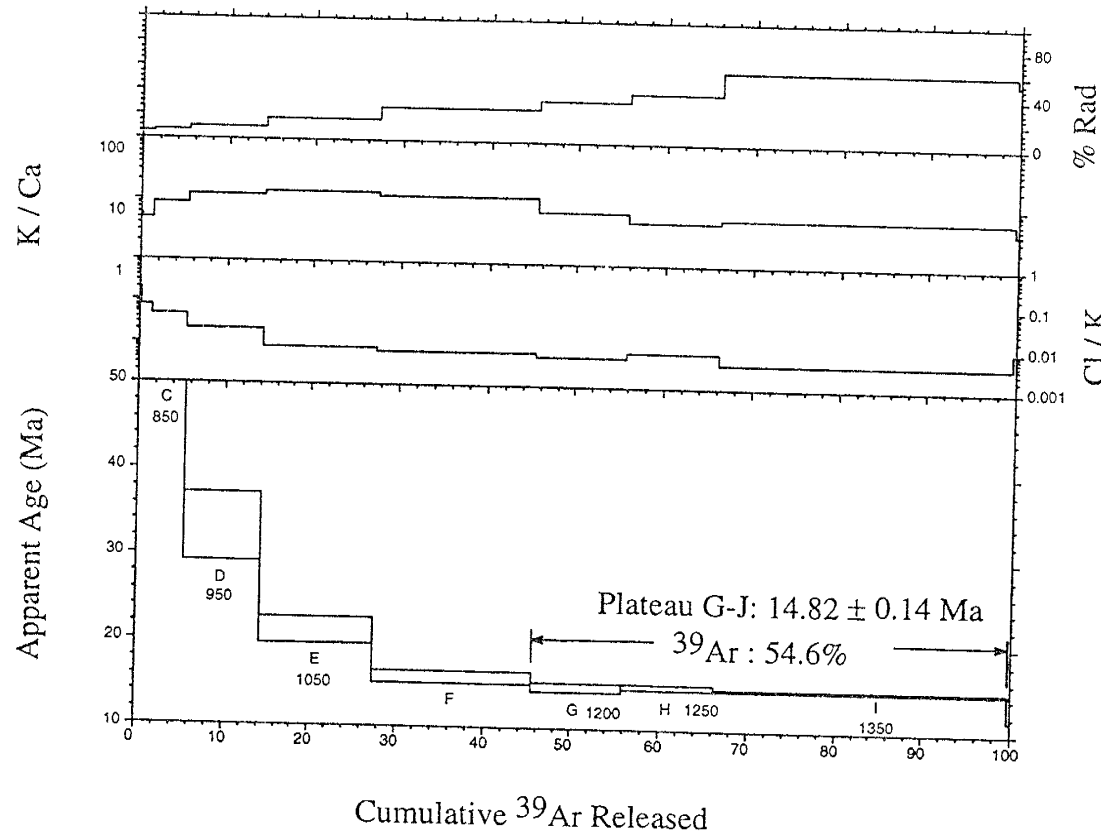
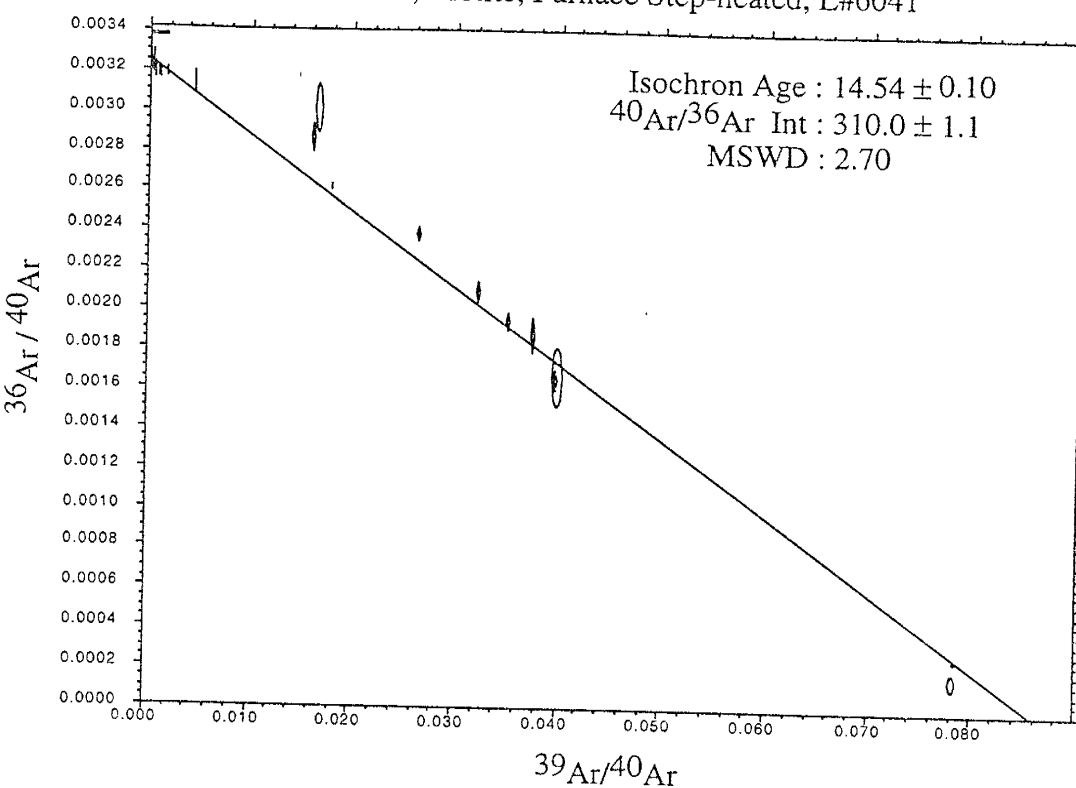
HN-32, Plagioclase, Furnace Step-heated, L#5844



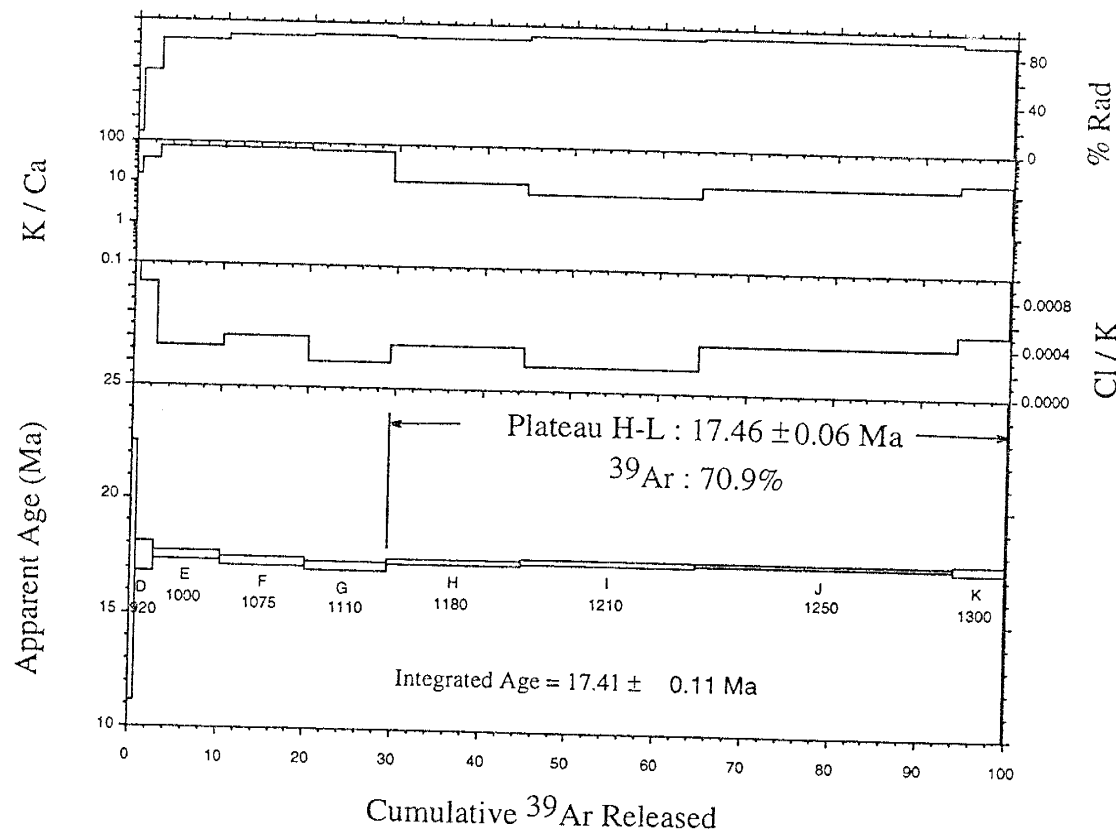
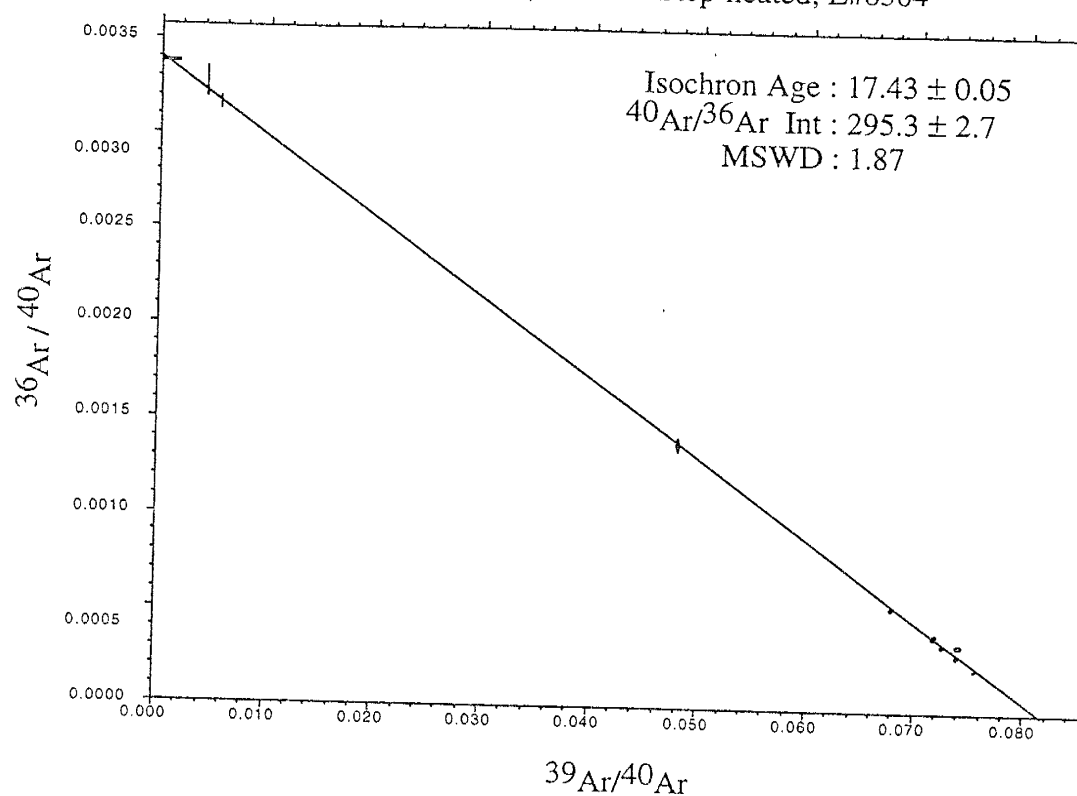
HN-33, Plagioclase, Furnace Step-heated, L#5845



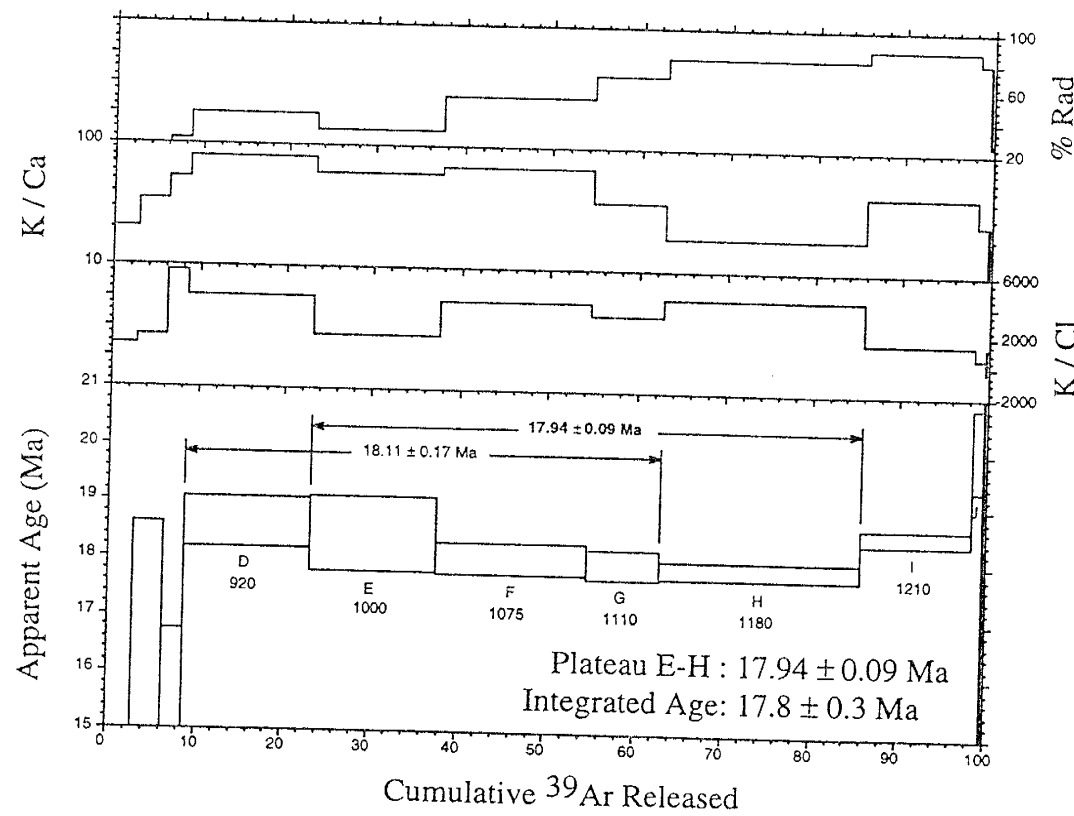
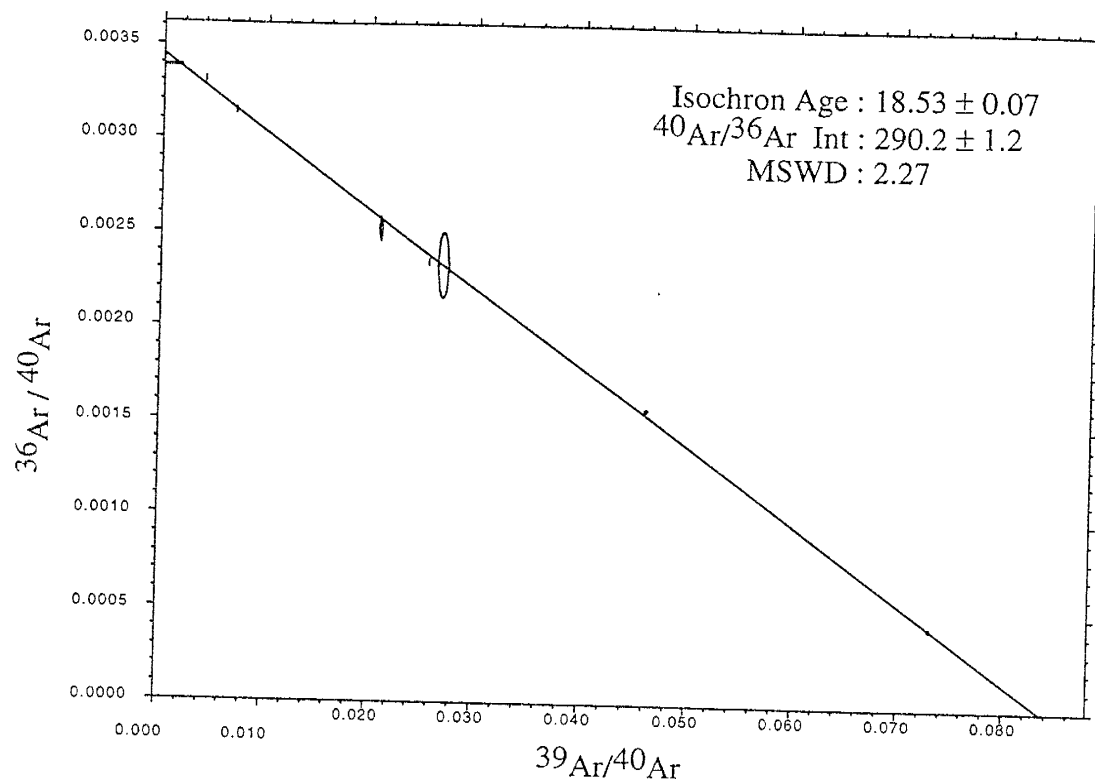
HN-37, Biotite, Furnace Step-heated, L#6041



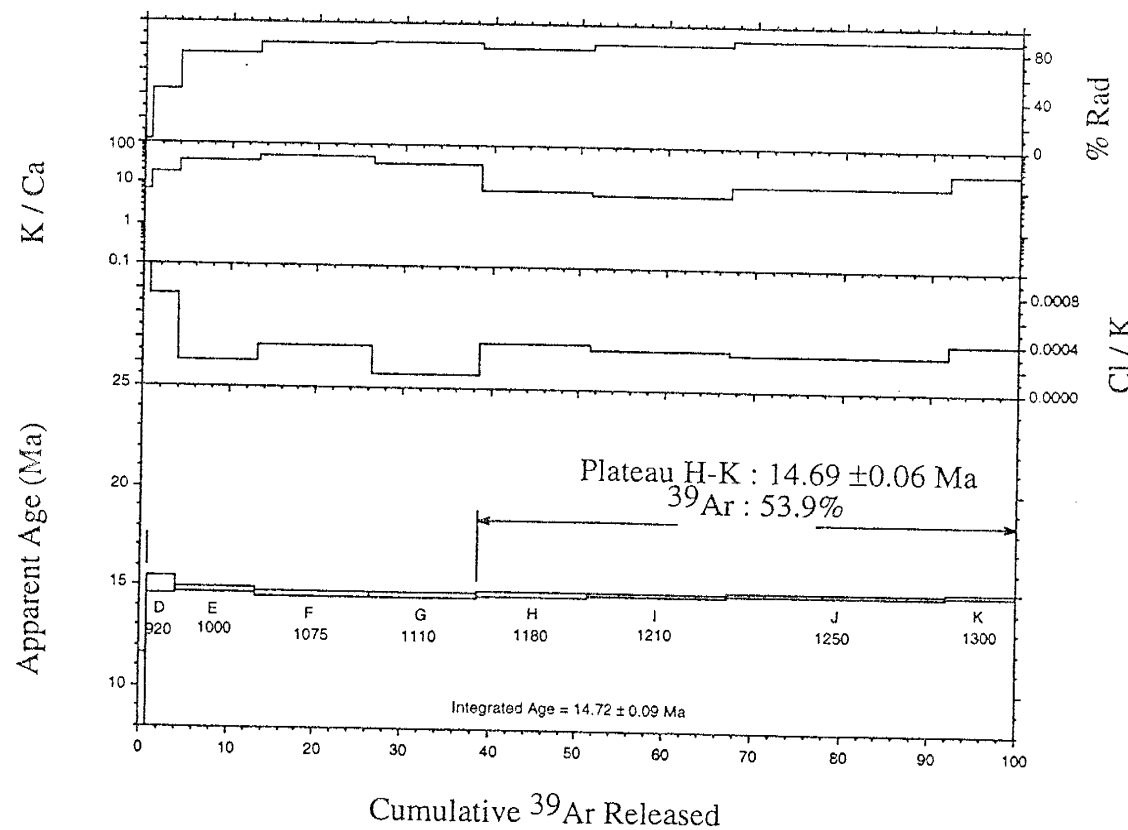
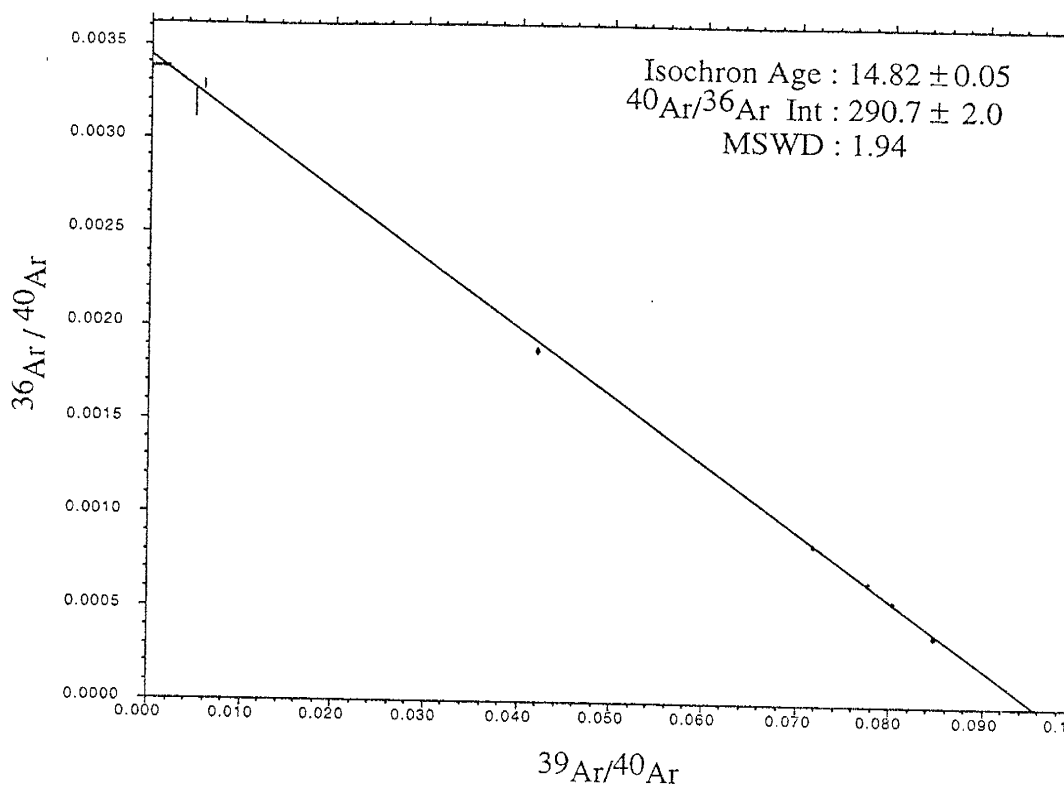
HN-41, Biotite, Furnace Step-heated, L#6364



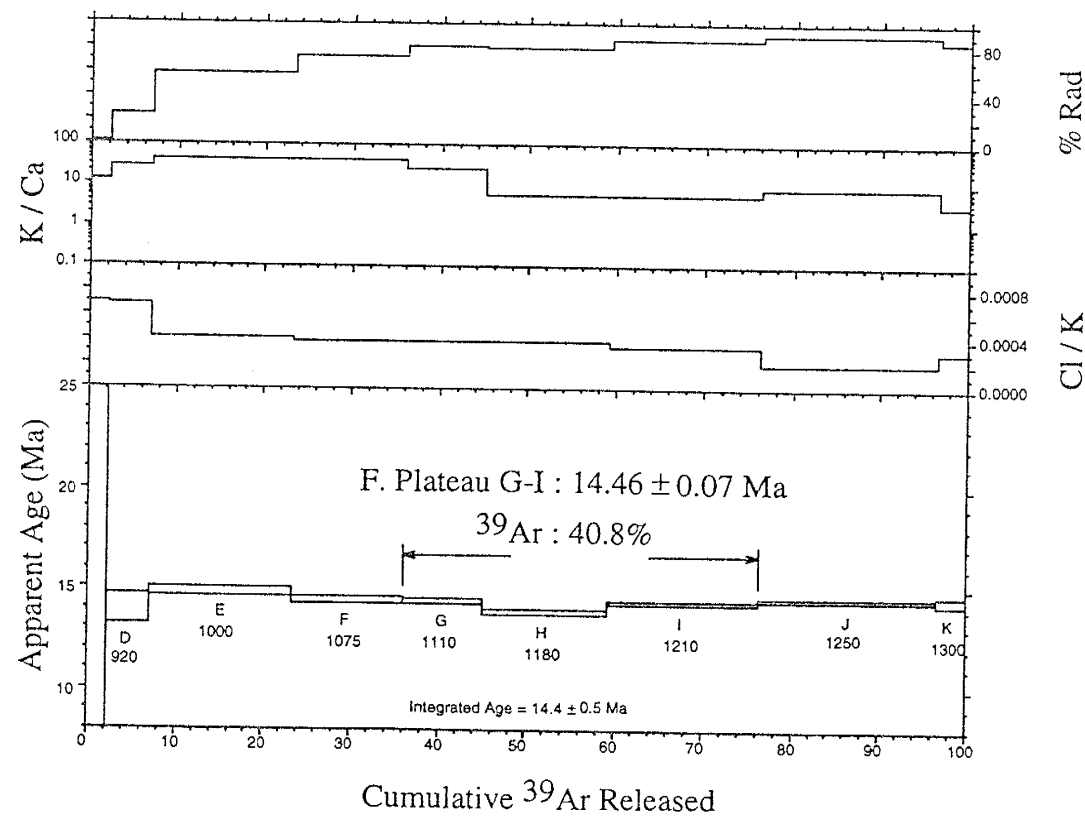
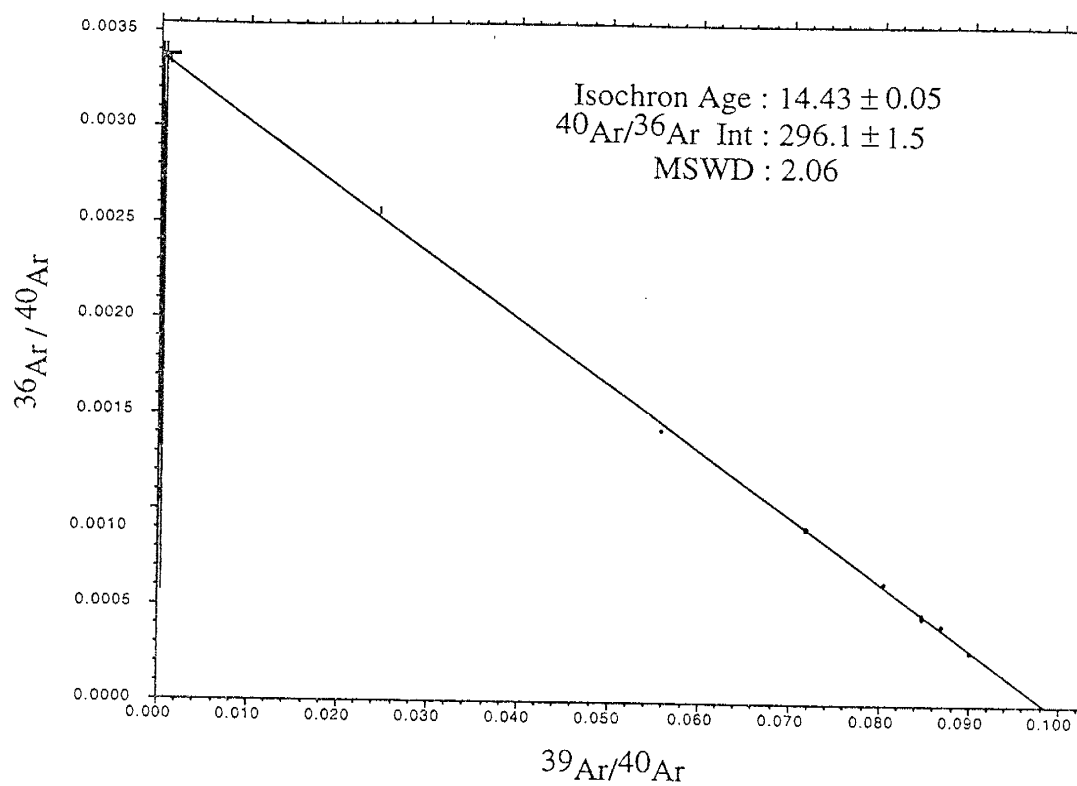
HN-43, Biotite, Furnace Step-heated, L#6577



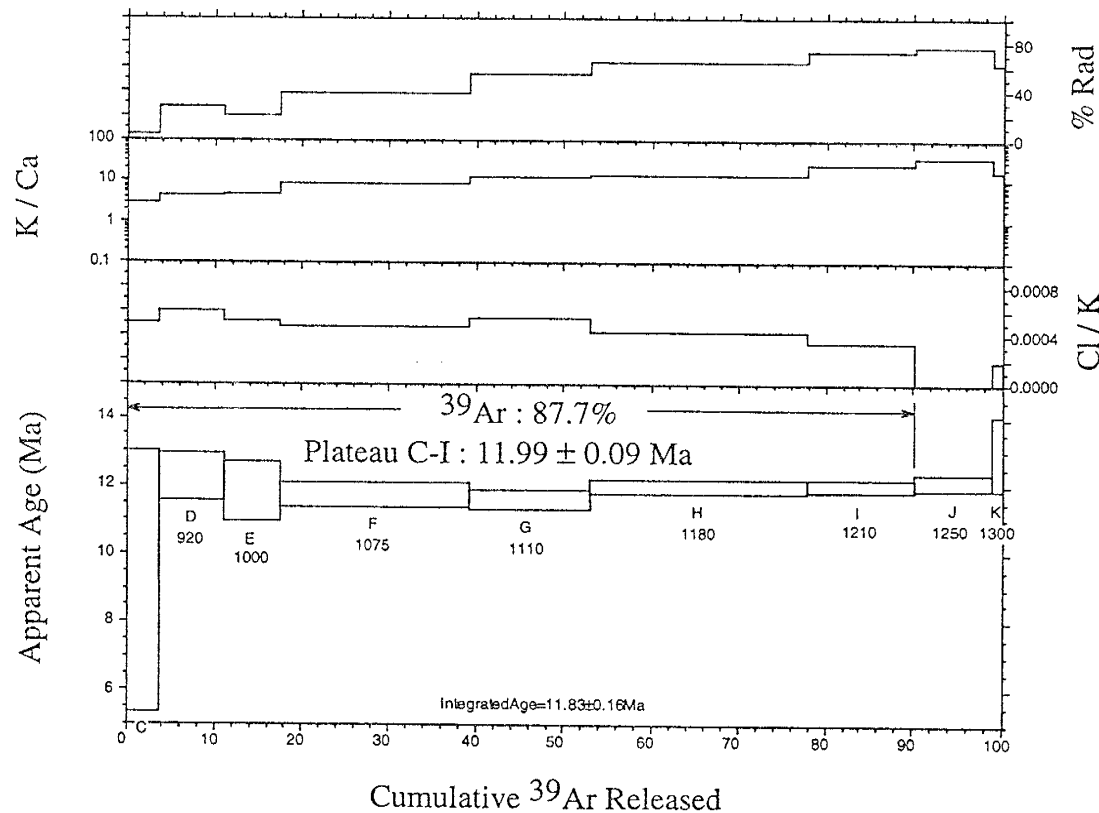
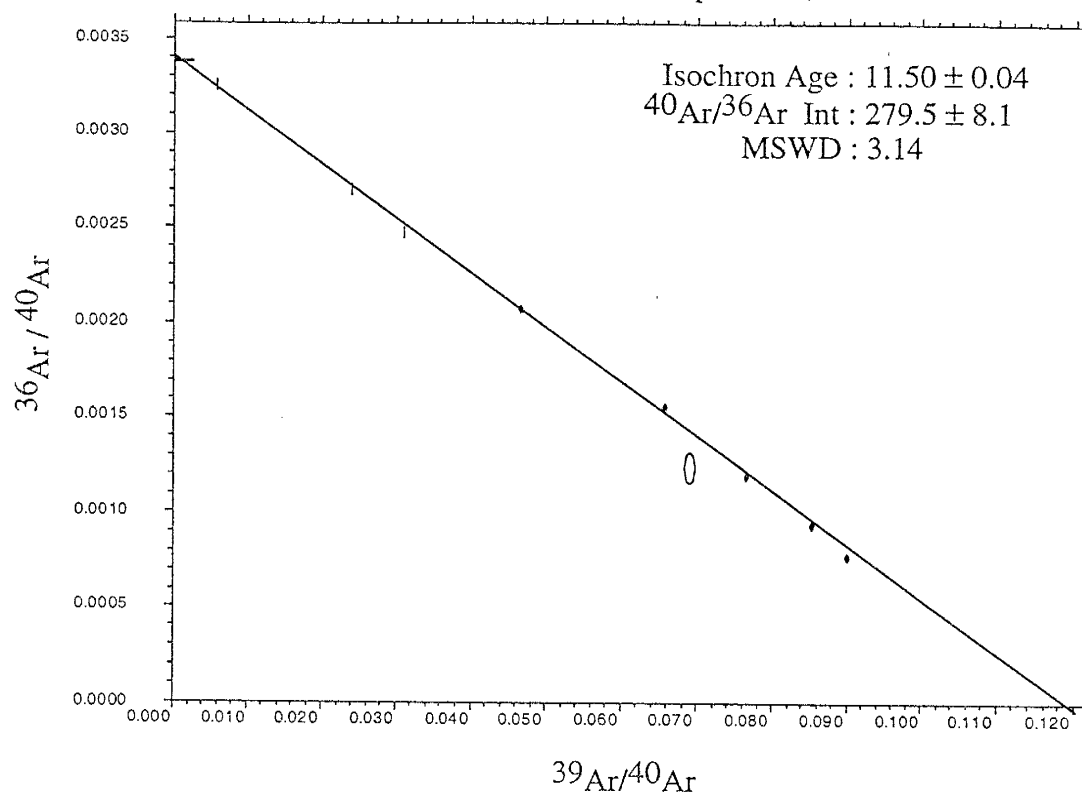
HN-45, Biotite, Furnace Step-heated, L#6361



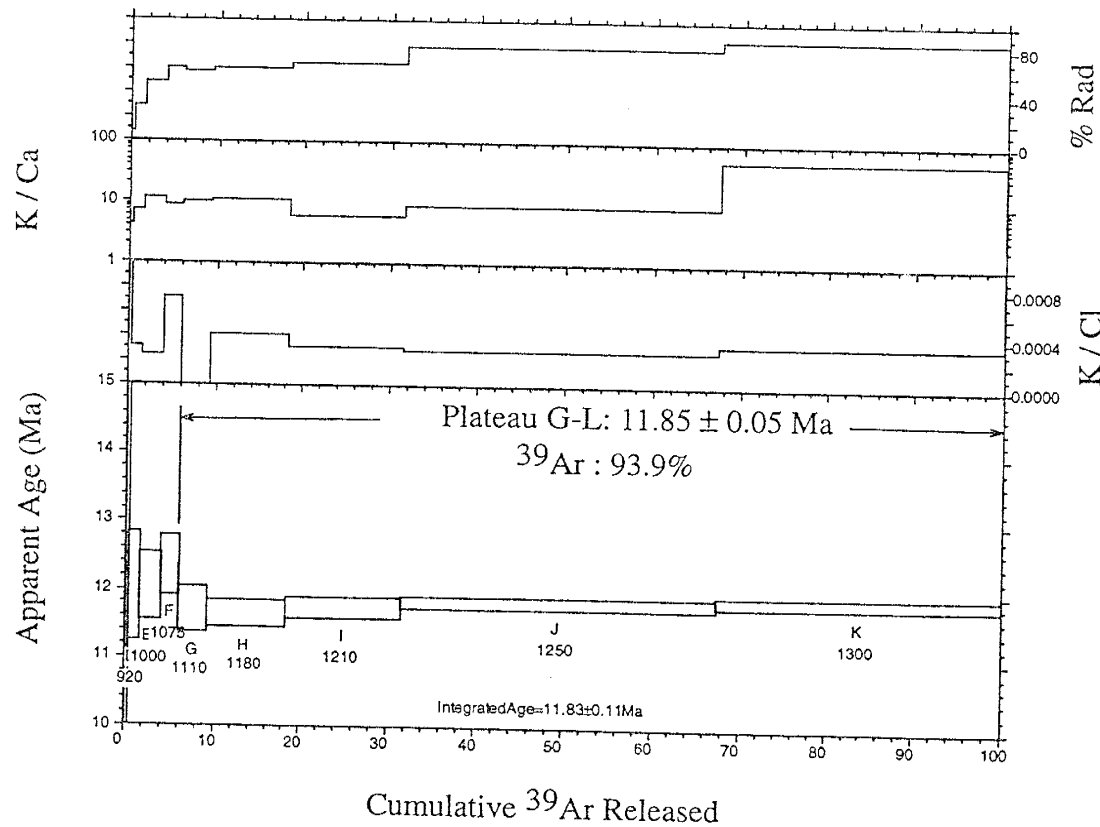
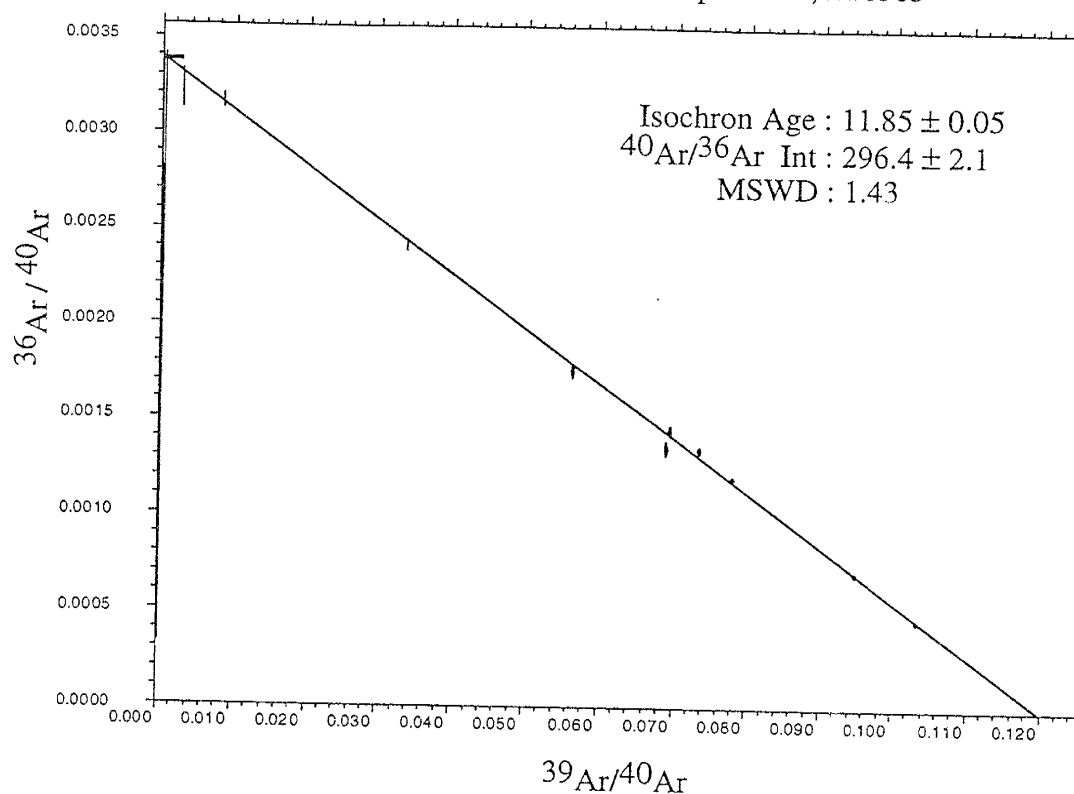
HN-46, Biotite, Furnace Step-heated, L#6363



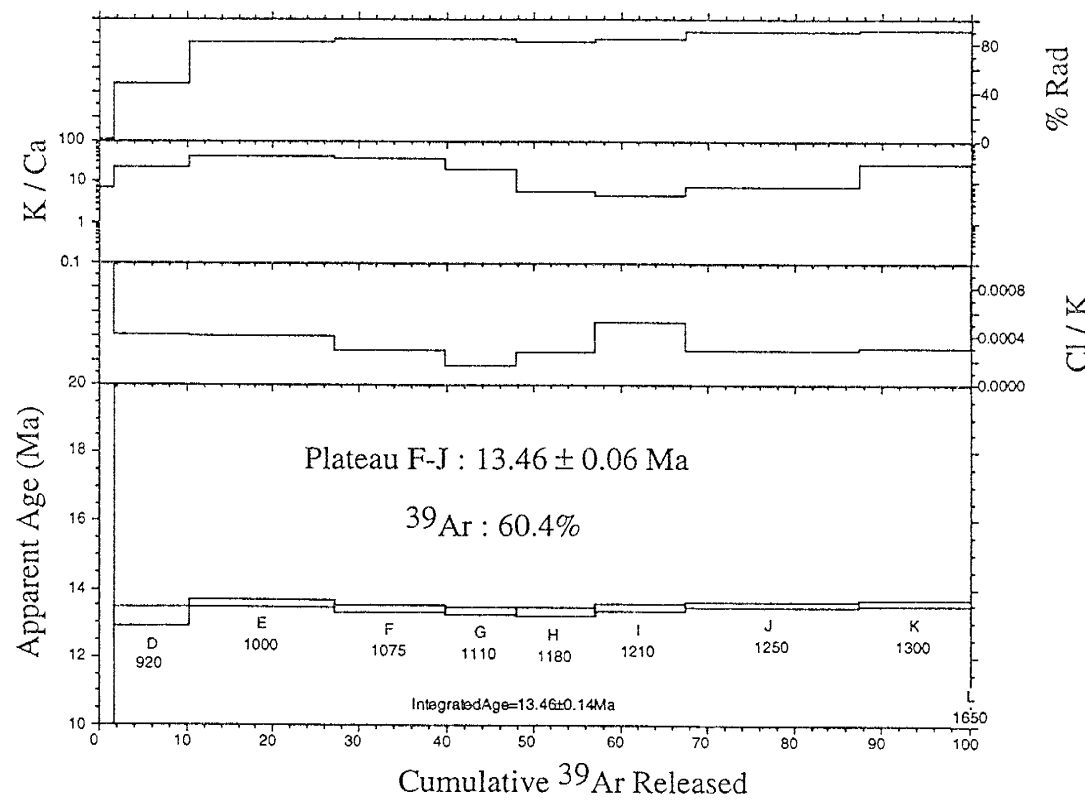
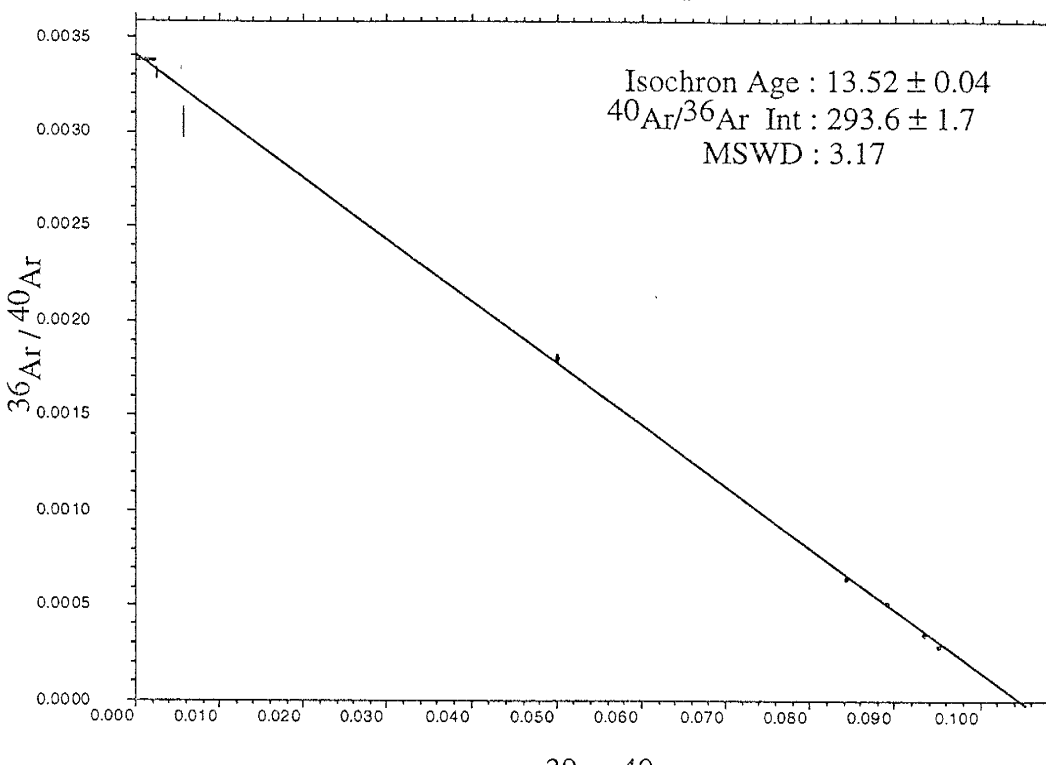
HN-55, Biotite, Furnace Step-heated, L#6369



HN-58, Biotite, Furnace Step-heated, L#6365



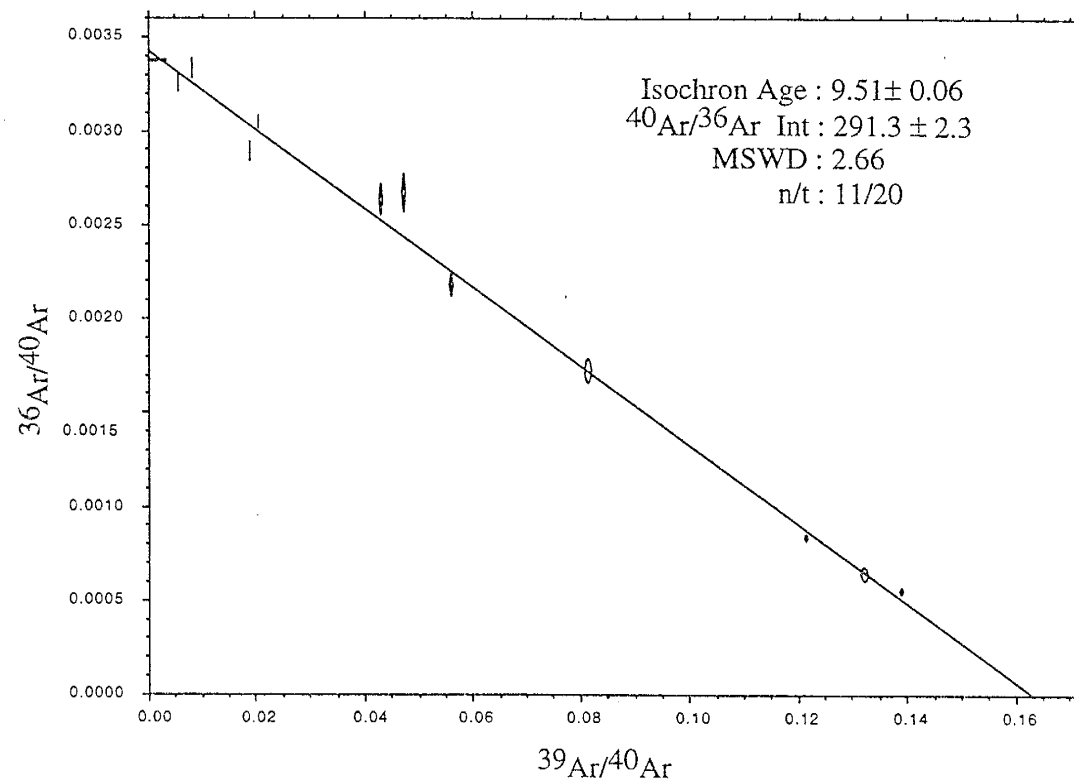
HN-59, Biotite, Furnace Step-heated, L#6367



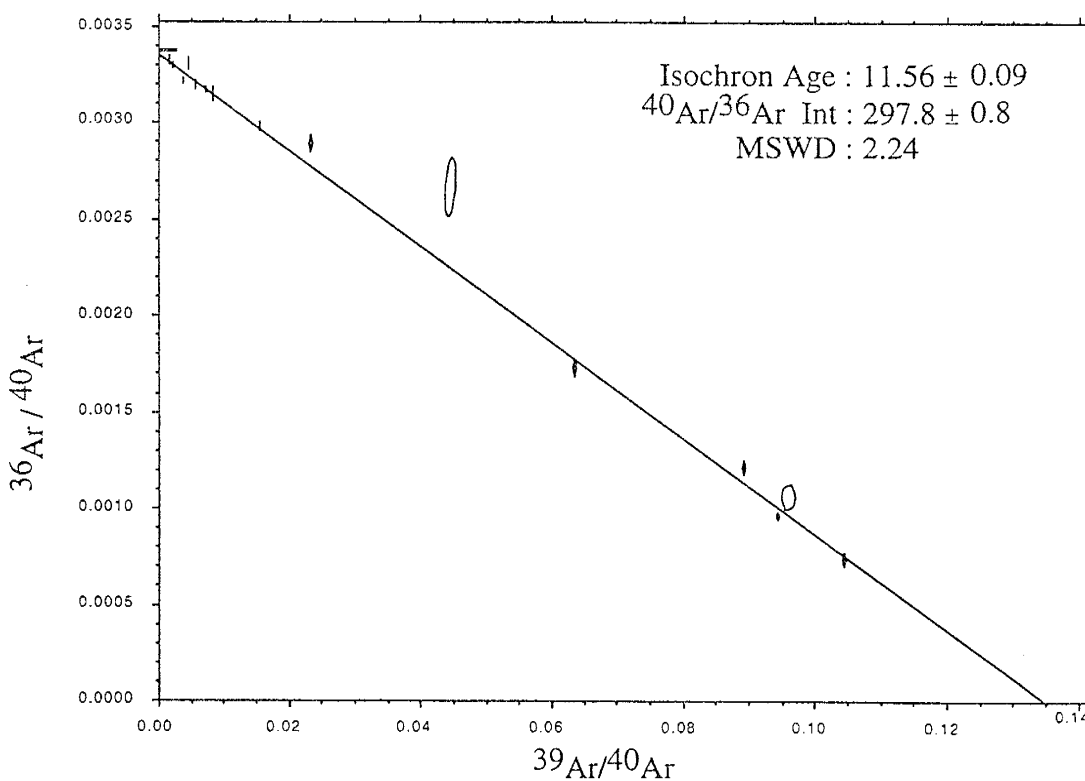
Appendix 6.c

Two-Step Laser Fusion Graphical Analysis biotite samples

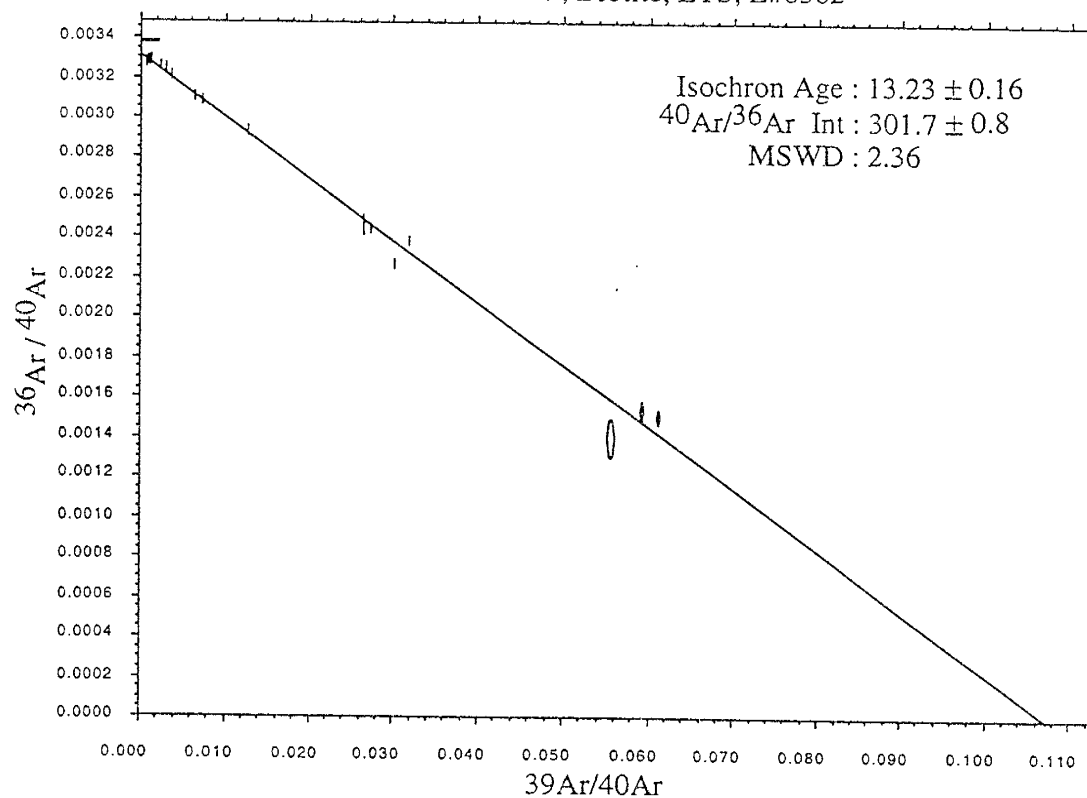
HN-2, Biotite, Laser Two Step Heating, L#6037



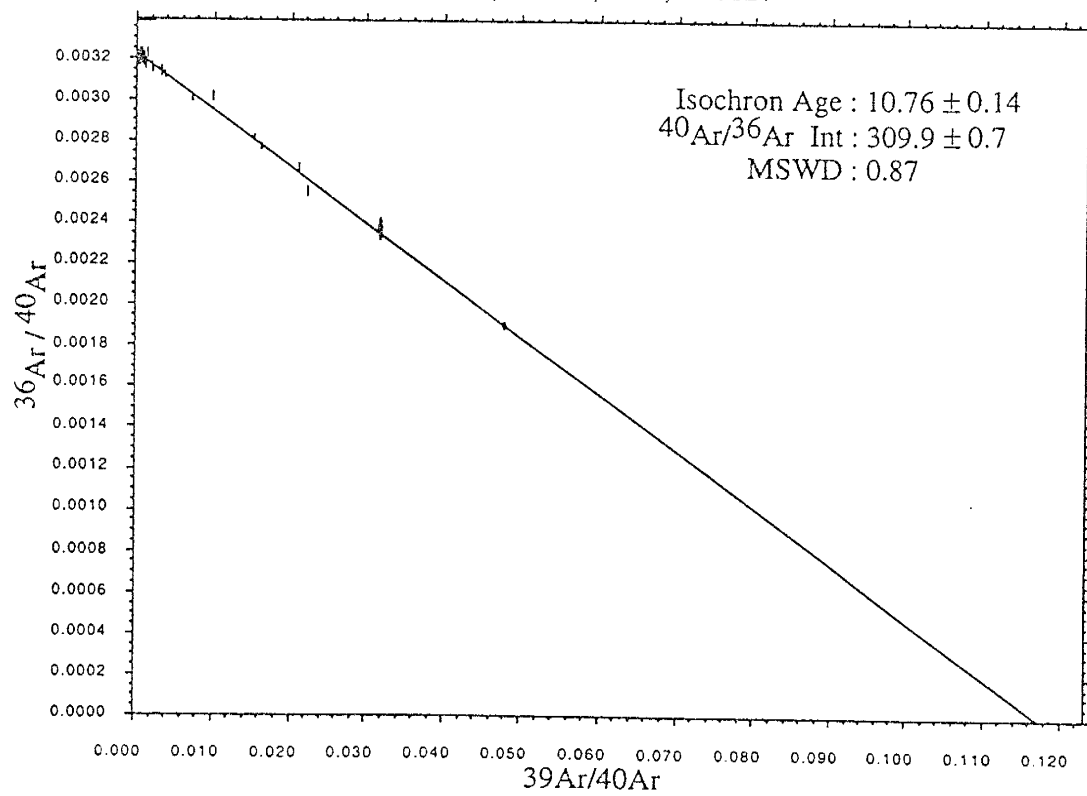
HN-3, Biotite, Laser Two Step Heating, L#6578



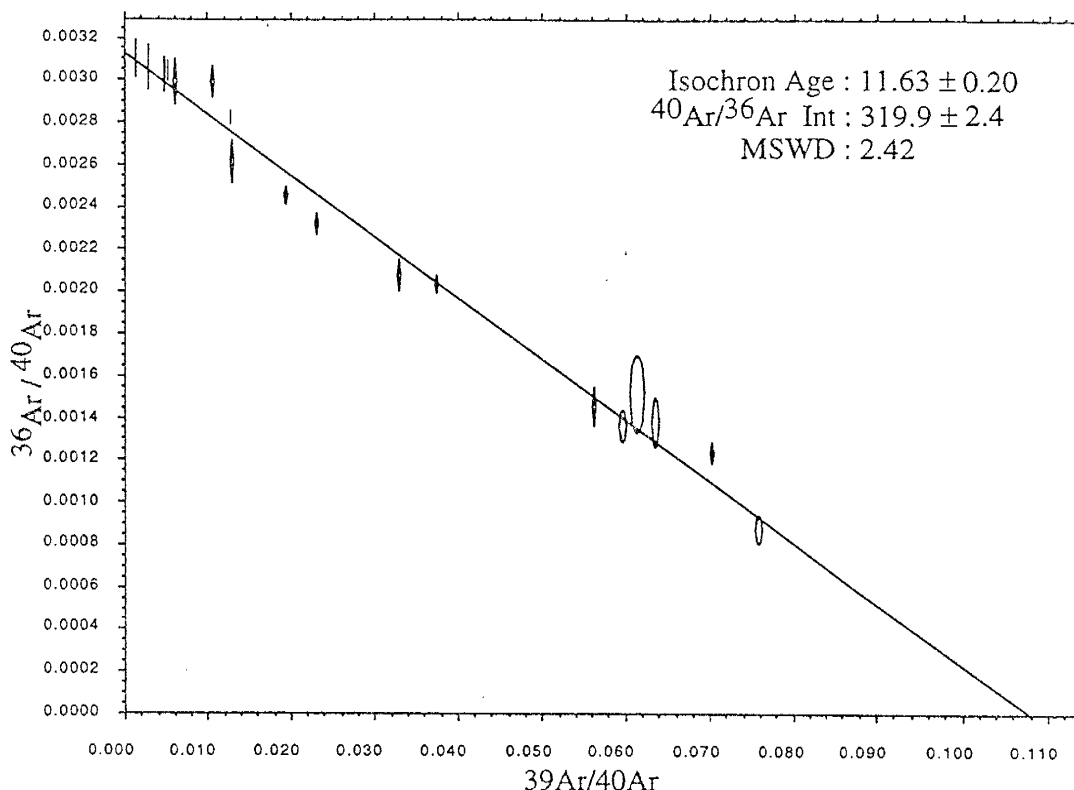
HN-9, Biotite, LTS, L#6362



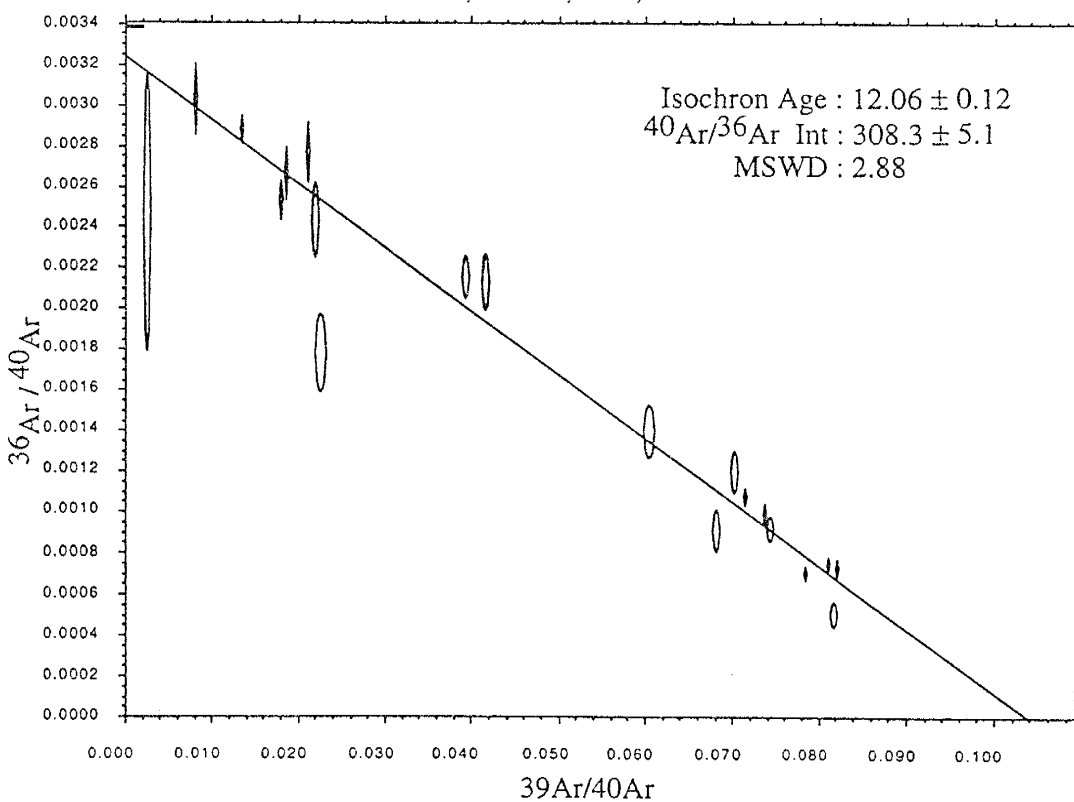
HN-12, Biotite, LTS, L#6027



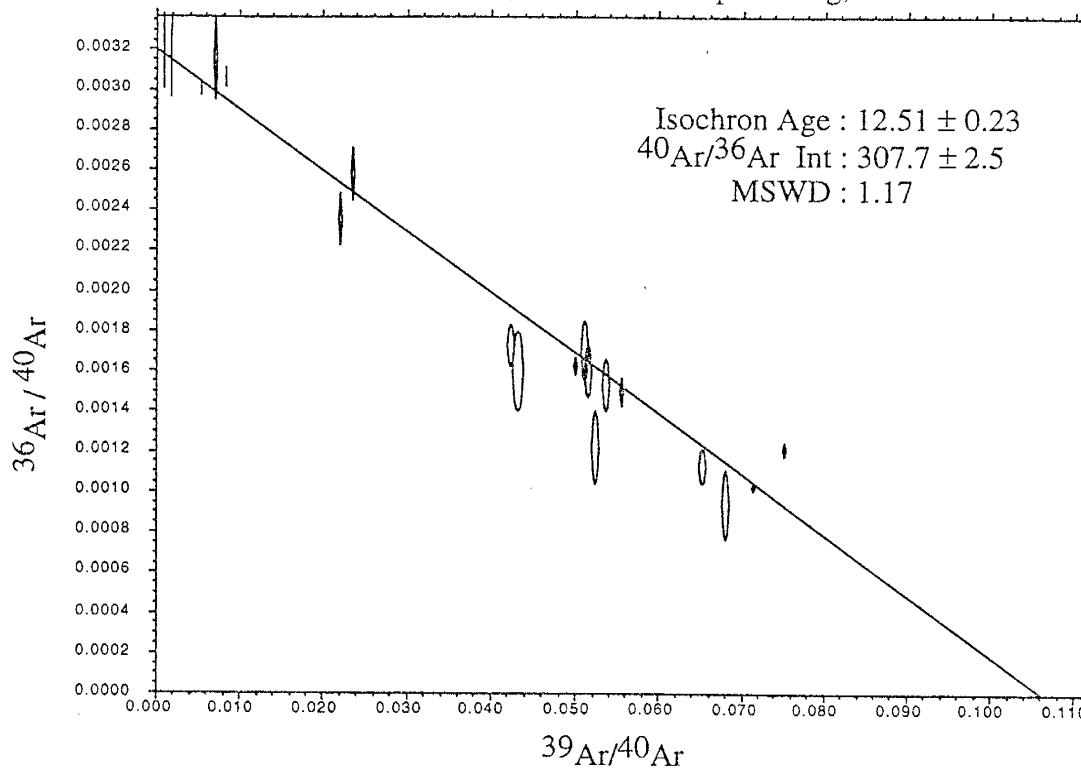
HN-17, Biotite, LTS, L#6029



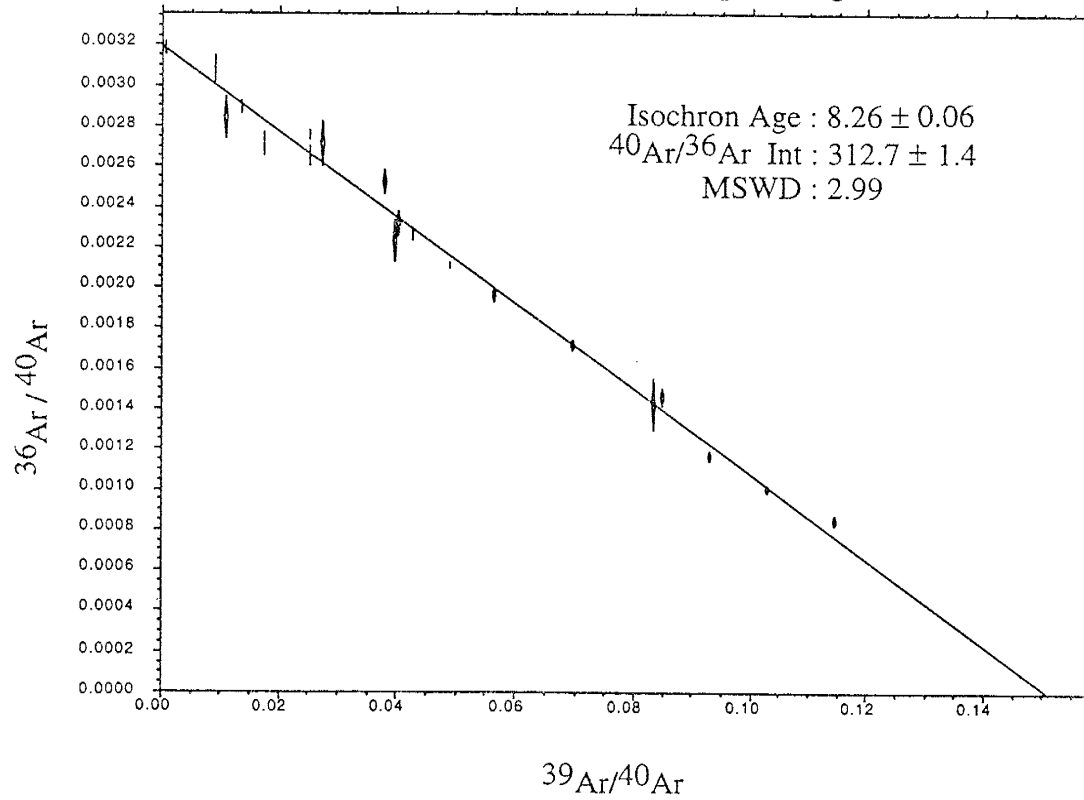
HN-18, Biotite, LTS, L#6030



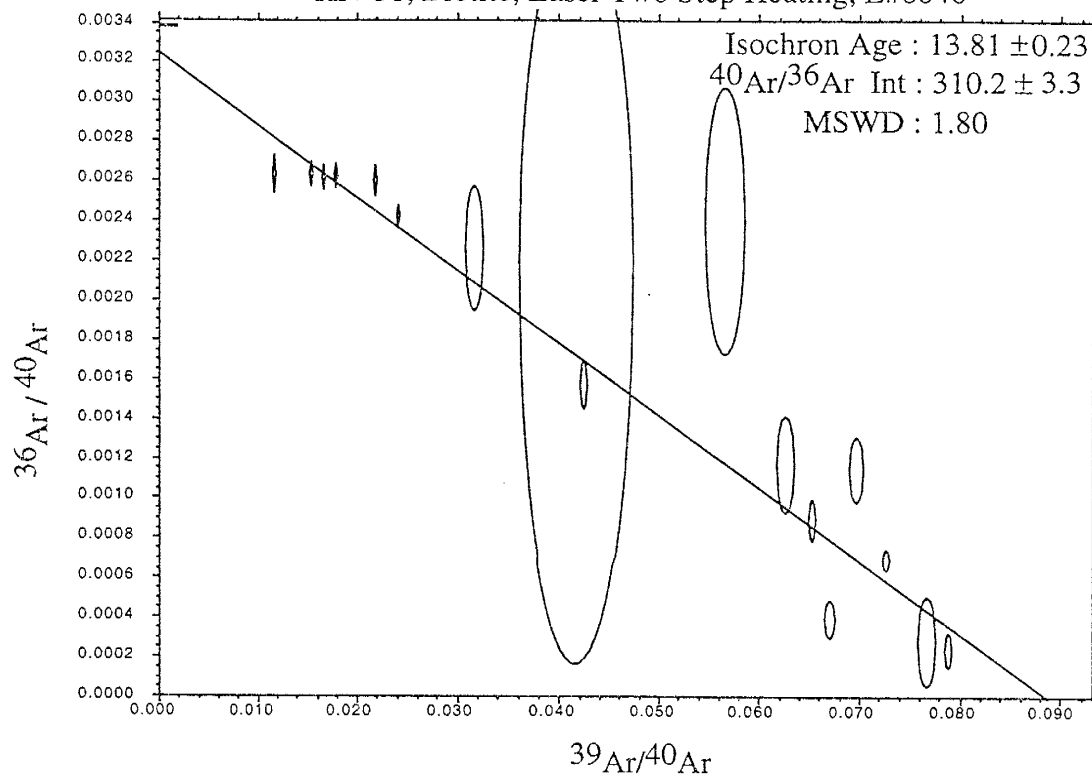
HN-20, Biotite, Laser Two Step Heating, L#6031



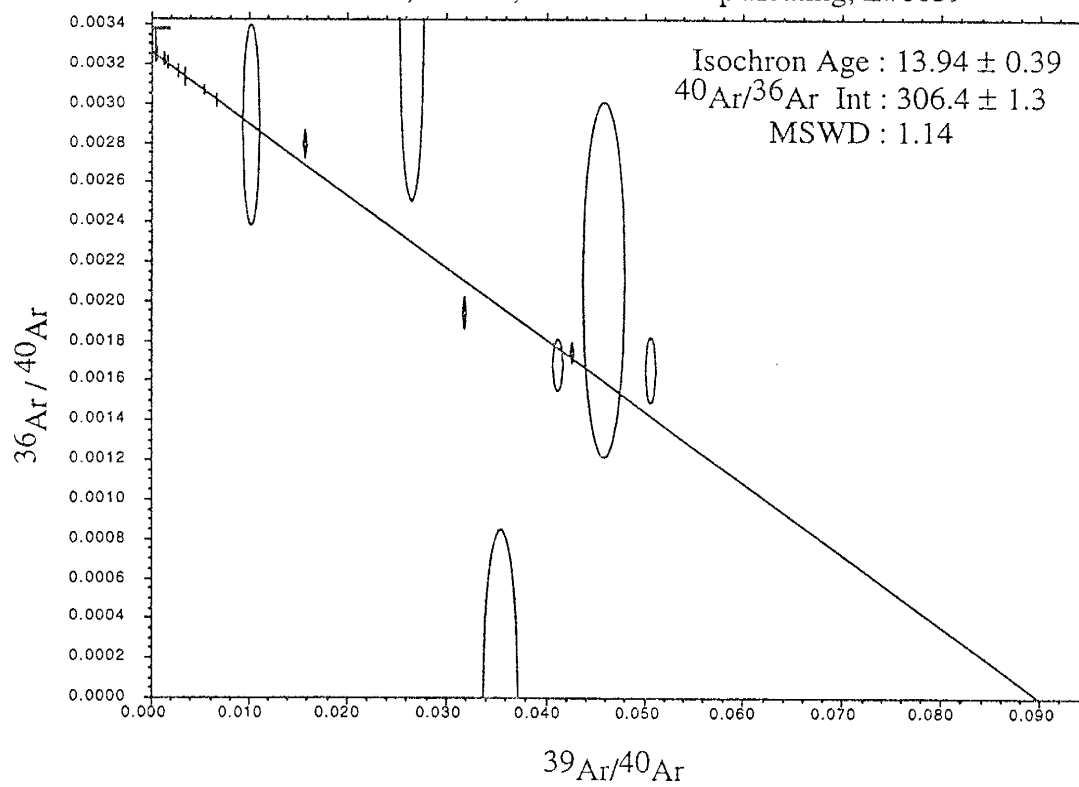
HN-24, Biotite, Laser Two Step Heating, L#6037

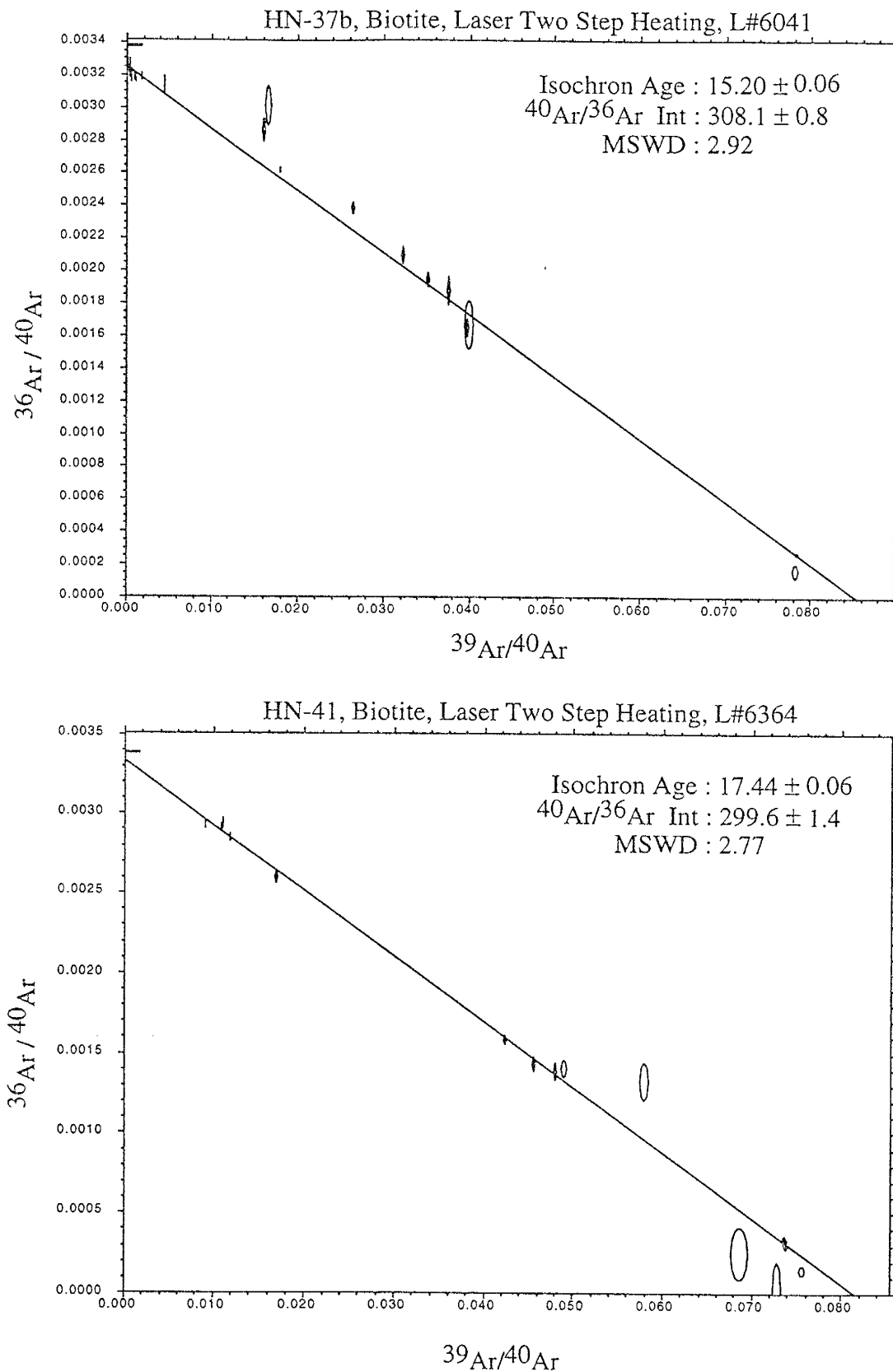


HN-31, Biotite, Laser Two Step Heating, L#6040

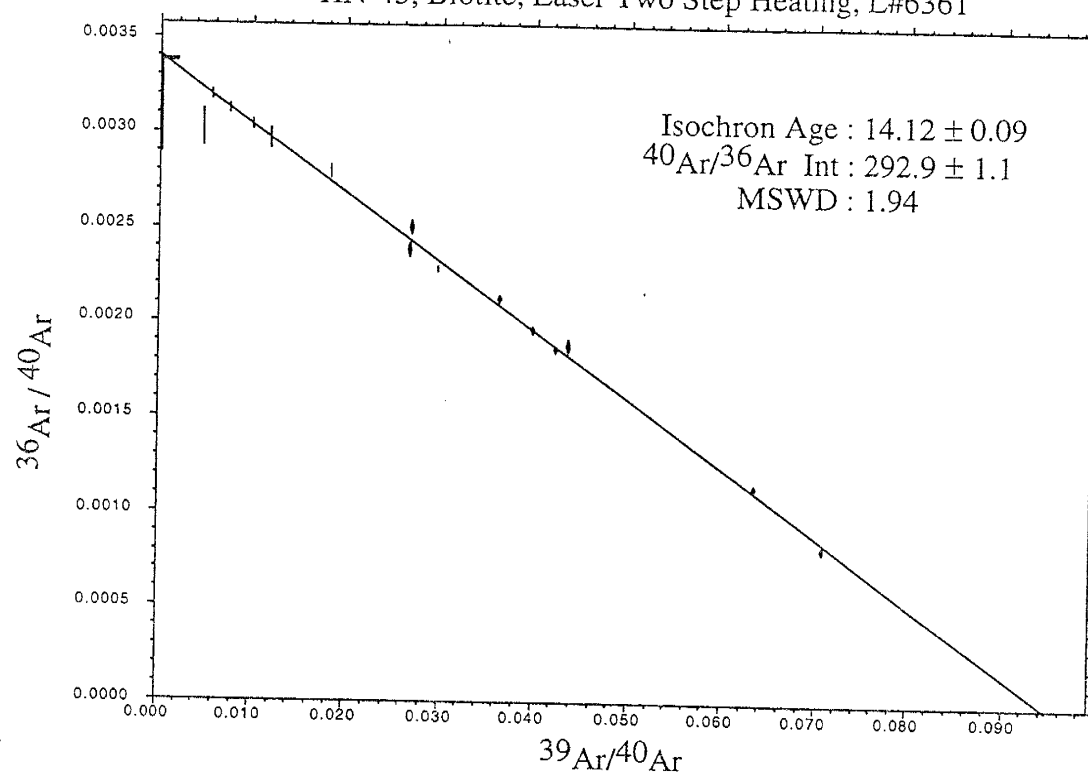


HN-32, Biotite, Laser Two Step Heating, L#6039

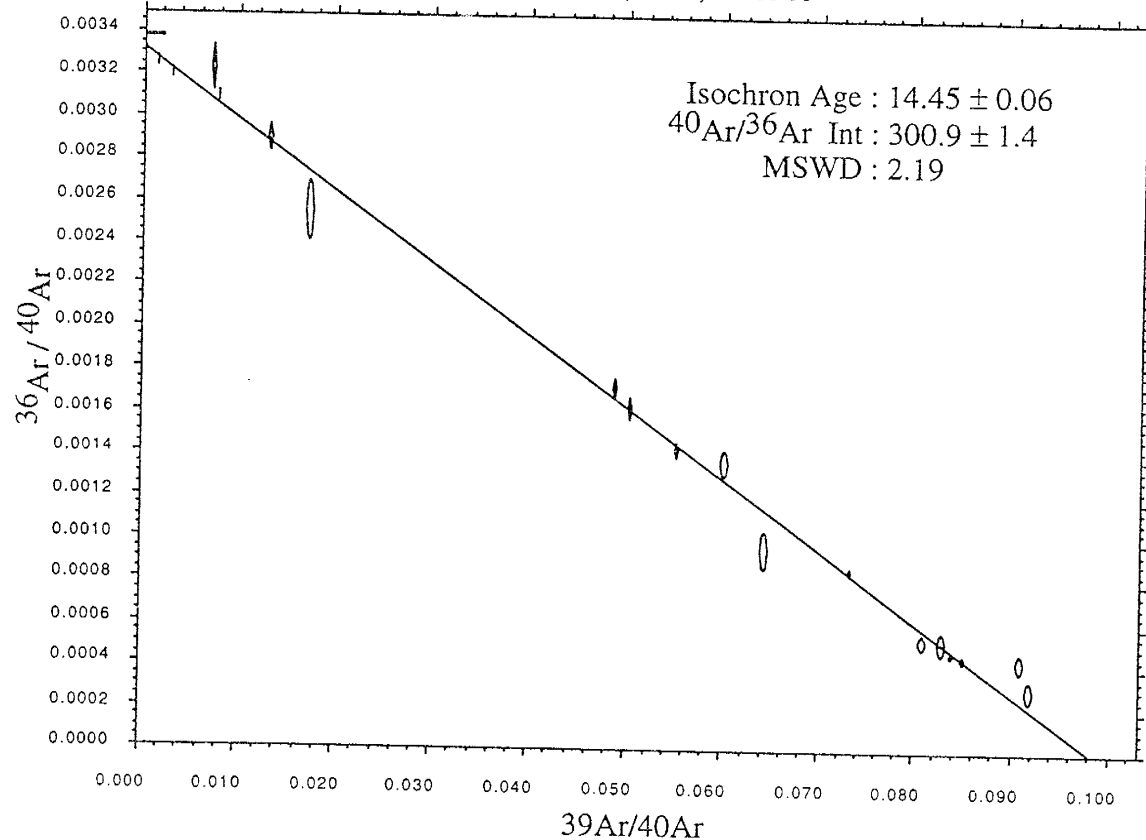




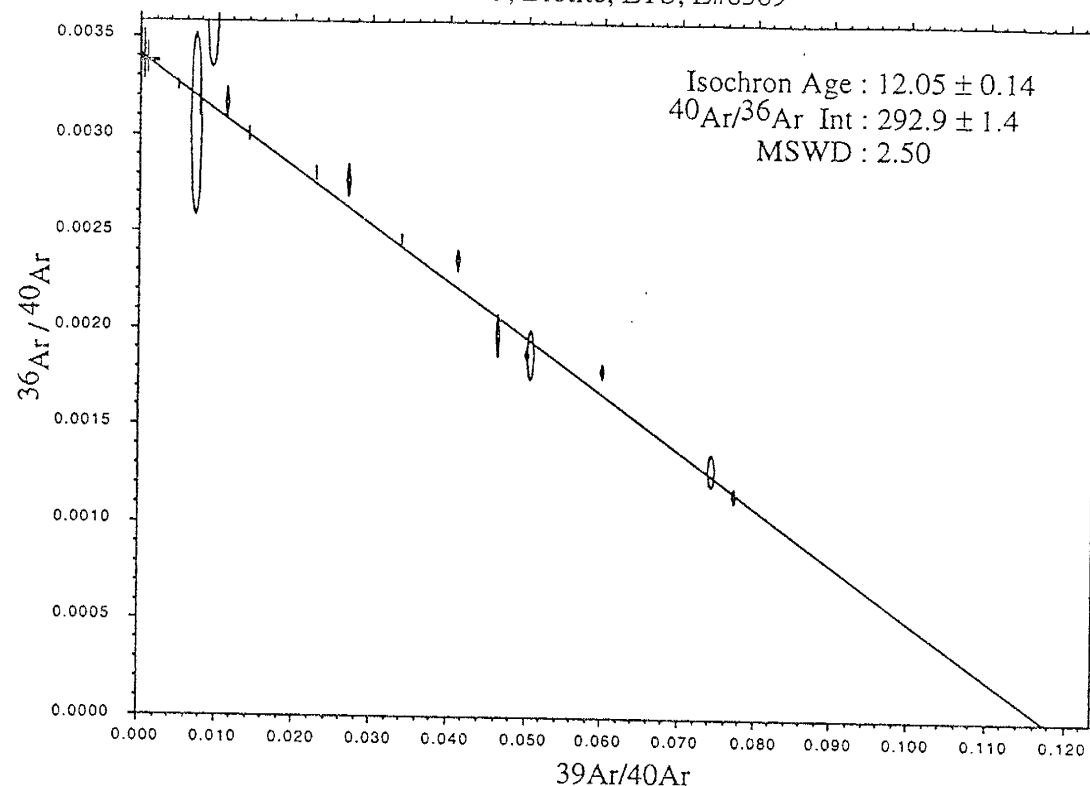
HN-45, Biotite, Laser Two Step Heating, L#6361



HN-46, Biotite, LTS, L#6363



HN-55, Biotite, LTS, L#6369



HN-58, Biotite, LTS, L#6365

